Walter Brand Increasing hesperetin bioavailability by modulating intestinal metabolism and transport

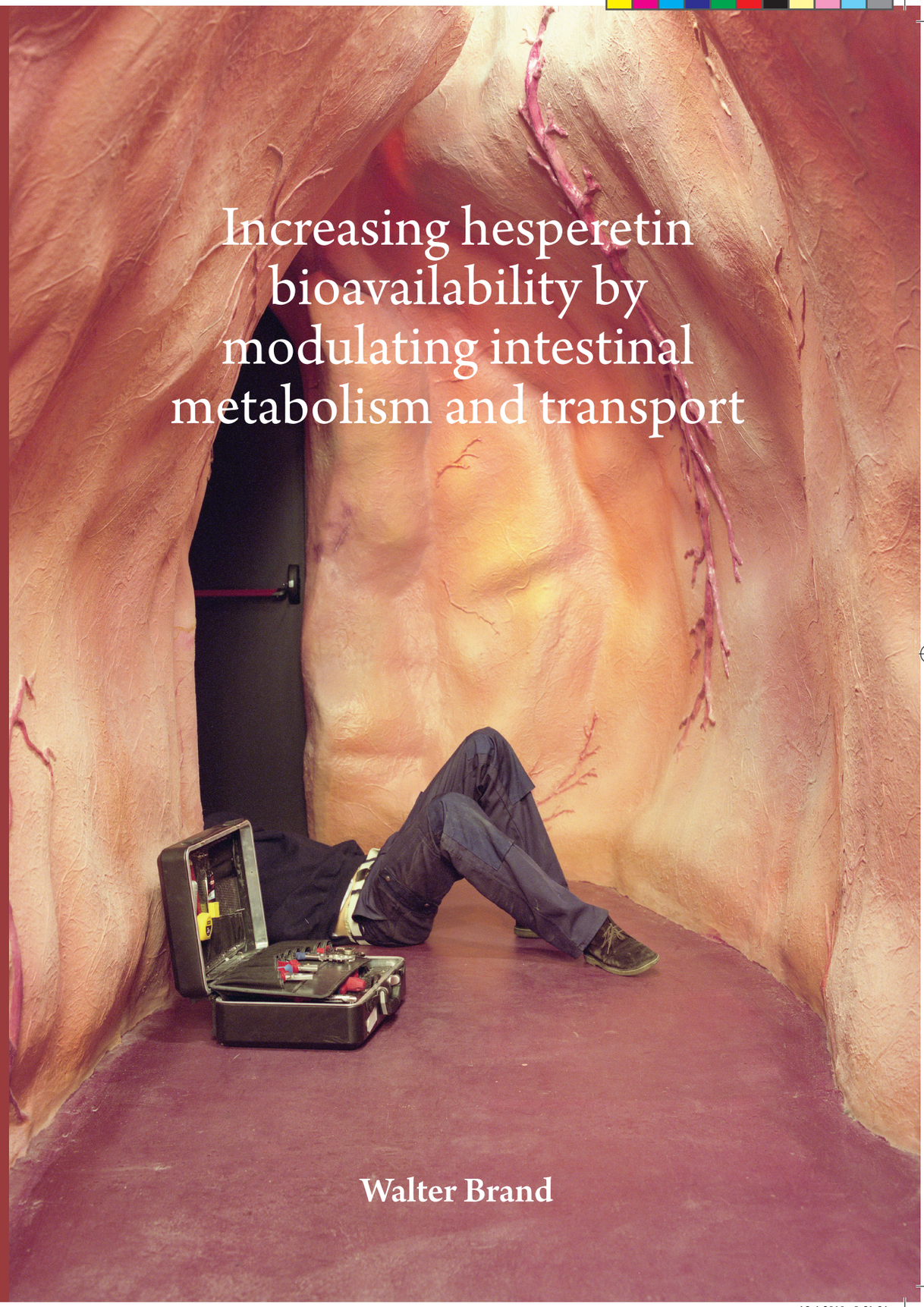

Increasing hesperetin bioavailability by modulating intestinal metabolism and transport

Walter Brand

Increasing hesperetin bioavailability by modulating intestinal metabolism and transport

Walter Brand

Thesis committee

Thesis supervisors

Prof. dr. ir. Ivonne M.C.M. Rietjens
Professor of Toxicology
Wageningen University

Prof. dr. Gary Williamson
Professor of Functional Food
University of Leeds, UK

Prof. dr. Peter J. van Bladeren
Professor of Toxico-kinetics and Biotransformation
Wageningen University

Other members

Prof. dr. Martin van den Berg, Institute for Risk Assessment Sciences, Utrecht

Dr. Peter C.H. Hollman, RIKILT, Wageningen

Prof. dr. Frans G.M. Russel, Radboud University Nijmegen

Prof. dr. Renger F. Witkamp, Wageningen University

This research was conducted under the auspices of the Graduate School VLAG

Increasing hesperetin bioavailability by modulating intestinal metabolism and transport

Walter Brand

Thesis
submitted in fulfilment of the requirements for the degree of doctor
at Wageningen University
by the authority of Rector Magnificus
Prof. dr. M.J. Kroppf,
in the presence of the
Thesis Committee appointed by the Academic Board
to be defended in public
on Friday 28 May 2010
at 4 p.m. in the Aula

Title: Increasing hesperetin bioavailability by modulating intestinal metabolism and transport

168 pages

Author: Walter Brand

Thesis Wageningen University, Wageningen, The Netherlands, 2010, with abstract, with references, and with summary in Dutch

ISBN: 978-90-8585-644-3

Je n'ay pas plus faict mon livre, que mon livre m'a faict
- Michel de Montaigne -

Voor Ada
(1946 - 2000)

Table of Contents

Chapter 1

General introduction, aim and outline of the thesis

General introduction

Bioavailability can be defined as the fraction of an administered dose of a compound that reaches the systemic circulation. Two important factors determining this bioavailability of a compound upon oral intake are its transport across the intestinal barrier and its first-pass metabolism. For most compounds the predominant route for intestinal absorption is through transcellular transport. Several mechanisms contribute to the efficiency of the transcellular transport and include passive diffusion, facilitated diffusion and active transport. Many factors can be of importance during this process, including the physical properties of a compound, *e.g.* size, hydrophobicity, acid dissociation constant, and solubility, but also the interaction with transport proteins and metabolizing enzymes.

Passive and facilitated diffusion occur along a concentration gradient and result in a net flux from the intestinal lumen at the apical side of the intestinal cells, to the blood at the basolateral side of the intestinal cells. The role of active transport in the overall outcome of the transcellular transport is more complex. First, because the transporters involved are able to transport compounds against a concentration gradient, and second, because they are located in either the apical or the basolateral membrane of the epithelial cells. Furthermore, some of these active transporters transport compounds into the intestinal cell, such as the sodium dependent glucose transporter (SGLT1) involved in active cellular uptake of for example certain flavonoid glycosides[1-3], but others, such as the ATP binding cassette (ABC) transporters preferentially result in efflux of compounds from the intestinal cell. In addition, transport from the intestinal cells by transporters in the basolateral membrane of the cells facilitates uptake thereby increasing bioavailability, whereas transport from the intestinal cells by transporters located in the apical membrane of the cells opposes uptake thereby decreasing bioavailability. Additionally, whenever a compound has entered the epithelial cells it is susceptible to conversion by intestinal metabolizing enzymes and this metabolism can be another important factor contributing to the limited bioavailability of the parent compound upon oral intake.

Compounds for which a limited bioavailability hampers their efficient use as functional food ingredients are flavonoids[4-6]. Even upon oral intake of doses up to several hundred milligrams, plasma levels achieved are generally in the low μM range and often even do not represent the parent compound but rather its glucuronidated, sulfated, and/or methylated metabolites[4,5]. Defining ways to increase the bioavailability of flavonoids is important in the development of their use as functional food ingredients. Therefore, the aim of this thesis was to investigate whether the bioavailability of the selected model flavonoid hesperetin could be increased by modulation of its intestinal metabolism and transport.

Flavonoids

Flavonoids consist of a large group of polyphenols that can be divided into different subclasses, including flavones, flavonols, isoflavones, flavanones, flavanols and anthocyanins and chalcones (Figure 1.1). Many of these compounds are present in plants and are believed to protect the plant against a variety of stress factors, and to have a role in plant pigmentation and flavoring[7]. Flavonoids are widely distributed in the human diet through fruits, vegetables and plant-derived products such as soy, wine, tea, coffee and cacao[7]. In plants and plant-derived food items flavonoids often occur as ß-glycosides, which become deglycosylated upon ingestion. Flavonoid glucosides can already be deglycosylated in the small intestine by lactase phloridzin hydrolase (LPH) or cytosolic ß-glucosidase, while disaccharides, such as rutinosides, are being deglycosylated by microbiota in the colon[8]. Upon uptake in the intestinal cells, flavonoids can be metabolized into glucuronidated, sulfonated or methylated derivates. Flavonoids, as well as their metabolites can be high affinity substrates for ABC transport proteins, which can facilitate uptake when located at the basolateral side of the intestinal cell, but also transport the flavonoid metabolites back to the intestinal lumen, opposing bioavailability[9].
Apart from substrates, flavonoids are also known as inhibitors or modulators of ABC transport proteins[10,11] and intestinal metabolizing enzymes[12] and therefore are compounds which can interact with the processes influencing the intestinal transport and metabolism of other compounds, thereby modulating their respective bioavailability.

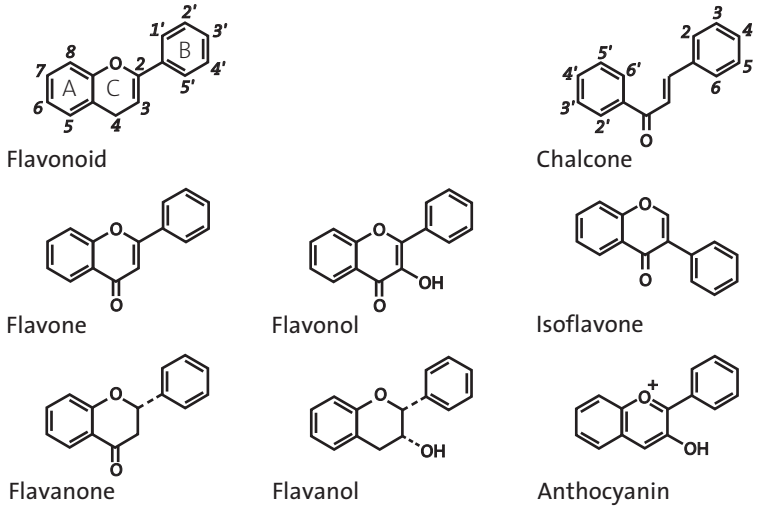

Figure 1.1 *Basic chemical flavonoid structure and basic chemical structures of different flavonoid subclasses.*

Hesperetin

The flavanone hesperetin (4'-methoxy-3',5,7-trihydroxyflavanone) (Figure 1.2) is the aglycone of hesperidin (hesperetin 7-*O*-rutinoside) (Figure 1.2) which is present in high amounts in sweet oranges (*Citrus sinensis*), orange juice and other citrus fruits including lemon, lime and mandarin[13]. Also certain herbs, spices, teas and other products have been reported to contain hesperidin, including rosemary[14], honeybush tea[15], and a large number of Chinese traditional medicinal products[16]. Hesperidin must by hydrolyzed by colonic microbiota before absorption whereas the aglycone hesperetin, as well as the monosaccharide hesperetin 7-*O*-glucoside, are already taken up earlier in the digestive tract[17,18]. Hesperetin 7-*O*-glucoside can be hydrolyzed by LPH followed by migration of the aglycone into the intestinal cell and/or the hesperetin 7-*O*-glucoside could be transported into the intestinal cell via a sodium-dependent glucose transporter (*e.g.* SGLT1) after which it is deglycosylated within the intestinal cell[1-3,19]. The resulting intracellular hesperetin aglycone is metabolized by UDP-glucuronosyl transferases (UGTs) and sulfotransferases (SULTs) into glucuronidated and sulfated metabolites which have been detected in human and rat plasma[20-25]. These conjugation reactions occurring in the intestinal cells have been reported to play an important role during the first pass metabolism of hesperetin[26] and the subsequent efflux of hesperetin metabolites to the intestinal lumen by apically located ABC transporters is believed to play an important factor in the limited bioavailability of hesperetin.

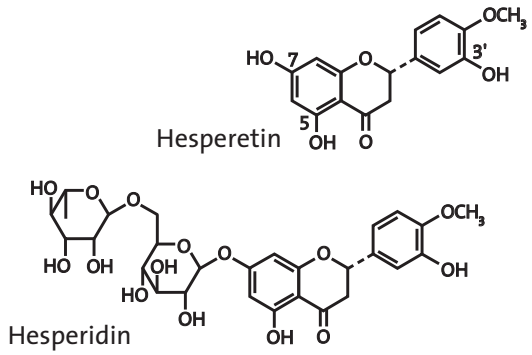

Figure 1.2 *Chemical structures of the rutinoside hesperidin and its aglycone hesperetin ((+/-)-4'-methoxy-3',5,7-trihydroxyflavone).*

Hesperidin, hesperetin 7-*O*-glucoside and hesperetin have been reported to provide several beneficial health effects, including anti-carcinogenic and anti-inflammatory effects and the capacity to reduce the chance on osteoporosis[27-30] and in addition also health beneficial effects have been reported for hesperetin glucuronides[31,32].

In general, hesperetin can make up an important part of the total flavonoid intake and its daily intake has been estimated to amount to 15.1 mg/day (after hydrolysis of glycosides)[33], although this daily intake is largely dependent on dietary habits because of the predominant occurrence of hesperidin in citrus fruits. The daily intake could be much higher since orange juice can easily contain up to 500 mg/l hesperidin[13]. Despite the potential high intake, plasma levels of hesperetin usually do not reach levels higher than 2 μM[22,34], indicating the limited bioavailability of hesperetin. Increasing the bioavailability of hesperetin is important to better exploit its beneficial properties. The conversion of hesperidin into hesperetin 7-*O*-glucoside prior to consumption has already shown to results in a 3-fold increase in the bioavailability of hesperetin[18].
Of importance to note is also that, unlike some other classes of flavonoid, flavanones like hesperetin have a chiral carbon atom in position 2 and therefore exist in an *S*(-)- and *R*(+)-configuration (Figure 1.3)[35,36], of which, in the case of hesperidin, one is naturally predominant in citrus fruits[37].

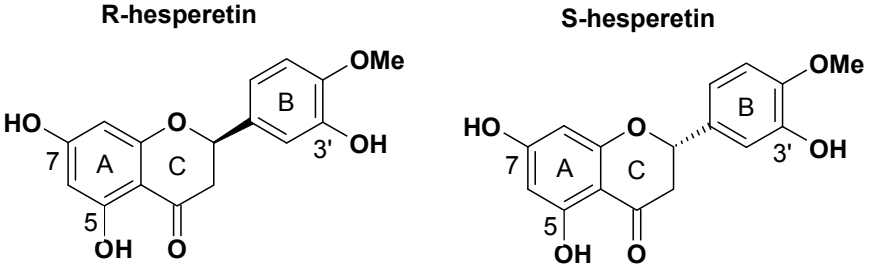

Figure 1.3 *Chemical structure of R(+)-hesperetin and S(-)-hesperetin.*

In sweet orange juice, hesperidin has been reported to exist in an epimeric ratio of at least 92:8 in favor of the 2*S*-epimer[38-40]. Although in nature the 2*S*-epimer of hesperidin, and subsequently the *S*-hesperetin enantiomers, are predominantly occurring, the 'pure' compounds are currently only commercially available as racemic mixtures. As a result, studies on hesperetin and hesperidin generally do not take the chirality into account whereas it can be foreseen that the two enantiomers may display distinct kinetic and dynamic properties[41]. For flavonoids, specific stereochemical properties have been demonstrated to influence for instance the bioavailability of the flavanol catechin[42], the estrogenic activity of the isoflavone metabolite equol[43,44] and the plasma and urinary kinetics of hesperetin[40,45], and may thus very well affect both the intestinal metabolism and transport of hesperetin, as well as its biological effects.

Aim and outline of the thesis

The aim of the present thesis was to investigate whether the bioavailability of the selected model flavonoid hesperetin could be increased by modulation of its intestinal metabolism and transport. It was hypothesized that, since other flavonoids may be converted by the same metabolic enzymes and transported by the same transporters as hesperetin, interactive effects upon simultaneous exposure may increase hesperetin bioavailability by modulating its intestinal metabolism and transport.

To further support this hypothesis chapter 2 of the thesis presents a literature study on the capacity of flavonoids to modulate the oral bioavailability of other compounds. In subsequent chapters of the thesis the concept is tested using different *in vitro* and *in vivo* model systems. The *in vitro* models used for these studies include a two-compartment transwell model with Caco-2 cell monolayers, simulating the intestinal transport barrier. After differentiation, Caco-2 cells are known to display morphological and biochemical characteristics of human enterocytes, including the expression of ABC transporters and phase II metabolizing enzymes, and to form a tight layer of polarized intestinal cells[46]. Grown on a membrane separating an apical compartment (simulating the intestinal lumen side) and a basolateral compartment (simulating the blood/plasma side) they form a well accepted model to study intestinal transport[47].

In chapter 3, the intestinal transport and metabolism of hesperetin was defined *in vitro* using Caco-2 cell monolayers in a two-compartment transwell model system simulating the intestinal transport barrier. The metabolites of hesperetin formed by the Caco-2 cells were identified using a combination of analytical techniques and available reference compounds combined with specific enzymatic deconjugation reactions. The ABC transporters responsible for the efflux of hesperetin metabolites were determined by co-administrating a series of transport inhibitors, and their cellular expression was confirmed using reverse transcription quantitative polymerase chain reaction (RT-qPCR) techniques. In chapter 4, the effect of co-administering other flavonoids, reported to be efficient modulators of ABC mediated transport, on the metabolism, transport and disposition of hesperetin and its metabolites by Caco-2 cell monolayers was studied. In chapter 5, the effect of co-administering quercetin, which proved to be a potent modulator *in vitro*, on the bioavailability of hesperetin was further studied *in vivo* using Sprague-Dawley rats. In Chapter 6 focus was on the phase II metabolism of hesperetin comparing its conversion by different model systems and identifying the UGT and SULT isoenzymes involved. The results provided insight in the relative importance of intestinal metabolism as compared to metabolism by liver tissue, both contributing to the reduced systemic availability of hesperetin aglycone.

Additionally, in chapter 7 the transport and metabolism characteristics so far studied for the commercially available racemic mixture of hesperetin were investigated for the *S*- and *R*-hesperetin enantiomers. To this end a chiral separation method on an analytical and semi-preparative scale was developed allowing small scale *in vitro* studies. Differences in intestinal metabolism and transport were studied by incubating *S*- or *R*-hesperetin with small intestinal microsomes and cytosol, and by exposing Caco-2 cell monolayers to either of the hesperetin enantiomers. In addition, to test stereochemical differences in bioactivity, mouse Hepa-1c1c7 cells transfected with human EpRE-controlled luciferase were exposed to *S*- or *R*-hesperetin to study induction of EpRE-mediated gene expression, a mechanism which is associated with some of the health beneficial effects associated with flavonoids[48].

The thesis concludes with chapter 8 presenting a summary of the results and conclusions, concluding remarks and future perspectives.

References

1 Day AJ, Gee JM, DuPont MS, Johnson IT, Williamson G. Absorption of quercetin-3-glucoside and quercetin-4'-glucoside in the rat small intestine: the role of lactase phlorizin hydrolase and the sodium-dependent glucose transporter. *Biochem Pharmacol* 65(7): 1199-1206, 2003.

2 Hollman PCH, De Vries JHM, Van Leeuwen SD, Mengelers MJB, Katan MB. Absorption of dietary quercetin glycosides and quercetin in healthy ileostomy volunteers. *Am J Clin Nutr* 62(6): 1276-1282, 1995.

3 Wolffram S, Blöck M, Ader P. Quercetin-3-glucoside is transported by the glucose carrier SGLT1 across the brush border membrane of rat small intestine. *J Nutr* 132(4): 630-635, 2002.

4 Manach C, Williamson G, Morand C, Scalbert A, Remesy C. Bioavailability and bioefficacy of polyphenols in humans. I. Review of 97 bioavailability studies. *Am J Clin Nutr* 81(1 Suppl): 230S-242S, 2005.

5 Scalbert A, Williamson G. Dietary intake and bioavailability of polyphenols. *J Nutr* 130(8S Suppl): 2073S-2085S, 2000.

6 Scholz S, Williamson G. Interactions affecting the bioavailability of dietary polyphenols in vivo. *Int J Vitam Nutr Res* 77(3): 224-235, 2007.

7 Ross JA, Kasum CM. Dietary flavonoids: bioavailability, metabolic effects, and safety. *Annu Rev Nutr* 22: 19-34, 2002.

8 Németh K, Plumb GW, Berrin J-G, Juge N, Jacob R, Naim HY, Williamson G, Swallow DM, Kroon PA. Deglycosylation by small intestinal epithelial cell beta-glucosidases is a critical step in the absorption and metabolism of dietary flavonoid glycosides in humans. *Eur J Nutr* 42(1): 29-42, 2003.

9 Liu Z, Hu M. Natural polyphenol disposition via coupled metabolic pathways. *Expert Opin Drug Metab Toxicol* 3(3): 389-406, 2007.

10 Aszalos A. Role of ATP-binding cassette (ABC) transporters in interactions between natural products and drugs. *Curr Drug Metab* 9(10): 1010-1018, 2008.

11 Brand W, Schutte ME, Williamson G, Van Zanden JJ, Cnubben NHP, Groten JP, Van Bladeren PJ, Rietjens IMCM. Flavonoid-mediated inhibition of intestinal ABC transporters may affect the oral bioavailability of drugs, food-borne toxic compounds and bioactive ingredients. *Biomed Pharmacother* 60(9): 508-519, 2006.

12 Moon YJ, Wang X, Morris ME. Dietary flavonoids: effects on xenobiotic and carcinogen metabolism. *Toxicol In Vitro* 20(2): 187-210, 2006.

13 Tomás-Barberán FA, Clifford MN. Flavanones, chalcones and dihydrochalcones - nature, occurrence and dietary burden. *J Sci Food Agric* 80(7): 1073-1080, 2000.

14 del Baño MJ, Lorente J, Castillo J, Benavente-García O, Marín MP, Del Río JA, Ortuño A, Ibarra I. Flavonoid distribution during the development of leaves, flowers, stems, and roots of Rosmarinus officinalis. postulation of a biosynthetic pathway. *J Agric Food Chem* 52(16): 4987-4992, 2004.

15 Joubert E, Otto F, Gruener S, Weinreich B. Reversed-phase HPLC determination of mangiferin, isomangiferin and hesperidin in Cyclopia and the effect of harvesting date on the phenolic composition of C. genistoides. *Eur Food Res Technol* 216(3): 270-273, 2003.
16 Lu Y, Zhang C, Bucheli P, Wei D. Citrus flavonoids in fruit and traditional Chinese medicinal food ingredients in China. *Plant Foods Hum Nutr* 61(2): 57-65, 2006.
17 Kanaze FI, Bounartzi MI, Georgarakis M, Niopas I. Pharmacokinetics of the citrus flavanone aglycones hesperetin and naringenin after single oral administration in human subjects. *Eur J Clin Nutr* 61(4): 472-477, 2007.
18 Nielsen ILF, Chee WSS, Poulsen L, Offord-Cavin E, Rasmussen SE, Frederiksen H, Enslen M, Barron D, Horcajada M-N, Williamson G. Bioavailability is improved by enzymatic modification of the citrus flavonoid hesperidin in humans: a randomized, double-blind, crossover trial. *J Nutr* 136(2): 404-408, 2006.
19 Walgren RA, Lin JT, Kinne RK, Walle T. Cellular uptake of dietary flavonoid quercetin 4'-beta-glucoside by sodium-dependent glucose transporter SGLT1. *J Pharmacol Exp Ther* 294(3): 837-843, 2000.
20 Ameer B, Weintraub RA, Johnson JV, Yost RA, Rouseff RL. Flavanone absorption after naringin, hesperidin, and citrus administration. *Clin Pharmacol Ther* 60(1): 34-40, 1996.
21 Gardana C, Guarnieri S, Riso P, Simonetti P, Porrini M. Flavanone plasma pharmacokinetics from blood orange juice in human subjects. *Br J Nutr* 98(1): 165-172, 2007.
22 Manach C, Morand C, Gil-Izquierdo A, Bouteloup-Demange C, Rémésy C. Bioavailability in humans of the flavanones hesperidin and narirutin after the ingestion of two doses of orange juice. *Eur J Clin Nutr* 57(2): 235-242, 2003.
23 Matsumoto H, Ikoma Y, Sugiura M, Yano M, Hasegawa Y. Identification and quantification of the conjugated metabolites derived from orally administered hesperidin in rat plasma. *J Agric Food Chem* 52(21): 6653-6659, 2004.
24 Mullen W, Archeveque M-A, Edwards CA, Matsumoto H, Crozier A. Bioavailability and metabolism of orange juice flavanones in humans: impact of a full-fat yogurt. *J Agric Food Chem* 56(23): 11157-11164, 2008.
25 Brett GM, Hollands W, Needs PW, Teucher B, Dainty JR, Davis BD, Brodbelt JS, Kroon PA. Absorption, metabolism and excretion of flavanones from single portions of orange fruit and juice and effects of anthropometric variables and contraceptive pill use on flavanone excretion. *Br J Nutr* 101(5): 664-675, 2009.
26 Silberberg M, Morand C, Mathevon T, Besson C, Manach C, Scalbert A, Remesy C. The bioavailability of polyphenols is highly governed by the capacity of the intestine and of the liver to secrete conjugated metabolites. *Eur J Nutr* 45(2): 88-96, 2006.
27 Chiba H, Uehara M, Wu J, Wang X, Masuyama R, Suzuki K, Kanazawa K, Ishimi Y. Hesperidin, a citrus flavonoid, inhibits bone loss and decreases serum and hepatic lipids in ovariectomized mice. *J Nutr* 133(6): 1892-1897, 2003.
28 Garg A, Garg S, Zaneveld LJD, Singla AK. Chemistry and pharmacology of the citrus bioflavonoid hesperidin. *Phytother Res* 15(8): 655-669, 2001.
29 Habauzit V, Nielsen IL, Gil-Izquierdo A, Morand C, Chee W, Barron D, Davicco MJ, Coxam V, Williamson G, Offord E, Horcajada MN. Increased bioavailability of hesperetin-7-glucoside compared to hesperidin results in more efficient prevention of bone loss in adult ovariectomized rats. *Br J Nutr* 102(7): 976-984, 2009.
30 Horcajada MN, Habauzit V, Trzeciakiewicz A, Morand C, Gil-Izquierdo A, Mardon J, Lebecque P, Davicco MJ, Chee WSS, Coxam V, Offord E. Hesperidin inhibits ovariectomized-induced osteopenia and shows differential effects on bone mass and strength in young and adult intact rats. *J Appl Physiol* 104(3): 648-654, 2008.
31 Proteggente AR, Basu-Modak S, Kuhnle G, Gordon MJ, Youdim K, Tyrrell R, Rice-Evans CA. Hesperetin glucuronide, a photoprotective agent arising from flavonoid metabolism in human skin fibroblasts. *Photochem Photobiol* 78(2): 256-261, 2003.
32 Trzeciakiewicz A, Habauzit V, Mercier S, Barron D, Urpi-Sarda M, Manach C, Offord E, Horcajada M-N. Molecular mechanism of hesperetin-7-O-glucuronide, the main circulating metabolite of hesperidin, involved in osteoblast differentiation. *J Agric Food Chem* 58(1): 668-675, 2010.
33 Knekt P, Kumpulainen J, Järvinen R, Rissanen H, Heliövaara M, Reunanen A, Hakulinen T, Aromaa A. Flavonoid intake and risk of chronic diseases. *Am J Clin Nutr* 76(3): 560-568, 2002.
34 Erlund I, Meririnne E, Alfthan G, Aro A. Plasma kinetics and urinary excretion of the flavanones naringenin and hesperetin in humans after ingestion of orange juice and grapefruit juice. *J Nutr* 131(2): 235-241, 2001.
35 Arakawa H, Nakazaki M. Absolute configuration of (-)hesperetin and (-)liquiritigenin. *Chem Ind* 1960: 73, 1960.

36 Arakawa H, Nakazaki M. Die absolute Konfigurationen der optisch aktiven Flavanone. *Liebigs Ann Chem* 636(1): 111-117, 1960.
37 Yáñez JA, Andrews PK, Davies NM. Methods of analysis and separation of chiral flavonoids. *J Chromatogr B Analyt Technol Biomed Life Sci* 848(2): 159-181, 2007.
38 Aturki Z, Brandi V, Sinibaldi M. Separation of flavanone-7-O-glycoside diastereomers and analysis in citrus juices by multidimensional liquid chromatography coupled with mass spectrometry. *J Agric Food Chem* 52(17): 5303-5308, 2004.
39 Gel-Moreto N, Streich R, Galensa R. Chiral separation of diastereomeric flavanone-7-O-glycosides in citrus by capillary electrophoresis. *Electrophoresis* 24(15): 2716-2722, 2003.
40 Yáñez JA, Remsberg CM, Miranda ND, Vega-Villa KR, Andrews PK, Davies NM. Pharmacokinetics of selected chiral flavonoids: hesperetin, naringenin and eriodictyol in rats and their content in fruit juices. *Biopharm Drug Dispos* 29(2): 63-82, 2008.
41 Ariëns EJ. Stereochemistry, a basis for sophisticated nonsense in pharmacokinetics and clinical pharmacology. *Eur J Clin Pharmacol* 26(6): 663-668, 1984.
42 Donovan JL, Crespy V, Oliveira M, Cooper KA, Gibson BB, Williamson G. (+)-Catechin is more bioavailable than (-)-catechin: relevance to the bioavailability of catechin from cocoa. *Free Radic Res* 40(10): 1029-1034, 2006.
43 Setchell KDR, Clerici C, Lephart ED, Cole SJ, Heenan C, Castellani D, Wolfe BE, Nechemias-Zimmer L, Brown NM, Lund TD, Handa RJ, Heubi JE. S-equol, a potent ligand for estrogen receptor beta, is the exclusive enantiomeric form of the soy isoflavone metabolite produced by human intestinal bacterial flora. *Am J Clin Nutr* 81(5): 1072-1079, 2005.
44 Setchell KDR, Zhao X, Jha P, Heubi JE, Brown NM. The pharmacokinetic behavior of the soy isoflavone metabolite S-(-)equol and its diastereoisomer R-(+)equol in healthy adults determined by using stable-isotope-labeled tracers. *Am J Clin Nutr* 90(4): 1029-1037, 2009.
45 Yáñez JA, Teng XW, Roupe KA, Davies NM. Stereospecific high-performance liquid chromatographic analysis of hesperetin in biological matrices. *J Pharm Biomed Anal* 37(3): 591-595, 2005.
46 Pinto M, Robine-Leon S, Appay M-D, Kedinger M, Triadou N, Dussaulx E, Lacroix B, Simon-Assmann P, Haffen K, Fogh J, Zweibaum A. Enterocyte-like differentiation and polarisation of the human colon carcinoma cell line Caco-2. *Biol Cell* 47: 323-330, 1983.
47 Karlsson J, Artursson P. A method for the determination of cellular permeability coefficients and aquous boundary layer thickness in monolayers of intestinal epithelial (Caco-2) cells grown in permeable filter chambers. *Int J Pharmaceutics* 71(1-2): 55-64, 1991.
48 Chen C, Kong AN. Dietary chemopreventive compounds and ARE/EpRE signaling. *Free Radic Biol Med* 36(12): 1505-1516, 2004.

Chapter 2

Flavonoid-mediated inhibition of intestinal ABC transporters may affect the oral bioavailability of drugs, food-borne toxic compounds and bioactive ingredients

Walter Brand, Maaike E. Schutte, Gary Williamson, Jelmer J. van Zanden, Nicole H.P. Cnubben, John P. Groten, Peter J. van Bladeren, and Ivonne M.C.M. Rietjens

Biomedicine & Pharmacotherapy 60(9): 508-519, 2006

Abstract

The transcellular transport of ingested food ingredients across the intestinal epithelial barrier is an important factor determining bioavailability upon oral intake. This transcellular transport of many chemicals, food ingredients, drugs or toxic compounds over the intestinal epithelium can be highly dependent on the activity of membrane bound ATP binding cassette (ABC) transport proteins, able to export the compounds from the intestinal cells. The present review describes the ABC transporters involved in the efflux of bioactive compounds from the intestinal cells, either to the basolateral blood side, facilitating absorption, or back into the intestinal lumen, reducing bioavailability. The role of the ABC transporters in intestinal transcellular uptake also implies a role for inhibitors of these transporters in modulation of the bioavailability upon oral uptake. The present paper focuses on the role of flavonoids as important modulators or substrates of intestinal ABC transport proteins. Several examples of such an effect of flavonoids are presented. It can be concluded that flavonoid-mediated inhibition of ABC transporters may affect the bioavailability of drugs, bioactive food ingredients and/or food-borne toxic compounds upon oral uptake. All together it appears that the flavonoid-mediated interactions at the level of the intestinal ABC transport proteins may be an important mechanism for unexpected food-drug, food-toxin or food-food interactions. The overview also indicates that future studies should focus on
i) *in vivo* validation of the flavonoid-mediated effects on bioavailability of drugs, toxins and beneficial bioactive food ingredients detected in *in vitro* models, and on
ii) the role of flavonoid phase II metabolism in modulating the activity of the flavonoids to act as ABC transporter inhibitors and/or substrates.

Introduction

The transport of ingested food ingredients across the intestinal barrier is an important factor determining bioavailability upon oral intake. This holds for biofunctional food ingredients, drugs and also for toxic compounds. For these small and generally hydrophilic compounds the predominant route for intestinal absorption is through transcellular transport. Several mechanisms contribute to the ultimate efficiency of this transcellular transport. These include passive diffusion, facilitated diffusion, and active transport. Passive and facilitated diffusion occur along a concentration gradient. Both processes result in a net flux from the intestinal lumen at the apical side of the intestinal cells, through the cytoplasm of the intestinal cells, to the blood stream at the basolateral side of the intestinal cells. The role of active transport in the ultimate outcome of the transcellular transport is more complex. This is because (1) the transporters involved are able to transport

compounds against a concentration gradient, (2) they are located in either the apical or the basolateral membrane of the epithelial cells, and (3) some of these active transporters transport compounds into the intestinal cell, such as the sodium dependent glucose transporter (SGLT1) involved in active cellular uptake of for example certain flavonoid glycosides[1-3], but others preferentially result in efflux of compounds and/or their metabolites from the intestinal cell. The overall absorption of a chemical, food ingredient, drug or toxic compound across the intestinal epithelium by transcellular transport can be largely dependent on the activity of these membrane bound transport proteins. The present review focuses especially on the ABC transporters involved in the efflux of bioactive compounds from the intestinal cells either to the basolateral blood side, facilitating absorption, or back into the intestinal lumen, reducing bioavailability.

Active transport proteins involved in efflux of chemicals from the intestinal cells

The intestinal ABC transporters involved in the efflux of chemicals from the intestinal cells include P-glycoprotein (Pgp/MDR1/ABCB1), Multidrug Resistance Proteins (MRPs/ABCCs) and Breast Cancer Resistance Protein (BCRP/ABCG2/ABCP/MXR)[4-7] (Table 2.1 on page 22). These transporters are generally located specifically in the apical (intestinal luminal side) or basolateral (blood/plasma side) membrane of the enterocytes (Figure 2.1). Pgp/MDR1, MRP2 (ABCC2) and BCRP are localized in the apical membrane[4,6,8], whereas MRP1 (ABCC1), MRP3 (ABCC3) and MRP5 (ABCC5) are localized in the basolateral membrane of the intestinal enterocytes[5,9-11]. Little is known about MRP4 (ABCC4) which could be located in the apical as well as in the basolateral membrane of the intestinal cells[4,12,13].

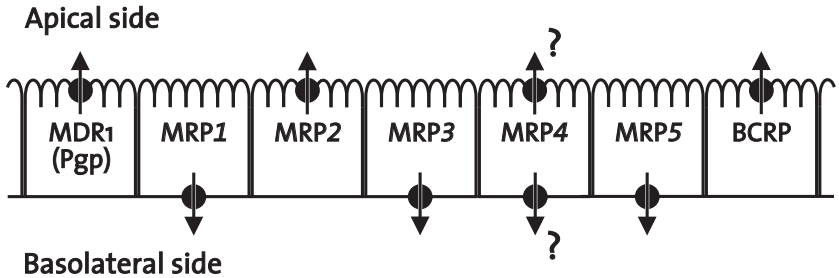

Figure 2.1 *Cellular localization of intestinal ABC transporters. P-glycoprotein (Pgp/MDR1/ABCB1), Multidrug Resistance Proteins MRP2 (ABCC2) and Breast Cancer Resistance Protein (BCRP/ABCG2/ABCP) are localized in apical membranes [4,6,8]. MRP1 (ABCC1), MRP3 (ABCC3) and MRP5 (ABCC5) are localized in basolateral membranes of enterocytes [5,9-11]. MRP4 (ABCC4) has been suggested to be located in the apical as well as in the basolateral membrane of the intestine [4,12,13].*

Table 2.1 *Relevant intestinal ABC transporters and literature describing their characteristics.*

Transporter	Tissues	Physiological substrates	References
Pgp (MDR1) (ABCB1)	Adrenal gland, blood-tissue barriers, brain, choroid plexus, epithelia, heart, intestine, kidney, liver, lung, ovary, placenta, prostate, skeletal muscle spleen, stomach.	Amphipathic drugs, neutral and positive charged hydrophobic compounds.	[4,6,43,65,125]
MRP1 (ABCC1)	Blood cerebral spinal fluid barrier, intestine, kidney, liver, lung, peripheral blood mononuclear cells, testis.	Anionic drug conjugates, leukotriene C4, GSH, oxidized GSH (GSSG), many glutathione, glucuronate and sulfate conjugated organic anions.	[4,43,52,65,125,126]
MRP2 (ABCC2)	Brain, intestine, kidney, liver, lung, placenta.	Acidic bile salts, amphipathic organic anions and xenobiotics, anionic drug-conjugates, bilirubin-glucuronides, GSSG, GSH, leukotriene C4, relative hydrophilic compounds, sulfate conjugates of endogenous and exogenous compounds.	[4,6,43,52, 65,125,126]
MRP3 (ABCC3)	Adrenal cortex, colon, intestine, kidney, liver, lung, pancreas, placenta, prostate, spleen.	Bile salts, endogenous organic anions.	[4,43,52,65]
MRP4 (ABCC4)	Adrenal gland, bladder, brain, gall bladder, kidney, liver, lung, ovary, pancreas prostate, skeletal muscle, small intestine, spleen, testis, thymus, tonsil.	cGMP, cAMP, conjugated steroids, bile acids, folic acid, folinic acid, estradiol-17-ß-glucuronide.	[4,43,52,65,127,128]
MRP5 (ABCC5)	Brain, erythrocyte, heart, intestine, kidney, liver, lung, skeletal muscle, testis.	cAMP, cGMP, folate, GSH, organic anions.	[4,43,52,65,126,127,129]
BCRP (ABCG2)	Breast, heart skeletal muscle, intestine, kidney, liver endothelium, lung, ovary, pancreas, placenta, spleen, thymus.	Amphipathic drugs, conjugated organic anions, organic anions, relative hydrophilic anticancer-agents, sulfate-, glucuronide- and gluthatione conjugates of many endogenous andexogenous compounds, weak bases.	[4,6,43,52,65,125,130-133]

Finally, MRP6 (ABCC6) seems to be located on the basolateral side[14,15] although it may only be expressed in the mucosal cells of the intestine[16]. More MRP homologues have been defined[17-19], but their function and location of expression is still uncertain.

Examples of the involvement of the transporters in the bioavailability of chemical compounds and bioactive ingredients can be found in the literature. There are several ways to study the food-drug interaction on transporters *in vitro* and these studies can use, for example, specific inhibitors of ABC transporters to show the effect on the transepithelial transport through monolayers of cultured epithelial cells (Caco-2, HCT*8*, MDCK)[20] in a two-compartment cell culture system (Figure 2.2)[21]. Such *in vitro* systems have been widely used to simulate interactions of chemical compounds with drugs or food ingredients and the effect on the human intestinal barrier function. Some other studies also provide *in vivo* data that support a role for the ABC transporters in bioavailability.

Transport by ATP dependent transporters has been well recognized as a determinant of drug absorption from the gastrointestinal tract[22,23]. Drug administration to *Pgp* knock-out mice demonstrated for example a role for Pgp in reducing the oral bioavailability of several drugs that are known substrates of Pgp, including cyclosporin, digoxin, quinidine, talinolol, vinblastine and HIV protease inhibitors[22,23]. Studies in humans indicated a role for intestinal Pgp in limiting the intestinal uptake of cyclosporine[24].

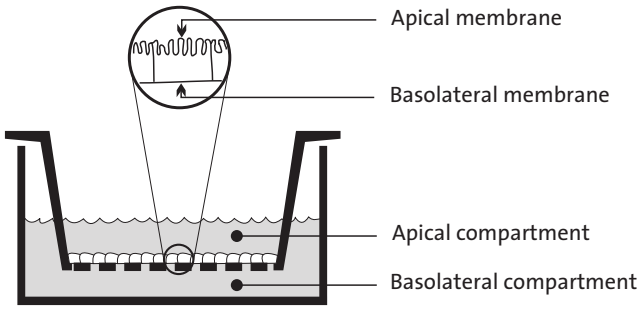

Figure 2.2 *The two-compartment cell culture system consists of a permeable cell culture filter insert that is placed in a well of a normal cell culture plate. The cells are seeded on the filter inserts and are cultured to cover the whole surface area. Caco-2 cells are known to display morphological and biochemical characteristics of human enterocytes after differentiation and form a layer of polarized intestinal cells [151]. The two compartments are designated the apical (luminal) compartment and the basolateral (serosal) compartment. Several advantages of this system include [152]: (1) that only small amounts of the compound suffice to perform a transport or effect experiment, (2) the experiments are relatively rapid and reproducible compared to other absorption models, (3) and real intestinal epithelial permeation rates can be determined (without gastrointestinal degradation, hepatic metabolism or complicating whole body kinetics).*

Furthermore, the reduced oral bioavailability of digoxin upon combination therapy with rifampicin has now been ascribed to rifampicin-mediated induction of Pgp[22,25].

Efficient transport of saquinavir, ritonavir and indinavir by *MRP2* transfected Madin-Darby Canine Kidney (MDCK)II cells, compared to MDCKII cells over-expressing other ABC transporters, indicated an important role for MRP2 in the efflux of these HIV protease inhibitors, thereby presumably limiting their oral bioavailability[26]. Merino *et al.* demonstrated a two-fold increase in the plasma concentration of the fluoroquinolone antibiotic ciprofloxacin after oral administration to Bcrp1 (the murine homologue of human BCRP) deficient *Bcrp1(-/-)* mice compared to wild-type mice, which suggests that Bcrp1 restricts the oral bioavailability of ciprofloxacin[27]. Also, the oral bioavailability of the NMDA receptor antagonist GV196771[28], and topotecan[29], seems affected by Bcrp1 and is increased in *Pgp* knockout mice by GF120918, an inhibitor of both Pgp and Bcrp1[30]. In humans co-administration with GF120918, in this case inhibiting BCRP as well as Pgp, increases the bioavailability of oral topotecan as well[31].

In addition to studies on the role of ABC transporters in the oral bioavailability of drugs more recent studies also focus on a role for the ABC transporters in determining the bioavailability of food ingredients, including toxic and bioactive compounds.

For the pro-carcinogen 2-amino-1-methyl-6-phenylimidazo-[4,5-*b*]pyridine (PhIP) it has been suggested that the apical ABC transporters MRP2, BCRP and probably Pgp reduce its oral bioavailability. The interaction of PhIP with these transport proteins was studied using various model systems such as the Caco-2 monolayers in a two-compartment system with specific inhibitors of Pgp- or MRP-associated transport proteins[32,33], MRP2 deficient rats[34], *MRP2* knockout mice[35], and *Bcrp1(-/-)* mice[36]. Following uptake in the intestine, PhIP has been demonstrated to be transported back into the lumen by apical ABC transporters, thereby providing the first line of defence against this harmful compound. In another study with Caco-2 cells it was demonstrated that an apical ABC transporter (not Pgp or MRP2) might be involved in luminal excretion of polar metabolites of the polycyclic aromatic hydrocarbon (PAH) benzo(*a*)pyrene formed by CYP1A1 or CYP1B1 inside the Caco-2 cells[37]. The authors suggest that this active transport of the intestinal benzo(*a*)pyrene metabolites may indicate a biochemical barrier function against potential mutagenic compounds through metabolism and luminally-directed transport. In subsequent studies, Ebert *et al.*[38] identified BCRP as an important transporter of benzo(*a*)pyrene conjugates metabolically formed in Caco-2 cells. Results from an *in vitro* system with Caco-2 cell monolayers and the MRP-associated transport inhibitor MK-571 suggest that MRP2 plays a role in the transport of the flavonoid genistein-7-*O*-glucoside from intestinal cells back into the intestinal

lumen, thereby limiting its bioavailability[39]. Using MRP2 deficient rats and *in situ* intestinal perfusion, as well as the specific Bcrp1 inhibitor fumitremorgin C (FTC) and MDCKII cells transfected with either human *MRP2* or murine *Bcrp1*, it was demonstrated that especially Bcrp1 and not MRP2 limits the net intestinal absorption of the flavonoid quercetin. This because of an efficient efflux of quercetin by *Bcrp1*-transfected MDCKII cells compared to control and *MRP2*-transfected cells, and of quercetin glucuronide metabolites from intestinal cells of *MRP2* deficient rats back into the intestinal lumen, which could be inhibited by FTC[40]. Using the specific Pgp inhibitor verapamil and Bcap37/MDR1 cells which are transfected with a Pgp gene construct Wang *et al.*[41] demonstrated that the flavonoids quercetin, kaempferol and isorhamnetin from *Ginkgo biloba* leaves were substrates for Pgp and that Pgp-mediated efflux of these flavonols might limit their bioavailability. A similar role for MRP2 in the bioavailability of epicatechin and possible other tea flavonoids is suggested by Vaidyanathan & Walle[42] based on studies with Caco-2 cells and the MRP-inhibitor MK-571.

Thus given the wide substrate selectivity of the intestinal ABC transporters an influence of these transporters on the bioavailability of not only a wide number of drugs, but also of many bioactive food ingredients and/or toxic compounds, can be foreseen. Although widely overlapping, the substrate specificities of Pgp, BCRP and the MRPs differ markedly (Table 2.1 on page 22). Pgp has a very broad spectrum of substrates including *e.g.* many anticancer drugs, cardiac drugs, immunosuppressants and antibiotics[4,43]. Most Pgp substrates are hydrophobic, neutral or mildly positive lipophilic compounds with a planar structure[44], whereas MRPs are able to transport lipophilic anions. MRP1 transports anionic conjugates of lipophilic compounds including glutathione (GSH), glucuronide and sulphate conjugates[45], but also some cations and neutral compounds using GSH as a co-factor[46,47]. MRP1 substrates also include lipid peroxidation products, herbicides, tobacco specific nitrosamines, mycotoxins, heavy metals, natural product and antifolate anticancer agents[48]. MRP2 and the other MRPs share similar but not identical substrate specificity with MRP1[4]. The importance of MRP4 and MRP5 as drug transporters and their role in intestinal drug disposition is unclear at present. BCRP seems to have an overlapping substrate specificity with Pgp, and like Pgp, substrates for BCRP include many anticancer agents like daunorubicine, doxorubicine, mitoxantrone and topotecan[4,29,43].

Role of the active transporters in multidrug resistance: need for non-cytotoxic inhibitors

Given the role of the various drug transporters in the cellular efflux of chemicals, including anticancer drugs, initial focus in the field of ABC transporters and ABC transport inhibitors was on multidrug resistance (MDR), rather than on intestinal uptake and oral bioavailability of drugs, food-borne toxic compounds and food ingredients. As a result, the role of the ABC efflux pumps and their inhibitors have been investigated in detail in studies on methods to overcome MDR. MDR is the resistance of a tumor cell population against drugs differing in chemical structure and cellular target, and is considered one of the major causes of failure of chemotherapy[49]. Upregulation of transport proteins involved in cellular efflux of compounds, against a concentration gradient with ATP-hydrolysis as a driving force, has shown to be of particular clinical importance in clinical multidrug resistance[50,51]. This includes resistance against anticancer drugs such as doxorubicine, etoposide, methotrexate, vincristine[48,52,53], irinotecan (CPT-11) and the unconjugated and conjugated forms of its metabolite SN-38[53], chlorambucil, cyclophosphamide, mephalan and thiotepa [54], flutamide and its metabolite hydroxyflutamide[55], and the HIV protease inhibitors ritonavir and saquinovar[56,57]. Over-expression of BCRP in cell lines confers resistance to a wide variety of anticancer drugs including daunorubicine, doxorubicine, epirubicin, mitoxantrone and topotecan[58], and the expression of BCRP has been implicated in multidrug resistance of acute myeloid leukemia and some solid tumors[58-60].
Because of the role of these transporters in multidrug resistance, one strategy to overcome transporter mediated drug resistance relies on the identification of transport inhibitors. Numerous compounds that inhibit Pgp, MRPs or BCRP transport activity have been described[61-63]. Different mechanisms by which these inhibitors might interact with the transporter proteins have been suggested and include an effect on drug binding, ATP binding, ATP hydrolysis, drug transport, and ADP release[64]. However, many of the inhibitors appeared to be relatively non-specific and exerted unwanted drug-drug interactions or interference with other physiological systems reducing their potential use in clinical settings[65,66]. This stimulated the quest for relatively non-cytotoxic inhibitors and the interest in flavonoids as relatively non-cytotoxic inhibitors of ABC transporters[67-69].

Flavonoids as inhibitors of transporter proteins

Flavonoids (Figure 2.3) consist of a large group of polyphenolic antioxidants found in fruits, vegetables and plant-derived beverages such as tea and red wine[70], as well as in dietary supplements. In foods, flavonoids are often present as ß-glycosides of

aglycones and methoxylated forms. Upon ingestion, flavonoid glycosides are deglycosylated and the aglycones are metabolized into glucuronide-, sulfate- and methylated conjugates[71-75]. Flavonoids and flavonoid-rich extracts have been implicated as beneficial agents in a multitude of disease states[76-78], including cancer[79-81], cardiovascular disease[82-84], neurodegenerative disorders[85-87] and osteoporosis[88].

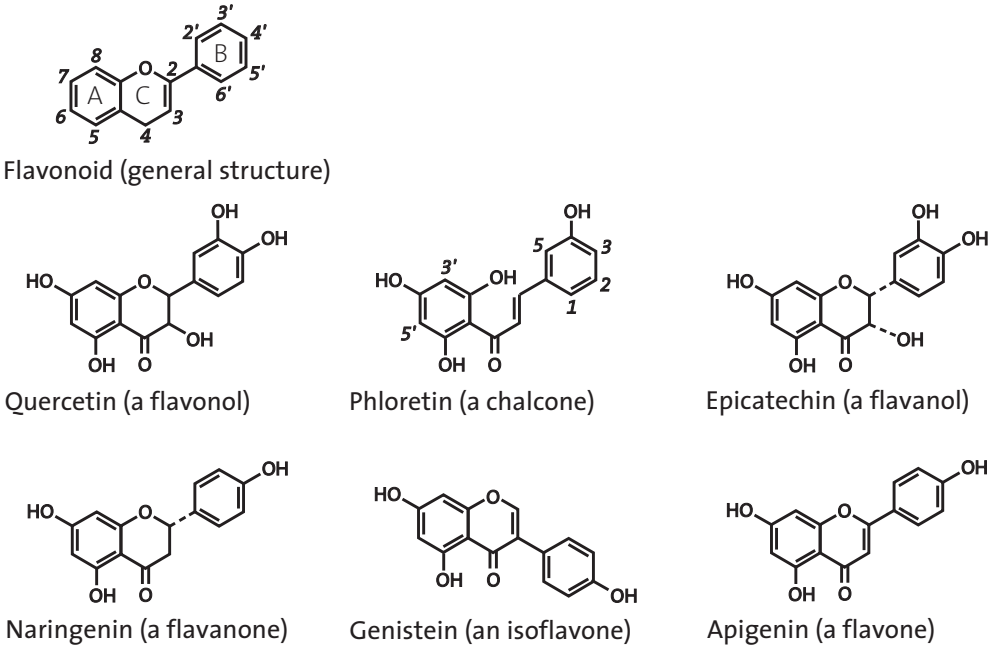

Figure 2.3 *Structural formula of examples of dietary flavonoid derivates representing the major classes of flavonoids (chalcones, flavanols, flavanones, flavones, flavonols and isoflavones) which are, apart from chalcones which have a different orientation and numbering, based on the different substitution and the oxidation status of ring C.*

Table 2.2 *Overview of selected literature on inhibition of ABC transporters present in the intestine by dietary flavonoids.*

Transporter	Flavonoid inhibitor	References
Pgp (MDR1)	biochanin A, EGCG, epigallocatechin, epicatechin-gallate, hesperetin, isoquercitrin, kaempferol, morin, naringenin, phloretin, quercetin.	[106,112,134-139]
MRP1	apigenin, baicalein, biochanin A, chalcone, galangin, genistein, hesperetin, kaempferol, luteolin, morin, myricetin, naringenin, phloretin, quercetin, robinetin.	[68,94,95,140-142]
MRP2	myricetin, quercetin-4'-*O*-glucoside, robinetin.	[94,95,138]
MRP3	-	
MRP4	daidzin, hesperetin, naringenin, quercetin, resveratrol.	[142]
MRP5	daidzin, hesperetin, naringenin, quercetin.	[142]
BCRP	acacetin, apigenin, biochanin A, chalcone, chrysin, daidzein, diosmetin, fisetin, flavone, galangin, genistein, hesperetin, kaempferide, kaempferol, luteolin, luteolin-4'-*O*-glucoside, 7-methoxyflavanone, naringenin, naringenin-7-*O*-glucoside, phloretin, quercetin, theaflavine, theaflavine-3-*O*-gallate.	[90-92,111,143-145]

Table 2.2 presents an overview of dietary flavonoids known to inhibit the activity of the various ABC transporter proteins. It has become clear that flavonoids or their metabolites are important modulators or substrates of intestinal membrane bound transport proteins including PgP, MRPs and BCRP (Figure 2.4). Their properties to modulate ABC transport proteins and multidrug resistance make them interesting therapeutic candidates[89].

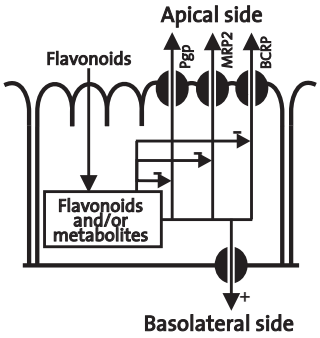

Figure 2.4 *Schematic presentation of the role of flavonoids, or their metabolites formed within intestinal cells, as substrates or inhibitors of apical intestinal ABC transport proteins (Pgp, MRP2 and BCRP).*

Effect of flavonoids as ABC transporter inhibitors on MDR, intracellular accumulation and bioavailability of bioactive chemicals

Given the involvement of the transport proteins in the efficiency of intestinal transport, it can be envisaged that the ABC transport inhibitors may not only affect multidrug resistance of tumor cells, but may also affect the bioavailability of a variety of drugs, bioactive food ingredients and/or toxic compounds upon oral uptake.

Some examples of such a role for flavonoids as ABC transport inhibitors affecting the bioavailability of drugs, toxic compounds or beneficial food ingredients can be found in recent literature. These include *in vitro* studies on the effect of flavonoids on intracellular accumulation of substrates for ABC transporters using for example BCRP over-expressing MCF-7 MX100 cells[90-92], and *MRP1*- or *MRP2*-transfected MDCKII cells[93-95]. Table 2.3 on page 32 presents an overview of studies reporting an effect of dietary flavonoids on intracellular accumulation and/or bioavailability of drugs, or food-borne toxins and bioactive ingredients. Some of the studies are discussed in more detail hereafter. For instance, the ethyl acetate extract of Seville orange juice containing the Pgp-inhibiting methoxyflavones tangeretin, heptamethoxyflavone and nobiletin, was shown to increase the uptake of vinblastine in Caco-2 cells and other cell types[96,97]. Also, the addition of epigallocatechin-gallate was shown to increase the accumulation of vinblastine in Caco-2 cells and potentiated the cytotoxicity of vinblastine in CH^RC5 cells, effects similar as observed for the Pgp inhibitor valspodar[98]. Co-treatment of MRP1 over-expressing MDCKII cells, and HT-29 human colon adenocarcinoma cells with isoflavones, increased epigallocatechin-3-gallate accumulation significantly, an effect also achieved by co-incubation of MRP1 over-expressing MDCKII cells with the MRP inhibitors indomethacin or probenecid[92]. These results suggest that MRP efflux pumps may limit the bioavailability of the tea polyphenol epigallocatechin-3-gallate, whereas isoflavonoid inhibitors of the apical MRPs may, as a consequence, increase its bioavailability. In addition, in *MRP1*- and *MRP2*-transfected MDCKII cells, it was shown that myricetin can inhibit cellular vincristine efflux by MRP1 and MRP2 thereby sensitizing the cells towards vincristine[94]. Further it has been shown that, quercetin and 3',4',7-trimethoxyquercetin, but not rutin, the naturally occuring 3-rhamosylglucoside of quercetin, were able to potentiate the effects of adriamycin on a multidrug resistant MCF-7 human breast cancer cell line, in which the MDR was associated to high levels of Pgp[99]. Using a sensitive and multidrug resistant human breast cancer MCF-7 cell line, it was demonstrated that biochanin A, genistein, morin quercetin, phloretin, chalcone, chrysin and silymarin significantly

increased the accumulation of daunomycin in the MDR resistant cells[100]. Di Pietro *et al.*[64] demonstrated the effect of various flavonoids on the intracellular accumulation of daunomycin in Pgp over-expressing K562/R7 cells, concluding that prenylation of the flavonoids increases both their affinity for Pgp and their effect on the duanomycin accumulation. Genistein inhibited Pgp-mediated transport thereby increasing the intracellular accumulation of rhodamine 123 and daunorubicin in Pgp expressing multidrug resistant BC19/3 cells, which are MCF-7 cells transfected with human *MDR1* [101].

In addition to these studies showing the effect of flavonoids on intracellular accumulation of chemicals, several other studies have investigated the effect of flavonoids on the intestinal transport of compounds using Caco-2 cells in transwell dishes as an *in vitro* model for the human intestinal barrier (Table 2.3 on page 32). Last, but not least, studies have shown this effect of flavonoids in *in vivo* models including rats and healthy volunteers. For instance, in Caco-2 cell monolayers, naringin was reported to increase the apical to basolateral transport of the HIV protease inhibitor saquinavir by inhibition of the Pgp mediated apical saquinavir efflux[102]. Furthermore, a significant increase in apical to basolateral transport as well as cellular accumulation, of ochratoxin A, a food-borne mycotoxin, in Caco-2 cells, was observed upon co-incubation with chrysin, quercetin, genistein, biochanin A or resveratrol, all at concentrations that can be expected in the gastrointestinal tract[103]. The authors hypothesise that the polyphenols may exert their effect though competitive inhibition of the MRP efflux pump involved, previously proposed to be MRP2[104].

Schutte *et al.*[32] demonstrated that addition of the flavonoid myricetin to Caco-2 cell monolayers exposed to the food-borne pro-carcinogen 2-amino-1-methyl-6-phenyl-imidazo[4,5-*b*]pyridine (PhIP) resulted in an increase in the transport of PhIP from the apical to the basolateral compartment. This effect was observed at physiologically relevant concentrations of PhIP and myricetin. The results indicate that myricetin inhibits the ABC transporter-mediated excretion of PhIP from the intestinal cells back to the apical luminal side, resulting in increased possibilities for transport to the basolateral side and a possibly increased bioavailability of the pro-carcinogen PhIP. In subsequent studies it was demonstrated that other flavonoids exert a similar effect on the transport of PhIP through Caco-2 monolayers[105] indicating a possible adverse effect of these supposed beneficial food ingredients. As an example, Figure 2.5 on page 31 depicts an increase in the apical to basolateral transport of PhIP in the presence of quercetin compared to the apical to basolateral transport of PhIP in the absence of quercetin through Caco-2 monolayers (Schutte *et al.*, unpublished results). In a study with Caco-2 cells, the apical to basolateral transport of digoxin was significantly increased, whereas the basolateral to apical transport was significantly decreased by biochanin A or

silymarin due to inhibition of the Pgp-mediated transport of digoxin by these flavonoids[106]. This suggests that these flavonoids could increase the absorption and bioavailability of co-administered drugs that are Pgp substrates. Furthermore, botanical ingredients other than flavonoids may result in altered absorption and bioavailability of drugs that are ABC transporter substrates because of their interaction with the ABC transport protein[107,108].

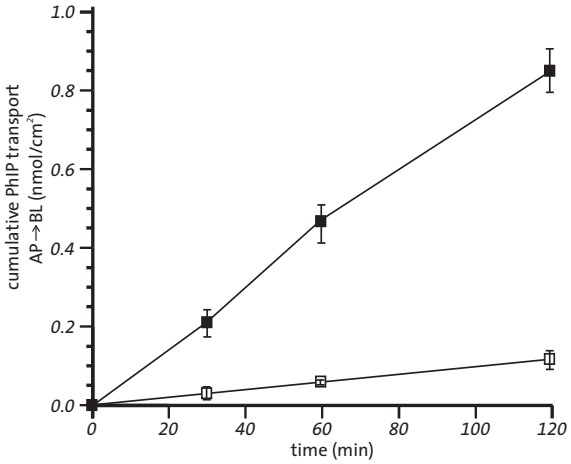

Figure 2.5 *PhIP transport through Caco-2 monolayers from the apical (AP) to the basolateral (BL) compartment. Caco-2 monolayers were exposed to 5 µM PhIP in the apical compartment in the absence (□) or presence (■) of 20 µM quercetin in both compartments, all in the presence of 1mM ascorbic acid (unpublished results, Schutte et al.. For experimental details see Schutte et al., 2006 [32]).*

It is also important to emphasise that the various effects observed in cells *in vitro* need *in vivo* validation. Only a few studies actually demonstrate a role for flavonoids as ABC transporter inhibitors or substrates leading to modulation of the *in vivo* bioavailability of other bioactive ingredients (Table 2.3 on page 32). Zhang *et al.*[90], for example, used Sprague-Dawley (SD) rats and *mdr1a/1b(-/-)* mice to investigate the bioavailability of topotecan in the presence and absence of the flavonoids chrysin or 7,8-benzoflavone. Neither chrysin nor 7,8-benzoflavone altered topotecan bioavailability in rats or in *mdr1a/1b(-/-)* mice after oral co-administration. The authors indicate that this might be due to the fact that the two flavonoids are only weak inhibitors of mouse or rat Bcrp1-mediated topotecan transport. This suggestion was based on the observation that chrysin and 7,8-benzoflavone inhibited the human BCRP mediated transport of topotecan in human BCRP over-expressing MCF-7 MX100 cells to a level comparable to that observed for the potent BCRP inhibitor FTC, but not in MDCK/Bcrp-1 cells over-expressing mouse Bcrp-1[90].

Table 2.3 *Overview of the literature on the effect of dietary flavonoids on cellular accumulation, transport or bioavailability of drugs and other xenobiotics in different model systems.*

Flavonoids	Model system Cell models	Compounds of which cellular accumulation, transport or bioavailability is increased	References
genistein	BC19/3, MCF-7, MCF-7 VP, BALB/c-3T3, BALB/c-3T3-1000	daunorubicin, rhodamine-123	[101]
biochanin A	Caco-2	digoxin, vinblastine	[106]
heptamethoxy-flavone, nobiletin, tangeretin	Caco-2	vinblastine	[146]
catechin-gallate, EGCG, epicatechin-gallate	Caco-2, CH^RC5	rhodamine-123, vinblastine	[98]
genistein	GLC4, GLC4 ADR	daunorubicin	[147]
quercetin, theaflavine, theaflavine-3-*O*-gallate	HEK-293/R482-ABCG2	SN-38	[145]
apigenin, galengin, genistein, naringenin	HEK-293/R482-ABCG2, HEK-293/T482-ABCG2, MDA-MB-231, MDA-MB-231/T482-ABCG2	mitoxantrone, rhodamine-6G	[143]
kaempferol, naringin	HK-2	calcium-AM, cyclosporine A, vinblastine	[112]
acacetin, apigenin, chrysin, diosmetin, genistein, kaempferide, kaempferol, luteolin, luteolin-4'-*O*-glucoside, naringenin, naringenin-7-glucoside	K562, K562/BCRP	mitoxantrone, SN-38, topotecan	[111]
heptamethoxy-flavone, nobiletin, tangeretin	K562, K562 ADM	vinblastine	[96]
baicalein, epicatechin-gallate, epigallocatechin, epigallocatechin-gallate, fisetin, kaempferol, morin, myricetin, quercetin	KB-3-1, KB-C2	daunorubicin, rhodamine-123	[135,136]
daidzein, genistein, kaempferol, quercetin	KB-3-1, KB-V1	paclitaxel, rhodamine-123, vinblastine	[148]
quercetin	MCF-7, MCF-7 ADM	doxorubicin	[99]
biochanin A, morin, naringenin, quercetin	MCF-7, MCF-7 ADR	daunomycin	[134]
biochanin A, chalcone, chrysin, genistein, morin, phloretin, quercetin	MCF-7, MCF-7 ADR	daunomycin	[100]
chrysin	MCF-7, MCF-7 MX100	topotecan	[90]
apigenin, biochanin A, chrysin, genistein, hesperetin, kaempferol, naringenin	MCF-7, MCF-7 MX100	mitoxantrone	[92]
biochanin A, morin, phloretin	MCF-7, MCF-7 ADR, MDA435/LCC6, MDA435/LCC6MDR	daunomycin, doxorubicin	[139]

apigenin, biochanin A, chrysin, fisetin, genistein, hesperetin, kaempferol, luteolin, naringenin, phloretin, quercetin	MCF-7, MCF-7 MX100, NCI-H460, NCI-H460 MX20	mitoxantrone	[91]
biochanin A, daidzein, formononetin, genistein	HT-29, MDCKII/Pgp, MDCKII/MRP1, MDCKII/MRP2,	EGCG	[93]
myricetin	MDCKII, MDCKII/MRP1, MDCKII/MRP2	vincristine	[95]
biochanin A, chalcone, chrysin, epigallocatechin, genistein, kaempferol, morin, phloretin, quercetin	Panc-1	daunomycin, vinblastine	[141]
galangin, kaempferol, quercetin	rat hepatocytes	rhodamine-123	[149]
	Transport models		
biochanin A	Caco-2, AP to BL	digoxin, vinblastine	[106]
biochanin A, chrysin, genistein, quercetin, resveratrol	Caco-2, AP to BL	ochratoxin A	[103]
myricetin	Caco-2, AP to BL	PhIP	[32]
6',7'-dihydroxy-bergamottin, naringin	Caco-2, AP to BL	saquinavir	[102]
hesperetin, quercetin, kaempferol, naringin	Caco-2, AP to BL	talinolol	[137]
epigallocatechin-gallate	Caco-2, AP to BL	vinblastine	[98]
naringenin, naringin	Caco-2, AP to BL	vinblastine	[146]
epicatechin-gallate, epigallocatechin-gallate, genistein, genistin, naringenin, quercetin, xanthohumol	Caco-2, MDCKII, MDCKII/Pgp, AP to BL	cycolosporin A, digoxin	[150]
quercetin	rat everted gut sac	etoposide	[123]
flavonoid containing grapefruit juice and orange juice	rat everted gut sac	fexofenadine, rhodamine-123, saquinavir	[117]
	In vivo models		
morin, naringin	male SD-rats	diltiazem	[113,114]
flavone, quercetin	male SD-rats	paclitaxel	[109,110]
flavonoid containing grapefruit juice	male SD-rats	talinolol	[118,119]
flavonoid containing grapefruit juice	healthy volunteers	cyclosporine	[115]
flavonoid containing grapefruit juice and orange juice	healthy volunteers	dextromethorphan	[120]

In the same study, co-administration of topotecan with GF120918, a potent BCRP and Pgp inhibitor[30], to the SD rats or *mdr1a/1b(-/-)* mice appeared to significantly increase the bioavailability of topotecan by more than 4-fold, indicating the possibility to increase oral bioavailability *in vivo* by inhibitors of ABC transport proteins. Choi *et al.*[109] showed that the pre-treatment with quercetin in male SD rats significantly increased the bioavailability of paclitaxel or its water soluble prodrug. Furthermore, co-administration with flavone resulted in a significant increase of the bioavailability of this drug and the authors suggest that this might be caused by the inhibition of Pgp or CYP3A[110].
Another example of validation of *in vitro* data by *in vivo* studies can be found in the results reported for the effects of flavonoids from fruit juices on the bioavailability of chemicals. The effects of morin, grapefruit juice and/or naringin on the pharmacokinetics of several drugs *in vitro*, resulting in, for example, increased cellular accumulation of topotecan and increased cellular toxicity of vinblastine in cultured cells[111,112], have also been observed in *in vivo* models resulting in increased bioavailability upon oral administration of diltiazem in rats[113,114], or of cyclosporine in man[115]. These effects have been ascribed to inhibition of Pgp-mediated transport, in addition to inhibition of the CYP3A4 drug oxidation[97,115,116].
Flavonoid containing ethyl acetate extracts of grapefruit and orange juice were also able to inhibit the Pgp-mediated efflux of saquinavir, rhodamine-123 and fexofenadine from everted sacs of rat intestine[117].
Grapefruit juice was able to enhance the intestinal absorption of the Pgp substrate talinolol both *in vitro* in the Caco-2 cell transport model, and also *in vivo* in rats[118,119]. Also, grapefruit juice and Seville orange juice increased the bioavailability of dextromethorphan in healthy volunteers via inhibition of Pgp and CYP3A[120]. In contrast, in another study, grapefruit juice consumption showed no significant effect on the pharmacokinetics of digoxin in 12 healthy subjects[121], or even enhanced the Pgp mediated efflux of cyclosporine, digoxin, fexofenadine and losartan across MDCK/MDR1 cell monolayers[122].
In an everted gut sac model, quercetin was able to stimulate the absorption of etoposide[123]. However, when rats were fed a flavonoid containing “natural” rodent diet there was no effect on the absorption of etoposide as compared to the rats fed the synthetic flavonoid-free diet[123]. These examples clearly illustrate the importance of *in vivo* validation of *in vitro* data on the effect of ABC transporter inhibitors on bioavailability. This validation is also important because of possible consequences of the extensive *in vivo* phase II metabolism of the flavonoids for their ultimate activity as ABC transporter inhibitors and/or substrates.

Physiological relevance of flavonoid interactions

All together it can be concluded that flavonoid-mediated inhibition of ABC transporters may affect the bioavailability of drugs, bioactive food ingredients and/or food-borne toxic compounds upon oral intake. Flavonoids, which are an important class of bioactive food ingredients, are expected to result in these interactions at physiologically relevant levels of intake. The relevance of this finding is further supported if one takes into consideration the actual (permitted) use level in food products and currently marketed food supplements. It can be calculated that intestinal levels that might be reached upon intake of a supplement capsule containing 100 to 200 mg flavonoids, may amount to about 35 to 70 μM. Thus, reported K_i values of *e.g.* 2.4 to 20.8 μM for the competitive inhibition of MRP1 activity mediated by different dietary flavonoids, using LTC_4 as substrate[68], or similar K_i values for the flavonoid-mediated inhibition of the efflux of calcein-acetoxymethyl ester (calcein-AM) by MRP1 or MRP2[95] are within a physiologically relevant range. This indicates that flavonoid intake might be an important factor in the regulation of the uptake of compounds, including drugs but also pro-carcinogens and bioactive beneficial food ingredients.

Conclusions

Inhibition of ABC transporters has originally been studied within the framework of multidrug resistance. Many of the inhibitors appeared to exert unwanted side effects, and this stimulated the interest in flavonoids as relatively non-cytotoxic inhibitors of ABC transporters. It has become clear that flavonoids are important modulators or substrates of intestinal transport proteins including Pgp, MRPs and BCRP.

Flavonoids are a ubiquitous component in the human diet with an intake level of about two thirds of the total intake of polyphenols, which has been estimated to be about 1g/day[124], The precise amount and composition are largely dependent on specific food contents, dietary habits and the possible use of flavonoids as dietary supplements. Because of their ubiquity it can be concluded that flavonoid mediated inhibition of ABC transporters may affect the bioavailability of a variety of drugs, bioactive food ingredients and/or toxins upon oral uptake. Since this reflects an increased bioavailability it will depend on the transported compound of interest as to whether this effect of flavonoids can be considered beneficial or adverse. For the effect on bioavailability of the pro-carcinogen PhIP, benzo(*a*)pyrene or the mycotoxin ochratoxin A it would imply an adverse side effect of supposed beneficial food ingredients. On the other hand, flavonoid mediated inhibition of ABC transporters might be a simple and safe approach of increasing the oral

bioavailability of beneficial food ingredients and/or drugs that are substrates of these ABC transporters. It is clear that these interactions at the level of the transport proteins may be an important mechanism for unexpected food-drug, food-toxin or food-food interactions in the field of risk and safety assessment. Future studies should focus especially on (1) *in vivo* validation of the flavonoid-mediated effects on bioavailability of drugs, toxins and beneficial bioactive food ingredients detected in *in vitro* models, and on (2) the role of flavonoid phase II metabolism in modulating the activity of the flavonoids to act as ABC transporter inhibitors and/or substrates.

References

1 Day AJ, Gee JM, DuPont MS, Johnson IT, Williamson G. Absorption of quercetin-3-glucoside and quercetin-4'-glucoside in the rat small intestine: the role of lactase phlorizin hydrolase and the sodium-dependent glucose transporter. *Biochem Pharmacol* 65(7): 1199-1206, 2003.

2 Hollman PCH, De Vries JHM, Van Leeuwen SD, Mengelers MJB, Katan MB.Absorption of dietary quercetin glycosides and quercetin in healthy ileostomy volunteers. *Am J Clin Nutr* 62(6): 1276-1282, 1995.

3 Wolffram S, Blöck M, Ader P. Quercetin-3-glucoside is transported by the glucose carrier SGLT1 across the brush border membrane of rat small intestine. *J Nutr* 132(4): 630-635, 2002.

4 Chan LMS, Lowes S, Hirst BH. The ABCs of drug transport in intestine and liver: efflux proteins limiting drug absorption and bioavailability. *Eur J Pharm Sci* 21(1): 25-51, 2004.

5 Taipalensuu J, Törnblom H, Lindberg G, Einarsson C, Sjöqvist F, Melhus H, Garberg P, Sjöström B, Lundgren B, Artursson P. Correlation of gene expression of ten drug efflux proteins of the ATP-binding cassette transporter family in normal human jejunum and in human intestinal epithelial Caco-2 cell monolayers. *J Pharmacol Exp Ther* 299(1): 164-170, 2001.

6 Takano M, Yumoto R, Murakami T. Expression and function of efflux drug transporters in the intestine. *Pharmacol Ther* 109(1-2): 137-161, 2006.

7 Zimmermann C, Gutmann H, Hruz P, Gutzwiller J-P, Beglinger C, Drewe J. Mapping of multidrug resistance gene 1 and multidrug resistance-associated protein isoform 1 to 5 mRNA expression along the human intestinal tract. *Drug Metab Dispos* 33(2): 219-224, 2005.

8 Dietrich CG, Geier A, Oude Elferink RPJ. ABC of oral bioavailability: transporters as gatekeepers in the gut. *Gut* 52(12): 1788-1795, 2003.

9 Hirohashi T, Suzuki H, Chu X-Y, Tamai I, Tsuji A, Sugiyama Y. Function and expression of multidrug resistance-associated protein family in human colon adenocarcinoma cells (Caco-2). *J Pharmacol Exp Ther* 292(1): 265-270, 2000.

10 Prime-Chapman HM, Fearn RA, Cooper AE, Moore V, Hirst BH. Differential multidrug resistance-associated protein 1 through 6 isoform expression and function in human intestinal epithelial Caco-2 cells. *J Pharmacol Exp Ther* 311(2): 476-484, 2004.

11 Scheffer GL, Kool M, de Haas M, de Vree JML, Pijnenborg ACLM, Bosman DK, Oude Elferink RPJ, van der Valk P, Borst P, Scheper RJ. Tissue distribution and induction of human multidrug resistant protein 3. *Lab Invest* 82(2): 193-201, 2002.

12 Lee K, Klein-Szanto AJ, Kruh GD. Analysis of the MRP4 drug resistance profile in transfected NIH3T3 cells. *J Natl Cancer Inst* 92(23): 1934-1940, 2000.

13 Van Aubel RA, Smeets PH, Peters JG, Bindels RJ, Russel FG. The MRP4/ABCC4 gene encodes a novel apical organic anion transporter in human kidney proximal tubules: putative efflux pump for urinary cAMP and cGMP. *J Am Soc Nephrol* 13(3): 595-603, 2002.

14 Kool M, Van der Linden M, De Haas M, Baas F, Borst P. Expression of human MRP6, a homologue of the multidrug resistance protein gene MRP1, in tissues and cancer cells. *Cancer Res* 59(1): 175-182, 1999.

15 Madon J, Hagenbuch B, Landmann L, Meier PJ, Stieger B. Transport function and hepatocellular localization of mrp6 in rat liver. *Mol Pharmacol* 57(3): 634-641, 2000.

16 Beck K, Hayashi K, Dang K, Hayashi M, Boyd CD. Analysis of ABCC6 (MRP6) in normal human tissues. *Histochem Cell Biol* 123(4-5): 517-528, 2005.

17 Bera TK, Iavarone C, Kumar V, Lee S, Lee B, Pastan I. MRP9, an unusual truncated member of the ABC transporter superfamily, is highly expressed in breast cancer. *Proc Natl Acad Sci U S A* 99(10): 6997-7002, 2002.

18 Bortfeld M, Rius M, Konig J, Herold-Mende C, Nies AT, Keppler D. Human multidrug resistance protein 8 (MRP8/ABCC11), an apical efflux pump for steroid sulfates, is an axonal protein of the CNS and peripheral nervous system. *Neuroscience* 137(4): 1247-1257, 2006.

19 Chen Z-S, Hopper-Borge E, Belinsky MG, Shchaveleva I, Kotova E, Kruh GD. Characterization of the transport properties of human multidrug resistance protein 7 (MRP7, ABCC10). *Mol Pharmacol* 63(2): 351-358, 2003.

20 Feron VJ, Groten JP, Hermus RJJ, Jonker D, Meijerman I, Mulder GJ, Salmon F, Schoen ED. Designing experiments for food-drug synergy: Safety aspects. In: Thompson LU, Ward WE, editors. Food-drug synergy and safety. Boca Raton: CRC Press, 2006. pp. 431-460.

21 Artursson P, Karlsson J. Correlation between oral drug absorption in humans and apparent drug permeability coefficients in human intestinal epithelial (Caco-2) cells. *Biochem Biophys Res Commun* 175(3): 880-885, 1991.

22 Fromm MF. P-glycoprotein: a defense mechanism limiting oral bioavailability and CNS accumulation of drugs. *Int J Clin Pharmacol Ther* 38(2): 69-74, 2000.

23 Spahn-Langguth H, Baktir G, Radschuweit A, Okyar A, Terhaag B, Ader P, Hanafy A, Langguth P. P-glycoprotein transporters and the gastrointestinal tract: evaluation of the potential in vivo relevance of in vitro data employing talinolol as model compound. *Int J Clin Pharmacol Ther* 36(1): 16-24, 1998.

24 Lown KS, Mayo RR, Leichtman AB, Hsiao H-L, Turgeon DK, Schmiedlin-Ren P, Brown MB, Guo W, Rossi SJ, Benet LZ, Watkins PB. Role of intestinal P-glycoprotein (mdr1) in interpatient variation in the oral bioavailability of cyclosporine. *Clin Pharmacol Ther* 62(3): 248-260, 1997.

25 Greiner B, Eichelbaum M, Fritz P, Kreichgauer H-P, Von Richter O, Zundler J, Kroemer HK. The role of intestinal P-glycoprotein in the interaction of digoxin and rifampin. *J Clin Invest* 104(2): 147-153, 1999.

26 Huisman MT, Smit JW, Crommentuyn KML, Zelcer N, Wiltshire HR, Beijnen JH, Schinkel AH. Multidrug resistance protein 2 (MRP2) transports HIV protease inhibitors, and transport can be enhanced by other drugs. *AIDS* 16(17): 2295-2301, 2002.

27 Merino G, ¡lvarez AI, Pulido MM, Molina AJ, Schinkel AH, Prieto JG. Breast cancer resistance protein (BCRP/ABCG2) transports fluoroquinolone antibiotics and affects their oral availability, pharmacokinetics, and milk secretion. *Drug Metab Dispos* 34(4): 690-695, 2006.

28 Polli JW, Baughman TM, Humphreys JE, Jordan KH, Mote AL, Webster LO, Barnaby RJ, Vitulli G, Bertolotti L, Read KD, Serabjit-Singh CJ. The systemic exposure of an N-methyl-$_D$-aspartate receptor antagonist is limited in mice by the P-glycoprotein and breast cancer resistance protein efflux transporters. *Drug Metab Dispos* 32(7): 722-726, 2004.

29 Jonker JW, Smit JW, Brinkhuis RF, Maliepaard M, Beijnen JH, Schellens JHM, Schinkel AH. Role of breast cancer resistance protein in the bioavailability and foetal penetration of topotecan. *J Natl Cancer Inst* 92(20): 1651-1656, 2000.

30 Allen JD, Brinkhuis RF, Wijnholds J, Schinkel AH. The mouse Bcrp1/Mxr/Abcp gene: amplification and overexpression in cell lines selected for resistance to topotecan, mitoxantrone, or doxorubicin. *Cancer Res* 59(17): 4237-4241, 1999.

31 Kruijtzer CMF, Beijnen JH, Rosing H, Ten Bokkel Huinink WW, Schot M, Jewell RC, Paul EM, Schellens JHM. Increased oral bioavailability of topotecan in combination with the breast cancer resistance protein and P-glycoprotein inhibitor GF120918. *J Clin Oncol* 20(13): 2943-2950, 2002.

32 Schutte ME, Van de Sandt JJM, Alink GM, Groten J, P., Rietjens IMCM. Myricetin stimulates the absorption of the pro-carcinogen PhIP. *Cancer Lett* 231(1): 36-42, 2006.

33 Walle UK, Walle T. Transport of the cooked-food mutagen 2-amino-1-methyl-6-phenylimidazo-[4,5-b]pyridine (PhIP) across the human intestinal Caco-2 cell monolayer: role of efflux pumps. *Carcinogenesis* 20(11): 2153-2157, 1999.

34 Dietrich CG, De Waart DR, Ottenhoff R, Schoots IG, Oude Elferink RPJ. Increased bioavailability of the food-derived carcinogen 2-amino-1-methyl-6-phenylimidazo[4,5-b]pyridine in MRP2-deficient rats. *Mol Pharmacol* 59(5): 974-980, 2001.

35 Vlaming MLH, Mohrmann K, Wagenaar E, De Waart DR, Oude Elferink RPJ, Lagas JS, Van Tellingen O, Vainchtein LD, Rosing H, Beijnen JH, Schellens JHM, Schinkel AH. Carcinogen and anti-cancer drug transport by Mrp2 in vivo: studies using Mrp2 (Abcc2)knockout mice. *J Pharmacol Exp Ther* 318(1): 319-327, 2006.

36 Van Herwaarden AE, Jonker JW, Wagenaar E, Brinkhuis RF, Schellens JHM, Beijnen JH, Schinkel AH. The breast cancer resistance protein (Bcrp1/Abcg2) restricts exposure to the dietary carcinogen

2-amino-1-methyl-6-phenylimidazo[4,5-b]pyridine. *Cancer Res* 63(19): 6447-6452, 2003.
37 Buesen R, Mock M, Nau H, Seidel A, Jacob J, Lampen A. Human intestinal Caco-2 cells display active transport of benzo[a]pyrene metabolites. *Chem Biol Interact* 142(3): 201-221, 2003.
38 Ebert B, Seidel A, Lampen A. Identification of BCRP as transporter of benzo[a]pyrene conjugates metabolically formed in Caco-2 cells and its induction by Ah-receptor agonists. *Carcinogenesis* 26(10): 1754-1763, 2005.
39 Walle UK, French KL, Walgren RA, Walle T. Transport of genistein-7-glucoside by human intestinal CACO-2 cells: potential role for MRP2. *Res Commun Mol Pathol Pharmacol* 103(1): 45-56, 1999.
40 Sesink ALA, Arts ICW, De Boer VCJ, Breedveld P, Schellens JHM, Hollman PCH, Russel FGM. Breast cancer resistance protein (Bcrp1/Abcg2) limits net intestinal uptake of quercetin in rats by facilitating apical efflux of glucuronides. *Mol Pharmacol* 67(6): 1999-2006, 2005.
41 Wang Y, Cao J, Zeng SJ. Involvement of P-glycoprotein in regulating cellular levels of Ginkgo flavonols: quercetin, kaempferol, and isorhamnetin. *J Pharm Pharmacol* 57(6): 751-758, 2005.
42 Vaidyanathan JB, Walle T. Transport and metabolism of the tea flavonoid (-)-epicatechin by the human intestinal cell line Caco-2. *Pharm Res* 18(10): 1420-1425, 2001.
43 Kuppens IELM, Breedveld P, Beijnen JH, Schellens JHM. Modulation of oral drug bioavailability: from preclinical mechanism to therapeutic application. *Cancer Invest* 23(5): 443-464, 2005.
44 Gottesmann MM, Pastan I. Biochemistry of multidrug resistance mediated by the multidrug transporter. *Annu Rev Biochem* 62: 385-427, 1993.
45 König J, Nies AT, Cui Y, Leier I, Keppler D. Conjugate export pumps of the multidrug resistance protein (MRP) family: localization, substrate specificity, and MRP2-mediated drug resistance. *Biochim Biophys Acta* 1461(2): 377-394, 1999.
46 Evers R, De Haas M, Sparidans R, Beijnen J, Wielinga PR, Lankelma J, Borst P. Vinblastine and sulfinpyrazone export by the multidrug resistance protein MRP2 is associated with glutathione export. *Br J Cancer* 83(3): 375-383, 2000.
47 Grant CE, Valdimarsson G, Hipfner DR, Almquist KC, Cole SP, Deeley RG. Overexpression of multidrug resistance-associated protein (MRP) increases resistance to natural product drugs. *Cancer Res* 54(2): 357-361, 1994.
48 Leslie EM, Deeley RG, Cole SPC. Toxicological relevance of the multidrug resistance protein 1, MRP1 (ABCC1) and related transporters. *Toxicology* 167(1): 3-23, 2001.
49 Fojo T, Bates S. Strategies for reversing drug resistance. *Oncogene* 22(47): 7512-7523, 2003.
50 Juliano RL, Ling V. A surface glycoprotein modulating drug permeability in Chinese hamster ovary cell mutants. *Biochim Biophys Acta* 455(1): 152-162, 1976.
51 Leonard GD, Fojo T, Bates SE. The role of ABC transporters in clinical practice. *Oncologist* 8(5): 411-424, 2003.
52 Haimeur A, Conseil G, Deeley RG, Cole SPC. The MRP-related and BCRP/ABCG2 multidrug resistance proteins: biology, substrate specificity and regulation. *Curr Drug Metab* 5(1): 21-53, 2004.
53 Sparreboom A, Danesi R, Ando Y, Chan J, Figg WD. Pharmacogenomics of ABC transporters and its role in cancer chemotherapy. *Drug Resist Updat* 6(2): 71-84, 2003.
54 Cnubben NHP, Rommens AJM, Oudshoorn MJ, Van Bladeren PJ. Glutathione-dependent biotransformation of the alkylating drug thiotepa and transport of its metabolite monoglutathionylthiotepa in human MCF-7 breast cancer cells. *Cancer Res* 58(20): 4616-4623, 1998.
55 Grzywacz MJ, Yang J-M, Hait WN. Effect of the multidrug resistance protein on the transport of the antiandrogen flutamide. *Cancer Res* 63(10): 2492-2498, 2003.
56 Olson DP, Scadden DT, D'Aquila RT, De Pasquale MP. The protease inhibitor ritonavir inhibits the functional activity of the multidrug resistance related-protein 1 (MRP-1). *AIDS* 16(13): 1743-1747, 2002.
57 Williams GC, Liu A, Knipp G, Sinko PJ. Direct evidence that saquinavir is transported by multidrug resistance-associated protein (MRP1) and canalicular multispecific organic anion transporter (MRP2). *Antimicrob Agents Chemother* 46(11): 3456-3462, 2002.
58 Han B, Zhang JT. Multidrug resistance in cancer chemotherapy and xenobiotic protection mediated by the half ATP-binding cassette transporter ABCG2. *Curr Med Chem Anticancer Agents* 4(1): 31-42, 2004.
59 Mao Q, Unadkat JD. Role of the breast cancer resistance protein (ABCG2) in drug transport. *AAPS J* 7(1): E118-E133, 2005.
60 Plasschaert SLA, Van der Kolk DM, De Bont ESJM, Vellenga E, Kamps WA, De Vries EGE. Breast cancer resistance protein (BCRP) in acute leukemia. *Leuk Lymphoma* 45(4): 649-654, 2004.
61 Avendano C, Menendez JC. Inhibitors of multidrug resistance to antitumor agents (MDR). *Curr Med Chem* 9(2): 159-193, 2002.

62 Sikic BI, Fisher GA, Lum BL, Halsey J, Beketic-Oreskovic L, Chen G. Modulation and prevention of multidrug resistance by inhibitors of P-glycoprotein. *Cancer Chemother Pharmacol* 40(Suppl): S13-S19, 1997.

63 Sugimoto Y, Tsukahara S, Ishikawa E, Mitsuhashi J. Breast cancer resistance protein: molecular target for anticancer drug resistance and pharmacokinetics/pharmacodynamics. *Cancer Sci* 96(8): 457-465, 2005.

64 Di Pietro A, Conseil G, Perez-Victoria JM, Dayan G, Baubichon-Cortay H, Trompier D, Steinfels E, Jault J-M, De Wet H, Maitrejean M, Comte G, Boumendjel A, Mariotte A-M, Dumontet C, McIntosh DB, Goffeau A, Castanys S, Gamarro F, Barron D. Modulation by flavonoids of cell multidrug resistance mediated by P-glycoprotein and related ABC transporters. *Cell Mol Life Sci* 59(2): 307-322, 2002.

65 Borst P, Oude Elferink R. Mammalian ABC transporters in health and disease. *Annu Rev Biochem* 71: 537-592, 2002.

66 Tan B, Piwnica-Worms D, Ratner L. Multidrug resistance transporters and modulation. *Curr Opin Oncol* 12(5): 450-458, 2000.

67 Conseil G, Baubichon-Cortay H, Dayan G, Jault J-M, Barron D, Di Pietro A. Flavonoids: a class of modulators with bifunctional interactions at vicinal ATP- and steroid-binding sites on mouse P-glycoprotein. *Proc Natl Acad Sci U S A* 95(17): 9831-9836, 1998.

68 Leslie EM, Mao Q, Oleschuk CJ, Deeley RG, Cole SPC. Modulation of multidrug resistance protein 1 (MRP1/ABCC1) transport and ATPase activities by interaction with dietary flavonoids. *Mol Pharmacol* 59(5): 1171-1180, 2001.

69 Trompier D, Baubichon-Cortay H, Chang X-B, Maitrejean M, Barron D, Riordon JR, Di Pietro A. Multiple flavonoid-binding sites within multidrug resistance protein MRP1. *Cell Mol Life Sci* 60(10): 2164-2177, 2003.

70 Aherne SA, O'Brien NM. Dietary flavonols: chemistry, food content, and metabolism. *Nutrition* 18(1): 75-81, 2002.

71 Ader P, Wessmann A, Wolffram S. Bioavailability and metabolism of the flavonol quercetin in the pig. Free Radic Biol Med 28(7): 1056-1067, 2000.

72 Day AJ, Bao Y, Morgan MRA, Williamson G. Conjugation position of quercetin glucuronides and effect on biological activity. *Free Radic Biol Med* 29(12): 1234-1243, 2000.

73 Day AJ, Mellon F, Barron D, Sarrazin G, Morgan MRA, Williamson G. Human metabolism of dietary flavonoids: identification of plasma metabolites of quercetin. *Free Radic Res* 35(6): 941-952, 2001.

74 Mullen W, Graf BA, Caldwell ST, Hartley RC, Duthie GG, Edwards CA, Lean MEJ, Crozier A. Determination of flavonol metabolites in plasma and tissues of rats by HPLC-radiocounting and tandem mass spectrometry following oral ingestion of [2-(14)C]quercetin-4'-glucoside. *J Agric Food Chem* 50(23): 6902-6909, 2002.

75 Spencer JPE, Abd-el-Mohsen MM, Rice-Evans C. Cellular uptake and metabolism of flavonoids and their metabolites: implications for their bioactivity. *Arch Biochem Biophys* 423(1): 148-161, 2004.

76 Havsteen BH. The biochemistry and medical significance of the flavonoids. *Pharmacol Ther* 96(2-3): 67-202, 2002.

77 Rice-Evans C. Flavonoid antioxidants. *Curr Med Chem* 8(7): 797-807, 2001.

78 Williams RJ, Spencer JPE, Rice-Evans C. Flavonoids: antioxidants or signalling molecules? *Free Radic Biol Med* 36(7): 838-849, 2004.

79 Le Marchand L. Cancer preventive effects of flavonoids--a review. *Biomed Pharmacother* 56(6): 296-301, 2002.

80 Lopez-Lazaro M. Flavonoids as anticancer agents: structure-activity relationship study. *Curr Med Chem Anticancer Agents* 2(6): 691-714, 2002.

81 Yang CS, Landau JM, Huang M-T, Newmark HL. Inhibition of carcinogenesis by dietary polyphenolic compounds. *Annu Rev Nutr* 21: 381-406, 2001.

82 Kris-Etherton PM, Keen CL. Evidence that the antioxidant flavonoids in tea and cocoa are beneficial for cardiovascular health. *Curr Opin Lipidol* 13(1): 41-49, 2002.

83 Ross JA, Kasum CM. Dietary flavonoids: bioavailability, metabolic effects, and safety. *Annu Rev Nutr* 22: 19-34, 2002.

84 Steinberg FM, Bearden MM, Keen CL. Cocoa and chocolate flavonoids: implications for cardiovascular health. *J Am Diet Assoc* 103(2): 215-213, 2003.

85 Inanami O, Watanabe Y, Syuto B, Nakano M, Tsuji M, Kuwabara M. Oral administration of (-)catechin protects against ischemia-reperfusion-induced neuronal death in the gerbil. *Free Radic Res* 29(4): 359-365, 1998.

86 Joseph JA, Shukitt-Hale B, Denisova NA, Bielinski D, Martin A, McEwen JJ, Bickford PC. Reversals of age-related declines in neuronal signal transduction, cognitive, and motor behavioral deficits with blueberry, spinach, or strawberry dietary supplementation. *J Neurosci* 19(18): 8114-8121, 1999.

87 Joseph JA, Shukitt-Hale B, Denisova NA, Prior RL, Cao G, Martin A, Taglialatela G, Bickford PC. Long-term dietary strawberry, spinach, or vitamin E supplementation retards the onset

of age-related neuronal signal-transduction and cognitive behavioral deficits. *J Neurosci* 18(19): 8047-8055, 1998.
88 Potter SM, Baum JA, Teng H, Stillman RJ, Shay NF, Erdman JWJ. Soy protein and isoflavones: their effects on blood lipids and bone density in postmenopausal women. *Am J Clin Nutr* 68(6 Suppl): 1375S-1379S, 1998.
89 Boumendjel A, Baubichon-Cortay H, Trompier D, Perrotton T, Di Pietro A. Anticancer multidrug resistance mediated by MRP1: recent advances in the discovery of reversal agents. *Med Res Rev* 25(4): 453-472, 2005.
90 Zhang S, Wang X, Sagawa K, Morris ME. Flavonoids chrysin and benzoflavone, potent breast cancer resistance protein inhibitors, have no significant effect on topotecan pharmacokinetics in rats or mdr1a/1b (-/-) mice. *Drug Metab Dispos* 33(3): 341-348, 2005.
91 Zhang S, Yang X, Morris ME. Flavonoids are inhibitors of breast cancer resistance protein (ABCG2)-mediated transport. *Mol Pharmacol* 65(5): 1208-1216, 2004.
92 Zhang S, Yang X, Morris ME. Combined effects of multiple flavonoids on breast cancer resistance protein (ABCG2)-mediated transport. *Pharm Res* 21(7): 1263-1273, 2004.
93 Hong J, Lambert JD, Lee S-H, Sinko PJ, Yang CS. Involvement of multidrug resistance-associated proteins in regulating cellular levels of (-)-epigallocatechin-3-gallate and its methyl metabolites. *Biochem Biophys Res Commun* 310(1): 222-227, 2003.
94 Van Zanden JJ, De Mul A, Wortelboer HM, Usta M, Van Bladeren PJ, Rietjens IMCM, Cnubben NHP. Reversal of in vitro cellular MRP1 and MRP2 mediated vincristine resistance by the flavonoid myricetin. *Biochem Pharmacol* 69(11): 1657-1665, 2005.
95 Van Zanden JJ, Wortelboer HM, Bijlsma S, Punt A, Usta M, Van Bladeren PJ, Rietjens IMCM, Cnubben NHP. Quantitative structure activity relationship studies on the flavonoid mediated inhibition of multidrug resistance proteins 1 and 2. *Biochem Pharmacol* 69(4): 699-708, 2005.
96 Ikegawa T, Ushigome F, Koyabu N, Morimoto S, Shoyama Y, Naito M, Tsuruo T, Ohtani H, Sawada Y. Inhibition of P-glycoprotein by orange juice components, polymethoxyflavones in adriamycin-resistant human myelogenous leukemia (K562/ADM) cells. *Cancer Lett* 160(1): 21-28, 2000.
97 Takanaga H, Ohnishi A, Yamada S, Matsuo H, Morimoto S, Shoyama Y, Ohtani H, Sawada Y. Polymethoxylated flavones in orange juice are inhibitors of P-glycoprotein but not cytochrome P450 3A4. *J Pharmacol Exp Ther* 293(1): 230-236, 2000.
98 Jodoin J, Demeule M, Béliveau R. Inhibition of the multidrug resistance P-glycoprotein activity by green tea polyphenols. *Biochim Biophys Acta* 1542(1-3): 149-159, 2002.
99 Scambia G, Ranelletti FO, Panici PB, De Vincenzo R, Bonanno G, Ferrandina G, Piantelli M, Bussa S, Rumi C, Cianfriglia M. Quercetin potentiates the effect of adriamycin in a multidrug-resistant MCF-7 human breast-cancer cell line: P-glycoprotein as a possible target. *Cancer Chemother Pharmacol* 34(6): 459-464, 1994.
100 Tseng E, Liang W, Wallen C, Morris ME. Effect of flavonoids of P-glycoprotein-mediated transport in a human breast cancer cell line. AAPS National Meetings. Denver, USA, 2001.
101 Castro AF, Altenberg GA. Inhibition of drug transport by genistein in multidrug-resistant cells expressing P-glycoprotein. *Biochem Pharmacol* 53(1): 89-93, 1997.
102 Eagling VA, Profit L, Back DJ. Inhibition of the CYP3A4-mediated metabolism and P-glycoprotein-mediated transport of the HIV-1 protease inhibitor saquinavir by grapefruit juice components. *Br J Clin Pharmacol* 48(4): 543-552, 1999.
103 Sergent T, Garsou S, Schaut A, De Saeger S, Pussemier L, Van Peteghem C, Larondelle Y, Schneider Y-J. Differential modulation of ochratoxin A absorption across Caco-2 cells by dietary polyphenols, used at realistic intestinal concentrations. *Toxicol Lett* 159(1): 60-70, 2005.
104 Berger V, Gabriel A-F, Sergent T, Trouet A, Larondelle Y, Schneider Y-J. Interaction of ochratoxin A with human intestinal Caco-2 cells: possible implication of a multidrug resistance-associated protein (MRP2). *Toxicol Lett* 140-141: 465-476, 2003.
105 Schutte ME, Freidig AP, van de Sandt JJM, Alink GM, Rietjens IMCM, Groten JP. An in vitro and in silico study on the flavonoid-mediated modulation of the transport of 2-amino-1-methyl-6-phenylimidazo[4,5-b]pyridine (PhIP) through Caco-2 monolayers. *Toxicol Appl Pharmacol* 217: 204-215, 2006.
106 Zhang S, Morris ME. Effect of the flavonoids biochanin A and silymarin on the P-glycoprotein-mediated transport of digoxin and vinblastine in human intestinal Caco-2 cells. *Pharm Res* 20(8): 1184-1191, 2003.
107 Deferme S, Augustijns P. The effect of food components on the absorption of P-gp substrates: a review. *J Pharm Pharmacol* 55(2): 153-162, 2003.
108 Zhou S, Lim LY, Chowbay B. Herbal modulation of P-glycoprotein. *Drug Metab Rev* 36(1): 57-104, 2004.
109 Choi J-S, Jo B-W, Kim Y-C. Enhanced paclitaxel bioavailability after oral administration of paclitaxel or prodrug to rats pretreated with

quercetin. *Eur J Pharm Biopharm* 57(2): 313-318, 2004.
110 Choi J-S, Choi H-K, Shin S-C. Enhanced bioavailability of paclitaxel after oral coadministration with flavone in rats. *Int J Pharm* 275(1-2): 165-170, 2004.
111 Imai Y, Tsukahara S, Asada S, Sugimoto Y. Phytoestrogens/flavonoids reverse breast cancer resistance protein/ABCG2-mediated multidrug resistance. *Cancer Res* 64(12): 4346-4352, 2004.
112 Romiti N, Tramonti G, Donati A, Chieli E. Effects of grapefruit juice on the multidrug transporter P-glycoprotein in the human proximal tubular cell line HK-2. *Life Sci* 76(3): 293-302, 2004.
113 Choi J-S, Han H-K. Enhanced oral exposure of diltiazem by the concomitant use of naringin in rats. *Int J Pharm* 305(1-2): 122-128, 2005.
114 Choi J-S, Han H-K. Pharmacokinetic interaction between diltiazem and morin, a flavonoid, in rats. *Pharmacol Res* 52(5): 386-391, 2005.
115 Edwards DJ, Fitzsimmons ME, Schuetz EG, Yasuda K, Ducharme MP, Warbasse LH, Woster PM, Schuetz JD, Watkins P. 6',7'-Dihydroxybergamottin in grapefruit juice and Seville orange juice: effects on cyclosporine disposition, enterocyte CYP3A4, and P-glycoprotein. *Clin Pharmacol Ther* 65(3): 237-244, 1999.
116 Flanagan D. Understanding the grapefruit-drug interaction. *Gen Dent* 53(4): 282-285, 2005.
117 Tian R, Koyabu N, Takanaga H, Matsuo H, Ohtani H, Sawada Y. Effects of grapefruit juice and orange juice on the intestinal efflux of P-glycoprotein substrates. *Pharm Res* 19(6): 802-809, 2002.
118 Spahn-Langguth H, Langguth P. Grapefruit juice enhances intestinal absorption of the P-glycoprotein substrate talinolol. *Eur J Pharm Sci* 12(4): 361-367, 2001.
119 Wagner D, Spahn-Langguth H, Hanafy A, Koggel A, Langguth P. Intestinal drug efflux: formulation and food effects. *Adv Drug Deliv Rev* 50(Suppl 1): S13-S31, 2001.
120 Di Marco MP, Edwards DJ, Wainer IW, Ducharme MP. The effect of grapefruit juice and seville orange juice on the pharmacokinetics of dextromethorphan: the role of gut CYP3A and P-glycoprotein. *Life Sci* 71(10): 1149-1160, 2002.
121 Becquemont L, Verstuyft C, Kerb R, Brinkmann U, Lebot M, Jaillon P, Funck-Brentano C. Effect of grapefruit juice on digoxin pharmacokinetics in humans. *Clin Pharmacol Ther* 70(4): 311-316, 2001.
122 Soldner A, Christians U, Susanto M, Wacher VJ, Silverman JA, Benet LZ. Grapefruit juice activates P-glycoprotein-mediated drug transport. *Pharm Res* 16(4): 478-485, 1999.
123 Lo YL, Huang JD. Comparison of effects of natural or artificial rodent diet on etoposide absorption in rats. *In Vivo* 13(1): 51-55, 1999.
124 Scalbert A, Williamson G. Dietary intake and bioavailability of polyphenols. *J Nutr* 130(8S Suppl): 2073S-2085S, 2000.
125 Leslie EM, Deeley RG, Cole SPC. Multidrug resistance proteins: role of P-glycoprotein, MRP1, MRP2, and BCRP (ABCG2) in tissue defense. *Toxicol Appl Pharmacol* 204(3): 216-237, 2005.
126 Borst P, Evers R, Kool M, Wijnholds J. A family of drug transporters: the multidrug resistance-associated proteins. *J Natl Cancer Inst* 92(16): 1295-1302, 2000.
127 Ritter CA, Jedlitschky G, Meyer zu Schwabedissen H, Grube M, Köck K, Kroemer HK. Cellular export of drugs and signaling molecules by the ATP-binding cassette transporters MRP4 (ABCC4) and MRP5 (ABCC5). *Drug Metab Rev* 37(1): 253-278, 2005.
128 Zelcer N, Reid G, Wielinga P, Kuil A, Van der Heijden I, Schuetz JD, Borst P. Steroid and bile acid conjugates are substrates of human multidrug-resistance protein (MRP) 4 (ATP-binding cassette C4). *Biochem J* 371(Pt 2): 361-367, 2003.
129 Wielinga P, Hooijberg JH, Gunnarsdottir S, Kathmann I, Reid G, Zelcer N, Van der Born K, De Haas M, Van der Heijden I, Kaspers G, Wijnholds J, Jansen G, Peters G, Borst P. The human multidrug resistance protein MRP5 transports folates and can mediate cellular resistance against antifolates. *Cancer Res* 65(10): 4425-4430, 2005.
130 Krishnamurthy P, Schuetz JD. Role of ABCG2/BCRP in biology and medicine. *Annu Rev Pharmacol Toxicol* 46: 381-410, 2006.
131 Sarkadi B, Özvegy-Laczka C, Német K, Váradi A. ABCG2 - a transporter for all seasons. *FEBS Lett* 567(1): 116-120, 2004.
132 Staud F, Pavek P. Breast cancer resistance protein (BCRP/ABCG2). *Int J Biochem Cell Biol* 37(4): 720-725, 2005.
133 Van Herwaarden AE, Schinkel AH. The function of breast cancer resistance protein in epithelial barriers, stem cells and milk secretion of drugs and xenotoxins. *Trends Pharmacol Sci* 27(1): 10-16, 2006.
134 Chung SY, Sung MK, Kim NH, Jang JO, Go EJ, Lee HJ. Inhibition of P-glycoprotein by natural products in human breast cancer cells. *Arch Pharm Res* 28(7): 823-828, 2005.
135 Kitagawa S, Nabekura T, Kamiyama S. Inhibition of P-glycoprotein function by tea catechins in KB-C2 cells. *J Pharm Pharmacol* 56(8): 1001-1005, 2004.
136 Kitagawa S, Nabekura T, Takahashi T, Nakamura Y, Sakamoto H, Tano H, Hirai M,

Tsukahara G. Structure-activity relationships of the inhibitory effects of flavonoids on P-glycoprotein-mediated transport in KB-C2 cells. *Biol Pharm Bull* 28(12): 2274-2278, 2005.

137 Ofer M, Wolffram S, Koggel A, Spahn-Langguth H, Langguth P. Modulation of drug transport by selected flavonoids: Involvement of P-gp and OCT? *Eur J Pharm Sci* 25(2-3): 263-271, 2005.

138 Walgren RA, Karnaky KJJ, Lindenmayer GE, Walle T. Efflux of dietary flavonoid quercetin-4'-glucoside across human Intestinal Caco-2 cell monolayers by apical multidrug resistance-associated protein-2. *J Pharmacol Exp Ther* 294(3): 830-836, 2000.

139 Zhang S, Morris ME. Effects of the flavonoids biochanin A, morin, phloretin, and silymarin on P-glycoprotein-mediated transport. *J Pharmacol Exp Ther* 304(3): 1258-1267, 2003.

140 Lania-Pietrzak B, Michalak K, Hendrich AB, Mosiadz D, Grynkiewicz G, Motohashi N, Shirataki Y. Modulation of MRP1 protein transport by plant, and synthetically modified flavonoids. *Life Sci* 77(15): 1879-1891, 2005.

141 Nguyen H, Zhang S, Morris ME. Effect of flavonoids on MRP1-mediated transport in Panc-1 cells. *J Pharm Sci* 92(2): 250-257, 2003.

142 Wu C-P, Calcagno AM, Hladky SB, Ambudkar SV, Barrand MA. Modulatory effects of plant phenols on human multidrug-resistance proteins 1, 4 and 5 (ABCC1, 4 and 5). *FEBS J* 272(18): 4725-4740, 2005.

143 Ahmed-Belkacem A, Pozza A, Muñ oz-Martinez F, Bates SE, Castanys S, Gamarro F, Di Pietro A, Pérez-Victoria JM. Flavonoid structure-activity studies identify 6-prenylchrysin and tectochrysin as potent and specific inhibitors of breast cancer resistance protein ABCG2. *Cancer Res* 65(11): 4852-4860, 2005.

144 Cooray HC, Janvilisri T, Van Veen HW, Hladky B, Barrand MA. Interaction of the breast cancer resistance protein with plant polyphenols. *Biochem Biophys Res Commun* 317(1): 269-275, 2004.

145 Yoshikawa M, Ikegami Y, Sano K, Yoshida H, Mitomo H, Sawada S, Ishikawa T. Transport of SN-38 by the wild type of human ABC transporter ABCG2 and its inhibition by quercetin, a natural flavonoid. *J Exp Ther Oncol* 4(1): 25-35, 2004.

146 Takanaga H, Ohnishi A, Matsuo H, Sawada Y. Inhibition of vinblastine efflux mediated by P-glycoprotein by grapefruit juice components in Caco-2 cells. *Biol Pharm Bull* 21(10): 1062-1066, 1998.

147 Versantvoort CHM, Broxterman HJ, Lankelma J, Feller N, Pinedo HM. Competitive inhibition by genistein and ATP dependence of daunorubicin transport in intact MRP overexpressing human small cell lung cancer cells. *Biochem Pharmacol* 48(6): 1129-1136, 1994.

148 Limtrakul P, Khantamat O, Pintha K. Inhibition of P-glycoprotein function and expression by kaempferol and quercetin. *J Chemother* 17(1): 86-95, 2005.

149 Chieli E, Romiti N, Cervelli F, Tongiani R. Effects of flavonols on P-glycoprotein activity in cultured rat hepatocytes. *Life Sci* 57(19): 1741-1751, 1995.

150 Rodriguez-Proteau R, Mata JE, Miranda CL, Fan Y, Brown JJ, Buhler DR. Plant polyphenols and multidrug resistance: effects of dietary flavonoids on drug transporters in Caco-2 and MDCKII-MDR1 cell transport models. *Xenobiotica* 36(1): 41-58, 2006.

151 Pinto M, Robine-Leon S, Appay M-D, Kedinger M, Triadou N, Dussaulx E, Lacroix B, Simon-Assmann P, Haffen K, Fogh J, Zweibaum A. Enterocyte-like differentiation and polarisation of the human colon carcinoma cell line Caco-2. *Biol Cell* 47: 323-330, 1983.

152 Karlsson J, Artursson P. A method for the determination of cellular permeability coefficients and aquous boundary layer thickness in monolayers of intestinal epithelial (Caco-2) cells grown in permeable filter chambers. *Int J Pharmaceutics* 71(1-2): 55-64, 1991.

Chapter 3

Metabolism and transport of the citrus flavonoid hesperetin in Caco-2 cell monolayers

Walter Brand, Petronella A. I. van der Wel, Maarit J. Rein, Denis Barron, Gary Williamson, Peter J. van Bladeren, and Ivonne M.C.M. Rietjens

Drug Metabolism and Disposition 36(9): 1794-1802, 2008

Abstract

Metabolism and transport from intestinal cells back into the lumen by ATP binding cassette (ABC) transporters is believed to limit the bioavailability of flavonoids. We studied metabolism and transport of the citrus flavonoid hesperetin, the aglycone of hesperidin, using a two-compartment transwell Caco-2 cell monolayer system, simulating the intestinal barrier. The role of apically located ABC transporters P-glycoprotein (Pgp/MDR1/ABCB1), Multidrug Resistance Protein 2 (MRP2/ABCC2) and Breast Cancer Resistance Protein (BCRP/ABCG2) in the efflux of hesperetin and its metabolites was studied by co-administration of compounds known to inhibit several classes of ABC transporters, including cyclosporin A, GF120918, Ko143, MK571, and PSC-833. Apically-applied hesperetin (10 μM) was metabolized into hesperetin 7-*O*-glucuronide and hesperetin 7-*O*-sulfate, identified using HPLC-DAD, uPLC-DAD-MS-MS and authentic standards, which were transported predominantly to the apical side of the Caco-2 cell monolayer (1.12 cm^2), at average (SD) rates of 14.3 (3.7) pmol/min/monolayer and 2.1 (0.8) pmol/min/monolayer, respectively. Hesperetin aglycone also permeated to the basolateral side, and this process was unaffected by the inhibitors used, possibly implying a passive diffusion process. Inhibition studies, however, showed that efflux of hesperetin conjugates to the apical side involved active transport, which from the pattern of inhibition, appeared to involve mainly BCRP. Upon inhibition by the BCRP inhibitor Ko143 (5 μM), the apical efflux of hesperetin conjugates was 1.9-fold reduced ($P \leq 0.01$) and transport to the basolateral side was 3.1-fold increased ($P \leq 0.001$). These findings elucidate a novel pathway of hesperetin metabolism and transport, and show that BCRP-mediated transport could be a limiting step for hesperetin bioavailability.

Introduction

Flavonoids consist of a large group of polyphenols which can be divided into different classes and are present in fruits, vegetables and other plant-derived products. In foods, flavonoids often occur as ß-glycosides of aglycones, which become deglycosylated upon ingestion. The flavanone hesperetin (Figure 3.1 on page 47) is the aglycone of hesperidin (hesperetin-7-*O*-rutinoside), which is the major flavonoid present in sweet oranges (*Citrus sinensis*) and orange juice[1]. Both hesperidin and hesperetin exhibit some anti-inflammatory and anti-microbial effects[2].

Flavanones occur in the diet almost exclusively in citrus fruits or citrus fruit derived products, and as a result the daily intake of hesperidin is largely dependent on dietary habits. In general, the amount of hesperidin can form an important part of

the total flavonoid intake, and has been estimated 15.1 mg/day (after hydrolysis of glycosides)[3]. According to data on urinary and plasma concentrations, however, bioavailability of hesperetin is limited[4-7].

It is believed that hesperidin (Figure 3.1), which has a disaccharide rutinoside at position C7, has to be hydrolyzed by colonic microflora prior to its absorption whereas hesperetin aglycone, as well as the monosaccharide hesperetin 7-*O*-glucoside, can already be absorbed in the small intestine[6]. Passive diffusion, absorption of hesperetin 7-*O*-glucoside, as well as hydrolysis of hesperidin by colonic microflora, result in occurrence of intestinal intracellular hesperetin aglycone[6], which is subsequently conjugated into glucuronidated and sulfated metabolites, which were detected in human blood and urine[4,5,7].

Flavonoids and/or their metabolites are well known substrates of ATP binding cassette (ABC) transporters[8], which are present in epithelial cells throughout the intestinal tract[9,10]. In general, ABC transporters are specifically located in the apical (lumen side) or basolateral (blood/plasma side) membrane of enterocytes and facilitate excretion back into the intestinal lumen or uptake into the blood, respectively.

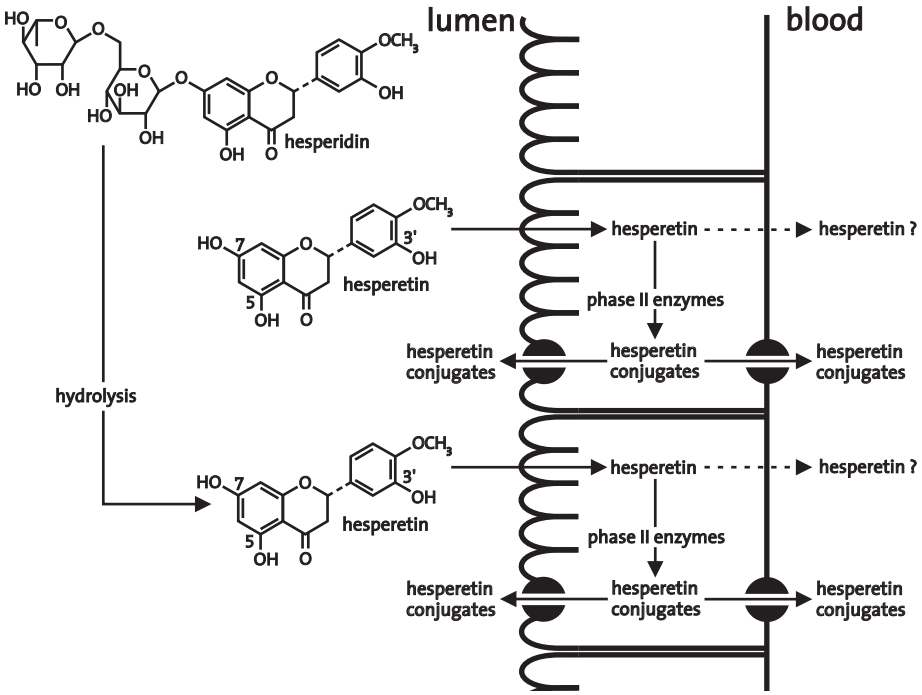

Figure 3.1 *Chemical structures of the rutinoside hesperidin and its aglycone hesperetin (4'-methoxy-3',5,7-trihydroxyflavanone) and an illustration of possible pathways for their intestinal uptake.*

Intestinal ABC transporters that have been related to flavonoid transport include P-glycoprotein (Pgp/MDR1/ABCB1), multidrug resistance proteins (MRPs/ABCCs) and breast cancer resistance protein (BCRP/ABCG2), of which Pgp, MRP2 and BCRP are localized in the apical membrane[8].

A common way to investigate the role of ABC transporters is co-exposure to compounds which more or less specifically inhibit individual ABC transport proteins. In the present study we used cyclosporin A, GF120918, Ko143, MK571 and PSC-833 (Table 3.1 on page 49). Cyclosporin A is a broad-spectrum inhibitor reported to inhibit Pgp, MRPs as well as BCRP[11,12], GF120918 is a dual inhibitor of both Pgp and BCRP[13], PSC-833 is a more specific inhibitor of Pgp[11], Ko143 is a highly specific inhibitor of BCRP[14,15], and MK571 is an MRP inhibitor[16,17].

Efficient intestinal metabolism and efflux mediated by ABC transporters located in the apical membrane are believed to be the main reasons for poor bioavailability of flavonoids and their metabolites[18]. Metabolites of the flavonoid quercetin, for instance, have been demonstrated to interact with MRP2[19] and BCRP[20]. In the present study, we focused on intestinal metabolism and transport of hesperetin *in vitro*, using Caco-2 cell monolayers grown on a permeable filter separating a two-compartment cell culture system, simulating the intestinal membrane barrier. Differentiated Caco-2 cells are known to display morphological and biochemical properties of intestinal enterocytes, including expression of Pgp, MRP2 and BCRP[9,10,21,22], of which we studied the mRNA expression levels in Caco-2 cell monolayers with RT-qPCR. By exposing Caco-2 cell monolayers to hesperetin (10 μM), in absence or presence of inhibitors, we studied formation and transport of hesperetin conjugates, which were identified by HPLC and uPLC retention times and diode-array detector (DAD) spectra, by co-elution with authentic synthesized standards, by confirmation with uPLC-DAD-MS-MS and by specific enzymatic de-conjugation. By co-administering hesperetin with a range of different inhibitors we investigated the role of Pgp, MRP2 and BCRP, in the transport of hesperetin and its metabolites in Caco-2 cell monolayers.

Table 3.1 *Overview from selected literature on the ability of the inhibitors used in this study to inhibit different ABC transporters in different specific model systems.*

Inhibitor	Concentration(s) used in present study	Affected ABC transporter(s)	Effect reported in literature	References
Cyclosporin A	10 μM	Pgp, MRP1 and BCRP	2.5 μM inhibited mitoxantrone efflux in Pgp, MRP1 and BCRP overexpressing cell lines.	[11,12]
GF120918	1, 5 and 10 μM	BCRP and Pgp	25-250 nM inhibited rhodamine efflux in Pgp overexpressing cells and 1-10 μM inhibited mitoxantrone efflux in BCRP overexpressing cells.	[13]
Ko143	1, 2 and 5 μM	BCRP	EC90's of 23 and 26 nM for inhibiting mitoxantrone and topotecan efflux, respectively, in Bcrp1 overexpressing cells.	[14]
MK571	2.4 and 24 μM	MRP1/MRP2	Inhibited LTC4 transport in MRP overexpressing cells with a K_i of 0.6 μM and 30 μM completely inhibited vincristine efflux in MRP overexpressing cells.	[16,17]
PSC-833	5 μM	Pgp, MRPs	2.5 μM inhibited mitoxantrone efflux in Pgp overexpressing cells.	[11,12]

Materials and methods

Materials

Chloroform, hesperetin (purity ≥95%), L-ascorbic acid and sulfatase (from *Helix pomatia*) were purchased from Sigma (St.Louis, MO). GF120918 was a generous gift from GlaxoSmithKline (Hertfordshire, UK), Ko143 from Dr. Alfred H. Schinkel from the Netherlands Cancer Institute (Amsterdam, The Netherlands) and PSC-833 from Novartis Pharma AG (Basel, Switzerland). MK571 was purchased from Biomol (Plymouth Meeting, PA) and cyclosporin A from Fluka (Buchs, Switzerland). Acetonitrile for the HPLC system and methanol were purchased from Sigma-Aldrich (Steinheim, Germany), acetontrile for the uPLC system and trifluoroacetic acid from J.T. Baker (Philipsburg, NJ), isopropanol (for molecular biology) from Acros (Geel, Belgium) and TRIzol reagent from Invitrogen (Paisley, UK). Di-potassium hydrogen phosphate, dimethyl sulfoxide (DMSO), ethanol (for molecular biology), ethylene dinitrilotetraacetic acid (EDTA) disodium salt dihydrate, ethyl acetate, formic acid, glacial acetic acid, hydrochloric acid, potassium di-hydrogen phosphate and sodium acetate were purchased from Merck (Darmstadt, Germany), and ß-glucuronidase (from *Escherichia coli*) from Roche (Mannheim, Germany). All cell culture reagents were purchased from Gibco (Paisley, UK). Authentic standards of hesperetin 7-*O*-glucuronide (purity 92.8%) and hesperetin 7-*O*-sulfate (purity <50%) were obtained from Nestlé Research Center (Lausanne, Switzerland).

Cell culture

Caco-2 cells were obtained from ATCC (Rockville, MD) and cultured in a humidified atmosphere of 5% CO2 and 95% air at 37°C in Dulbecco's Modified Eagle Medium (DMEM) containing 25 mM HEPES buffer, 4500 mg/l glucose, L-glutamine and phenol red, and was supplemented with 10% (v/v) heat inactivated (30 min at 56°C) fetal bovine serum, 1% (v/v) MEM non-essential amino acids and 0.2% (v/v) 50 mg/ml gentamycin. When the cell culture reached 70 to 90% confluency, it was rinsed with phosphate buffered saline (PBS) containing 22 mg/l EDTA and split using trypsin. The cell density of the suspension was determined using a Bürker-Türk counting chamber from Labor Optik (Friedrichsdorf, Germany). For transport experiments, 1×10^5 cells per cm2 (0.5 ml of 2.24×10^5 cells/ml) were seeded in Costar 12-well transwell plate inserts from Corning (Corning, NY) with an insert membrane pore size of 0.4 µm and a growth area of 1.12 cm^2. The passage number of the cells used in the experiments was between 37 and 47. The medium was changed 3 times a week and the transport experiments were performed 18 or 19 days post seeding.

RNA isolation

Medium was removed from a culture flask containing a Caco-2 cell monolayer (passage number 46) and the cells were lyzed in TRIzol reagent (100 µl/cm^2) and stored at -80°C. After defreezing, 200 µl chloroform was added to 1 ml aliquots, which were shaken (1 min), incubated at room temperature (3 min) and centrifuged at 15500 *g* and 4°C (15 min). The aqueous phases were transferred to a sterile tube, followed by addition of an equal volume isopropanol to precipitate the RNA. The samples were mixed and left to incubate at room temperature (10 min), after which they were centrifuged at 15500 *g* and 4°C (10 min). After removing the supernatant the pellets were washed with 70% (v/v) ethanol. After centrifugation at 12000 *g* and 4°C (5 min), the supernatant was removed and the pellets were air dried and resuspended in 100 µl RNase free water. The samples were pooled, cleaned and concentrated using a RNeasy Mini kit from Qiagen (Hilden, Germany) following the instructions of the manufacturer. The RNA concentration was spectophotometrically determined using a Nanodrop ND-1000 from Nanodrop Technologies (Wilmington, DE).

Real time RT-qPCR

A 5 µl mix containing 2 µg total RNA was reverse transcribed using 0.25 µg random primers from Invitrogen (Paisley, UK), 2 µl dNTPs (10 mM) from Fermentas (Vilnius, Lithuania) and RNase free water, together incubated at 65°C for 5 min in an iCycler from Bio-Rad (Hercules, CA). The product was added to a 9 µl enzyme mix containing RT-buffer, 2 µl DTT (100 mM), 0.5 µl RNase OUT (40 units/µl), 1 µl M-MLV (200 units/µl) from Invitrogen (Paisley, UK) and RNase free water, and incubated for 10 min at 25°C, 50 min at 37°C, 15 min at 70°C and cooled to 4°C, in the iCycler. To quantify the amount of mRNA of Pgp, MRP2 and BCRP real time qPCR was performed in duplicate with a dilution series (5, 10, 20, 40, 80, 160 times) of the cDNA using the iCycler and iQ SYBR Green from Bio-Rad (Hercules, CA). Each 25 µl PCR reaction contained 5 µl cDNA, 12.5 µl Mastermix SYBR Green, RNase free water and 1 µl of both the specific forward and reverse primers (10 mM) which were synthesized by Biolegio (Nijmegen, The Netherlands). The sequences of the primers used were described by Taipalensuu et al.[9] and are given in Table 3.2 on page 52. Villin, an actin cross-linking structural protein, was used to normalize the mRNA expression levels[23]. The amplification program consisted of a 15 min pre-incubation at 95°C, followed by 45 amplification cycles with denaturation at 95°C for 30 s, annealing at 60°C (MDR1, MRP2 and BCRP) or 56°C (villin) for 30 s, and extension at 72°C for 45 s. The cycle number at the threshold (C_T), was used for semi-quantification of the PCR product and the relative ABC transporter mRNA expression levels, normalized to villin, are given by $\Delta C_T = C_{T\ ABC\ transporter} - C_{T\ villin}$, converted to $2^{-\Delta C_T}$.

Table 3.2 *Gene specific PCR primers.*

Gene	Forward primer	Reverse primer	Reference
MDR1	5'-CAGACAGCAGGAAATGAAGTTGAA-3'	5'-TGAAGACATTTCCAAGGCATCA-3'	[9]
MRP2	5'-TGCAGCCTCCATAACCATGAG-3'	5'-GATGCCTGCCATTGGACCTA-3'	[9]
BCRP	5'-CAGGTCTGTTGGTCAATCTCACA-3'	5'-TCCATATCGTGGAATGCTGAAG-3'	[9]
Villin	5'-CATGAGCCATGCGCTGAAC-3'	5'-TCATTCTGCACCTCCACCTGT-3'	[9]

Transport experiments

Before experiments were started, Caco-2 cell monolayers were washed with DMEM (without phenol red). The integrity of the monolayers was checked by measuring trans-epithelial electrical resistance (TEER) values with a Millicell ERS volt/ohmmeter from Millipore (Bedford, MA). Only monolayers that demonstrated a TEER value between 500 and 1000 $\Omega \cdot cm^2$ were used. Transport experiments were carried out with transport medium consisting of DMEM (without phenol red) supplemented with 1% (v/v) MEM non-essential amino acids and 1 mM ascorbic acid to prevent auto-oxidation, which was filtered through a sterile 0.2 µm filter unit from Schleicher & Schuell (Dassel, Germany). To study the transport of hesperetin and the formation of metabolites with time, transport studies were performed in which the monolayers were exposed at the apical side to 10 µM hesperetin for 0, 20, 40, 60, 80, 100 or 120 min, whereupon samples of medium were taken from both the apical and basolateral compartment. To study the role of metabolism and different ABC transporters, Caco-2 cell monolayers were exposed at the apical side to 10 µM hesperetin, in the absence or presence of an inhibitor, all added from 400 times concentrated stock solutions in DMSO. Cyclosporin A, GF120918, Ko143, MK571 and PSC-833 were used in concentrations which are often used in inhibition studies and have demonstrated to potently inhibit specific ABC transporters (Table 3.1 on page 49). The concentration of DMSO at the apical side was kept at 0.5% in each transport experiment. After 120 min exposure, in which the apical efflux of hesperetin metabolites was linear with time, 150 µl samples were taken from both basolateral and apical compartment. Finally, the TEER value was re-checked to confirm the quality of the monolayer after the experiment. On some occasions the filters covered with Caco-2 cell monolayers were washed with PBS, cut out of the insert, dissolved in 250 or 500 µl 65% (v/v) methanol and sonificated for 15 min in a Bandelin Sonorex RK100 (Berlin, Germany) in order to collect the intracellular contents. All samples were stored at -80 °C until further analysis.

HPLC-DAD analysis

The HPLC system consisted of a Waters (Milford, MA) Alliance 2695 separation module connected to a Waters 2996 photodiode array detector, equipped with an Alltech (Breda, The Netherlands) Alltima C18 5 µm 150×4.6 mm reverse phase column with 7.5×4.6 mm guard column. Before injection, samples were centrifuged at 16000 *g* for 4 min and 50 µl was injected and eluted at a flow rate of 1 ml/min starting at 0% acetonitrile in nanopure water containing 0.1% trifluoroacetic acid, increasing to 10% acetonitrile in 5 min, to 15% in the following 16 min, and to 50% in the next 16 min. Thereafter the percentage acetonitrile was increased to 80% in 1 min, which condition was kept for 1 min, followed by a decrease to 0% acetonitrile

in 1 min, keeping this condition for 10 minutes allowing the column to re-equilibrate at the initial conditions (total run time: 50 min). DAD spectra were detected between 200 and 420 nm and HPLC chromatograms acquired at 280 nm were used for quantification and presentation.

uPLC-DAD analysis

The uPLC system consisted of a Waters Acquity binary solvent manager, sample manager and photodiode array detector, equipped with a Waters BEH C18 1.7 µm 50×2.1 mm column. After centrifugation at 16000 *g* for 4 min samples of 10 µl were injected and eluted at a flow rate of 0.440 ml/min starting at 95% millipore water and 5% acetonitrile, both containing 0.1% formic acid, increasing to 21% acetonitrile in 2 min, keeping this condition for 1.5 min, followed by an increase to 25% acetonitrile in 0.25 min, which condition was kept for 1.75 min, and followed to 80% acetontrile in 0.5 min. This percentage was kept for 0.5 min after which the percentage acetonitrile was decreased to 5% in 0.5 min, keeping this condition for 1 min allowing the column to re-equilibrate at the initial conditions (total run time: 8 min). DAD spectra were detected between 230 and 400 nm and UPLC chromatograms acquired at 280 nm were used for quantification.

uPLC-DAD-MS-MS analysis

Before injecting, samples were pre-treated by a solvent extraction in which 300 µl of sample was mixed with an equal volume of 200 mM HCl/methanol and 3 times extracted with 900 µl ethyl acetate. The collected organic fractions were pooled, dried under nitrogen and dissolved in 60 µl in millipore water containing 5% acetonitrile and 0.1% formic acid. A sample injection of 1.5 µl was eluted according to the uPLC-DAD method described above, however, with a 1 mm inner diameter column at a flow rate of 0.1 ml/min, on a similar Waters Acquity UPLC system connected to a Micromass (Manchester, UK) Quattro Micro Triple Quadrupole equipped with an electrospray ionization (ESI) probe. The instrument was operated on negative ion scan mode. The following parameters were used for the ion source for the MS Scans: 3kV capillary needle voltage, 38V cone voltage, source block temperature 100°C, desolvation temperature 400°C, cone gas (nitrogen) flow 50 L/h, and desolvation gas (nitrogen) flow 500 L/h. The scanned mass range was between 200-700 *m/z* and the scan time 0.4 s with interscan delay of 0.05 s. For the selective ion recording mode (SIR) the following masses of metabolites were monitored: 217, 301, 381, 395, 463, 477, 491, and 609 *m/z*. For the SIR mode, the cone voltage change was between 30 to 40V depending on the analyte. Dwell time was 0.02 s and the other parameters as above.

Enzymatic deconjugation

To confirm the presence of glucuronide or sulfate conjugates, samples were treated with ß-glucuronidase or sulfatase/ß-glucuronidase. For ß-glucuronidase incubations 50 µl sample was added to 50 µl 400 mM potassium phosphate buffer (pH 6.2) and after addition of 4 µl ß-glucuronidase solution (0.8 units), the mixture was incubated for 60 min at 37°C. To hydrolyze both glucuronide and sulfate conjugates, samples were treated with sulfatase (containing ß-glucuronidase activity). A sample volume of 50 µl was added to 50 µl 1 M sodium acetate buffer (pH 4.5) and upon addition of 4 µl sulfatase/ß-glucuronidase solution (0.8 units) the sample was incubated for 18 h at 37°C. Control samples were given the same treatment but with 4 µl water instead of enzyme solution. After incubation the mixtures were stored at -80°C until further analysis by HPLC-DAD.

Quantification

Hesperetin was quantified by peak area measurement using HPLC-DAD analysis, based on detection at 280 nm, using a ten-point linear (R^2>0.99) calibration line of a concentration range of 0.02 to 20 µM hesperetin in transport medium containing a final concentration of 0.5% DMSO. Similarly, the amount of hesperetin 7-*O*-glucuronide was quantified based on an eight-point linear (R^2>0.99) calibration curve of a concentration range of 0.02 to 2.5 µM with the authentic synthesized standard of hesperetin 7-*O*-glucuronide. The limit of detection of both compounds in transport medium was 0.02 µM (injection volume 50 µl). The amount of hesperetin 7-*O*-sulfate was quantified using the calibration curve of hesperetin 7-*O*-glucuronide since the authentic hesperetin 7-*O*-sulfate sample was not pure enough to allow definition of a calibration curve and the enzymatic deconjugation of hesperetin metabolites with sulfatase/ß-glucuronidase, compared with the deconjugation with only ß-glucuronidase, demonstrated a comparable molar extinction coefficient for hesperetin 7-*O*-sulfate and hesperetin 7-*O*-glucuronide metabolites.

Stability

The stability of hesperetin, hesperetin 7-*O*-glucuronide and 7-*O*-sulfate standards under experimental conditions was tested separately by taking samples with time (at 0, 1, 2, 3, 6 and 24 hours) from wells on a Corning Costar 12-well plate (Corning, NY) which was stored in the incubator used for cell culture and contained in each well 2 ml transport medium supplemented with known concentrations of hesperetin aglycone, hesperetin 7-*O*-glucuronide or hesperetin 7-*O*-sulfate standards (final concentration 0.5% DMSO). The samples were stored at -80°C until analysis by HPLC-DAD.

Partition coefficient determination

The log *P* value of hesperetin was calculated using the online LogKow (KowWin) program (available at http://www.syrres.com/esc/est_kowdemo.htm) from Syracuse Research Corporation (Syracuse, NY). This program uses fragmental analysis of the chemical structure for the prediction and obtained log *P* values demonstrate high correlation with quoted experimental log *P* values (R^2=0.98).

Statistical analysis

Student's two-tailed unpaired *t*-test was used to evaluate statistical differences. Differences were considered significant when *p*-values were less than 0.05. Values are expressed as mean ± standard deviation (SD).

Results

Metabolism and transport of hesperetin by Caco-2 cell monolayers

Using the Caco-2 cell monolayer two-compartment transwell system we studied transport and metabolism of hesperetin. Figure 3.2 shows representative sections of HPLC chromatograms of samples taken from the 0.5 ml apical (A) and 1.5 ml basolateral (B) compartment of a Caco-2 cell monolayer upon 120 min exposure to 10 µM hesperetin added to the apical compartment. Hesperetin was detected at the basolateral side (t_R 36.7 min), as well as 2 major metabolites, M1 (t_R 30.9 min) and M2 (t_R 31.4 min), which were detected at about 3.9- and 3.1-fold higher amounts in the apical compartment compared with the basolateral compartment, respectively.

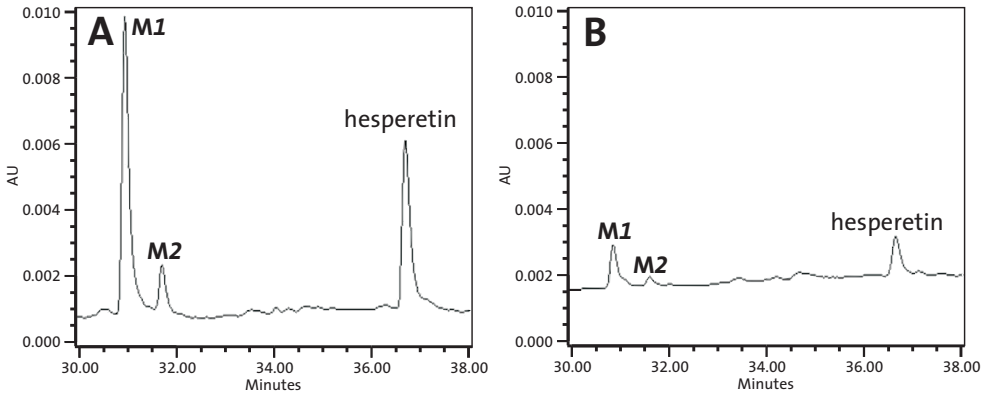

Figure 3.2 *Representative sections of the HPLC chromatograms of medium samples from the apical (A) and basolateral (B) side of a Caco-2 monolayer 120 min upon exposure to 10 µM hesperetin added to the apical medium. The volume of the apical and basolateral compartment is 0.5 and 1.5 ml, respectively. M1 = hesperetin 7-O-glucuronide, M2 = hesperetin 7-O-sulfate.*

Upon further analysis by uPLC-DAD, the major metabolite M*1* (amounting to 86% of the total amount of metabolites determined by peak area), demonstrated the same retention time (3.50 min) and DAD spectrum (UV_{max} 284.1 nm) as the authentic hesperetin 7-*O*-glucuronide standard, and metabolite M*2* demonstrated the same retention time (4.30 min) and UV spectrum (UV_{max} 280.5 nm, sholder at 335 nm) as the authentic hesperetin 7-*O*-sulfate standard. Equal retention times and DAD spectra for M*1* and the hesperetin 7-*O*-glucuronide standard, as well as for M*2* and the hesperetin 7-*O*-sulfate standard, were demonstrated by co-elution on the HPLC-DAD system as well.
Additional identification of M*1* as hesperetin 7-*O*-glucuronide was achieved by confirming the correct molecular mass by uPLC-DAD-MS-MS. Both M*1* from the transport medium and the corresponding peak from the metabolite standard showed an [M-H]- ion of *m/z* 477, consistent with the molecular mass of hesperetin (302 Da) containing a deprotonated additional glucuronic acid moiety (175 Da). The mass of M*2*, however, could not be determined on the uPLC-DAD-MS-MS system, due to instability of the sulfate moiety during the required sample preparation. However, enzymatic deconjugation with sulfatase (which contains also ß-glucuronidase activity) hydrolysed both M*1* and M*2*, as well as the corresponding standards, into hesperetin aglycone, whereas treatment with ß-glucuronidase deconjugated only M*1*. In control incubations, without enzyme activity added, M*1* and M*2* were unaffected.
We also tested the stability of the hesperetin derivates dissolved in transport medium and incubated under applied experimental conditions. The concentration of hesperetin 7-*O*-glucuronide from the authentic standard was stable and present after 120 min at 97% and after 24 hours at 95% of its initial concentration. Hesperetin 7-*O*-sulfate from the authentic standard also was very stable and present after both 120 min and 24 hours at >98% of its initial concentration. Hesperetin aglycone, however, seemed less stable (or soluble) and after 120 min was present at 88%, and after 24 hours at only 67% of the initial concentration.
Hesperetin was extensively metabolized into hesperetin 7-*O*-glucuronide and hesperetin 7-*O*-sulfate, which were predominantly excreted to the apical side, linear with time up to 120 min (Figure 3.3 on page 58), at average rates of 14.3±3.7 pmol/min/monolayer and 2.1±0.8 pmol/min/monolayer, respectively, in the transport experiments (Figure 3.4 on page 58). Figure 3.4 shows the amounts of hesperetin, hesperetin 7-*O*-glucuronide and hesperetin 7-*O*-sulfate in the apical and basolateral compartment of the transwell system, 120 min upon exposure to 10 µM hesperetin (5 nmol/0.5 ml). Upon 120 min incubation, the residual amount of hesperetin at the donor side amounts to only 0.78 nmol (15.5% of the initial amount added). The amount of hesperetin appearing in the basolateral compartment and

the amount of both hesperetin metabolites transported to the apical and basolateral compartment together make up for only 59.3% of the initial amount hesperetin added. The residual 25.2% may be accounted for by the amount of hesperetin and/or hesperetin metabolites accumulating in the cellular compartment of the Caco-2 monolayer transwell system. Indeed, we detected intracellular amounts of hesperetin, hesperetin 7-*O*-glucuronide and hesperetin 7-*O*-sulfate. The total amount, however, accounted for only 6% of the initial dose. At least part of the explanation for the residual 19.2% loss of hesperetin that remained unaccounted for could be the apparent instability or insolubility of hesperetin aglycone under experimental conditions, or during storage, leading to losses in the overall amount of hesperetin plus metabolites.

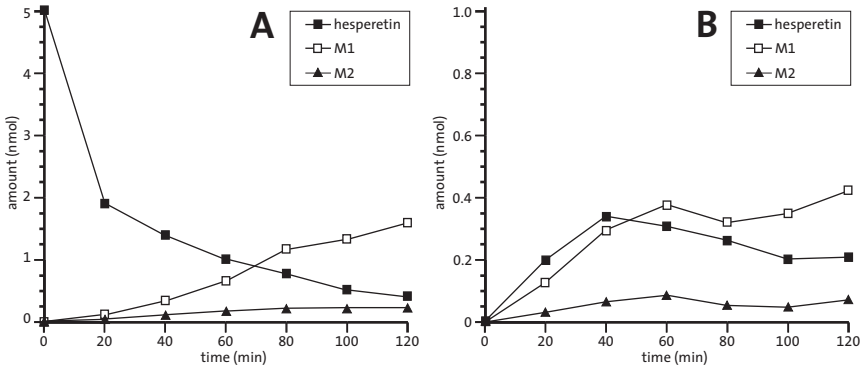

Figure 3.3 *Amounts of hesperetin 7-O-glucuronide (M1), hesperetin 7-O-sulfate (M2) and hesperetin aglycon in the apical compartment (A) and basolateral compartment (B) with time upon exposure to 5 nmol (=10 µM / 0.5 ml) apically-applied hesperetin. Data are the average of 2 determinations.*

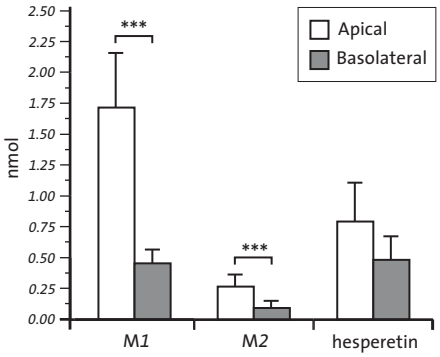

Figure 3.4 *Mean amounts of hesperetin 7-O-glucuronide (M1), hesperetin 7-O-sulfate (M2) and hesperetin aglycone in the apical compartment and basolateral compartment 120 min upon exposure to 5 nmol (=10 µM / 0.5 ml) apically-applied hesperetin (n=7), *** = p<0.001 significantly different.*

Real time RT-qPCR

From the cDNA dilution series, the C_T values were for all genes most stable between 10- and 40-fold dilution, and so the real time qPCR data from the 20-fold diluted cDNA was used for the calculations. Figure 3.5 depicts the relative mRNA expression levels of Pgp, MRP2 and BCRP normalized to villin. All three ABC transporter genes are expressed, with the relative levels of Pgp and MRP2 mRNA being respectively 12- and 41-fold higher compared to the mRNA expression level of BCRP.

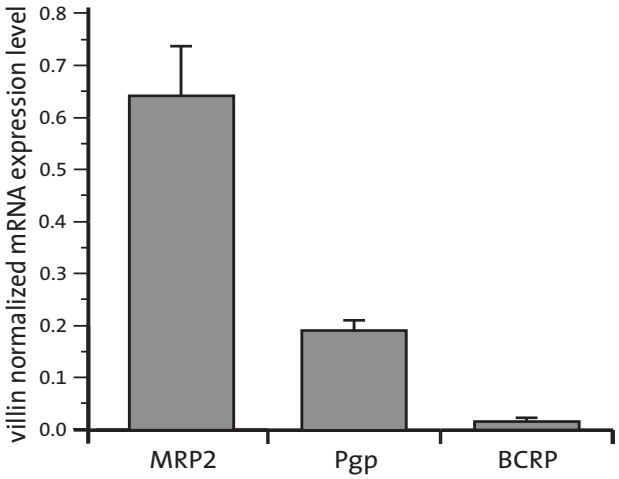

Figure 3.5 *Relative ABC transporter mRNA expression levels in Caco-2 cells normalized to the expression of villin. Mean ±SD values of two determinations are shown.*

Effect of ABC transporter inhibitors on hesperetin metabolism and efflux by Caco-2 cell monolayers

Since flavonoids and/or their metabolites are known to be substrates of ABC transporters, the effect of co-administering different ABC transporter inhibitors to the apical compartment on the transport of hesperetin aglycone and the hesperetin metabolites was investigated. Figure 3.6 on page 60 demonstrates no significant effect of the range of several co-administrated inhibitors on the appearance of hesperetin aglycone at the basolateral side, which could indicate that hesperetin moves through the Caco-2 monolayer by passive paracellular or transcellular diffusion. The relatively high lipophilicity of hesperetin, represented by the calculated log *P* value of 2.44, and the molecular weight (302 Da), would imply the latter.

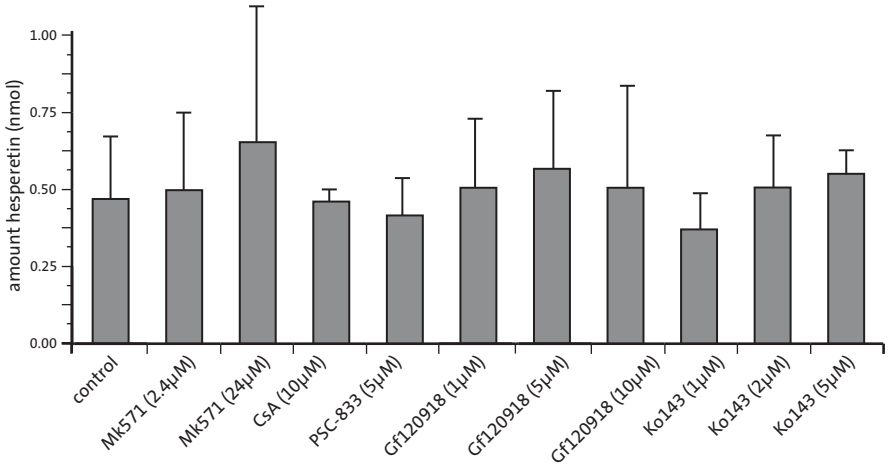

Figure 3.6 *Effect of different ABC transport inhibitors on basolateral amounts of hesperetin detected 120 min upon apical addition of 10 μM hesperetin compared with the control (10 μM hesperetin without inhibitors). Mean ±SD values are shown (n=4, control n=7). CsA = cyclosporin A.*

The efflux of hesperetin metabolites (Figure 3.7, and Table 3.3 on page 62), however, was affected by the dual Pgp/BCRP inhibitor GF120918, which caused a concentration-dependent decrease in the apical efflux, accompanied by a concentration-dependent increase in basolateral efflux, of hesperetin 7-*O*-glucuronide. Relevant doses of other Pgp inhibiting compounds did not alter the efflux of hesperetin metabolites significantly, which suggested BCRP to be the major ABC transport protein involved in the apical efflux of hesperetin metabolites. This was corroborated by the effect of co-administration of the highly specific BCRP inhibitor Ko143, which caused an even greater decrease in the apical efflux, for both hesperetin 7-*O*-glucuronide (Figure 3.7A) and hesperetin 7-*O*-sulfate (Figure 3.7B), and a concomitant increase in basolateral efflux of both hesperetin metabolites. Co-administration of 5 μM Ko143 resulted in a 1.9-fold decrease ($P \leq 0.01$) in the total amount of hesperetin metabolites transported to the apical side of the Caco-2 cell monolayer and in a 3.1-fold increase ($P \leq 0.001$) in the total amount of hesperetin metabolites transported to the basolateral compartment (Figure 3.7C).

Figure 3.7 *Effect of different ABC transport inhibitors on amounts of hesperetin 7-O-glucuronide (A), hesperetin 7-O-sulfate (B) and on the sum of both hesperetin metabolites (C) in the apical and basolateral medium 120 min after addition of 10 μM hesperetin to the apical side of Caco-2 monolayers compared to the control (10 μM hesperetin without inhibitors). Mean ±SD values shown (n=4, control n=7), (1) = p<0.05, (2) = p<0.01 and (3) = p<0.001 significantly different compared to the control. CsA = cyclosporin A.*

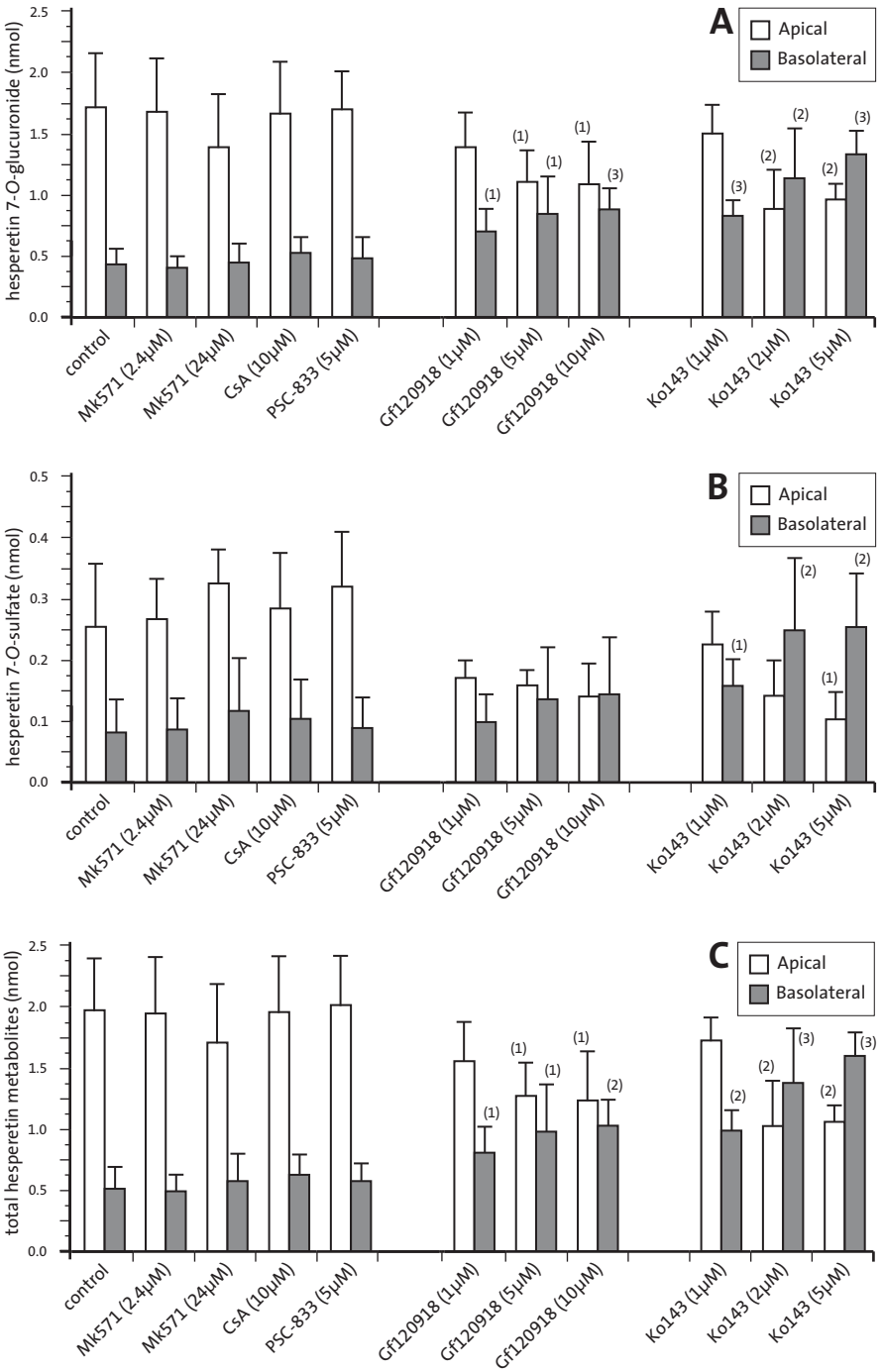
A
Apical
Basolateral
hesperetin 7-O-glucuronide (nmol)
2.5
2.0
1.5
1.0
0.5
0.0
control
Mk571 (2.4µM)
Mk571 (24µM)
CsA (10µM)
PSC-833 (5µM)
Gf120918 (1µM)
Gf120918 (5µM)
Gf120918 (10µM)
Ko143 (1µM)
Ko143 (2µM)
Ko143 (5µM)
B
Apical
Basolateral
hesperetin 7-O-sulfate (nmol)
0.5
0.4
0.3
0.2
0.1
0.0
control
Mk571 (2.4µM)
Mk571 (24µM)
CsA (10µM)
PSC-833 (5µM)
Gf120918 (1µM)
Gf120918 (5µM)
Gf120918 (10µM)
Ko143 (1µM)
Ko143 (2µM)
Ko143 (5µM)
C
Apical
Basolateral
total hesperetin metabolites (nmol)
2.5
2.0
1.5
1.0
0.5
0.0
control
Mk571 (2.4µM)
Mk571 (24µM)
CsA (10µM)
PSC-833 (5µM)
Gf120918 (1µM)
Gf120918 (5µM)
Gf120918 (10µM)
Ko143 (1µM)
Ko143 (2µM)
Ko143 (5µM)

As a result, the predominant side of both hesperetin 7-*O*-glucuronide and hesperetin 7-*O*-sulfate efflux was reversed from the apical to the basolateral side. Although not significant, co-administration of MK571 (24 µM) decreased the apical efflux of hesperetin 7-*O*-glucuronide by 19% (Figure 3.7A and Table 3.3), implying a minor role for apically localized MRP transporters (*i.e.* MRP2) in the transport of hesperetin 7-*O*-glucuronide as well.

Table 3.3 *Effect of different ABC transport inhibitors on amounts of hesperetin 7-O-glucuronide and hesperetin 7-O-sulfate in the apical and basolateral medium 120 min after addition of 10 µM hesperetin at the apical side of Caco-2 monolayers compared to the control (10 µM hesperetin without inhibitors) Mean + SD values (n=4, control n=7), (1)= p<0.05 , (2)= p<0.01, (3)= p<0.001 significantly different compared to the control. CsA = cyclosporine A.*

.

Inhibitor	(µM)	hesperetin 7-O-glucuronide (nmol)		hesperetin 7-O-sulfate (nmol)	
		Apical	Basolateral	Apical	Basolateral
Control		1.71 ± 0.44	0.44 ± 0.12	0.25 ± 0.10	0.08 ± 0.05
MK571	2.4	1.68 ± 0.42	0.41 ± 0.09	0.27 ± 0.06	0.09 ± 0.05
	24	1.39 ± 0.44	0.46 ± 0.15	0.32 ± 0.06	0.12 ± 0.08
CsA	10	1.66 ± 0.43	0.53 ± 0.12	0.29 ± 0.09	0.11 ± 0.06
PSC-833	5	1.70 ± 0.31	0.48 ± 0.10	0.32 ± 0.09	0.09 ± 0.05
GF120918	1	1.39 ± 0.28	0.71 ± 0.17(1)	0.17 ± 0.03	0.10 ± 0.04
	5	1..11 ± 0.25(1)	0.85 ± 0.30(1)	0.16 ± 0.03	0.14 ± 0.08
	10	1.09 ± 0.34(1)	0.88 ± 0.17(3)	0.14 ± 0.05	0.14 ± 0.09
Ko143	1	1.50 ± 0.23	0.82 ± 0.12(3)	0.23 ± 0.05	0.16 ± 0.04(1)
	2	0.89 ± 0.31(2)	1.14 ± 0.40(2)	0.14 ± 0.06	0.25 ± 0.11(2)
	5	0.96 ± 0.13(2)	1.34 ± 0.18(3)	0.10 ± 0.04(1)	0.26 ± 0.09(2)

Discussion

The present study showed that hesperetin was intensively metabolized by Caco-2 cells into 7-*O*-glucuronide and 7-*O*-sulfate metabolites. Other studies describing metabolism of flavonoids by Caco-2 cells also reported a relatively high rate of conjugation into glucuronidated, sulfated and/or methylated metabolites, the relative formation of all these metabolites depending on the type of flavonoid[24-27]. About 86% of the total amount of hesperetin metabolites formed consisted of hesperetin 7-*O*-glucuronide, a percentage similar as reported in a study in which the rutinoside hesperidin was given to humans and 87% of hesperetin in plasma consisted of glucuronides[5]. The remaining 13% in this human study consisted of sulfoglucuronides, while no conjugates were detected which were only sulfated[5]. Systemic plasma analysis does not reveal the organs in which conjugation has taken place, but likely at least part of the conjugation reactions of hesperetin take place in the intestinal epithelia. The results with the Caco-2 cells in the present study would support a role for intestinal cells in phase II metabolism of hesperetin and of hesperidin after its deglycosylation.

Co-administration of compounds known to potently inhibit BCRP-mediated transport, including the specific BCRP inhibitor Ko143 and the dual BCRP/Pgp inhibitor GF120918, decreased efflux of hesperetin metabolites to the apical compartment and consequently increased efllux of hesperetin metabolites to the basolateral side, while co-administration of PSC-833, MK571 and cyclosporin A, known to inhibit several other classes of ABC transporters (Table 3.1 on page 49), did not modify the efflux of hesperetin metabolites significantly (Figure 3.7 on page 60, Table 3.3 on page 62). Co-administration of 10 μM cyclosporin A, which is generally regarded as a non-specific inhibitor of Pgp but has been reported to inhibit BCRP as well[11,12], did not demonstrate any effect on disposition of hesperetin metabolites in the present study. A reason for this could be that its BCRP inhibiting properties were demonstrated in a cell line specifically overexpressing BCRP, whereas in Caco-2 cells, cyclosporin A might have a higher affinity for other ABC transporters present. In addition, Ejendal and Hrycyna did not demonstrate inhibition of BCRP by cyclosporin A in BCRP overexpressing HeLa and MCF-7 derived cells[28]. The addition of Ko143 seemed to have a more profound effect on inhibition of the apical efflux of hesperetin 7-*O*-sulfate than hesperetin 7-*O*-glucuronide, which further supports a role of BCRP in the transport of hesperetin metabolites, since the affinity of BCRP for sulfated metabolites has been reported to be greater than that for glucuronidated metabolites[29]. Altogether, our results suggest that efflux of hesperetin metabolites to the apical compartment in our Caco-2 cell transwell system mainly involves BCRP.

Specific flavonoids, and/or their metabolites, interact with apically located ABC transporters, especially with Pgp and BCRP[8], representing high affinity substrates. Hesperetin, and/or its metabolites, have been demonstrated to interact with BCRP in vitro[30,31], while co-administration of up to 50 μM hesperetin did not interact with Pgp-mediated transport in Caco-2 cell monolayers[32] and interactions of hesperetin with MRP2, on the basis of structural similarity to other flavonoids, seem unlikely[33], together further supporting a role for BCRP in the efflux of hesperetin metabolites. The important role for BCRP in the intestinal efflux of sulfate and glucuronide conjugates has also been established for other compounds[34,35], including glucuronide metabolites of the flavonol quercetin[20].

Previous studies on the transport and metabolism of flavonoids other than hesperetin by Caco-2 cell monolayers demonstrated a decreased apical efflux of flavonoids and their metabolites by co-administration of MK571, suggesting MRP2 to be responsible for the transport of flavonoid metabolites back to the intestinal lumen[25,26,36]. For instance, 10 μM MK571 inhibited both the apical and basolateral efflux of glucuronidated and sulfated metabolites of the flavone apigenin in Caco-2 monolayers[36]. Our findings do not rule out a role for MRP2 in the transport of flavonoid hesperetin conjugates completely, since co-administration of 24 μM MK571 did seem to negatively affect the apical efflux of hesperetin 7-*O*-glucuronide, although not significantly. Both BCRP and MRP2, as well as other ABC transporters, have an overlapping substrate specificity[37,38], thus, the class of transporter contributing most to specific transport will depend on the available dose of a substrate and the specific affinity, together with the specific levels of transporter expression. Earlier studies did not always focus on BCRP mediated transport, and other studies sometimes used concentrations of 50 μM MK571, or higher, which could be problematic when studying the metabolism of the flavonoid together with transport of its metabolites because MK571 has shown to inhibit glucuronidation at concentrations higher than 25 μM[36].

Since BCRP is a highly expressed ABC transporter throughout the intestinal tract[9,10,22,39], an important role for BCRP in the intestinal efflux of hesperetin conjugates in vivo is very likely. Furthermore, the expression of BCRP in Caco-2 cells is often considered to be relatively low compared with the expression level of other classes of ABC transporters, including Pgp and MRP2, and with expression of BCRP in the intestine[9,10,22], which could both result in an underestimation of its relevance in in vitro experiments. The real time RT-qPCR analyses in the present study demonstrated a 12- and 41-times lower mRNA expression of BCRP compared to the expression of Pgp and MRP2, respectively. This MRP>Pgp>>BCRP rank order of gene expression is in line with earlier studies on Caco-2 cells[10,22]. The expression of ultimate BCRP protein in Caco-2 cells has been demonstrated by Western blotting by

Xia *et al.*[15], making the Caco-2 cells used in the present study represent a good model to study intestinal BCRP mediated transport, keeping in mind that effects observed may even be of greater importance in vivo.
Our experiments demonstrated that a portion of the apically-applied hesperetin aglycone appeared at the basolateral side unconjugated. Administration of the different inhibitors did not affect this process, which could indicate that the small and relatively lipophilic hesperetin molecule moves through the Caco-2 monolayer by passive transcellular diffusion (*i.e.* non-transporter mediated). This suggests that passive diffusion of hesperetin could play a role in permeation across intestinal cells, not only in the Caco-2 monolayers, but possibly also in vivo. Lipophilicity is an important determinant of flavonoids for transfer across the intestinal barrier, as demonstrated in situ in rat models[40], however, in a study by Silberberg *et al.* , in which hesperetin (15 μM) was perfused in situ in rats, more than 95% of the hesperetin found in the mesenteric vein was conjugated[41]. In the study of Manach *et al.*, in which humans were given hesperidin, no unconjugated hesperetin was detected in plasma[5] and in the study of Gardana *et al.*, in which juice from blood oranges was given to humans, also more than 95% of hesperetin in plasma was conjugated[7]. Unfortunately, the only study in which the aglycone itself was given to humans did not study the chemical forms present in plasma[42], thus, the fate of hesperetin in vivo in humans remains to be elucidated.
In conclusion, hesperetin is extensively metabolized by Caco-2 cell monolayers into 7-*O*-glucuronide and 7-*O*-sulfate metabolites, which are predominantly transported to the apical side. Hesperetin aglycone, however, also permeates to the basolateral side of the Caco-2 cell monolayer unconjugated. The pattern of inhibition by different ABC transporter inhibitors suggests the apical efflux of hesperetin metabolites involves mainly BCRP. Moreover, inhibition of BCRP results not only in a decreased apical efflux, but also in an increased transport of hesperetin metabolites to the basolateral side of Caco-2 cell monolayers. Altogether, these findings elucidate a novel pathway of hesperetin metabolism and transport, and show that BCRP mediated transport could be one of the main limiting steps for hesperetin bioavailability.

Acknowledgements

The authors wish to thank Dr. Alfred H. Schinkel of The Netherlands Cancer Institute (NKI) for supplying Ko143, GlaxoSmithKline for supplying GF120918, Novartis Pharma AG for supplying PSC-833, and Laura H.J. de Haan of the Division of Toxicology of Wageningen University for her kind and excellent assistance with the RNA isolation and real time RT-qPCR analyses.

References

1 Tomás-Barberán FA, Clifford MN. Flavanones, chalcones and dihydrochalcones - nature, occurrence and dietary burden. *J Sci Food Agric* 80(7): 1073-1080, 2000.

2 Garg A, Garg S, Zaneveld LJD, Singla AK. Chemistry and pharmacology of the citrus bioflavonoid hesperidin. *Phytother Res* 15(8): 655-669, 2001.

3 Knekt P, Kumpulainen J, Järvinen R, Rissanen H, Heliövaara M, Reunanen A, Hakulinen T, Aromaa A. Flavonoid intake and risk of chronic diseases. *Am J Clin Nutr* 76(3): 560-568, 2002.

4 Ameer B, Weintraub RA, Johnson JV, Yost RA, Rouseff RL. Flavanone absorption after naringin, hesperidin, and citrus administration. *Clin Pharmacol Ther* 60(1): 34-40, 1996.

5 Manach C, Morand C, Gil-Izquierdo A, Bouteloup-Demange C, Rémésy C. Bioavailability in humans of the flavanones hesperidin and narirutin after the ingestion of two doses of orange juice. *Eur J Clin Nutr* 57(2): 235-242, 2003.

6 Nielsen ILF, Chee WSS, Poulsen L, Offord-Cavin E, Rasmussen SE, Frederiksen H, Enslen M, Barron D, Horcajada M-N, Williamson G. Bioavailability is improved by enzymatic modification of the citrus flavonoid hesperidin in humans: a randomized, double-blind, crossover trial. *J Nutr* 136(2): 404-408, 2006.

7 Gardana C, Guarnieri S, Riso P, Simonetti P, Porrini M. Flavanone plasma pharmacokinetics from blood orange juice in human subjects. *Br J Nutr* 98(1): 165-172, 2007.

8 Morris ME, Zhang S. Flavonoid-drug interactions: effects of flavonoids on ABC transporters. *Life Sci* 78(18): 2116-2130, 2006.

9 Taipalensuu J, Törnblom H, Lindberg G, Einarsson C, Sjöqvist F, Melhus H, Garberg P, Sjöström B, Lundgren B, Artursson P. Correlation of gene expression of ten drug efflux proteins of the ATP-binding cassette transporter family in normal human jejunum and in human intestinal epithelial Caco-2 cell monolayers. *J Pharmacol Exp Ther* 299(1): 164-170, 2001.

10 Englund G, Rorsman F, Rönnblom A, Karlbom U, Lazorova L, GrÂsjö J, Kindmark A, Artursson P. Regional levels of drug transporters along the human intestinal tract: Co-expression of ABC and SLC transporters and comparison with Caco-2 cells. *Eur J Pharm Sci* 29(3-4): 269-277, 2006.

11 Qadir M, O'Loughlin KL, Fricke SM, Williamson NA, Greco WR, Minderman H, Baer MR. Cyclosporin A is a broad-spectrum multidrug resistance modulator. *Clin Cancer Res* 11(6): 2320-2326, 2005.

12 Pawarode A, Shukla S, Minderman H, Fricke SM, Pinder EM, O'Loughlin KL, Ambudkar SV, Baer MR. Differential effects of the immunosuppressive agents cyclosporin A, tacrolimus and sirolimus on drug transport by multidrug resistance proteins. *Cancer Chemother Pharmacol* 60(2): 179-188, 2007.

13 De Bruin M, Miyake K, Litman T, Robey R, Bates SE. Reversal of resistance by GF120918 in cell lines expressing the ABC half-transporter, MXR. *Cancer Lett* 146(2): 117-126, 1999.

14 Allen JD, Van Loevezijn A, Lakhai JM, Van der Valk M, Van Tellingen O, Reid G, Schellens JHM, Koomen G-J, Schinkel AH. Potent and specific inhibition of the breast cancer resistance protein multidrug transporter in vitro and in mouse intestine by a novel analogue of fumitremorgin C. *Mol Cancer Ther* 1(6): 417-425, 2002.

15 Xia CQ, Liu N, Yang D, Miwa G, Gan L-S. Expression, localization, and functional characteristics of breast cancer resistance protein in Caco-2 cells. *Drug Metab Dispos* 33(5): 637-643, 2005.

16 Gekeler V, Ise W, Sanders KH, Ulrich WR, Beck J. The leukotriene LTD4 receptor antagonist MK571 specifically modulates MRP associated multidrug resistance. *Biochem Biophys Res Commun* 208(1): 345-352, 1995.

17 Leier I, Jedlitschky G, Buchholz U, Cole SPC, Deeley RG, Keppler D. The MRP gene encodes an ATP-dependent export pump for leukotriene C4 and structurally related conjugates. *J Biol Chem* 269(45): 27807-27810, 1994.

18 Liu Z, Hu M. Natural polyphenol disposition via coupled metabolic pathways. *Expert Opin Drug Metab Toxicol* 3(3): 389-406, 2007.

19 Williamson G, Aeberli I, Miguet L, Zhang Z, Sanchez M-B, Crespy V, Barron D, Needs P, Kroon PA, Glavinas H, Krajcsi P, Grigorov M. Interaction of positional isomers of quercetin glucuronides with the transporter ABCC2 (cMOAT, MRP2). *Drug Metab Dispos* 35(8): 1262-1268, 2007.

20 Sesink ALA, Arts ICW, De Boer VCJ, Breedveld P, Schellens JHM, Hollman PCH, Russel FGM. Breast cancer resistance protein (Bcrp1/Abcg2) limits net intestinal uptake of quercetin in rats by facilitating apical efflux of glucuronides. *Mol Pharmacol* 67(6): 1999-2006, 2005.

21 Hirohashi T, Suzuki H, Chu X-Y, Tamai I, Tsuji A, Sugiyama Y. Function and expression of multidrug resistance-associated protein family in human colon adenocarcinoma cells

(Caco-2). *J Pharmacol Exp Ther* 292(1): 265-270, 2000.

22 Seithel A, Karlsson J, Hilgendorf C, Björquist A, Ungell AL. Variability in mRNA expression of ABC- and SLC-transporters in human intestinal cells: comparison between human segments and Caco-2 cells. *Eur J Pharm Sci* 28(4): 291-299, 2006.

23 Lown KS, Mayo RR, Leichtman AB, Hsiao H-L, Turgeon DK, Schmiedlin-Ren P, Brown MB, Guo W, Rossi SJ, Benet LZ, Watkins PB. Role of intestinal P-glycoprotein (mdr1) in interpatient variation in the oral bioavailability of cyclosporine. *Clin Pharmacol Ther* 62(3): 248-260, 1997.

24 Galijatovic A, Otake Y, Walle UK, Walle T. Extensive metabolism of the flavonoid chrysin by human Caco-2 and Hep G2 cells. *Xenobiotica* 29(12): 1241-1256, 1999.

25 Vaidyanathan JB, Walle T. Transport and metabolism of the tea flavonoid (-)-epicatechin by the human intestinal cell line Caco-2. *Pharm Res* 18(10): 1420-1425, 2001.

26 Zhang L, Zheng Y, Chow MSS, Zuo Z. Investigation of intestinal absorption and disposition of green tea catechins by Caco-2 monolayer model. *Int J Pharm* 287(1-2): 1-12, 2004.

27 Liu Y, Hu M. Absorption and metabolism of flavonoids in the caco-2 cell culture model and a perused rat intestinal model. *Drug Metab Dispos* 30(4): 370-377, 2002.

28 Ejendal KFK, Hrycyna CA. Differential sensitivities of the human ATP-binding cassette transporters ABCG2 and P-glycoprotein to cyclosporin A. *Mol Pharmacol* 67(3): 902-911, 2005.

29 Chen Z-S, Robey RW, Belinsky MG, Shchaveleva I, Ren X-Q, Sugimoto Y, Ross DD, Bates SE, Kruh GD. Transport of methotrexate, methotrexate polyglutamates, and 17beta-estradiol 17-(beta-D-glucuronide) by ABCG2: effects of acquired mutations at R482 on methotrexate transport. *Cancer Res* 63(14): 4048-4054, 2003.

30 Cooray HC, Janvilisri T, Van Veen HW, Hladky B, Barrand MA. Interaction of the breast cancer resistance protein with plant polyphenols. *Biochem Biophys Res Commun* 317(1): 269-275, 2004.

31 Zhang S, Yang X, Morris ME. Flavonoids are inhibitors of breast cancer resistance protein (ABCG2)-mediated transport. *Mol Pharmacol* 65(5): 1208-1216, 2004.

32 Mertens-Talcott SU, De Castro WV, Manthey JA, Derendorf H, Butterweck V. Polymethoxylated flavones and other phenolic derivates from citrus in their inhibitory effects on P-glycoprotein-mediated transport of talinolol in Caco-2 cells. *J Agric Food Chem* 55(7): 2563-2568, 2007.

33 Van Zanden JJ, Wortelboer HM, Bijlsma S, Punt A, Usta M, Van Bladeren PJ, Rietjens IMCM, Cnubben NHP. Quantitative structure activity relationship studies on the flavonoid mediated inhibition of multidrug resistance proteins 1 and 2. *Biochem Pharmacol* 69(4): 699-708, 2005.

34 Adachi Y, Suzuki H, Schinkel AH, Sugiyama Y. Role of breast cancer resistance protein (Bcrp1/Abcg2) in the extrusion of glucuronide and sulfate conjugates from enterocytes to intestinal lumen. *Mol Pharmacol* 67(3): 923-928, 2005.

35 Ebert B, Seidel A, Lampen A. Identification of BCRP as transporter of benzo[a]pyrene conjugates metabolically formed in Caco-2 cells and its induction by Ah-receptor agonists. *Carcinogenesis* 26(10): 1754-1763, 2005.

36 Hu M, Chen J, Lin H. Metabolism of flavonoids via enteric recycling: mechanistic studies of disposition of apigenin in the Caco-2 cell culture model. *J Pharmacol Exp Ther* 307(1): 314-321, 2003.

37 Haimeur A, Conseil G, Deeley RG, Cole SPC. The MRP-related and BCRP/ABCG2 multidrug resistance proteins: biology, substrate specificity and regulation. *Curr Drug Metab* 5(1): 21-53, 2004.

38 Takano M, Yumoto R, Murakami T. Expression and function of efflux drug transporters in the intestine. *Pharmacol Ther* 109(1-2): 137-161, 2006.

39 Gutmann H, Hruz P, Zimmermann C, Beglinger C, Drewe J. Distribution of breast cancer resistance protein (BCRP/ABCG2) mRNA expression along the human GI tract. *Biochem Pharmacol* 70(5): 695-699, 2005.

40 Crespy V, Morand C, Besson C, Cotelle N, Vézin H, Demigné C, Rémésy C. The splanchnic metabolism of flavonoids highly differed according to the nature of the compound. *Am J Physiol Gastrointest Liver Physiol* 284(6): G980-G988, 2003.

41 Silberberg M, Morand C, Mathevon T, Besson C, Manach C, Scalbert A, Remesy C. The bioavailability of polyphenols is highly governed by the capacity of the intestine and of the liver to secrete conjugated metabolites. *Eur J Nutr* 45(2): 88-96, 2006.

42 Kanaze FI, Bounartzi MI, Georgarakis M, Niopas I. Pharmacokinetics of the citrus flavanone aglycones hesperetin and naringenin after single oral administration in human subjects. *Eur J Clin Nutr* 61(4): 472-477, 2007.

Chapter 4

The effect of co-administered flavonoids on the metabolism of hesperetin and the disposition of its metabolites in Caco-2 cell monolayers

Walter Brand, Beatriz Padilla, Peter J. van Bladeren,
Gary Williamson, and Ivonne M.C.M. Rietjens

Molecular Nutrition & Food Research, in press
(doi 10.1002/mnfr.2009 00183)

Abstract

Metabolism by phase II enzymes and transport from intestinal cells back into the lumen by ATP binding cassette (ABC) transporters limits the bioavailability of the flavanone hesperetin, the aglycone of hesperidin. This study investigates to what extent other flavonoids modulate the metabolism and transport of hesperetin by characterizing the effect of co-administrating a series of flavonoids using Caco-2 cell monolayers in a two-compartment transwell system. Flavonoids may interfere with hesperetin metabolism and can also inhibit the apically located ABC transporter BCRP (ABCG2) which was previously shown to be responsible for the apical transport of hesperetin metabolites. Co-exposure of Caco-2 cell monolayers to hesperetin with specific flavonoids reduced the ratio of apical efflux to basolateral transport of hesperetin metabolites, and in some cases, also reduced the amount of hesperetin metabolites detected extracellularly. Because intracellular accumulation of hesperetin metabolites did not account for this decrease, inhibition of metabolism of hesperetin is likely the underlying mechanism for the reduced metabolite formation and excretion. In spite of the reduction in metabolism the amount of hesperetin metabolites transported to the basolateral side significantly increased upon co-exposure with specific flavonoids and therefore co-administration of specific flavonoids could be a strategy to improve the bioavailability of hesperetin.

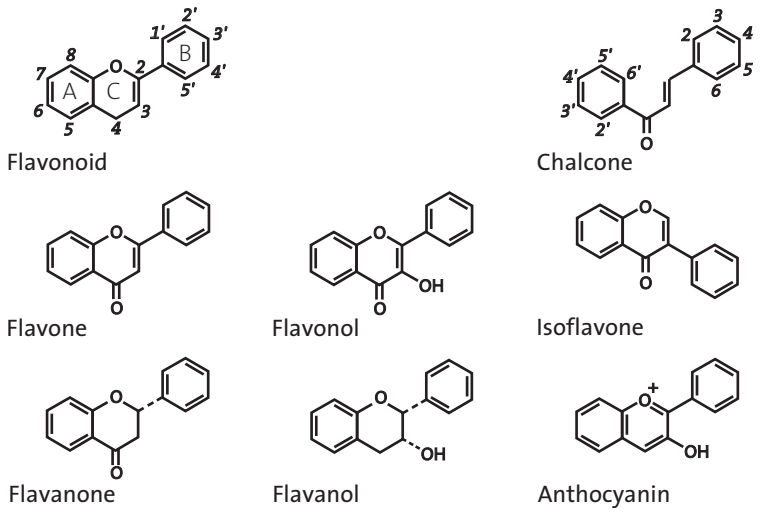

Figure 4.1 *Basic chemical flavonoid structure and basic chemical structures of different flavonoid subclasses.*

Introduction

Flavonoids are polyphenols and can be divided into different classes including flavones, flavonols (3-hydroxyflavones), isoflavones, flavanones, flavanols, chalcones and anthocyanins (Fig. 4.1 on page 70). They are present in fruits, vegetables and plant derived products, often occurring as ß-glycosides[1]. Flavonoids and flavonoid-rich products have been implicated as beneficial agents to reduce the risk of chronic diseases[2]. Despite their relatively high dietary intake, the bioavailability of many flavonoids and/or their metabolites is relatively poor[3]. Dependent on the type of flavonoid, a significant proportion can be attributed to efficient intestinal metabolism and/or efflux mediated by ATP binding cassette (ABC) transport proteins located in the apical membrane of enterocytes, including P-glycoprotein (Pgp/MDR1/ABCB1), multidrug resistance proteins (MRPs/ABCCs) and breast cancer resistance protein (BCRP/ABCG2)[4-7].

The flavanone hesperetin (3',5,7-trihydroxy-4'-methoxyflavanone) is the aglycone of hesperidin (hesperetin 7-*O*-rutinoside) which contains a disaccharide moiety (Figure 4.2), which is present in high amounts in sweet oranges (*Citrus sinensis*) and orange juice, but also in other citrus fruits including lemon, lime and mandarin[8]. For example, orange juice may contain more than 500 mg/l hesperidin[8]. Both hesperidin and hesperetin have been reported to provide beneficial health effects, as has been reviewed by Garg *et al.*[9]. The reported beneficial health effects of hesperetin include a reduced risk of osteoporosis, which has been demonstrated by an increased bone mineral density in ovariectomized or sham operated rats or mice given hesperidin[10,11]. Although the exact molecular mechanism for these effects have not yet been elucidated, some explanation arises from the anti-oxidant and anti-inflammatory properties of hesperetin affecting nuclear factor (NF)-κB and related signal transduction pathways[12].

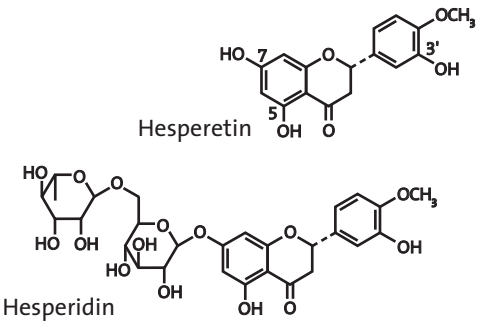

Figure 4.2 *Chemical structures of the rutinoside hesperidin and its aglycone hesperetin ((+/-)-4'-methoxy-3',5,7-trihydroxyflavone).*

Hesperidin must be hydrolyzed by colonic microflora before it can be absorbed, whereas the hesperetin aglycone, as well as the monosaccharide hesperetin 7-*O*-glucoside, is already taken up earlier in the digestive tract[13,14]. The latter could be hydrolyzed by lactase phlorizin hydrolase whereafter the hesperetin aglycone can migrate into the intestinal cells and/or the hesperetin glucoside could be transported into the intestinal cells via the sodium-dependent glucose transporter (SGLT1) after which it is deglucosylated by ß-glucosidase activity within the intestinal cell[13,15,16]. The resulting intracellularly located hesperetin aglycone is conjugated by UDP-glucuronosyltransferase (UGT) and sulfotransferase (SULT) enzymes into glucuronidated and sulfated metabolites, respectively, which have been detected in human and rat plasma[17-20]. An increased bioavailability of hesperetin by exposure to hesperetin 7-*O*-glucoside, which is already taken up in the small intestine, rather than to hesperidin[13], has been demonstrated to more efficiently prevent bone loss in ovariectomized rats[21].
Recently, we studied the intestinal metabolism and extracellular transport of hesperetin *in vitro* using Caco-2 cell monolayers in a two-compartment transwell system, simulating the intestinal transport barrier, and demonstrated that hesperetin was metabolized into hesperetin 7-*O*-glucuronide and hesperetin 7-*O*-sulfate metabolites which were preferentially transported to the apical compartment, simulating the intestinal lumen side[7]. Inhibition of the apically expressed BCRP by standard inhibitors reversed the predominant side of hesperetin metabolite efflux to the basolateral compartment, simulating the blood/plasma side[7]. Since intestinal BCRP-mediated apical efflux of hesperetin metabolites could be a limiting factor in the bioavailability of hesperetin, co-administration of hesperetin with dietary compounds inhibiting BCRP mediated efflux could be a strategy to increase hesperetin bioavailability. Some dietary flavonoids are potent BCRP inhibitors[22,23]. Furthermore, these flavonoids may also modulate the enzymes catalyzing phase II biotransformation thereby influencing the bioavailability of hesperetin and/or its metabolites by a second mechanism. The aim of the present study was to investigate to what extent other flavonoids modulate the metabolism and intestinal transport of hesperetin. To this end we tested the ability of a selection of different flavonoids (Table 4.1 on page 73) to modulate the metabolism and transport of hesperetin in Caco-2 cell monolayers as an intestinal *in vitro* model system. The results obtained provide insight in the flavonoid-mediated modulation of the two processes influencing hesperetin bioavailability: its metabolism by phase II enzymes and the extracellular transport of its conjugates. They also provide a possible strategy to improve the bioavailability of hesperetin.

Table 4.1 *Flavonoids used in the present study which have been reported to inhibit (+), or not to inhibit (-), BCRP in different in vitro studies.*

Flavonoid class	Flavonoid	Systematic name	Inhibition of BCRP	Effect reported in literature
Rutinosides	Hesperidin	Hesperetin-7-O-rutinoside		
	Rutin	Quercetin-3-O-rutinoside	-	SN-38 and mitoxantrone accumulation in BCRP transfected K562 cells[27,35].
Flavonols	Quercetin	3,3',4',5,7-pentahydroxyflavone	+	Mitoxantrone and bodipy-FL-prazosin accumulation in drug selected BCRP overexpressing MCF-7 cells and BCRP transfected K562 cells[34] and mitoxantrone accumulation in drug selected BCRP overexpressing MCF-7 and NCI-H460 cells[36].
			-	SN-38 and mitoxantrone accumulation in BCRP transfected K562 cells[27,35].
	Isorhamnetin	3,4',5,7-tetrahydroxy-3'-methoxyflavone		
	Galangin	3,5,7-trihydroxyflavone	+	SN-38 and mitoxantrone accumulation in BCRP transfected K562 cells[27,35] and mitoxantrone accumulation in BCRP transfected HEK-293 cells[28].
	Kaempferide	3,5,7-trihydroxy-4'-methoxyflavone	+	SN-38 and mitoxantrone accumulation in BCRP transfected K562 cells[27,35].
Flavones	Chrysin	5,7-dihydroxyflavone	+	SN-38 and mitoxantrone accumulation in BCRP transfected K562 cells[27,35], mitoxantrone accumulation in BCRP transfected HEK-293 cells[28] and mitoxantrone accumulation in drug selected BCRP overexpressing MCF-7 and NCI-H460 cells[36].
	Acacetin	5,7-dihydroxy-4'-methoxyflavone	+	SN-38 and mitoxantrone accumulation in BCRP transfected K562 cells[27,35].
Isoflavones	Genistein	4',5,7-trihydroxyisoflavone	+	SN-38 and mitoxantrone accumulation in BCRP transfected K562 cells[27,35], mitoxantrone accumulation in BCRP transfected HEK-293 cells[28] and mitoxantrone accumulation in drug selected BCRP overexpressing MCF-7 and NCI-H460 cells[36].
	Daidzein	4',7-dihydroxyisoflavone	+	SN-38 and mitoxantrone accumulation in BCRP transfected K562 cells[27,35], mitoxantrone and bodipy-FL-prazosin accumulation in drug selected BCRP overexpressing MCF-7 cells and BCRP transfected K562 cells[34] and mitoxantrone accumulation in drug selected BCRP overexpressing MCF-7 and NCI-H460 cells[36].
	Biochanin A	5,7-dihydroxy-4'-methoxyisoflavone	+	Mitoxantrone accumulation in drug selected BCRP overexpressing MCF-7 and NCI-H460 cells[36].
Flavanols	(+)-Catechin	(+)-3,3',4',5,7-pentahydroxyflavane	-	SN-38 and mitoxantrone accumulation in BCRP transfected K562 cells[27,35].
	(-)-EGCG	(-)-3,3',4',5,5',7-hexahydroxyflavan-3-gallate	-	Mitoxantrone accumulation in drug selected BCRP overexpressing MCF-7 and NCI-H460 cells [36].
	(-)-Epicatechin	(-)-3,3',4',5,7-pentahydroxyflavane		
Chalcones	Phloretin	2',4,4',6'-tetrahydroxydihydrochalcone	-	SN-38 and mitoxantrone accumulation in BCRP transfected K562 cells[27,35] and mitoxantrone accumulation in drug selected BCRP overexpressing MCF-7 and NCI-H460 cells[36].

Materials and methods

Materials

The flavonoids acacetin (purity ≥ 85 %), chrysin (purity ≥ 99 %) and genistein (purity ≥ 98 %) were obtained from ICN Biomedicals (Aurora, OH), biochanin A (purity ≥ 97 %), (+)-catechin hydrate (purity ≥ 98 %), (-)-epigallocatechin gallate (EGCG) (purity ≥ 97%), (-)-epicatechin (purity ≥ 90%), hesperetin (purity ≥ 95%), hesperidin (purity ~90%), phloretin (purity ≥ 98%) and quercetin dihydrate (purity ≥ 95%) from Sigma (St. Louis, MO), daidzein (purity ≥ 98%) from Indofine Chemical Company (Belle Mead, NJ), isorhamnetin (purity ≥ 99 %) and kaempferide (purity ≥ 99 %) from Extrasynthèse (Genay, France), galangin (purity ≥ 95 %) from Aldrich (Milwaukee, WI) and rutin (purity ≥ 97 %) from Acros (Morris Plains, NJ). Authentic standards of hesperetin 7-*O*-glucuronide (purity 92.8 %) and hesperetin 7-*O*-sulfate (purity <50 %) were obtained from the Nestlé Research Center (Lausanne, Switzerland). *L*-ascorbic acid was purchased from Sigma (St. Louis, MO), acetonitrile and methanol from Sigma-Aldrich (Steinheim, Germany), trifluoroacetic acid from J.T. Baker (Philipsburg, NJ), DMSO and EDTA disodium salt dihydrate from Merck (Darmstadt, Germany) and all cell culture reagents from Gibco (Paisley, UK).

Cell culture

Caco-2 cells from ATCC (Manassas, VA) were cultured in a humidified atmosphere of 5 % CO_2 and 95 % air at 37°C in Dulbecco's modified Eagle's medium (DMEM) supplemented with 10 % heat inactivated fetal bovine serum, MEM non-essential amino acids and 0.1 mg/ml gentamycin, as described before[7]. For transport experiments, 1×10^5 cells per cm^2 were seeded in Corning Costar 12-well transwell plate inserts with an insert membrane pore size of 0.4 µm and a growth area of 1.12 cm^2. The medium was changed 3 times a week and the experiments were performed 18 or 19 days post seeding. The passage number of the cells used in the experiments was between 39 and 50.

Caco-2 cell monolayer experiments

Before exposure, Caco-2 cell monolayers were washed with DMEM (without phenol red). The integrity of the monolayers was checked by measuring trans-epithelial electrical resistance (TEER) values with a Millicell ERS volt/ohmmeter from Millipore (Bedford, MA). Only monolayers demonstrating a TEER value between 500 and 1000 $\Omega \cdot cm^2$ were used. Transport experiments were carried out with medium consisting of DMEM (without phenol red) supplemented with 1% (v/v) MEM non-essential amino acids and 1 mM ascorbic acid to prevent auto-oxidation of the flavonoids, which was filtered through a cellulose acetate sterile syringe filter (0.2 µm) from VWR (West Chester, PA). To study the effect of co-administration of

flavonoids, Caco-2 cell monolayers were exposed at the apical side to 10 μM hesperetin, in the absence or presence of 10 μM of a specific flavonoid added to the apical side. The flavonoids tested are listed in Table 4.1 on page 73, and include flavonoids reported to inhibit BCRP as well as flavonoids reported not to inhibit BCRP. References reporting these flavonoid characteristics with respect to BCRP are also presented in Table 4.1. The concentration of 10 μM reflects a physiologically relevant dose and corresponds with our earlier study[7]. All flavonoids were added to the exposure medium from 400 times concentrated stock solutions in DMSO. The concentration of DMSO at the apical side was kept at 0.5% in each transport experiment. After 120 min exposure, 150 μl samples were taken from both the basolateral and apical compartment and the TEER value was re-checked to confirm the quality of the monolayer after the experiment. In an additional experiment Caco-2 cell monolayers were exposed to hesperetin in the presence or absence of quercetin and in addition to the hesperetin metabolites in the basolateral and apical media also the intracellular levels of hesperetin metabolites and hesperetin were determined. To determine the intracellular hesperetin and hesperetin metabolite levels, the filters of 2 transwell plates covered with Caco-2 cell monolayers exposed for 120 minutes to 10 μM hesperetin with or without 10 μM quercetin added at the apical side were washed with phosphate-buffered saline containing 22 mg/l EDTA, cut out of the insert, suspended in 200 μl of 65 % (v/v) methanol and sonicated for 15 min using a Bandalin Sonorex RK100 (Berlin, Germany). All samples were stored at -80 °C until further analysis by HPLC-DAD.

HPLC-DAD analysis

The HPLC system consisted of a Waters (Milford, MA) Alliance 2695 separation module with autosampler connected to a Waters 2996 photodiode array detector and was equipped with an Alltech (Breda, The Netherlands) Alltima C18 5 μm 150×4.6 mm^2 reverse phase column with 7.5×4.6 mm^2 guard column. Before injection, samples were centrifuged at 16,000 *g* for 4 min and 50 μl of the supernatant was injected and eluted at a flow rate of 1 ml/min. The gradient of the method to analyze the medium samples from the Caco-2 monolayer transport and metabolism experiments was reported previously[7]. The HPLC chromatograms of the medium from Caco-2 cell monolayers co-exposed with other flavonoids demonstrated no peak overlap of hesperetin or hesperetin metabolite peaks with other peaks resulting from the simultaneously added flavonoids, which was confirmed by analysis of medium from Caco-2 monolayers exposed only to the flavonoids used for co-administration (data not shown). All DAD spectra were recorded between 200 and 420 nm, and HPLC chromatograms acquired at 280 nm were used for quantification.

Quantification

Hesperetin and hesperetin 7-*O*-glucuronide were quantified by peak area measurement using calibration curves (R^2>0.99) of relevant concentration series of available reference compounds. The limit of detection was 0.02 µM, and the lower limit of quantification was 0.06 µM (injection volume 50 µl). Hesperetin 7-*O*-sulfate was quantified on the basis of the hesperetin 7-*O*-glucuronide calibration curve, since it demonstrated a comparable molar extinction coefficient and maximum absorption wavelength[7].

Statistics

The Student's two-tailed paired *t*-test was used to evaluate statistical differences between the hesperetin metabolite transport in Caco-2 monolayers exposed to hesperetin in the presence of another flavonoid and the control (only exposed to hesperetin) from the same transwell plate. Statistical differences in the experiment analyzing the intracellular content were evaluated using Student's two-tailed unpaired *t*-test. Differences were considered significant when *p*-values were less than 0.05. Values are expressed as mean and variances as standard deviation (SD).

Results

When hesperetin (10 µM) is incubated for 120 min with Caco-2 cell monolayers, it is efficiently metabolized into hesperetin 7-*O*-glucuronide and hesperetin 7-*O*-sulfate, of which the efflux is linear with time, and 28% of the initial amount of hesperetin aglycone can be recovered from the apical, basolateral and intracellular compartment[7]. On average (±SD) 1.73 (±0.48) nmol and 0.47 (±0.18) nmol of hesperetin 7-*O*-glucuronide were transported to the apical and basolateral side, respectively, and 0.34 (±0.24) nmol and 0.19 (±0.36) nmol of hesperetin 7-*O*-sulfate were transported to the apical and basolateral side, respectively (average values of all controls, n= 18).

On co-incubation with 10 µM of several of the tested flavonoids the efflux of hesperetin metabolites to the apical side of the Caco-2 cell monolayer decreased, while the transport to the basolateral side increased (Table 4.2 on page 77 and Figure 4.3 on page 78). Co-incubation with hesperetin and especially flavonols, including galangin, isorhamnetin, kaempferide and quercetin, as well as with the flavones acacetin and chrysin, had the most pronounced effect. Significant effects were also demonstrated upon co-incubation of Caco-2 cell monolayers with hesperetin and the isoflavones biochanin A, daidzein and genistein. Interestingly, the apical efflux of specifically hesperetin 7-*O*-sulfate was increased instead of decreased by the co-administration of the isoflavones (Table 4.2 on page 77).

Table 4.2 *Effect of different flavonoids (10 µM) on the apical and basolateral amounts of hesperetin metabolites as percentage of the control detected after 120 min incubation of Caco-2 cell monolayers with 10 µM hesperetin with or without 10 µM of the respective flavonoids added to the apical side expressed as mean (± SD) percent of control (only 10 µM hesperetin). n = 9-11. M1=hesperetin 7-O-glucuronide, M2=hesperetin 7-O-sulfate. (1) = p<0.05, (2) = p<0.01 and (3) = p<0.001 significantly different from the corresponding controls.*

	Apical			Basolateral		
	M1 (%)	**M2 (%)**	**Sum (%)**	**M1 (%)**	**M2 (%)**	**Sum (%)**
Acacetin	*59.1 ± 14.4*$^{(3)}$	*80.2 ± 19.5*$^{(1)}$	*61.0 ± 13.7*$^{(3)}$	*165 ± 39*$^{(3)}$	*154 ± 38*$^{(1)}$	*163 ± 36*$^{(3)}$
Biochanin A	*64.0 ± 11.7*$^{(3)}$	*143 ± 34*$^{(3)}$	*75.5 ± 9.4*$^{(3)}$	*160 ± 51*$^{(2)}$	*171 ± 30*$^{(3)}$	*159 ± 38*$^{(3)}$
(+)-Catechin	*112 ± 37*	*95.3 ± 10.3*	*104 ± 25*	*124 ± 67*	*103 ± 30*	*115 ± 51*
Chrysin	*61.4 ± 11.6*$^{(3)}$	*84.5 ± 17.6*$^{(1)}$	*64.6 ± 11.5*$^{(3)}$	*201 ± 53*$^{(2)}$	*136 ± 45*	*179 ± 49*$^{(3)}$
Daidzein	*70.4 ± 19.5*$^{(2)}$	*130 ± 22*$^{(3)}$	*79.4 ± 17.7*$^{(2)}$	*129 ± 48*	*114 ± 29*	*122 ± 36*
(-)-EGCG	*115 ± 39*	*94.1 ± 11.5*	*107 ± 27*	*105 ± 53*	*90.5 ± 28*	*99.3 ± 42*
(-)-Epicatechin	*114 ± 36*	*94.1 ± 16.4*	*106 ± 26*	*122 ± 55*	*111 ± 37*	*117 ± 45*
Galangin	*47.6 ± 6.8*$^{(3)}$	*111 ± 33*	*56.2 ± 6.2*$^{(3)}$	*140 ± 37*$^{(2)}$	*190 ± 46*$^{(2)}$	*151 ± 55*$^{(2)}$
Genistein	*59.9 ± 14.5*$^{(3)}$	*119 ± 23*$^{(1)}$	*71.1 ± 14.4*$^{(3)}$	*167 ± 46*$^{(3)}$	*144 ± 39*$^{(1)}$	*157 ± 38*$^{(3)}$
Hesperidin	*94.4 ± 11.7*	*101 ± 13*	*95.5 ± 11.7*	*95.2 ± 22.6*	*88.3 ± 24.6*	*93.4 ± 21.7*
Isorhamnetin	*49.3 ± 16.6*$^{(2)}$	*79.2 ± 3.0*$^{(3)}$	*38.6 ± 1.3*$^{(3)}$	*176 ± 42*$^{(3)}$	*336 ± 46*$^{(3)}$	*178 ± 23*$^{(2)}$
Kaempferide	*51.0 ± 15.8*$^{(3)}$	*94.0 ± 20.8*	*55.7 ± 12.6*$^{(3)}$	*164 ± 51*$^{(2)}$	*227 ± 61*$^{(3)}$	*175 ± 43*$^{(3)}$
Phloretin	*91.0 ± 21.5*$^{(1)}$	*78.1 ± 13.8*$^{(2)}$	*86.7 ± 16.0*$^{(2)}$	*120 ± 39*	*120 ± 51*	*120 ± 43*
Quercetin	*38.0 ± 11.8*$^{(3)}$	*80.6 ± 52.8*	*43.2 ± 15.3*$^{(3)}$	*202 ± 77*$^{(3)}$	*235 ± 92*$^{(3)}$	*202 ± 76*$^{(3)}$
Rutin	*103 ± 23*	*98.6 ± 14.3*	*99.1 ± 17.4*	*87.0 ± 14.1*$^{(1)}$	*97.2 ± 20.4*	*91.3 ± 10.9*

Co-incubation with hesperetin and the chalcone phloretin significantly decreased the apical efflux of hesperetin metabolites only by 13.3%, and co-incubation with flavanols including (+)-catechin, EGCG and (-)-epicatechin, as well as with the rutinosides hesperidin and rutin, did not affect the disposition of hesperetin metabolites under the applied experimental conditions (Table 4.2 on page 77) and Figure 4.3.

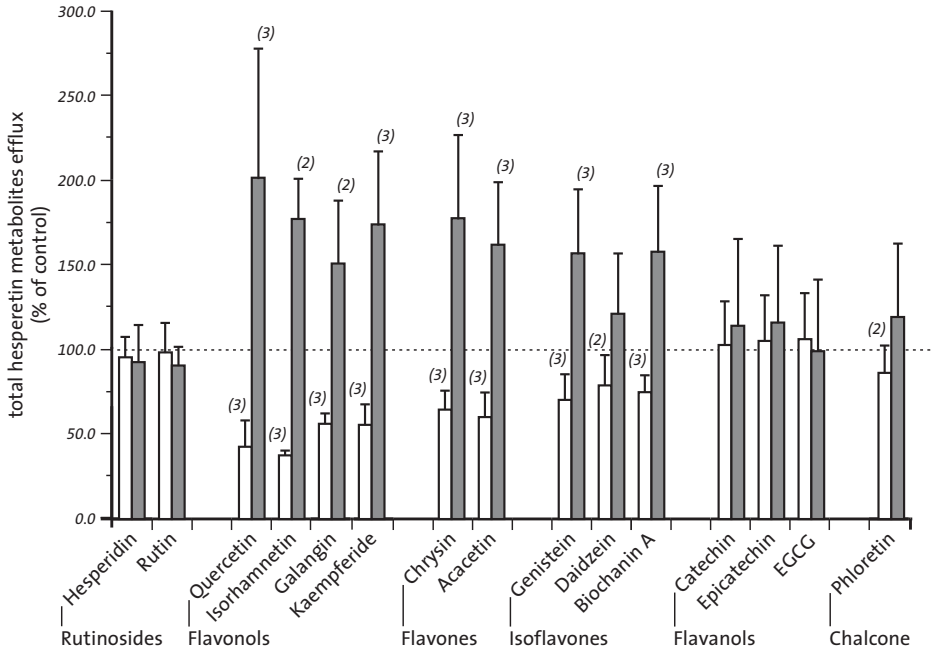

Figure 4.3 *Effect of different flavonoids, grouped per class, on the apical (□) and basolateral (■) efflux of hesperetin metabolites (hesperetin 7-O-glucuronide plus hesperetin 7-O-sulfate) as percentage of the control, detected after 120 min incubation of Caco-2 cell monolayers with 10 µM hesperetin with or without 10 µM of the respective flavonoids added to the apical side. Mean ± SD values shown (n= 9-11). (2) = p<0.01; (3) = p<0.001 significantly different compared with the paired controls.*

In the controls, the average basolateral/apical (BL/AP) ratio of hesperetin metabolite transport was 0.36 (Figure 4.4 on page 79). Co-incubation of the Caco-2 cell monolayers with hesperetin and chrysin, isorhamnetin or quercetin increased this ratio above 1 which effectively reverses the predominant side of hesperetin metabolite efflux (Figure 4.4 on page 79), with quercetin being the most potent modulator (BL/AP ratio 1.7).

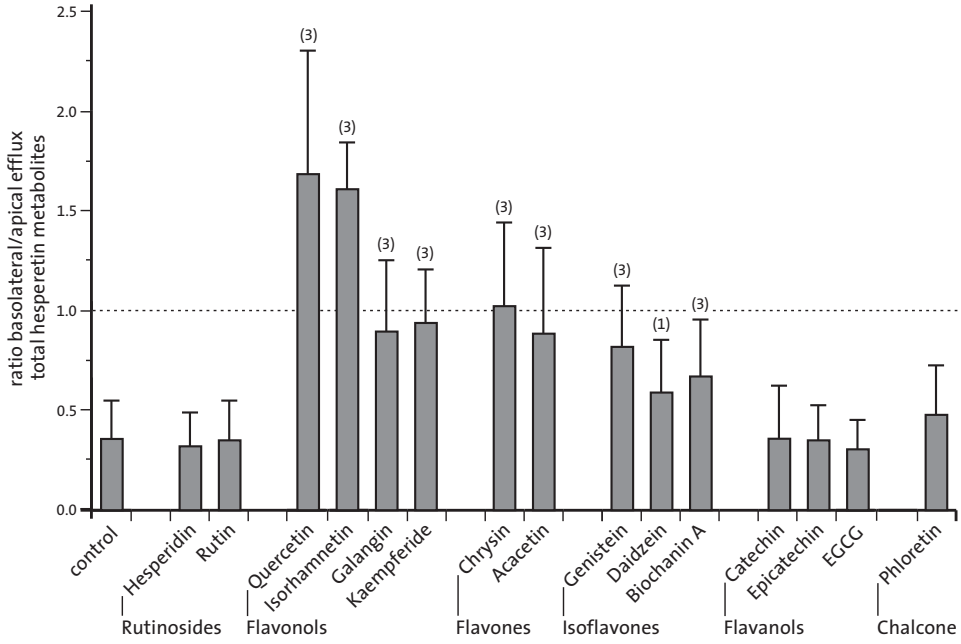

Figure 4.4 *Effect of co-administration of different flavonoids, grouped per class, on the ratio basolateral/apical efflux of hesperetin metabolites (hesperetin 7-O-glucuronide plus hesperetin 7-O-sulfate), detected after 120 min incubation of Caco-2 cell monolayers with 10 µM hesperetin with or without 10 µM of the respective flavonoids added to the apical side. Mean ± SD values shown (n= 9-11, control n=18). (1) = p<0.05; (2) = p<0.001 significantly different compared with the paired controls.*

However, co-administration of the flavonoids affecting the disposition of hesperetin metabolites also negatively affected the sum of amounts of hesperetin metabolite transported to the apical and basolateral side (Figure 4.5 on page 80). The possible mechanism underlying this effect was investigated further for the experiments with co-administration with quercetin, which significantly ($p<0.01$) decreased the total amount of hesperetin metabolites detected in the apical and basolateral side by 23% (Figure 4.5 on page 80). An additional experiment was performed in which the intracellular contents of the Caco-2 cell monolayers exposed to hesperetin or the combination of hesperetin and quercetin after 120 min was analyzed. Only small amounts (~3%) of the total amount of hesperetin metabolites detected were present inside the Caco-2 cells (Figure 4.6 on page 81). Although co-administration of quercetin showed a significant ($p<0.05$) increase of 16% in the amount of hesperetin metabolites inside the cell, this amount accounts for only 5% of the total decrease of hesperetin metabolites detected extracellularly, demonstrating that the major part of the decrease (95%) in the total amount of hesperetin metabolites (0.69 nmol) is

likely caused by inhibition of the phase II conjugation by co-exposure to quercetin. This is also reflected by a 70% higher total amount of hesperetin aglycone (0.68 nmol) (Figure 4.6 on page 81).

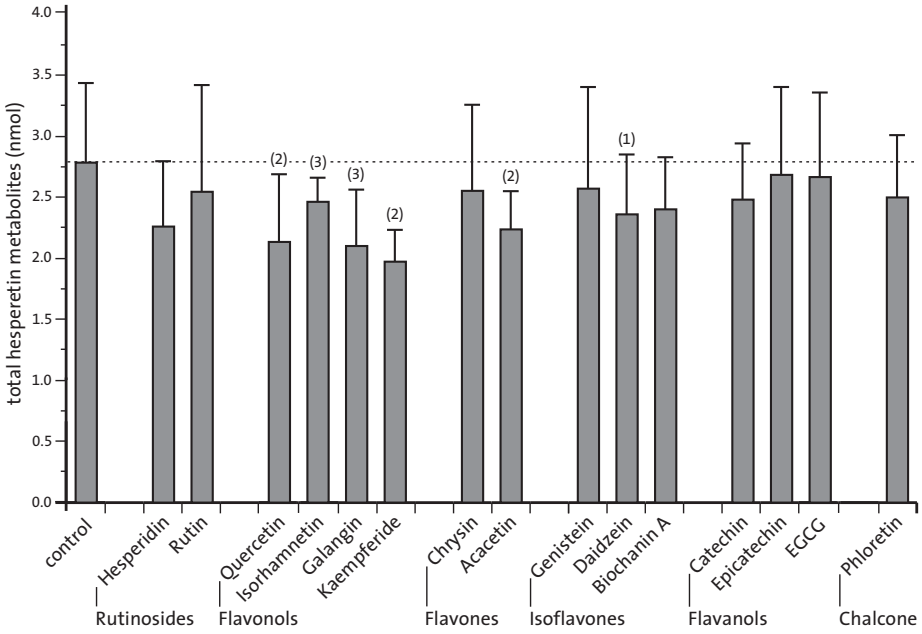

Figure 4.5 *Effect of co-administration of different flavonoids, grouped per class, on the sum of hesperetin metabolites at the basolateral and apical side of Caco-2 cell monolayers, detected after 120 min incubation of Caco-2 cell monolayers with 10 µM hesperetin with or without 10 µM of the respective flavonoids added to the apical side. Mean ± SD values shown (n= 9-11, control n=18). (1) = p<0.05; (2) = P<0.01; (3) = p<0.001 significantly different compared with the paired controls.*

The amount of 3.5 nmol of hesperetin and hesperetin metabolites recovered 120 min upon exposure in the apical, basolateral and intracellular compartments account for only 70% of the initial dose (5 nmol). At least part of the explanation for the residual loss of hesperetin unaccounted for could be the apparent instability or insolubility of hesperetin aglycone under experimental conditions or during storage, leading to losses in the overall amount of hesperetin plus metabolites[7].

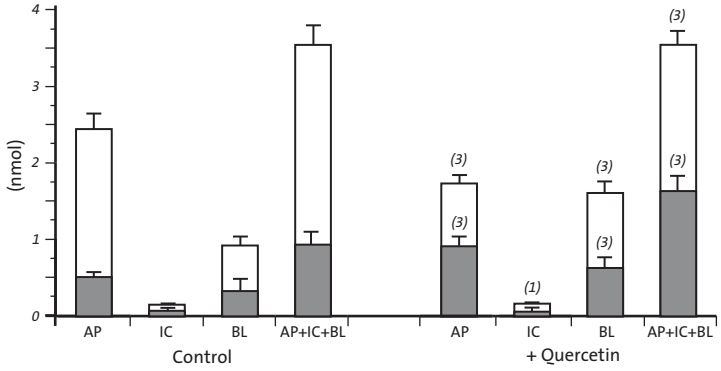

Figure 4.6 *Effect of co-administration of quercetin (10 µM) on the amount of hesperetin metabolites (hesperetin 7-O-glucuronide plus hesperetin 7-O-sulfate) (□) and hesperetin aglycone (■) detected in the apical (AP), intracellular (IC) and basolateral (BL) compartment of the Caco-2 cell monolayers, and the sum of amounts in these compartments (AP+IC+BL), detected after 120 min, compared with the Caco-2 cell monolayers only exposed to hesperetin (control). Mean + SD values shown (n=10). (1) = p<0.05; (3) = p<0.001 significantly different compared with the control.*

Discussion

Metabolism by phase II enzymes and transport from intestinal cells back into the lumen by ATP binding cassette (ABC) transporters limit the bioavailability of flavonoids[4-7]. Recently we demonstrated an important role for the ABC transporter BCRP in the efflux of hesperetin metabolites to the apical side of Caco-2 cell monolayers, an *in vitro* model of the intestinal barrier, by co-administration of standard BCRP inhibitors such as GF120918 and Ko143[7]. The objective of the present study was to identify whether this effect could also be achieved by co-administration of hesperetin with other flavonoids, since certain flavonoids were demonstrated to be potent inhibitors of BCRP (Table 1 and references therein), and also to define to what extent flavonoids may affect the phase II metabolism of hesperetin, representing the second mechanism that may influence the bioavailability of hesperetin[24].

Hesperetin is metabolized by Caco-2 cell monolayers into hesperetin 7-*O*-glucuronide and hesperetin 7-*O*-sulfate which are mainly transported to the apical side[7], and hesperetin partly migrates through the monolayer passively[7,25,26]. Co-administration of hesperetin with flavonoids, previously reported to inhibit BCRP *in vitro*, decreased the apical efflux of hesperetin metabolites and increased the transport to the basolateral side, while flavonoids from classes reported not to inhibit BCRP (flavanols, rutinosides) did not affect the disposition (Table 4.1 on page 73 and Table 4.2 on page 77, Figure 4.3 on page 78 and Figure 4.4 on page 79).

In general, the order of potency was flavonols>flavones>isoflavones. This order is in line with structure-activity relationships which have been proposed for flavonoid-mediated BCRP inhibition: the 2,3-double bond in ring C as well as ring B attached at position 2, are structural requirements for effective BCRP inhibition, although the lack of hydroxylation at position 3, as in flavones, not flavonols, has been defined as an important structural requirement as well[27-29]. The rutinoside hesperidin is probably not taken up by Caco-2 cells[25], although there is one report where rutin has been proposed to occur intracellularly in Caco-2 cells[26]. Moreover, rutin has been described to decrease the apical to basolateral transport of genistein through Caco-2 cell monolayers, albeit at relatively high concentrations of 50 and 150 μM rutin[30]. This effect might be due to an inhibitory effect of rutin on a basolateral transporter, which is in line with the slight decrease in the basolateral amount of hesperetin 7-*O*-glucuronide detected in our studies upon co-exposure to rutin (Table 4.2).

Under the applied experimental conditions in this study, that include the use of only a single dose, quercetin, isorhamnetin and chrysin were demonstrated to be the most potent modulator of hesperetin metabolite disposition, reversing the predominant side of efflux from the apical to the basolateral side (Figure 4.4). Co-exposure to flavonoids that significantly modulated the BL/AP ratio also resulted in a decreased amount of hesperetin metabolites excreted from the cells (Figure 4.5 on page 80), but intracellular accumulation of hesperetin metabolites did not account for this decrease (Figure 4.6 on page 81). In fact, only a small amount of the total amount of hesperetin metabolites was detected in the cellular compartment, which indicates a high affinity of ABC transporters towards conjugates of hesperetin, a conclusion advanced previously to explain the negligible amounts of metabolites of the flavone baicalein in Caco-2 cells[31]. Since quercetin is also known to be metabolized by Caco-2 cells into glucuronidated and sulfonated metabolites[32,33], a (competitive) inhibitory effect of quercetin on the phase II metabolism of hesperetin might be the reason for the 27% decrease in the total amount of hesperetin metabolites formed by the Caco-2 cells upon co-exposure with quercetin.

Specific flavonoids have been described as potent modulators of BCRP-mediated activity[22,23], including hesperetin itself[27,34-37], and specific combinations of flavonoids have demonstrated an additive effect on the inhibition of BCRP *in vitro*[37], although the exact mechanism of interaction is not precisely defined. Flavonoids and/or their metabolites could interact directly with BCRP associated ATP-ase activity[34], however, as high affinity substrates they probably also (competitively) inhibit BCRP-mediated transport. Since different flavonoids are substrates and/or modulators, interaction between different flavonoids may affect

their respective bioavailability.

Inhibition of murine BCRP (Bcrp1) has been demonstrated to increase the bioavailability of total plasma quercetin while limiting the intestinal efflux of quercetin glucuronide metabolites[5], indicating a role for BCRP *in vivo* in the efflux of quercetin glucuronides to the intestinal lumen and bioavailability of total plasma quercetin. In a study on the bioavailability of biochanin A, a single oral co-administration of biochanin A together with the combination of quercetin and EGCG did increase the bioavailability of biochanin A in Sprague-Dawley rats[38]. This could be explained by the fact that BCRP plays an important role in limiting the bioavailability of both quercetin[5] and biochanin A[39], and that both have been demonstrated to interact with BCRP[34,36,37]. In another study, a 3-week period of co-administration of quercetin and (+)-catechin, the latter was reported not to interact with BCRP[27,35], did not result in an increased bioavailability of both compounds in Wistar rats fed a diet containing (+)-catechin, quercetin, or both[40]. Flavanols including (+)-catechin, (-)-epicatechin and EGCG, and/or their metabolites, preferably interact with other classes of ABC transporters such as MRPs[41-43]. Modulation of the intracellular amount or bioavailability of EGCG has been successfully demonstrated in HT-29 cells and CF-1 mice, respectively, in combination with genistein[44], which could be explained by the fact that both compounds have been reported to be substrates of MRPs[41,45].

In conclusion, the amount of hesperetin metabolites excreted to the basolateral side of the Caco-2 cell monolayer, representing the blood/plasma side of the intestinal barrier, was doubled upon co-exposure with μM concentrations of quercetin, in spite of the 27% reduction in phase II metabolite formation also resulting from the co-exposure with quercetin. Since the effect of quercetin on transport dominates over the effect on metabolism, co-administration of quercetin, or other specific flavonoids, could be a strategy to improve the limited bioavailability of hesperetin, which in turn could lead to an improved bioefficacy. Altogether, whether co-administration of other flavonoids could indeed increase the bioavailability of hesperetin *in vivo* remains to be elucidated and is currently under investigation in our laboratory.

Acknowledgements

We thank Dr. Denis Barron of Nestlé Research Center for supplying the hesperetin metabolite standards and Inge van der Wel and Karin Ruigrok for their initial experiments with Caco-2 monolayers and combinations of flavonoids. This study was supported by a research grant from Nestlé Research Center (Lausanne, Switzerland).

References

1 Scalbert A, Williamson G. Dietary intake and bioavailability of polyphenols. *J Nutr* 130(8S Suppl): 2073S-2085S, 2000.

2 Havsteen BH. The biochemistry and medical significance of the flavonoids. *Pharmacol Ther* 96(2-3): 67-202, 2002.

3 anach C, Williamson G, Morand C, Scalbert A, Remesy C. Bioavailability and bioefficacy of polyphenols in humans. I. Review of 97 bioavailability studies. *Am J Clin Nutr* 81(1 Suppl): 230S-242S, 2005.

4 Liu Z, Hu M. Natural polyphenol disposition via coupled metabolic pathways. *Expert Opin Drug Metab Toxicol* 3(3): 389-406, 2007.

5 Sesink ALA, Arts ICW, De Boer VCJ, Breedveld P, Schellens JHM, Hollman PCH, Russel FGM. Breast cancer resistance protein (Bcrp1/Abcg2) limits net intestinal uptake of quercetin in rats by facilitating apical efflux of glucuronides. *Mol Pharmacol* 67(6): 1999-2006, 2005.

6 Walle UK, Galijatovic A, Walle T. Transport of the flavonoid chrysin and its conjugated metabolites by the human intestinal cell line Caco-2. *Biochem Pharmacol* 58(3): 431-438, 1999.

7 Brand W, Van der Wel PAI, Rein MJ, Barron D, Williamson G, Van Bladeren PJ, Rietjens IMCM. Metabolism and transport of the citrus flavonoid hesperetin in Caco-2 cell monolayers. *Drug Metab Dispos* 36(9): 1794-1802, 2008.

8 Tomás-Barberán FA, Clifford MN. Flavanones, chalcones and dihydrochalcones - nature, occurrence and dietary burden. *J Sci Food Agric* 80(7): 1073-1080, 2000.

9 Garg A, Garg S, Zaneveld LJD, Singla AK. Chemistry and pharmacology of the citrus bioflavonoid hesperidin. *Phytother Res* 15(8): 655-669, 2001.

10 Horcajada MN, Habauzit V, Trzeciakiewicz A, Morand C, Gil-Izquierdo A, Mardon J, Lebecque P, Davicco MJ, Chee WSS, Coxam V, Offord E. Hesperidin inhibits ovariectomized-induced osteopenia and shows differential effects on bone mass and strength in young and adult intact rats. *J Appl Physiol* 104(3): 648-654, 2008.

11 Chiba H, Uehara M, Wu J, Wang X, Masuyama R, Suzuki K, Kanazawa K, Ishimi Y. Hesperidin, a citrus flavonoid, inhibits bone loss and decreases serum and hepatic lipids in ovariectomized mice. *J Nutr* 133(6): 1892-1897, 2003.

12 Kim JY, Jung KJ, Choi JS, Chung HY. Modulation of the age-related nuclear factor-kappaB (NF-kappaB) pathway by hesperetin. *Aging Cell* 5(5): 401-411, 2006.

13 Nielsen ILF, Chee WSS, Poulsen L, Offord-Cavin E, Rasmussen SE, Frederiksen H, Enslen M, Barron D, Horcajada M-N, Williamson G. Bioavailability is improved by enzymatic modification of the citrus flavonoid hesperidin in humans: a randomized, double-blind, crossover trial. *J Nutr* 136(2): 404-408, 2006.

14 Kanaze FI, Bounartzi MI, Georgarakis M, Niopas I. Pharmacokinetics of the citrus flavanone aglycones hesperetin and naringenin after single oral administration in human subjects. *Eur J Clin Nutr* 61(4): 472-477, 2007.

15 Day AJ, Gee JM, DuPont MS, Johnson IT, Williamson G. Absorption of quercetin-3-glucoside and quercetin-4'-glucoside in the rat small intestine: the role of lactase phlorizin hydrolase and the sodium-dependent glucose transporter. *Biochem Pharmacol* 65(7): 1199-1206, 2003.

16 Walgren RA, Lin JT, Kinne RK, Walle T. Cellular uptake of dietary flavonoid quercetin 4'-beta-glucoside by sodium-dependent glucose transporter SGLT1. *J Pharmacol Exp Ther* 294(3): 837-843, 2000.

17 Ameer B, Weintraub RA, Johnson JV, Yost RA, Rouseff RL. Flavanone absorption after naringin, hesperidin, and citrus administration. *Clin Pharmacol Ther* 60(1): 34-40, 1996.

18 Gardana C, Guarnieri S, Riso P, Simonetti P, Porrini M. Flavanone plasma pharmacokinetics from blood orange juice in human subjects. *Br J Nutr* 98(1): 165-172, 2007.

19 Manach C, Morand C, Gil-Izquierdo A, Bouteloup-Demange C, Rémésy C. Bioavailability in humans of the flavanones hesperidin and narirutin after the ingestion of two doses of orange juice. *Eur J Clin Nutr* 57(2): 235-242, 2003.

20 Mullen W, Archeveque M-A, Edwards CA, Matsumoto H, Crozier A. Bioavailability and metabolism of orange juice flavanones in humans: impact of a full-fat yogurt. *J Agric Food Chem* 56(23): 11157-11164, 2008.

21 Habauzit V, Nielsen IL, Gil-Izquierdo A, Morand C, Chee W, Barron D, Davicco MJ, Coxam V, Williamson G, Offord E, Horcajada MN. Increased bioavailability of hesperetin-7-glucoside compared to hesperidin results in more efficient prevention of bone loss in adult ovariectomized rats. *Br J Nutr* 102(7): 976-984, 2009.

22 Morris ME, Zhang S. Flavonoid-drug interactions: effects of flavonoids on ABC transporters. *Life Sci* 78(18): 2116-2130, 2006.

23 Brand W, Schutte ME, Williamson G, Van Zanden JJ, Cnubben NHP, Groten JP, Van

Bladeren PJ, Rietjens IMCM. Flavonoid-mediated inhibition of intestinal ABC transporters may affect the oral bioavailability of drugs, food-borne toxic compounds and bioactive ingredients. *Biomed Pharmacother* 60(9): 508-519, 2006.

24 Moon YJ, Wang X, Morris ME. Dietary flavonoids: effects on xenobiotic and carcinogen metabolism. *Toxicol In Vitro* 20(2): 187-210, 2006.

25 Serra H, Mendes T, Bronze MR, Simplício AL. Prediction of intestinal absorption and metabolism of pharmacologically active flavones and flavanones. *Bioorg Med Chem* 16(7): 4008-4018, 2008.

26 Tian X-J, Yang X-W, Yang X, Wang K. Studies of intestinal permeability of 36 flavonoids using Caco-2 cell monolayer model. *Int J Pharm* 367(1-2): 58-64, 2009.

27 Katayama K, Masuyama K, Yoshioka S, Hasegawa H, Mitsuhashi J, Sugimoto Y. Flavonoids inhibit breast cancer resistance protein-mediated drug resistance: transporter specificity and structure-activity relationship. *Cancer Chemother Pharmacol* 60(6): 789-797, 2007.

28 Ahmed-Belkacem A, Pozza A, Muñoz-Martinez F, Bates SE, Castanys S, Gamarro F, Di Pietro A, Pérez-Victoria JM. Flavonoid structure-activity studies identify 6-prenylchrysin and tectochrysin as potent and specific inhibitors of breast cancer resistance protein ABCG2. *Cancer Res* 65(11): 4852-4860, 2005.

29 Zhang S, Yang X, Coburn RA, Morris ME. Structure activity relationships and quantitative structure activity relationships for the flavonoid-mediated inhibition of breast cancer resistance protein. *Biochem Pharmacol* 70(4): 627-639, 2005.

30 Oitate M, Nakaki R, Koyabu N, Takanaga H, Matsuo H, Ohtani H, Sawada Y. Transcellular transport of genistein, a soybean-derived isoflavone, across human colon carcinoma cell line (Caco-2). *Biopharm Drug Dispos* 22(1): 23-29, 2001.

31 Zhang L, Lin G, Kovács B, Jani M, Krajcsi P, Zuo Z. Mechanistic study on the intestinal absorption and disposition of baicalein. *Eur J Pharm Sci* 31(3-4): 221-231, 2007.

32 Williamson G, Aeberli I, Miguet L, Zhang Z, Sanchez M-B, Crespy V, Barron D, Needs P, Kroon PA, Glavinas H, Krajcsi P, Grigorov M. Interaction of positional isomers of quercetin glucuronides with the transporter ABCC2 (cMOAT, MRP2). *Drug Metab Dispos* 35(8): 1262-1268, 2007.

33 Dihal AA, Woutersen RA, Van Ommen B, Rietjens IMCM, Stierum RH. Modulatory effects of quercetin on proliferation and differentiation of the human colorectal cell line Caco-2. *Cancer Lett* 238(2): 248-259, 2006.

34 Cooray HC, Janvilisri T, Van Veen HW, Hladky B, Barrand MA. Interaction of the breast cancer resistance protein with plant polyphenols. *Biochem Biophys Res Commun* 317(1): 269-275, 2004.

35 Imai Y, Tsukahara S, Asada S, Sugimoto Y. Phytoestrogens/flavonoids reverse breast cancer resistance protein/ABCG2-mediated multidrug resistance. *Cancer Res* 64(12): 4346-4352, 2004.

36 Zhang S, Yang X, Morris ME. Flavonoids are inhibitors of breast cancer resistance protein (ABCG2)-mediated transport. *Mol Pharmacol* 65(5): 1208-1216, 2004.

37 Zhang S, Yang X, Morris ME. Combined effects of multiple flavonoids on breast cancer resistance protein (ABCG2)-mediated transport. *Pharm Res* 21(7): 1263-1273, 2004.

38 Moon YJ, Morris ME. Pharmacokinetics and bioavailability of the bioflavonoid biochanin A: effects of quercetin and EGCG on biochanin A disposition in rats. *Mol Pharm* 4(6): 865-872, 2007.

39 Wang SWJ, Chen Y, Joseph T, Hu M. Variable Isoflavone Content of Red Clover Products Affects Intestinal Disposition of Biochanin A, Formononetin, Genistein, and Daidzein. *J Altern Complement Med* 14(3): 287-297, 2008.

40 Silberberg M, Morand C, Manach C, Scalbert A, Remesy C. Co-administration of quercetin and catechin in rats alters their absorption but not their metabolism. *Life Sci* 77(25): 3156-3167, 2005.

41 Hong J, Lambert JD, Lee S-H, Sinko PJ, Yang CS. Involvement of multidrug resistance-associated proteins in regulating cellular levels of (-)-epigallocatechin-3-gallate and its methyl metabolites. *Biochem Biophys Res Commun* 310(1): 222-227, 2003.

42 Vaidyanathan JB, Walle T. Cellular uptake and efflux of the tea flavonoid (-)epicatechin-3-gallate in the human intestinal cell line Caco-2. *J Pharmacol Exp Ther* 307(2): 745-752, 2003.

43 Zhang L, Zheng Y, Chow MSS, Zuo Z. Investigation of intestinal absorption and disposition of green tea catechins by Caco-2 monolayer model. *Int J Pharm* 287(1-2): 1-12, 2004.

44 Lambert JD, Kwon S-J, Ju J, Bose M, Lee M-J, Hong J, Hao X, Yang CS. Effect of genistein on the bioavailability and intestinal cancer chemopreventive activity of (-)-epigallocatechin-3-gallate. *Carcinogenesis* 29(10): 2019-2024, 2008.

45 Wortelboer HM, Usta M, Van Zanden JJ, Van Bladeren PJ, Rietjens IMCM, Cnubben NHP. Inhibition of multidrug resistance proteins MRP1 and MRP2 by a series of alpha,beta-unsaturated carbonyl compounds. *Biochem Pharmacol* 69(12): 1879-1890, 2005.

Chapter 5

Effect of co-administering quercetin on the bioavailability of hesperetin 7-*O*-glucoside in rats

Walter Brand, Bert Spenkelink, Marelle G. Boersma,
Sylvie Pridmore-Merten, Fabiola Dionisi, Peter J. van Bladeren,
Gary Williamson, and Ivonne M.C.M. Rietjens

in preparation

Abstract

The citrus flavonoid hesperetin (4'-methoxy-3',5,7-trihydroxyflavanone) has been associated with beneficial health effects including a reduced risk of osteoporosis. In spite of the relative high dietary intake of hesperetin from citrus consumption, the bioavailability of this flavonoid is limited. This is partly due to its efficient intestinal phase II metabolism and ABC transporter-mediated excretion from the intestinal cells back into the intestinal lumen during uptake. Our previous *in vitro* study revealed that co-administration of quercetin may increase the basolateral transport of hesperetin through intestinal cell monolayers at the cost of its apical transport, pointing at a possible way to increase hesperetin bioavailability. The objective of the present study was to investigate whether this observation could be confirmed in an *in vivo* rat model. Quercetin was previously shown to exert this effect in part by acting as an inhibitor of BCRP mediated apical intestinal transport. In the present study hesperetin 7-*O*-glucoside (15 or 3 mg/kg body weight (bw)) was administrated by oral gavage to Sprague-Dawley rats in the presence or absence of quercetin (15 mg/kg bw), and systemic blood was taken 15, 30, 45, 60, 90, 120, 240 and 480 min after dosing. The concentration of plasma hesperetin and its demethylated and remethylated metabolites (eriodictyol and homoeriodictyol) after treatment of blood samples with ß-glucuronidase/sulfatase were determined by uPLC-DAD. Co-administration of quercetin did increase total hesperetin plasma concentrations especially in the early phase of the concentration time curve when elimination was not yet dominating over uptake, but did not significantly increase the $AUC_{0\text{-}8h}$ (area under the concentration time curve from 0 to 8 hours). It is concluded that the effect of co-administration of quercetin as an inhibitor of apical intestinal ABC transporter mediated transport may result in an increased bioavailability of hesperetin especially during the early phase of exposure when absorption processes still dominate over elimination processes.

Introduction

Flavonoids are a large class of polyphenols present in fruits, vegetables and plant derived products, in which they often occur as ß-glycosides[1]. Despite their relatively high dietary intake (~1 g/day)[2], the bioavailability of many flavonoids and/or their metabolites is limited[3]. Dependent on the type of flavonoid, this limited bioavailability can for an important part be attributed to efficient intestinal metabolism and/or efflux from intestinal cells to the intestinal lumen mediated by ATP-binding cassette (ABC) transporters located in the apical membrane of enterocytes.

The flavanone hesperetin (4'-methoxy-3',5,7-trihydroxyflavanone) (Figure 5.1) is the

aglycone of hesperidin (hesperetin 7-*O*-rutinoside) which is present in high amounts in sweet oranges, orange juice and other citrus fruits including lemon, lime and mandarin[4]. Also certain herbs, spices, teas and other products have been reported to contain hesperidin: such as rosemary[5], honeybush tea[6], and a large number of Chinese traditional medicinal products[7]. Hesperidin must by hydrolyzed by colonic microbiota prior to absorption whereas the aglycone hesperetin, as well as the monosaccharide hesperetin 7-*O*-glucoside, are already taken up earlier in the digestive tract[8,9]. Hesperetin 7-*O*-glucoside can be hydrolyzed by lactase phloridzin hydrolase (LPH) followed by migration of the aglycone into the intestinal cell and/or the hesperetin 7-*O*-glucoside could be transported into the intestinal cell via a sodium-dependent glucose transporter (*e.g.* SGLT1) after which it is deglucosylated within the intestinal cell[10,11].

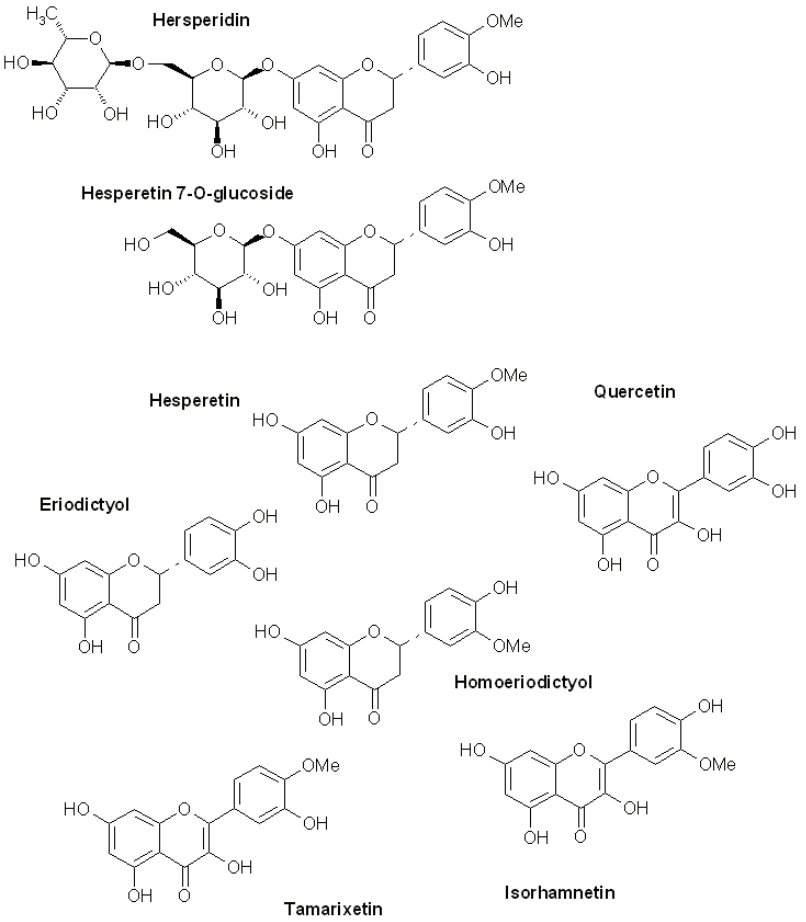

Figure 5.1 *Chemical structures of hesperetin, hesperidin, hesperetin 7-O-glucoside, eriodictyol, homoeriodictyol, quercetin, isorhamnetin and tamarixetin.*

The resulting intracellular hesperetin aglycone is conjugated into glucuronidated and sulfonated metabolites which have been detected in human and rat plasma[12-17]. These conjugation reactions occurring in the intestinal cells have been reported to play an important role during first pass metabolism[18,19]. In rat, after oral administration of hesperidin (50 mg/kg body weight (bw)), hesperetin is mainly present in plasma as hesperetin 7-*O*-glucuronide and hesperetin 3'-*O*-glucuronide, and as glucuronides of homoeriodictyol[15], which can be formed after demethylation of hesperetin into eriodictyol[20], and remethylation into homoeriodictyol or hesperetin[21].
Although largely dependent on dietary habits (*i.e.* citrus consumption), the amount of hesperidin can form a major part of the total flavonoid intake since orange juice can reach 0.5 to 1 g/l hesperidin[4,22]. Conversion of hesperidin in citrus juice into hesperetin 7-*O*-glucoside by enzymatic-treatment has demonstrated to increase the bioavailability of hesperetin from orange juice substantially[9]. Hesperidin, hesperetin as well as hesperetin conjugates have been reported to provide beneficial health effects including the reduction of the risk of osteoporosis[23-25].
Previously we studied the intestinal metabolism and transport of hesperetin *in vitro* using Caco-2 cell monolayers in a two-compartment transwell system as a model for the intestinal barrier[26]. We demonstrated that hesperetin is metabolized and transported back to the apical compartment, simulating the intestinal lumen side, by the ABC transporter Breast Cancer Resistance Protein (BCRP)[26]. In addition, we demonstrated that co-administering hesperetin with flavonoids reported to inhibit BCRP, reduced the apical efflux of hesperetin metabolites and increased the transport of hesperetin metabolites to the basolateral side, simulating the blood/plasma side. This increase in basolateral transport was up to 2-fold in the case of co-administration of hesperetin with quercetin, resulting in reversal of the preferential side for cellular efflux of hesperetin metabolites from Caco-2 cell monolayers, and preferentially basolateral instead of apical excretion[27]. Based on this *in vitro* result one might postulate that co-administration with specific flavonoids could be a strategy to improve the limited bioavailability of hesperetin *in vivo*. Therefore, the objective of the present study was to investigate the effect of co-administration of quercetin on the bioavailability of hesperetin 7-*O*-glucoside. In this *in vivo* study hesperetin 7-*O*-glucoside was used instead of hesperetin itself, because previous studies in rats revealed hesperetin to be already absorbed to a significant extent in the stomach excluding the possibility to study the effects of co-administering quercetin on the intestinal uptake of hesperetin (unpublished results). Hesperetin 7-*O*-glucoside was found to be absorbed in the small intestine and thus provided a better model compound to study the effect of quercetin on its intestinal uptake and subsequent bioavailability[9]. In the present study rats were orally administered hesperetin 7-*O*-glucoside (15 or 3 mg/kg bw), in the presence or

absence of quercetin (15 mg/kg bw). Systemic blood was taken at different time points upon dosing (15, 30, 45, 60, 90, 120, 240 and 480 min) and after enzymatic hydrolysis the plasma concentrations of hesperetin, eriodicyiol and homoeriodictyol were determined by uPLC-DAD. Quercetin was chosen for co-administration since it was found to be a potent inhibitor of BCRP *in vitro*[28,29], able to significantly influence and even reverse the preferential side for cellular efflux of hesperetin metabolites from Caco-2 cell monolayers[27]. In a previous study in rats[30], *in vivo* co-administration of quercetin (10 mg/kg bw) resulted in a 1.3-fold increased oral bioavailability of the procarcinogen 2-amino-1-methyl-6-phenylimidazo[4,5-*b*]-pyridine (PhIP), which is also a substrate of BCRP[31,32].

Materials and Methods

Materials

L-ascorbic acid, eriodictyol (purity ≥95%), ß-glucuronidase from *Helix pomatia* (type HP-2, aqueous solution), hesperetin (purity ≥95%) and quercetin dihydrate were obtained from Sigma (St. Louis, MO), homoeriodictyol (purity ≥ 99%), isorhamnetin (purity ≥ 99%) and tamarixetin (purity ≥ 99%) were purchased from Extrasynthése (Genay, France), and daidzein (purity ≥ 98%) from Indofine Chemical Company (Belle Mead, NJ), hesperetin 7-*O*-glucoside from Nestlé Research Center (Lausanne, Switzerland), dimethyl sulfoxide (DMSO), glacial acetic acid and sodium acetate trihydrate from Merck (Darmstadt, Germany), ethyl acetate and 2-hydroxypropyl-ß-cyclodextrin from Aldrich (Steinheim, Germany), trifluoroacetic acid (TFA) from Fluka (Buchs, Switzerland), and acetonitrile and methanol from Biosolve (Valkenswaard, The Netherlands).

Animal experiment

The animal study complied with the Dutch Act on Animal Experimentation (Stb. 1977, 67; Stb. 1996, 565), revised February 5, 1997. The study has been approved by the animal experimentation committee of Wageningen University; all procedures used were considered to avoid or minimize discomfort, distress and pain to the animals[33]. Five week old male Sprague-Dawley rats were obtained from Harlan (Horst, The Netherlands) and acclimatized for 1 wk. The rats were housed, multiple rats per cage, under standard conditions, including a temperature of ± 20 °C, a 12 hrs light/dark cycle and a humidity of 55%. Rats were fed *ad libitum* with standard Harlan Teklad diet, but fasted the night prior to the experiment. The rats had unlimited access to water at all times.

First, an experiment was done with 4 rats in 2 groups: a control group only receiving hesperetin 7-*O*-glucoside (15 mg/kg bw) (n=2), and a group co-administrated with

quercetin (15 mg/kg bw) (n=2). This experiment was repeated three times with a lower dose of hesperetin 7-*O*-glucoside (3 mg/kg bw), co-administered or not with quercetin (15 mg/kg bw) including 3 rats in each dose group.
The rats were randomly divided over the dosing groups. The experiment was started by weighing the rats, housing them separately. The average (±SD) weight of the rats was 172.3 ± 20.3 g (n=22). The rats received 1 ml test solution by oral gavage containing hesperetin 7-*O*-glucoside in the presence or absence quercetin in 25% (w/v) 2-hydroxypropyl-ß-cyclodextrin in fresh tap water. Blood samples of ~ 0.15 ml were taken from the tail vein at 15, 30, 45, 60, 90, 120, 240 and 480 min after dosing and collected in Microvette CB 300 tubes containing lithium-heparin from Sarstedt (N¸mbrecht, Germany) and stored on ice. The plasma was separated by centrifugation at 2000 *g* for 5 min in a cooled centrifuge and stored at -20°C. After the last blood sample was taken, the rats were euthanized by CO_2/O_2 gas.

Plasma sample preparation

Plasma samples (50 µl) were spiked with 2.5 µl daidzein (200 µM / DMSO) as internal standard (IS), and to this solution 5 µl 0.78 M sodium acetate (pH 4.8), 5 µl 1.0 M ascorbic acid in water, 135 µl nanopure water, and 2.5 µl ß-glucuronidase from *Helix pomatia* (type HP-2, aqueous solution, containing sulfatase activity) were added. The mixture was incubated for 18 hrs at 37°C in a shaking water bath, after which the water phase was extracted with 0.5 ml ethyl acetate followed by centrifugation at 16,000 *g* for 4 min. The ethyl acetate was removed and this extraction was repeated twice. The collected ethyl acetate fractions were pooled and evaporated to dryness under a stream of nitrogen, at 30°C. The residue was re-suspended in 100 µl 50:50 methanol:0.1% trifluoroacetic acid (TFA) in nanopure water by sonication for 4 min. Spiking samples with daidzein allowed adjustment of the concentration according to the extraction efficiency from the plasma (recovery of daidzein was always > 85%).

uPLC-DAD analysis

The uPLC-DAD system consisted of a Waters (Milford, MA) Acquity binary solvent manager, sample manager, and photodiode array detector, equipped with a Waters BEH C18 1.7µm 50- × 2.1-mm column. After centrifugation of the samples at 16,000 *g* for 4 min, 3.5 µl of the supernatant was injected and eluted at a flow rate of 600 µl/min using 20% acetonitrile in 0.1% trifluoroacetic acid in nanopure water for 2 min. Thereafter the percentage of acetonitrile was increased to 25% in 4 min, and to 80% in 30 sec, which condition was kept for 30 sec as a cleaning step. Thereafter the percentage of acetonitrile was brought back to its initial value in 30 sec, a condition that was kept for 42 sec to re-equilibrate the column (total run time 8.12 min). DAD spectra were detected between 210 and 420 nm, and uPLC chromatograms

acquired at 280 nm were used for quantification. Hesperetin, homoeriodictyol and eriodictyol were quantified on the basis of calibration curves made with the pure compounds.

Pharmacokinetics

The plasma peak concentration (C_{max}), the time to reach the peak concentration (T_{max}) and the area under the plasma concentration-time curve was determined from time zero to 2 hours or to the time of the last sample which was 8 hours after dosing ($AUC_{0\text{-}2hr}$ and $AUC_{0\text{-}8hr}$, respectively). Values were calculated for hesperetin, homoeriodictyol and eriodictyol, using Graphpad Prism (version 5.02) from Graphpad Software (San Diego, CA). The Student's two-tailed unpaired *t* test was applied to evaluate statistical differences. Differences were considered significant when p values were less than 0.05.

Results

Plasma analysis

Figure 5.2 on page 94 shows a uPLC chromatogram (Figure 5.2A on page 94) of a mixture containing standards of the compounds of interest which were to be expected in the plasma samples from the animal experiment after enzymatic hydrolysis: hesperetin (t_R 5.2 min, UV_{max} 287.7 nm), homoeriodictyol (t_R 4.7 min, UV_{max} 287.1 nm) and eriodictyol (t_R 2.5 min, UV_{max} 287.7 nm), as well as the compounds to be expected in the plasma after enzymatic hydrolysis of the animals co-exposed to quercetin: quercetin (t_R 2.7 min, UV_{max} 255.1 and 371.3 nm), isorhamnetin (t_R 5.5 min, UV_{max} 254.5 and 369.4 nm) and tamarixetin (t_R 5.7 min, UV_{max} 254.5 and 373.2 nm). The uPLC method was able to separate hesperetin from its demethylated and remethylated metabolites, eriodictyol and homoeriodictyol, as well as from quercetin and its methylated metabolites isorhamnetin (3'-*O*-methylquercetin) and tamarixetin (4'-*O*-methylquercetin). The internal standard daidzein exhibited a t_R of 2.0 min (UV_{max} 249.0 nm, shoulder at 303.1 nm). Figure 5.2B on page 94 shows a representative uPLC-DAD chromatogram of a hydrolyzed plasma sample from a rat exposed to hesperetin 7-*O*-glucoside co-administered with quercetin. The presence of hesperetin and quercetin is clearly demonstrated, as well as small amounts of eriodictyol, homoeriodictyol, isorhamnetin and tamarixetin (Figure 5.2B).

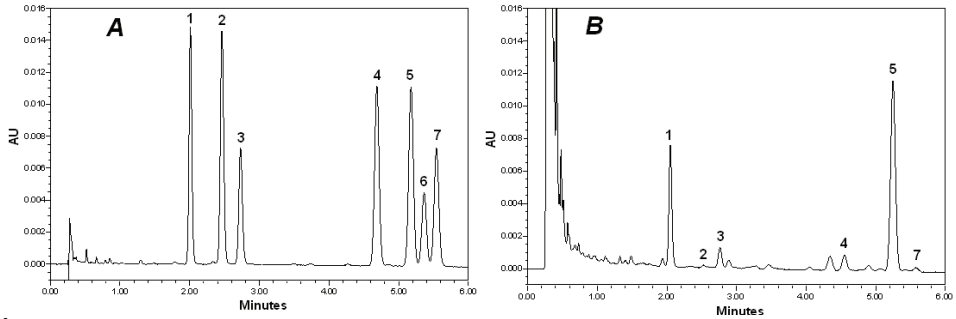

Figure 5.2 *uPLC chromatogram of a mixture containing standards of the compounds expected in the plasma samples from the animal experiment after enzymatic hydrolysis (A), and a representative uPLC chromatogram of a hydrolyzed plasma sample from a rat exposed to hesperetin 7-O-glucoside and quercetin (B). 1 = daidzein, 2 = eriodictyol, 3 = quercetin, 4 = homoeriodictyol, 5 = hesperetin, 6 = tamarixetin, 7 = isorhamnetin. AU = absorption units.*

Pharmacokinetics

Figure 5.3A depicts the total plasma hesperetin in rats exposed to 15 mg/kg bw hesperetin 7-*O*-glucoside in the presence or absence of quercetin (15 mg/kg bw), and Table 5.1 on page 95 shows the pharmacokinetic parameters derived from these measurements. The $AUC_{o\text{-}8hr}$ as determined for total plasma hesperetin in rats exposed to 15 mg/kg bw was 53.8 µmol/L/h (Table 5.1 on page 95, Figure 5.3A). Co-administration of quercetin did not result in a significantly increase in C_{max} or the AUC values, although both the $AUC_{o\text{-}2hr}$ and $AUC_{o\text{-}8hr}$ did show a tendency to be increased, amounting to respectively 118% and 119% of the corresponding value obtained for rats exposed to hesperetin 7-*O*-glucuronide alone (Table 5.1, Figure 5.3A). Hardly any eriodictyol was detected, whereas homoeriodictyol was present up to a plasma concentration of 1.5 µM at 30 min (Figure 5.3B), amounting to about 5% of the hesperetin plasma concentration.

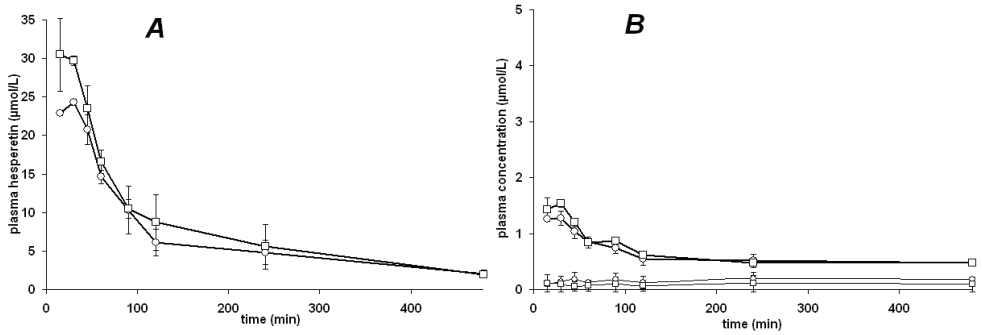

Figure 5.3 *Plasma concentration vs. time of A) total hesperetin and B) homoeriodictyol (thick line) and eriodictyol (thin line) in rats after oral exposure to 15 mg/kg bw hesperetin 7-O-glucoside in the absence (○) or presence (□) of 15 mg/kg bw quercetin. Values are mean ± SD, n=2.*

Table 5.1 *Pharmacokinetic parameters for total plasma hesperetin in rats (n=2) given 15 mg/kg bw hesperetin 7-O-glucoside by oral gavage in the absence or presence of quercetin (15 mg/kg bw). Mean (±SD) values shown.*

Parameter	unit	control	+quercetin
n		*2*	*2*
C_{max}	(µmol/L)	*24.4 (±0.4)*	*30.5 (±4.7)*
T_{max}	(min)	*30*	*15*
AUC_{o-2hr}	(µmol/L/h)	*29.2 (±2.8)*	*34.6 (±4.2)*
AUC_{o-8hr}	(µmol/L/h)	*53.8 (±10.5)*	*63.8 (±16.8)*

In order to investigate whether the effect of quercetin on the bioavailability of hesperetin 7-*O*-glucoside would be more significant when the relative ratio between quercetin and hesperetin 7-*O*-glucoside would be increased enabling easier competition by quercetin for the relevant ABC transporter, the experiment was repeated using a lower dose of hesperetin 7-*O*-glucoside (3 mg/kg bw) but keeping the dose of quercetin at 15 mg/kg bw. Figure 5.4 on page 96 depicts the total plasma hesperetin from an experiment in which three rats were exposed to the lower dose of 3 mg/kg hesperetin 7-*O*-glucoside either in the presence or in the absence of quercetin (15 mg/kg bw) and Table 5.2 on page 96 presents the corresponding pharmacokinetic parameters. The results of this experiment demonstrated that co-administration of 15 mg/kg bw did result in a significant 1.3-fold higher C_{max} and a significant 1.3-fold higher AUC_{o-2hr} (Table 5.2, Figure 5.4), whereas the 1.4 fold increase in the AUC_{o-8hr} appeared not to be significant. To increase the sensitivity of the analysis the experiment was repeated twice. However, in these subsequent experiments an increased plasma concentration of hesperetin and its metabolites upon co-administration with quercetin was only observed for the samples at 15 minutes following exposure and a significant increase in the AUC_{o-2hr} or AUC_{o-8hr} were not observed.

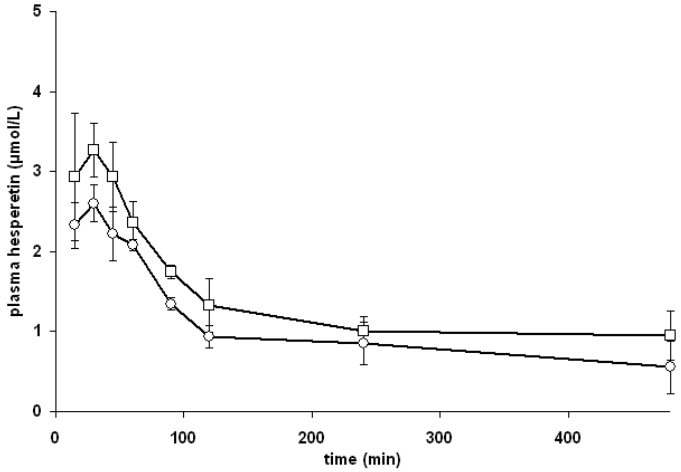

Figure 5.4 *Plasma concentration vs. time of hesperetin in rats after oral exposure to 3 mg/kg bw hesperetin 7-O-glucoside in the absence (○) or presence (□) of 15 mg/kg bw quercetin. Values are mean (± SD), n=3.*

Figure 5.5 on page 97 presents a summary of the combined data of all 4 experiments (n=11 for all data points), expressing the plasma concentrations of hesperetin and its metabolites observed upon co-administration with quercetin as percentage of the amount detected in the plasma of the corresponding rats dosed with hesperetin 7-*O*-glucoside alone. From these results it can be concluded that a statistically significant 32 % ($p<0.05$) increase in hesperetin bioavailability is observed especially at 15 min post dosing, whereas at subsequent time points the relative increase was no longer statistically significant (Figure 5.5).

Table 5.2 *Pharmacokinetic parameters for total plasma hesperetin in rats (n=3) given 3 mg/kg bw hesperetin 7-O-glucoside per oral gavage in the absence or presence of quercetin (15 mg/kg bw). Mean (±SD) values shown. *, $p < 0.05$ significantly different compared to the control group.*

Parameter	unit	control	+quercetin
n		3	3
C_{max}	(µmol/L)	2.6 (±0.2)	3.3 (±0.3)*
T_{max}	(min)	*30*	30
AUC_{0-2hr}	(µmol/L/h)	3.5 (±0.2)	4.4 (±0.3)*
AUC_{0-8hr}	(µmol/L/h)	7.7 (±1.8)	10.7 (±2.3)

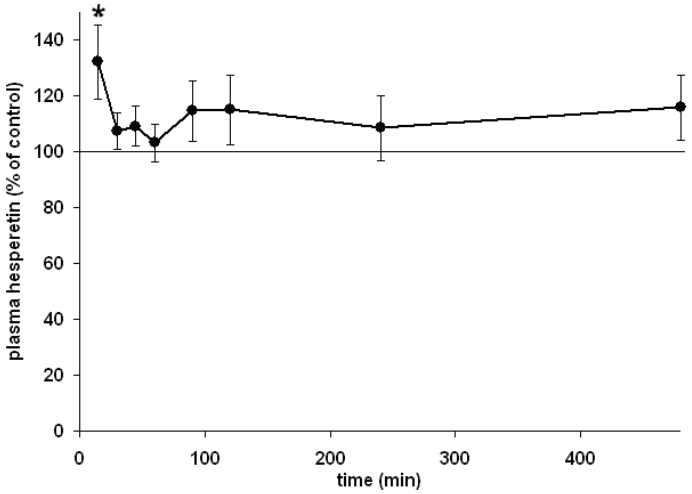

Figure 5.5 *Plasma hesperetin levels in rats exposed to hesperetin 7-O-glucoside in the presence of quercetin, expressed as percentage of the plasma hesperetin levels in the corresponding controls exposed to hesperetin 7-O-glucoside in the absence of quercetin. Mean values (±SEM) (n=11). *, p <0.05 significantly different compared to the control.*

Discussion

Flavonoids can be potent modulators of intestinal metabolism and ABC transporter mediated transport, which can affect the oral bioavailability of other compounds[34]. Co-administration of quercetin *in vitro* to a Caco-2 cell monolayer, as a model system for the intestinal transport barrier, increased the transport to the basolateral side of several compounds including drugs such as talinolol[35] or cimetidine[36], as well as toxins such as ochratoxin A[37] and PhIP[38]. These effects were confirmed in *in vivo* studies using rats demonstrating that co-administration with quercetin resulted in an increased relative oral bioavailability ($AUC_{0\text{-}24hr}$) of paclitaxel[39] and PhIP ($AUC_{0\text{-}8hr}$)[30]. In the present paper we studied whether co-administration of quercetin resulted in an increased oral bioavailability of hesperetin 7-*O*-glucoside. Sprague-Dawley rats were dosed by gavage to hesperetin 7-*O*-glucoside rather than to hesperetin because hesperetin, having a log*P* value of 2.44[26] and a molecular weight of 302 g/mol, is already taken up in the stomach (unpublished results) excluding the possibility to study the effects of co-administration of quercetin on intestinal uptake. Hesperetin 7-*O*-glucoside was found to be absorbed in the small intestine and thus provides a better model compound to study the effect of quercetin on intestinal uptake and subsequent bioavailability of hesperetin. Our previous studies using Caco-2 cells[26,27] were performed with hesperetin aglycone since Caco-2 cells, in contrast to the intestinal cells, have a very low LPH activity[10]

resulting in a slow hydrolysis and hence uptake of hesperetin 7-*O*-glucoside, making hesperetin 7-*O*-glucoside an adequate model compound *in vivo* but not *in vitro* using Caco-2 cells.

Results of the present study revealed that only the rats exposed to the highest concentration of hesperetin 7-*O*-glucoside (15 mg/kg bw) showed quantifiable plasma concentrations of homoeriodictyol (Figure 3B), but only low plasma levels of eriodictyol, often below the limit of quantification. In the rats exposed to lower concentrations of hesperetin 7-*O*-glucoside (3 mg/kg bw), no eriodictyol and only a little homoeriodictyol, mostly below quantification limits, were detected. Interestingly, the presence of homoeriodictyol conjugates (mainly glucuronides) in addition to hesperetin conjugates amounted to about 40% of the total flavanone metabolites in the plasma of Wistar rats exposed to 50 mg/kg bw hesperidin [15], or to 0.25 or 0.5% (v/v) hesperidin in the diet[41], a level that was not observed in our experiments. Given that hesperidin, in contrast to hesperetin 7-*O*-glucoside, is believed to be deconjugated and absorbed in the colon, this observation suggests that hesperetin might not be primarily demethylated into eriodictyol, and remethylated into hesperetin or homoeriodictyol in the liver, but that this conversion may be mainly performed by gut microbiota, which have been reported before to efficiently transmethylate hesperetin into homoeriodictyol[42].

In the present study the C_{max} values were observed at the first two time points collected (15 or 30 min) and in the first case it cannot even be excluded that the real C_{max} already occurs even before 15 min post dosing. In human studies in which healthy volunteers (after fasting) were given enzymatically-treated orange juice containing hesperetin 7-*O*-glucoside (1.21 mg/kg bw), the C_{max} of 2.6 μM plasma hesperetin was detected at 30 min, the first time point measured[9]. Similar results were obtained for the flavanone naringenin 7-*O*-glucoside, both indicating a rapid uptake of hesperetin 7-*O*-glucoside in human as well[40].

Co-administration of quercetin did increase total hesperetin plasma concentrations especially in the early phase of the concentration time curve when elimination was not yet dominating over uptake, but did not significantly increase the $AUC_{0\text{-}8hr}$. At 15 min post dosing, the amount of total plasma hesperetin was 32% higher ($p<0.05$) compared to the control, whereas at subsequent time points the relative increase was no longer statistically significant (Figure 5). It is concluded that the effect of co-administration of quercetin as an inhibitor of apical intestinal ABC transporter mediated transport may result in an increased bioavailability of hesperetin especially during the early phase of exposure when absorption processes still dominate over elimination processes. In addition, the uptake of hesperetin at relatively later time points will occur in a reduced presence of quercetin, since this compound is taken up as well, which could also help to explain the transient effect of the co-administration of quercetin.

Other groups studied the effect of co-administration of other flavonoids on flavonoid bioavailability. Moon & Morris[43] demonstrated that co-administration of the isoflavone biochanin A with both quercetin and the flavanol (-)-epigallocatechin-3-gallate (EGCG) (50 mg/kg bw each via oral gavage in 1:20 DMSO:olive oil) significantly increased the $AUC_{0\text{-}24hr}$ of biochanin A by 2-fold in Sprague Dawley rats. This effect could be explained by the fact that BCRP plays an important role in limiting the bioavailability of both biochanin A and quercetin[44,45], and that both have been demonstrated to interact with BCRP[28,29,46]. However, in another study, a 3-week period of co-administration of quercetin and (+)-catechin did not result in an increased bioavailability of both compounds in Wistar rats fed a diet containing (+)-catechin, or quercetin or both [47]. This might be explained by the fact that flavanols such as catechin and/or their metabolites preferably interact with other classes of ABC transporters such as MRPs[48].

Altogether it is concluded that co-administration of quercetin as an inhibitor of apical intestinal ABC transporter mediated transport may result in increased bioavailability of hesperetin especially during the early phase of exposure when absorption processes still dominate over elimination processes.

Acknowledgements

We thank the co-workers of the center for laboratory animals (CKP) of Wageningen University (Wageningen, The Netherlands) for their excellent zootechnical assistance during the animal experiments. This study was supported by a research grant from Nestlé Research Center (Lausanne, Switzerland).

References

1 Manach C, Scalbert A, Morand C, Rémésy C, Jiménez L. Polyphenols: food sources and bioavailability. *Am J Clin Nutr* 79: 727-747, 2004.

2 Scalbert A, Williamson G. Dietary intake and bioavailability of polyphenols. *J Nutr* 130(8S Suppl): 2073S-2085S, 2000.

3 Manach C, Williamson G, Morand C, Scalbert A, Remesy C. Bioavailability and bioefficacy of polyphenols in humans. I. Review of 97 bioavailability studies. *Am J Clin Nutr* 81(1 Suppl): 230S-242S, 2005.

4 Tomás-Barberán FA, Clifford MN. Flavanones, chalcones and dihydrochalcones - nature, occurrence and dietary burden. *J Sci Food Agric* 80(7): 1073-1080, 2000.

5 del Baño MJ, Lorente J, Castillo J, Benavente-García O, Marín MP, Del Río JA, Ortuño A, Ibarra I. Flavonoid distribution during the development of leaves, flowers, stems, and roots of Rosmarinus officinalis. postulation of a biosynthetic pathway. *J Agric Food Chem* 52(16): 4987-4992, 2004.

6 Joubert E, Otto F, Gruener S, Weinreich B. Reversed-phase HPLC determination of mangiferin, isomangiferin and hesperidin in Cyclopia and the effect of harvesting date on the phenolic composition of C. genistoides. *Eur Food Res Technol* 216(3): 270-273, 2003.

7 Lu Y, Zhang C, Bucheli P, Wei D. Citrus flavonoids in fruit and traditional Chinese medicinal food ingredients in China. *Plant Foods Hum Nutr* 61(2): 57-65, 2006.

8 Kanaze FI, Bounartzi MI, Georgarakis M, Niopas I. Pharmacokinetics of the citrus flavanone aglycones hesperetin and naringenin after single oral administration in human subjects. *Eur J Clin Nutr* 61(4): 472-477, 2007.

9 Nielsen ILF, Chee WSS, Poulsen L, Offord-Cavin E, Rasmussen SE, Frederiksen H, Enslen M, Barron D, Horcajada M-N, Williamson G. Bioavailability is improved by enzymatic modification of the citrus flavonoid hesperidin in humans: a randomized, double-blind, crossover trial. *J Nutr* 136(2): 404-408, 2006.

10 Day AJ, Gee JM, DuPont MS, Johnson IT, Williamson G. Absorption of quercetin-3-glucoside and quercetin-4'-glucoside in the rat small intestine: the role of lactase phlorizin hydrolase and the sodium-dependent glucose transporter. *Biochem Pharmacol* 65(7): 1199-1206, 2003.

11 Walgren RA, Lin JT, Kinne RK, Walle T. Cellular uptake of dietary flavonoid quercetin 4'-beta-glucoside by sodium-dependent glucose transporter SGLT1. *J Pharmacol Exp Ther* 294(3): 837-843, 2000.

12 Ameer B, Weintraub RA, Johnson JV, Yost RA, Rouseff RL. Flavanone absorption after naringin, hesperidin, and citrus administration. *Clin Pharmacol Ther* 60(1): 34-40, 1996.

13 Gardana C, Guarnieri S, Riso P, Simonetti P, Porrini M. Flavanone plasma pharmacokinetics from blood orange juice in human subjects. *Br J Nutr* 98(1): 165-172, 2007.

14 Manach C, Morand C, Gil-Izquierdo A, Bouteloup-Demange C, Rémésy C. Bioavailability in humans of the flavanones hesperidin and narirutin after the ingestion of two doses of orange juice. *Eur J Clin Nutr* 57(2): 235-242, 2003.

15 Matsumoto H, Ikoma Y, Sugiura M, Yano M, Hasegawa Y. Identification and quantification of the conjugated metabolites derived from orally administered hesperidin in rat plasma. *J Agric Food Chem* 52(21): 6653-6659, 2004.

16 Mullen W, Archeveque M-A, Edwards CA, Matsumoto H, Crozier A. Bioavailability and metabolism of orange juice flavanones in humans: impact of a full-fat yogurt. *J Agric Food Chem* 56(23): 11157-11164, 2008.

17 Brett GM, Hollands W, Needs PW, Teucher B, Dainty JR, Davis BD, Brodbelt JS, Kroon PA. Absorption, metabolism and excretion of flavanones from single portions of orange fruit and juice and effects of anthropometric variables and contraceptive pill use on flavanone excretion. *Br J Nutr* 101(5): 664-675, 2009.

18 Brand W, Boersma MG, Bik H, Van den Hil EF, Vervoort J, Barron D, Meinl W, Glatt H, Williamson G, Van Bladeren PJ, Rietjens IMCM. Phase II metabolism of hesperetin by individual UDP-glucuronosyltransferases (UGTs) and sulfotransferases (SULTs) and rat and human tissue samples. *Drug Metab Dispos*, submitted.

19 Silberberg M, Morand C, Mathevon T, Besson C, Manach C, Scalbert A, Remesy C. The bioavailability of polyphenols is highly governed by the capacity of the intestine and of the liver to secrete conjugated metabolites. *Eur J Nutr* 45(2): 88-96, 2006.

20 Nielsen SE, Breinholt V, Justesen U, Cornett C, Dragsted LO. *In vitro* biotransformation of flavonoids by rat liver microsomes. *Xenobiotica* 28: 389-401, 1998.

21 Miyake Y, Shimoi K, Kumazawa S, Yamamoto K, Kinae N, Osawa T. Identification and antioxidant activity of flavonoid metabolites in plasma and urine of eriocitrin-treated rats. *J Agric Food Chem* 48: 3217-3224, 2000.

22 Yáñez JA, Remsberg CM, Miranda ND, Vega-Villa KR, Andrews PK, Davies NM. Pharmacokinetics of selected chiral flavonoids: hesperetin, naringenin and eriodictyol in rats and their content in fruit juices. *Biopharm Drug Dispos* 29(2): 63-82, 2008.

23 Chiba H, Uehara M, Wu J, Wang X, Masuyama R, Suzuki K, Kanazawa K, Ishimi Y. Hesperidin, a citrus flavonoid, inhibits bone loss and decreases serum and hepatic lipids in ovariectomized mice. *J Nutr* 133(6): 1892-1897, 2003.

24 Horcajada MN, Habauzit V, Trzeciakiewicz A, Morand C, Gil-Izquierdo A, Mardon J, Lebecque P, Davicco MJ, Chee WSS, Coxam V, Offord E. Hesperidin inhibits ovariectomized-induced osteopenia and shows differential effects on bone mass and strength in young and adult intact rats. *J Appl Physiol* 104(3): 648-654, 2008.

25 Trzeciakiewicz A, Habauzit V, Mercier S, Barron D, Urpi-Sarda M, Manach C, Offord E, Horcajada M-N. Molecular mechanism of hesperetin-7-O-glucuronide, the main circulating metabolite of hesperidin, involved in osteoblast differentiation. *J Agric Food Chem* 58(1): 668-675, 2010.

26 Brand W, Van der Wel PAI, Rein MJ, Barron D, Williamson G, Van Bladeren PJ, Rietjens IMCM. Metabolism and transport of the citrus flavonoid hesperetin in Caco-2 cell monolayers. *Drug Metab Dispos* 36(9): 1794-1802, 2008.

27 Brand W, Padilla B, Van Bladeren PJ, Williamson G, Rietjens IMCM. The effect of co-administered flavonoids on the metabolism of hesperetin and the disposition of its metabolites in Caco-2 cell monolayers. *Mol Nutr Food Res*, in press.

28 Cooray HC, Janvilisri T, Van Veen HW, Hladky B, Barrand MA. Interaction of the breast cancer resistance protein with plant polyphenols. *Biochem Biophys Res Commun* 317(1): 269-275, 2004.

29 Zhang S, Yang X, Morris ME. Flavonoids are inhibitors of breast cancer resistance protein (ABCG2)-mediated transport. *Mol Pharmacol* 65(5): 1208-1216, 2004.

30 Schutte ME, Alink GM, Freidig AP, Spenkelink B, Vaessen JCH, van de Sandt JJM, Groten JP, Rietjens IMCM. Quercetin increases the bioavailability of 2-amino-1-methyl-6-phenylimidazo[4,5-b]pyr idine (PhIP) in rats. *Food Chem Toxicol* 46: 3422-3428, 2008.

31 Ebert B, Seidel A, Lampen A. Identification of BCRP as transporter of benzo[a]pyrene conjugates metabolically formed in Caco-2 cells and its induction by Ah-receptor agonists. *Carcinogenesis* 26(10): 1754-1763, 2005.

32 Van Herwaarden AE, Jonker JW, Wagenaar E, Brinkhuis RF, Schellens JHM, Beijnen JH, Schinkel AH. The breast cancer resistance protein (Bcrp1/Abcg2) restricts exposure to the dietary carcinogen 2-amino-1-methyl-6-phenylimidazo[4,5-b]pyr idine. *Cancer Res* 63(19): 6447-6452, 2003.

33 Balls M, A.M. G, Fentem JH, Broadhead CL, Burch RL, M.F.W. F, Frazier JM, Hendriksen CFM, Jennings M, Van der Kamp MDO, Morton DB, Rowan AN, Russell C, Russell WMS, Spielmann H, Stephens ML, Stokes W, S., Straughan DW, Yager JD, Zurlo J, Van Zutphen BFM. The three Rs: the way forward: the report and recommendations of ECVAM Workshop 11. *Altern Lab Anim* 23: 838-866, 1995.

34 Brand W, Schutte ME, Williamson G, Van Zanden JJ, Cnubben NHP, Groten JP, Van Bladeren PJ, Rietjens IMCM. Flavonoid-mediated inhibition of intestinal ABC transporters may affect the oral bioavailability of drugs, food-borne toxic compounds and bioactive ingredients. *Biomed Pharmacother* 60(9): 508-519, 2006.

35 Ofer M, Wolffram S, Koggel A, Spahn-Langguth H, Langguth P. Modulation of drug transport by selected flavonoids: Involvement of P-gp and OCT? *Eur J Pharm Sci* 25(2-3): 263-271, 2005.

36 Taur J-S, Rodriguez-Proteau R. Effects of dietary flavonoids on the transport of cimetidine via P-glycoprotein and cationic transporters in Caco-2 and LLC-PK1 cell models. *Xenobiotica* 38: 1536-1550, 2008.

37 Sergent T, Garsou S, Schaut A, De Saeger S, Pussemier L, Van Peteghem C, Larondelle Y, Schneider Y-J. Differential modulation of ochratoxin A absorption across Caco-2 cells by dietary polyphenols, used at realistic intestinal concentrations. *Toxicol Lett* 159(1): 60-70, 2005.

38 Schutte ME, Freidig AP, van de Sandt JJM, Alink GM, Rietjens IMCM, Groten JP. An in vitro and in silico study on the flavonoid-mediated modulation of the transport of 2-amino-1-methyl-6-phenylimidazo[4,5-b]pyr idine (PhIP) through Caco-2 monolayers. *Toxicol Appl Pharmacol* 217: 204-215, 2006.

39 Choi J-S, Jo B-W, Kim Y-C. Enhanced paclitaxel bioavailability after oral administration of paclitaxel or prodrug to rats pretreated with quercetin. *Eur J Pharm Biopharm* 57(2): 313-318, 2004.

40 Bredsdorff L, Nielsen ILF, Rasmussen SE, Cornett C, Barron D, Bouisset F, Offord E, Williamson G. Absorption, conjugation and excretion of the flavanones, naringenin and hesperetin from alpha-rhamnosidase-treated orange juice in human subjects. *Br J Nutr*.

41 Habauzit V, Nielsen IL, Gil-Izquierdo A, Morand C, Chee W, Barron D, Davicco MJ, Coxam V, Williamson G, Offord E, Horcajada MN. Increased bioavailability of hesperetin-7-glucoside compared to hesperidin results in more efficient prevention of bone loss in adult ovariectomized rats. *Br J Nutr* 102(7): 976-984, 2009.

42 DeEds F, Booth AN, Jones TF. Methylation and dehydroxylation of phenolic compounds by rats and rabbits. *J Biol Chem* 225(2): 615-621, 1957.

43 Moon YJ, Morris ME. Pharmacokinetics and bioavailability of the bioflavonoid biochanin A: effects of quercetin and EGCG on biochanin A disposition in rats. *Mol Pharm* 4(6): 865-872, 2007.

44 Sesink ALA, Arts ICW, De Boer VCJ, Breedveld P, Schellens JHM, Hollman PCH, Russel FGM. Breast cancer resistance protein (Bcrp1/Abcg2) limits net intestinal uptake of quercetin in rats by facilitating apical efflux of glucuronides. *Mol Pharmacol* 67(6): 1999-2006, 2005.

45 Wang SWJ, Chen Y, Joseph T, Hu M. Variable Isoflavone Content of Red Clover Products Affects Intestinal Disposition of Biochanin A, Formononetin, Genistein, and Daidzein. *J Altern Complement Med* 14(3): 287-297, 2008.

46 Zhang S, Yang X, Morris ME. Combined effects of multiple flavonoids on breast cancer resistance protein (ABCG2)-mediated transport. *Pharm Res* 21(7): 1263-1273, 2004.

47 Silberberg M, Morand C, Manach C, Scalbert A, Remesy C. Co-administration of quercetin and catechin in rats alters their absorption but not their metabolism. *Life Sci* 77(25): 3156-3167, 2005.

48 Zhang L, Zheng Y, Chow MSS, Zuo Z. Investigation of intestinal absorption and disposition of green tea catechins by Caco-2 monolayer model. *Int J Pharm* 287(1-2): 1-12, 2004.

Chapter 6

Phase II metabolism of hesperetin by individual UDP-glucuronosyl transferases and sulfotransferases and rat and human tissue samples

Walter Brand, Marelle G. Boersma, Hanneke Bik, Elisabeth F. Hoek-van den Hil, Jacques Vervoort, Denis Barron, Walter Meinl, Hansruedi Glatt, Gary Williamson, Peter J. van Bladeren, and Ivonne M.C.M. Rietjens

Drug Metabolism and Disposition 38(4): 617-625, 2010

Abstract

Phase II metabolism by UDP-glucuronosyltransferases (UGTs) and sulfotransferases (SULTs) is the predominant metabolic pathway during the first pass metabolism of hesperetin (4'-methoxy-3',5,7-trihydroxyflavanone). In the present study we have determined the kinetics for glucuronidation and sulfonation of hesperetin by 12 individual UGT and 12 individual SULT enzymes as well as by human or rat small intestinal, colonic and hepatic microsomal and cytosolic fractions. Results demonstrate that hesperetin is conjugated at positions 7 and 3', and that major enzyme-specific differences in kinetics and regioselectivity for the UGT and SULT catalyzed conjugations exist. UGT1A9, UGT1A1, UGT1A7, UGT1A8 and UGT1A3 are the major enzymes catalyzing hesperetin glucuronidation, the latter only producing 7-*O*-glucuronide, while UGT1A7 mainly produced 3'-*O*-glucuronide. Furthermore, UGT1A6 and UGT2B4 only produce hesperetin 7-*O*-glucuronide, while UGT1A1, UGT1A8, UGT1A9, UGT1A10, UGT2B7 and UGT2B15 conjugate both positions. SULT1A2 and SULT1A1 catalyze preferably and most efficiently the formation of hesperetin 3'-*O*-sulfate, and SULT1C4 preferably and most efficiently the formation of hesperetin 7-*O*-sulfate. Based on expression levels also SULT1A3 and SULT1B1 will likely play a role in the sulfo-conjugation of hesperetin *in vivo*. The results help to explain discrepancies in metabolite patterns determined in tissues or systems with different expression of UGTs and SULTs, *e.g.* hepatic and intestinal fractions or Caco-2 cells. The incubations with rat and human tissue samples support an important role for the intestinal cells during first pass metabolism in the formation of hesperetin 3'-*O*-glucuronide and 7-*O*-glucuronide, which appear to be the major hesperetin metabolites found *in vivo*.

Introduction

The flavanone hesperetin (4'-methoxy-3',5,7-trihydroxyflavanone) (Figure 6.1 on page 105) is the aglycone of hesperidin (hesperetin 7-*O*-rutinoside), which is the major flavonoid present in sweet oranges (*Citrus sinensis*) and orange juice, and also occurs in other citrus fruits and some herbs[1]. Hesperidin and hesperetin have been reported to provide beneficial effects on health, including a reduced risk of osteoporosis[2].

Upon ingestion, hesperidin has to be hydrolyzed into hesperetin aglycone by colonic microbiota prior to its absorption[3]. Enzymatic conversion of hesperidin prior to consumption to the monosaccharide hesperetin-7-*O*-glucoside has been demonstrated to result in absorption already in the small intestine after deglucosylation by phloridzin hydrolase and/or facilitated transport into the intestinal cells by a sugar transporter such as SGLT1 followed by intracellular

deglucosylation[4]. In the intestinal cells, or during further first pass metabolism, hesperetin aglycone is metabolized by UDP-glucuronosyltransferases (UGTs) and sulfotransferases (SULTs) into respectively glucuronidated and sulfonated metabolites, which have been detected in human and rat plasma[5-8]. The intestinal barrier is believed to play a dominant role in the phase II conjugation during the first pass metabolism of hesperetin[9], and in its limited bioavailability because of efflux of the metabolites back to the intestinal lumen by ABC transport proteins[10,11].

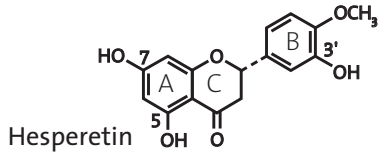

Figure 6.1 *Chemical structure of hesperetin (4'-methoxy-3',5,7 trihydroxyflavanone).*

UGTs form a gene superfamily and currently a total of 22 different UGT proteins have been detected in human tissues, belonging to either the UGT1A (UGT1A1, UGT1A3, UGT1A4, UGT1A5, UGT1A6, UGT1A7, UGT1A8, UGT1A9 and UGT1A10), the UGT2A (UGT2A1, UGT2A2 and UGT2A3), the UGT2B (UGT2B4, UGT2B7, UGT2B10, UGT2B11, UGT2B15, UGT2B17 and UGT2B28), the UGT3 (UGT3A1 and UGT3A2) or the UGT8 (UGT8A1) family[12]. *SULTs* form a gene superfamily and a total of ten different SULT proteins have been detected in human tissues including SULT1A1, SULT1A2, SULT1A3 (encoded by *SULT1A3* and *SULT1A4* and therefore also called SULT1A3/4), SULT1B1, SULT1C2, SULT1C4, SULT1E1, SULT2A1, SULT2B1_v2 and SULT4A1_v2[13,14]. In addition, there are some SULTs which have only been detected at the mRNA level: SULT2B1_v1, SULT1C3 and SULT6B1[15], the latter solely in testis[16]. SULT1C2, SULT1C4, SULT2B1_v1, SULT2B1_v2 and SULT4A1_v2 are respectively also referred to as SULT1C1, SULT1C2, SULT2B1a, SULT2B1b and SULT4A1 in literature not following the nomenclature proposed by Blanchard *et al.*[17].

We previously characterized the metabolism of hesperetin *in vitro* using Caco-2 cell monolayers as a model for the small intestinal barrier and reported that hesperetin is metabolized into 7-*O*-glucuronide and 7-*O*-sulfate metabolites[11]. However, analysis of metabolites in plasma demonstrated the existence of other glucuronide and sulfo-conjugates as well[6-8]. Different individual UGTs and SULTs probably possess different kinetics and regioselectivity for the conjugation of hesperetin, as has been reported for the glucuronidation and sulfonation of other flavonoids[18-21], and therefore different levels of expression of UGTs and SULTs might lead to different metabolite patterns.

In the present paper we determined the kinetics for the conversion of hesperetin into glucuronidated and sulfonated metabolites by individual UGT and SULT enzymes, respectively. The metabolites formed were identified by HPLC-DAD in combination with authentic standards or ^{1}H-NMR. The UGT isoforms tested include 12 individual UGTs reported to be expressed, at least at the mRNA level, in human intestinal and hepatic cells: UGT1A1, UGT1A3, UGT1A4, UGT1A6, UGT1A7, UGT1A8, UGT1A9, UGT1A10, UGT2B4, UGT2B7, UGT2B15 and UGT2B17[22-25]. The SULT isoforms tested include 12 individual SULTs which have been detected in human intestinal and hepatic tissues: SULT1A1, SULT1A2, SULT1A3, SULT1B1, SULT1C2, SULT1E1, SULT1C4 and SULT2A1[13,14,26], and in addition SULT1C3, SULT2B1_v1, SULT2B1_v2 and SULT4A1_v2 which have not been detected on the protein level in these tissues[15,27]. Furthermore, we studied the apparent kinetics of glucuronidation and sulfonation using respectively microsomes and cytosol derived from tissues from human and rat playing a role during the first pass metabolism of hesperetin after ingestion of hesperidin or hesperetin 7-*O*-glucoside: the small intestine, the colon and the liver.

Materials and Methods

Materials

Alamethicin (from *Trichoderma viride*), hesperetin (purity ≥ 95%), L-ascorbic acid and uridine 5'-diphosphoglucuronic acid (UDPGA) were obtained from Sigma (St. Louis, MO), 3'-phosphoadenosine 5'-phosphosulfate (PAPS) from Fluka (Buchs, Switzerland), deuterated acetic acid, dimethyl sulfoxide (DMSO), dipotassium hydrogen phosphate trihydrate, hydrochloric acid and potassium dihydrogen phosphate from Merck (Darmstadt, Germany), acetonitrile and methanol from Sigma-Aldrich (Steinheim, Germany), Tris from Invitrogen (Carlsbad, CA), and trifluoroacetic acid from J.T. Baker (Philipsburg, NJ). Deuterated methanol-*d4* (99.96% *d*) was obtained from Euriso-Top (Gif-sur-Yvette, France). Authentic standards of hesperetin 7-*O*-glucuronide (purity > 90%), hesperetin 3'-*O*-glucuronide (purity > 90%) and hesperetin 7-*O*-sulfate (purity < 50%) were provided by Nestlé Research Center (Lausanne, Switzerland).

UGT supersomes from cDNA transfected insect cells expressing individual human UGTs were obtained from Gentest (Woburn, MA) and their glucuronidation activities toward standard substrates as described by the supplier were as follows: UGT1A1 (lot 95244) and UGT1A3 (lot 70200): 817 and 190 pmol min^{-1} mg protein^{-1} estradiol 3-glucuronidation activity, respectively; UGT1A4 (lot 95375): 1100 pmol min^{-1} mg protein^{-1} trifluoperazine glucuronidation activity; UGT1A6 (lot 70201), UGT1A7 (lot 68106), UGT1A8 (lot 95862), UGT1A9 (lot 81291), UGT1A10 (lot 96097), UGT2B4 (lot 93808), UGT2B7 (lot 83494) and UGT2B15 (lot 70203): 5200, 12000, 630,

7200, 86, 180, 1200 and 3000 pmol min^{-1} mg $protein^{-1}$ 7-hydroxy 4-trifluoromethylcoumarin glucuronidation activity, respectively; UGT2B17 (lot 09302): 1100 pmol min^{-1} mg $protein^{-1}$ eugenol glucuronidation activity. SULTs from cDNA transfected bacteria expressing quantified concentrations of individual human SULT enzymes were prepared as described elsewhere in detail[28].
Pooled human small intestinal microsomes (batch MIC318012), pooled rat (male Sprague-Dawley) small intestinal microsomes (batch MIC323019), pooled human small intestinal cytosol (batch CYT318004), and pooled rat (male Sprague-Dawley) small intestinal cytosol (batch CYT323008), were obtained from Biopredic (Rennes, France), without quantified glucuronidation or sulfonation activities. Human single donor colon microsomes from a 64 year old male (batch MIC317008), pooled colon microsomes from rat (male Sprague-Dawley) (batch MIC322003), human single donor colon cytosol from a 64 year old male (batch CYT317005), and pooled colon cytosol from rat (male Sprague-Dawley) (batch CYT322003) were provided by Biopredic (Rennes, France), without quantified glucuronidation or sulfonation activities. Ethical permission for the use of the human tissue extract was obtained by Biopredic (Rennes, France). Pooled human liver microsomes (lot 28831) with 920 pmol min^{-1} mg $protein^{-1}$ estradiol 3-glucuronidation activity, 890 pmol min^{-1} mg $protein^{-1}$ trifluoroperazine glucuronidation activity and 2400 pmol min^{-1} mg $protein^{-1}$ propofol glucuronidation activity, pooled rat (male Sprague-Dawley) liver microsomes (lot 83481) without quantified glucuronidation activity, pooled human liver cytosol (lot 99925) and pooled rat (male Sprague-Dawley) liver cytosol (lot 08003) with 320 and 1900 pmol min^{-1} mg $protein^{-1}$ 7-hydroxycoumarin sulfotransferase activity, respectively, as described by the supplier, were provided by Gentest (Woburn, MA).

Incubations with UGTs or rat or human microsomes

To study glucuronidation of hesperetin by individual UGTs or microsomal preparations, incubation mixtures (total volume 200 µl) were prepared containing 10 mM $MgCl_2$, 25 µg/ml alamethicin added from a 200 times concentrated stock solution in methanol (final concentration 0.5% methanol), 0.1, 0.2 or 0.5 mg/ml protein and 1 mM UDPGA, in 50 mM Tris-HCl (pH 7.5) [18]. The reaction was started by addition of hesperetin from a 200 times concentrated stock solution in DMSO (final concentration 0.5% DMSO) and incubated for 5 min (UGT1A10, UGT2B7 and human and rat liver microsomes), 10 min (UGT1A1, UGT1A3, UGT1A7, UGT1A8, UGT1A9, UGT2B15 and human and rat small intestinal microsomes), 15 min (human and rat colon microsomes) or 30 min (UGT1A4, UGT1A6, UGT2B4 and UGT2B17) at 37 °C. The final concentration series were 1, 2.5, 5, 10, 15, 25, 35 and 50 µM (n=1-2), or 2.5, 5, 10, 15, 25 and 50 µM (n=1-3) hesperetin for all UGTs tested. The reaction was

terminated by addition of 50 µl acetonitrile. Under these conditions metabolite formation was linear in time and with the amount of protein added (data not shown). Activity is expressed in nmol min^{-1} mg $protein^{-1}$.

Incubations with SULTs or rat or human cytosol

To study sulfonation of hesperetin, incubation mixtures (total volume 100 µl) were prepared containing 5 mM $MgCl_2$, 100 µM PAPS and 0.04-0.23 mg/ml protein (cytosol) or 0.03-0.1 mg/ml protein (individual SULTs) in 50 mM potassium phosphate (pH 7.4). The reaction was started by addition of hesperetin (the final concentration series were 1, 2.5, 5, 10, 15, 25, 35 and 50 µM hesperetin) from a 100-fold concentrated stock solution in DMSO (final concentration 1% DMSO) and incubated for 3 min (SULT1A1, SULT1A2, SULT1C4 and human and rat liver cytosol), 5 min (SULT1E1 and human small intestinal cytosol), 9 min (SULT1A3), 10 min (SULT1B1), 90 min (human colon cytosol), 120 min (SULT1C2 and SULT2A1), 150 min (rat small intestinal and colon cytosol) or 180 min (SULT1C3, SULT2B1_v1, SULT2B1_v2 and SULT4A1_v2) at 37°C. Because SULT1A1, SULT1A2, SULT1C4, SULT1E1 and some cytosolic fractions showed substrate inhibition at concentrations > 1 µM, > 1 µM and > 3 µM, respectively, additional series of 0.1, 0.15, 0.25, 0.35, 0.5, 0.75, 1 and 1.5 µM hesperetin (SULT1A1, SULT1A2 and SULT1C4), or a series of 0.1, 0.25, 0.5, 0.75, 1, 1.5, 2.5, 3.5 µM hesperetin (SULT1E1 and cytosolic fractions) were used. The reaction was terminated by addition of 25 µl acetonitrile. Under these conditions metabolite formation was linear with time and the amount of protein added (data not shown). Activity is expressed in nmol min^{-1} mg $protein^{-1}$ for the cytosolic fractions and in nmol min^{-1} mg SULT $protein^{-1}$ for the individual SULTs[28].

Enzyme kinetics

To determine the kinetics for glucuronidation and sulfonation, incubations were performed as described above. The maximum velocity (V_{max}) and Michaelisñ Menten constant (K_m) for the formation of the different phase II metabolites of hesperetin were determined by fitting the data to the Michaelis-Menten steady-state model $v = V_{max} / (1 + (K_m / [S]))$, with [S] being the hesperetin concentration, using the LSW data analysis toolbox (version 1.1.1) from MDL Information Systems (San Ramon, CA). For reactions demonstrating substrate inhibition the V_{max}, K_m and inhibition constant (K_i) were determined by fitting the data to the substrate inhibition equation $v = V_{max} \cdot [S] / (K_m + [S] \cdot (1 + [S] / K_i))$ using Graphpad Prism (version 5.02) from Graphpad Software (San Diego, CA).

HPLC analysis

To analyze the formation of hesperetin metabolites in the enzymatic incubations, reaction mixtures were centrifuged for 4 min at 16,000 *g* and samples of 50 µl of the supernatant were injected on a Waters Alliance 2695 separation module connected to a Waters 2996 DAD with an Alltech (Breda, The Netherlands) Alltima C18 5-µm 150- x 4.6 mm column with 7.5- x 4.6 mm guard column. Elution was at a flow rate of 1 ml/min. The gradient for the analysis of samples from the incubations with cytosol or SULTs started at 0% acetonitrile in nanopure water containing 0.1% trifluoroacetic acid, increasing to 10% acetonitrile in 5 min, to 15% in the following 16 min, and to 50% in the next 16 min, and to 80% in 1 min, followed by a cleaning and re-equilibration step. The gradient to analyze the samples from the incubations with microsomes or UGTs started at 0% acetonitrile in nanopure water containing 0.1% trifluoroacetic acid, increasing to 25% acetonitrile in 10 min, which condition was kept for 21 min, whereafter the percentage of acetonitrile was increased to 60% in 7 min, and to 80% in 1 min, followed by a cleaning and re-equilibration step. DAD-UV spectra were recorded between 200 and 420 nm, and chromatograms acquired at 280 nm were used for presentation and quantification.

Metabolite identification and quantification

Hesperetin 7-*O*-glucuronide, hesperetin 3'-*O*-glucuronide and hesperetin 7-*O*-sulfate were identified using authentic standards by their HPLC-DAD retention times and UV-spectra. Using the HPLC gradient for the analysis of the samples from the glucuronidation reactions, the retention times were as follows: hesperetin 37.2 min (UV_{max} 285.9 nm); hesperetin 7-*O*-glucuronide 17.7 min (UV_{max} 285.9 nm); hesperetin 3'-*O*-glucuronide 18.5 min (UV_{max} 285.9 nm). Using the HPLC gradient for the analysis of the samples from the sulfonation reactions, the retention times were as follows: hesperetin 36.7 min (UV_{max} 285.9 nm); hesperetin 7-*O*-sulfate 31.6 min (UV_{max} 281.2 nm, shoulder at 338 nm). Another metabolite resulting from the cytosolic and SULT incubations with PAPS at a retention time of 30.7 min (UV_{max} 290.7 nm) was repeatedly collected during HPLC-DAD separation, freeze dried and resolved in acidified, deuterated methanol for ^{1}H-NMR analysis. ^{1}H-NMR analysis revealed this metabolite to be hesperetin 3'-*O*-sulfate (for details see results section). Hesperetin 7-*O*-glucuronide and hesperetin 3'-*O*-glucuronide were quantified on the basis of a calibration curve made with authentic standards. Hesperetin 7-*O*-sulfate and hesperetin 3'-*O*-sulfate were quantified indirectly using the calibration curve for hesperetin and multiplication factors determined by enzymatic hydrolysis of hesperetin 7-*O*-sulfate (factor 1.27) and hesperetin 3'-*O*-sulfate (factor 0.86) into unconjugated hesperetin, which could be quantified with a calibration curve.

^{1}H-NMR analysis

^{1}H-NMR analysis was performed using a Bruker Avance III 600 MHz (Ettlingen, Germany) with cryoprobe. A Noesygppr1d pulse sequence with 3 s delay, 0.1 s mixing time and a 1.8 s acquisition time was used (18,028 Hz sweep width, 64 K data points). Spectra were obtained at 25°C. Resonances are reported relative to methanol-*d4* at 3.34 ppm.

Results

Identification of hesperetin metabolites

Figure 6.2 depicts part of a chromatogram from the HPLC-DAD analysis of the supernatant of an incubation of hesperetin with UGT1A9 and UDPGA. Two metabolites were formed and identified as hesperetin 7-*O*-glucuronide (t_R, 17.7 min; UV_{max}, 285.9 nm) and hesperetin 3'-*O*-glucuronide (t_R, 18.5 min; UV_{max}, 285.9 nm) on the basis of analysis of the corresponding authentic metabolite standards. Figure 6.3 on page 111 depicts part of a chromatogram from the HPLC-DAD analysis of the supernatant from an incubation of hesperetin with SULT1A3 and PAPS. Two metabolites were formed, one of which was identified as hesperetin 7-*O*-sulfate (t_R, 31.6 min; UV_{max}, 281.2 nm, shoulder at 338 nm) on the basis of analysis of the corresponding authentic metabolite standard. The fraction containing the second metabolite (t_R, 30.7 min; UV_{max}, 290.7 nm) which could not be identified with the available authentic standards, was collected, freeze dried, dissolved in acidified methanol and analyzed by ^{1}H-NMR. Modern NMR instruments with dedicated cryoprobes provide excellent sensitivity with relatively small amounts of material, provided that this material is of high purity. The sample analyzed contained about 0.5 nmol (150 ng) of the unknown sulfonated metabolite.

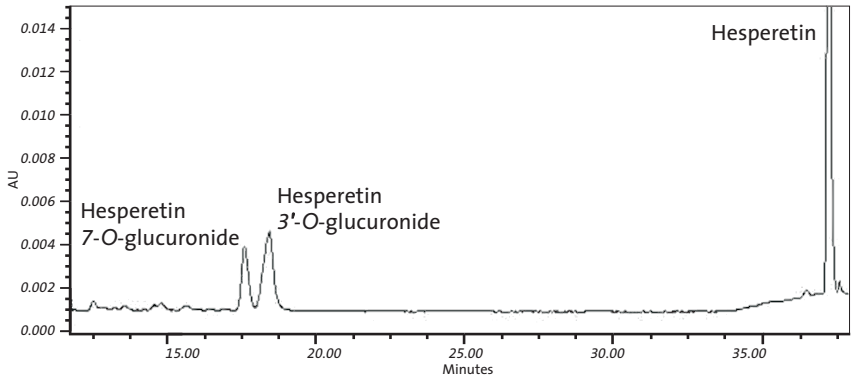

Figure 6.2 *Representative section of the HPLC chromatogram of the supernatant from the incubation of hesperetin with UGT1A9 and UDPGA showing the hesperetin glucuronide conjugates.*

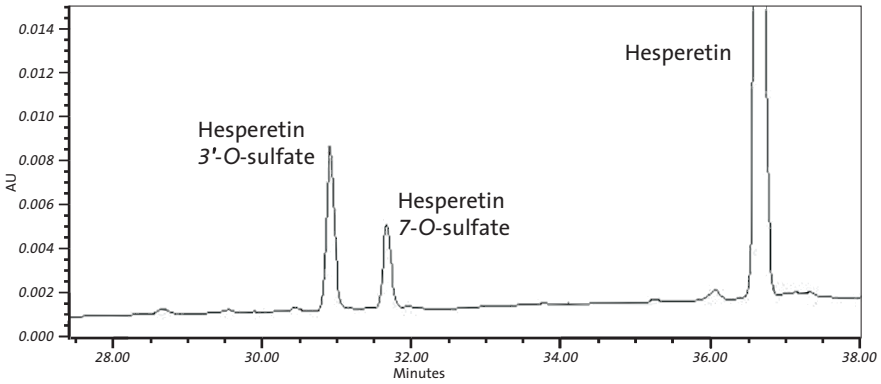

Figure 6.3 *Representative section of the HPLC chromatogram of the supernatant from the incubation of hesperetin with SULT1A3 and PAPS showing the hesperetin sulfo conjugates.*

Table 6.1 summarizes the ^{1}H-NMR data of this unknown sulfonated hesperetin metabolite, as well as of the parent compound hesperetin. Comparison of the chemical shift values and J-values of the corresponding protons in hesperetin and in the unknown sulfonated hesperetin metabolite reveals changes in especially the ^{1}H-NMR data of the protons of the B-ring upon conjugate formation: a relative shift of +0.66 ppm for H2', and a relative shift of +0.33 ppm for H6' (Table 6.1). This indicates a modification of the hydroxyl moiety at C3' resulting in a relatively large change in the chemical shift values of the protons H2' and H6' at the positions ortho and para with respect to the modified hydroxyl moiety. This is in line with earlier ^{1}H-NMR studies on metabolites of quercetin[29]. The signals of the protons H6 and H8 remained unchanged, excluding modification of the other hydroxyl-groups at position 5 or 7 of the hesperetin molecule. Together these data identify the unknown metabolite as hesperetin 3'-*O*-sulfate.

Table 6.1 *^{1}H-NMR data of hesperetin and the metabolite (identified as hesperetin 3'-O-sulfate) formed in the incubation mixture of hesperetin with specific SULT isoforms and human small intestinal cytosol and PAPS. The differences in chemical shift values of the protons in the metabolite as compared to the chemical shift values of the same protons in hesperetin are given in parentheses. d = doublet, dd = doublet of doublets.*

compound	**^{1}H-NMR chemical shift *(ppm)*, J-values *(Hz)* and peak splitting**							
	H6	**H8**	**H3 a**	**H3 b**	**H2**	**H2'**	**H5'**	**H6'**
hesperetin	*5.91* J=2.2 d	*5.95* J=2.2 d	*3.11* J=17.0; J=12.9 dd	*2.74* J=17.0; J=3.0 dd	*5.36* J=12.9; J=3.0 dd	*6.98* J=1.7 d	*6.96* J=8.4 d	*6.94* J=1.7; J=8.4 dd
metabolite	*5.91* J=*2.1* d	*5.95* J=*2.1* d	*3.10 (-0.01)* J=*17.1*; J=*12.9* dd	*2.80 (+0.06)* J=*17.1*; J=*3.0* dd	*5.41 (+0.05)* J=*12.9*; J=*3.0* dd	*7.64 (+0.66)* J=*2.1* d	*7.08 (+0.12)* J=*8.4* d	*7.27 (+0.33)* J=*2.1*; J=*8.4* dd

Glucuronidation by individual UGT enzymes

Glucuronidation of hesperetin was characterized using human recombinant UGT enzymes. The V_{max} and K_m values obtained for the formation of hesperetin 7-*O*-glucuronide and hesperetin 3'-*O*-glucuronide by the various UGT enzymes are shown in Table 6.2, as well as the catalytic efficiencies (V_{max}/K_m) derived from these values. The results reveal that hesperetin is most efficiently glucuronidated by UGT1A9. The efficiency of glucuronidation (V_{max}/K_m) decreases in the order of UGT1A9 > UGT1A1 > UGT1A7 > UGT1A3 > UGT1A8 > UGT1A10 > UGT2B7 = UGT2B15 > UGT2B4. The rate of formation of hesperetin 7-*O*-glucuronide by UGT1A6 was virtually linear with the applied concentration: 0.018 nmol min^{-1} mg $protein^{-1}$ 7-*O*-glucuronide formed per µM hesperetin, which excluded the determination of the kinetic parameters V_{max} and K_m by fitting the data to the Michaelis-Menten equation. Higher doses of hesperetin could not be tested because of the limited solubility of hesperetin in aqueous solutions.

Table 6.2 *V_{max} and K_m values (mean ± SEM) determined from 3-4 independent curves, and the catalytic efficiencies (V_{max}/K_m) derived from these values, for the glucuronidation of hesperetin (1 up to 50 µM) by individual UGT enzymes. n.d. = not detectable.*

UGT isoform	7-*O*-glucuronidation			3'-*O*-glucuronidation		
	K_m *(µM)*	V_{max} *(nmol min^{-1} mg $protein^{-1}$)*	(V_{max}/K_m) *(µl min^{-1} mg $protein^{-1}$)*	K_m *(µM)*	V_{max} *(nmol min^{-1} mg $protein^{-1}$)*	(V_{max}/K_m) *(µl min^{-1} mg $protein^{-1}$)*
UGT1A1	*4.0 ± 1.3*	*1.35 ± 0.29*	*339*	*1.2 ± 0.5*	*0.46 ± 0.06*	*376*
UGT1A3	*16.5 ± 4.6*	*3.94 ± 0.74*	*239*	n.d.	n.d.	-
UGT1A4	n.d.[a]	n.d.[a]	-[a]	n.d.	n.d.	-
UGT1A6	-[b]	-[b]	*18*[b]	n.d.	n.d.	-
UGT1A7	*105 ± 67.9*	*0.47 ± 0.04*	*5*	*8.7 ± 1.6*	*2.47 ± 0.63*	*285*
UGT1A8	*63.3 ± 11.8*	*2.33 ± 1.20*	*37*	*19.2 ± 3.9*	*3.18 ± 1.78*	*166*
UGT1A9	*5.3 ± 0.8*	*2.19 ± 0.10*	*411*	*4.0 ± 0.3*	*3.89 ± 0.20*	*981*
UGT1A10	*30.4 ± 8.2*	*2.82 ± 0.69*	*93*	*31.2 ± 12.6*	*0.89 ± 0.29*	*28*
UGT2B4	*119 ± 43.7*	*0.42 ± 0.09*	*4*	n.d	n.d	–
UGT2B7	*53.9 ± 17.6*	*1.53 ± 0.25*	*28*	*42.4 ± 13.9*	*0.88 ± 0.23*	*21*
UGT2B15	*34.5 ± 1.6*	*0.28 ± 0.01*	*8*	*29.9 ± 0.3*	*1.19 ± 0.02*	*40*
UGT2B17	n.d.[c]	n.d.[c]	-[c]	n.d.[c]	n.d.[c]	-[c]

[a] UGT1A4 very poorly glucuronidated hesperetin into solely hesperetin 7-O-glucuronide, only measurable at the highest test concentration (50 µM), precluding determination of kinetics. [b] Conjugation velocity by UGT1A6 of hesperetin into hesperetin 7-O-glucuronide occurred in a linear manner with dose (0.018 nmol min^{-1} mg $protein^{-1}$ µM $hesperetin^{-1}$), precluding determination of the individual Michaelis-Menten parameters Vmax and Km, but allowing the definition of the catalytic efficiency because the slope of the linear relationship between the rate of formation as a function of the substrate concentration equals Vmax/Km. [c] UGT2B17 very poorly glucuronidated hesperetin, only measurable at the highest test concentrations (50 µM).

The enzymes UGT1A4 and UGT2B17 only demonstrated very poor glucuronidation activity towards hesperetin under the conditions used in this study, precluding determination of the kinetics. Figure 6.4 presents an overview of the regioselectivity of the glucuronidation of hesperetin by the individual UGTs at a concentration of 10 μM hesperetin. For all UGTs the regioselectivity at 1 μM or 50 μM hesperetin was similar to that obtained at 10 μM. UGT1A3, UGT1A6 and UGT2B4 catalyze glucuronidation specifically at the hydroxyl moiety at C7 of hesperetin, while UGT1A7 almost solely conjugated the hydroxyl moiety at C3'. UGT1A1, UGT1A10 and UGT2B7 converted hesperetin into both hesperetin 3'-*O*-glucuronide and hesperetin 7-*O*-glucronide, however preferentially into the latter, while UGT1A8, UGT1A9 and UGT2B15 preferentially conjugated the hydroxyl moiety of hesperetin at position 3'. Overall, relatively more hesperetin 7-*O*-glucuronide is formed at higher substrate concentrations (Table 6.2).

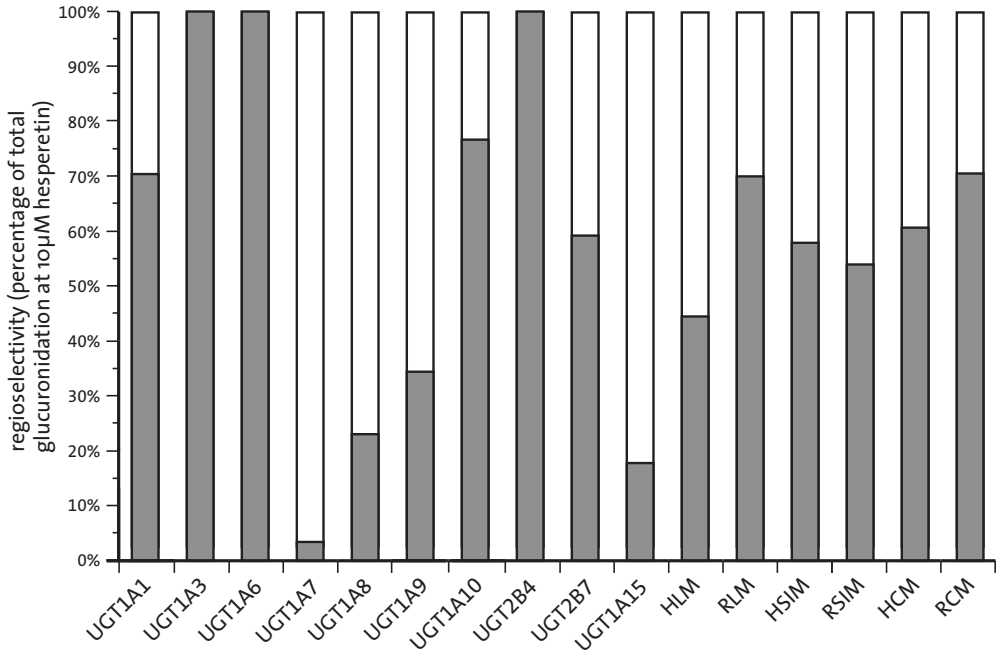

Figure 6.4 *Regioselectivity of the glucuronidation of hesperetin at position 7 (■) or position 3' (□) by different UGT enzymes and human and rat microsomes expressed as percentage of the total amount of hesperetin glucuronides formed at a 10 μM hesperetin concentration. HLM = human liver microsomes, RLM = rat liver microsomes, HSIM = human small intestinal microsomes, RSIM = rat small intestinal microsomes, HCM = human colon microsomes, RCM = rat colon microsomes.*

Sulfonation by individual SULT enzymes

The V_{max} and K_m values determined for the formation of hesperetin 7-*O*-sulfate and hesperetin 3'-*O*-sulfate by individual human SULTs are shown in Table 6.3, as well as the catalytic efficiencies (V_{max}/K_m) derived from these values. SULT1A1 demonstrated strong substrate inhibition already at hesperetin concentrations > 0.15 µM precluding determination of kinetic parameters. The high rate of 3'-*O*-sulfonation up to 117 nmol min^{-1} mg $SULT1A1^{-1}$ (at 0.15 µM hesperetin) indicates that SULT1A1 mediated sulfonation could likely play an important role in the conjugation of hesperetin at low concentrations. SULT1A2, SULT1C4 and SULT1E1 also demonstrated substrate inhibition at concentrations > 1 µM, > 1 µM and > 3 µM, respectively. The catalytic efficiency of sulfonation (V_{max}/K_m) of the SULTs (other than SULT1A1) decreases in the order of SULT1C4 > SULT1A2 > SULT1E1 > SULT1A3 > SULT1B1 > SULT1C2 > SULT2A1. The isoenzymes SULT1C3, SULT2B1_v1, SULT2B1_v2 and SULT4A1_v2 did not show any sulfonation activity toward hesperetin under the conditions used in this study.

Table 6.3 *V_{max} and K_m values (mean ± SEM) determined from 3 independent curves, and the catalytic efficiencies (V_{max}/K_m) derived from these values, for the sulfonation of hesperetin (1 up to 50 µM unless stated otherwise) by individual SULT enzymes. n.d. = not detectable.*

SULT isoform	7-*O*-sulfonation			3'-*O*-sulfonation		
	K_m *(µM)*	V_{max} *(nmol min^{-1} mg $SULT^{-1}$)*	(V_{max}/K_m) *(µl min^{-1} mg $SULT^{-1}$)*	K_m *(µM)*	V_{max} *(nmol min^{-1} mg $SULT^{-1}$)*	(V_{max}/K_m) *(µl min^{-1} mg $SULT^{-1}$)*
SULT1A1	n.d.	n.d.	-	*< 0.15*[a]	-[a]	-[a]
SULT1A2	n.d.	n.d.	-	*0.5 ± 0.2*[b]	*454 ± 94.8*[b]	*881,553*[b]
SULT1A3	*12.5 ± 3.3*	*89.9 ± 7.43*	*7,178*	*13.2 ± 3.0*	*276 ± 24.8*	*20,964*
SULT1B1	*3.9 ± 0.5*	*3.54 ± 0.66*	*899*	*4.3 ± 0.2*	*21.5 ± 2.14*	*5,003*
SULT1C2	*66.7 ± 16.1*	*18.8 ± 6.83*	*282*	*28.3 ± 14.5*	*1.45 ± 0.46*	*51*
SULT1C3	n.d.	n.d.	-	n.d.	n.d.	-
SULT1C4	*0.1 ± 0.0*[c]	*87.4 ± 8.13*[c]	*1,117,263*[c]	n.d.	n.d.	-
SULT1E1	n.d.	n.d.	-	*2.5 ± 1.0*[d]	*538 ± 134*[d]	*219,242*[d]
SULT2A1	*80.2 ± 21.0*	*10.2 ± 1.96*	*127*	n.d.	n.d.	-
SULT2B1_v1	n.d.	n.d.	-	n.d.	n.d.	-
SULT2B1_v2	n.d.	n.d.	-	n.d.	n.d.	-
SULT4A1_v2	n.d.	n.d.	-	n.d.	n.d.	-

[a] SULT1A1 demonstrated strong substrate inhibition at concentrations > 0.1 µM precluding determination of kinetic parameters. [b] SULT1A2 showed substrate inhibition at concentrations > 1 µM hesperetin; K_i = 1.9 µM. [c] SULT1C4 showed substrate inhibition at concentrations > 1 µM hesperetin; K_i = 23.5 µM. [d] SULT1E1 showed substrate inhibition at concentrations > 3 µM hesperetin; K_i = 12.9 µM.

SULT1C4 and SULT2A1 selectively catalyzed the sulfonation at the hydroxyl moiety of position 7 of hesperetin, while SULT1A1, SULT1A2 and SULT1E1 solely conjugated the hydroxyl moiety at position 3' (Figure 6.5). SULT1C2 converted hesperetin into both hesperetin 3'-*O*-sulfate and hesperetin 7-*O*-sulfate, however preferentially into the latter, while SULT1A3 and SULT1B1 preferentially conjugated the hydroxyl moiety of hesperetin at position 3' (Figure 6.5). For all SULTs the regioselectivity at 1 µM or 50 µM hesperetin was similar to that obtained at 10 µM.

Glucuronidation by human and rat tissue samples

The apparent V_{max} and K_m values for the formation of hesperetin 7-*O*-glucuonide and hesperetin 3'-*O*-glucuronide by human and rat microsomal fractions from different tissues are shown in Table 6.4 on page 116, as well as the apparent catalytic efficiencies (V_{max}/K_m) derived from these values. Hesperetin was converted into both glucuronide metabolites by microsomes from all human and rat tissues tested. Generally, the affinity was higher (K_m lower) for glucuronidation at position 3', whereas the capacity (V_{max}) was higher for glucuronidation at position 7 (Table 6.4), and as a result, at higher hesperetin concentrations relatively more hesperetin 7-*O*-glucuronide than hesperetin 3'-glucuronide is formed.

.

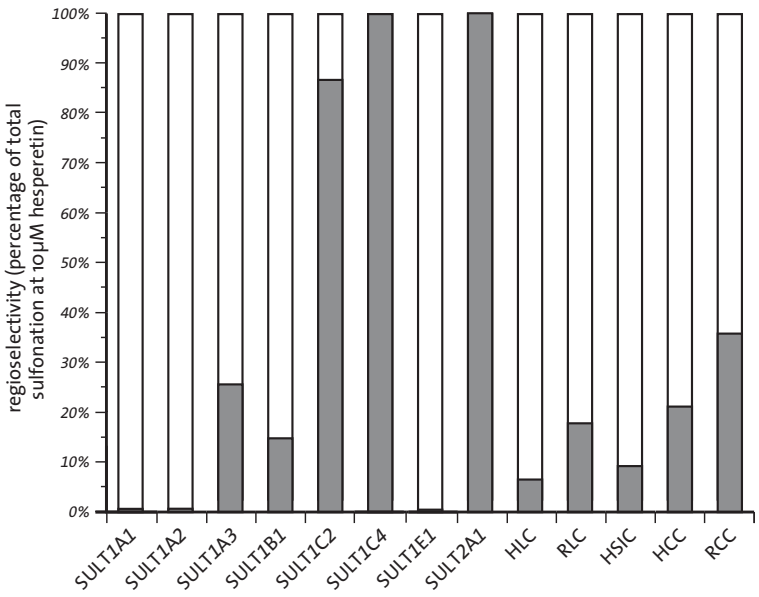

Figure 6.5 *Regioselectivity of the sulfonation of hesperetin at position 7 (■) or position 3' (□) by different SULT enzymes and human and rat cytosol expressed as percentage of the total amount of hesperetin sulfates formed at a 10 µM hesperetin concentration. HLC = human liver cytosol, RLC = rat liver cytosol, HSIC = human small intestinal cytosol, HCC = human colon cytosol, RCC = rat colon cytosol.*

Table 6.4 *Apparent V_{max} and K_m values (mean ± SEM) determined from 2-3 independentcurves of the glucuronidation or sulfonation of hesperetin (up to 50 μM unless stated otherwise) by microsomes or cytosol, respectively, from human and rat tissue fractions. n.d. = not detectable.*

	7-O-glucuronidation			*3'-O-glucuronidation*			*7-O-sulfonation*			*3'-O-sulfonation*		
	K_m(app) (μM)	V_{max}(app) (nmol min^{-1} mg protein^{-1})	(V_{max}(app)/K_m(app)) (μl min^{-1} mg protein^{-1})	K_m(app) (μM)	V_{max}(app) (nmol min^{-1} mg protein^{-1})	(V_{max}(app)/K_m(app)) (μl min^{-1} mg protein^{-1})	K_m(app) (μM)	V_{max}(app) (nmol min^{-1} mg protein^{-1})	(V_{max}(app)/K_m(app)) (μl min^{-1} mg protein^{-1})	K_m(app) (μM)	V_{max}(app) (nmol min^{-1} mg protein^{-1})	(V_{max}(app)/K_m(app)) (μl min^{-1} mg protein^{-1})
Small intestine												
Human	8.3 ± 1.9	3.80 ± 0.50	458	6.4 ± 1.2	2.49 ± 0.49	391	9.1 ± 1.5	0.14 ± 0.04	16	0.6 ± 0.2	0.79 ± 0.14	1240
Rat	15.3 ± 3.8	9.85 ± 0.70	643	7.7 ± 0.6	5.91 ± 0.71	764	n.d.	n.d.	-	n.d.	n.d.	-
Colon												
Human	3.7 ± 0.1	1.55 ± 0.08	415	3.4 ± 0.1	0.99 ± 0.02	294	8.6 ± 0.0	0.07 ± 0.00	8	3.3 ± 0.7[a]	0.20 ± 0.02[a]	61[a]
Rat	10.3 ± 0.0	5.41 ± 0.18	524	2.4 ± 0.0	1.41 ± 0.07	598	1.1 ± 0.4	0.01 ± 0.00	4	7.3 ± 1.1[a]	0.04 ± 0.00[a]	5[a]
Liver												
Human	20.1 ± 1.6	8.00 ± 0.23	398	10.6 ± 1.1	6.96 ± 0.79	657	1.5 ± 0.9	0.02 ± 0.00	15	< 0.1[b]	-[b]	-[b]
Rat	24.3 ± 0.4	21.08 ± 0.05	868	5.0 ± 0.1	4.04 ± 0.30	801	< 0.25[c]	-[c]	-[c]	< 0.25[b]	-[b]	-[b]

a) Human and rat colon cytosol showed 3'-O-sulfonation substrate inhibition at concentrations > 25 μM and > 15 μM, respectively; K_i human colon cytosol = 446 μM, K_i rat colon cytosol = 22.2 μM. b) Human and rat liver cytosol demonstrated strong 3'-O-sulfonation substrate inhibition at concentrations of respectively > 0.1 μM and > 0.25 μM precluding determination of kinetic parameters. c) Rat liver cytosol demonstrated strong 7-O-sulfonation substrate inhibition at concentrations of > 0.25 μM precluding determination of kinetic parameters.

Sulfonation by human and rat tissue samples

The apparent V_{max} and K_m values determined for the formation of hesperetin 7-*O*-sulfate and hesperetin 3'-*O*-sulfate by human and rat cytosol from different tissues are shown in Table 6.4 on page 116, as well as the apparent catalytic efficiencies (V_{max}/K_m) derived from these values. Hesperetin was predominately converted into hesperetin 3'-*O*-sulfate by human small intestinal cytosol with a K_m of 0.6 μM and a capacity of 0.79 nmol min^{-1} mg $protein^{-1}$, while rat small intestinal cytosol did not show sulfonation activity toward hesperetin (Table 6.4). Rat as well as human colonic cytosol showed low catalytic efficiencies. Liver cytosol of both species converted hesperetin into hesperetin 3'-*O*-sulfate already at low concentrations, and demonstrated substrate inhibition at hesperetin concentrations > 0.25 μM. Remarkably, rat liver cytosol also demonstrated efficient conversion of hesperetin into hesperetin 7-*O*-sulfate at low concentrations, with substrate inhibition at hesperetin concentrations > 0.25 μM, while the sample of human liver cytosol demonstrated very little 7-*O*-sulfate formation (Table 6.4).

Discussion

In the present study the kinetics for the conjugation of hesperetin by individual UGT and SULT enzymes and rat or human microsomes and cytosol from small intestine, colon and liver, were characterized. Hesperetin was conjugated at the C7 and C3' hydroxyl moieties. It is interesting to note that the conjugation at the C5 hydroxyl moiety was not catalyzed. This phenomenon can be explained by the strong intramolecular hydrogen bond between this hydroxyl moiety and the C4 carbonyl moiety preventing the phase II conjugation[30]. Of all UGTs tested, UGT1A9, UGT1A1, UGT1A7, UGT1A3 and UGT1A8 demonstrated the highest catalytic efficiencies (Table 6.2 on page 112). These UGTs have been reported to efficiently catalyze the glucuronidation of other flavonoids as well, as was recently reviewed by Zhang *et al.*[31], although the relative efficiency of different UGTs seems highly dependent on the flavonoid structure involved. Hesperetin, as other flavonoids, appears not to be a suitable substrate for UGT1A4[18,21,32]. The regioselectivity of hesperetin glucuronidation varied enzyme-specifically (Table 6.2 on page 112). Differences in the regioselectivity of the flavonoid conjugation by different individual UGTs has also been reported for the conjugation of other flavonoids[18-21], the regioselectivity being dependent on the isoenzyme involved, the flavonoid converted, and the substrate concentration. For instance luteolin (3',4',5,7-tetrahydroxyflavone) was almost solely (98% of HPLC chromatogram peak area) converted into a 7-*O*-glucuronide metabolite by UGT1A6, while quercetin (3,3',4',5,7-tetrahydroxy-flavone) bearing one extra hydroxyl moiety, was metabolized into its 4'-*O*-glucuronide (32%), 7-*O*-glucuronide (30%), 3'-*O*-glucuronide (22%) and

3-*O*-glucuronide (16%) by UGT1A6[18].
Of the SULT enzymes (apart from SULT1A1) SULT1A2, SULT1C4 and to a lesser extent SULT1E1 and SULT1A3 demonstrated the highest catalytic efficiencies for the sulfonation of hesperetin (Table 6.3 on page 114). SULT1A1, SULT1A3 and SULT1E1 have been reported to sulfonate other flavonoids as well[19,33,34]. In the present study, SULT1A1, SULT1A2 and SULT1E1 solely catalyzed the formation of hesperetin 3'-*O*-sulfate while SULT1C4 and SULT2A1 solely catalyzed the formation of hesperetin 7-*O*-sulfate (Figure 6.5 on page 115). The regioselectivity of flavonoid sulfonation appears to be dependent on the SULT isoenzyme as well as on the flavonoid studied: daidzein (4',7-dihydroxyisoflavone) and genistein (4',5,7-trihydroxyisoflavone) were reported to be predominantly sulfated by SULT1A1 at position 7 rather than at position 4', while the hydroxyl moieties at both positions were sulfonated with similar efficiency by SULT1E1[33]. At low concentrations of hesperetin SULT1A2, SULT1C4, SULT1E1 (Table 6.3 on page 114) and especially SULT1A1 demonstrated substrate inhibition. This property of SULTs in the conjugation of flavonoids at low concentrations is also reported for the SULT1A1 mediated sulfonation of daidzein (> 1.5 μM) and genistein (> 2 μM)[33], and for the SULT1E1 mediated sulfonation of quercetin and chrysin[34].
Incubations of hesperetin with human and rat microsomal fractions in the presence of UDPGA resulted in formation of hesperetin 7-*O*-glucuronide and hesperetin 3'-*O*-glucuronide (Table 6.4 on page 116). Based on the kinetics of the individual human UGTs (Table 6.2 on page 112) and the data on UGT mRNA expression levels[22-25], the 7-*O*-glucuronidation of hesperetin in human tissue fractions is likely catalyzed by UGT1A1 and UGT1A9. The 3'-*O*-glucuronidation of hesperetin by human microsomes is likely catalyzed by UGT1A9 and UGT1A1, whereas in the human small intestinal and colonic microsomes UGT1A7 and UGT1A8 may contribute as well. However, one should keep in mind that selectivity profiles by single UGTs in complete systems, in which protein-protein interactions may occur, may be different from those in *in vitro* model systems[35]. Taking the catalytic efficiencies (Table 6.2) and the mRNA expression levels of the rat orthologue UGTs into account[36], it can be foreseen that, in rat liver and rat intestinal microsomes, rat UGT1A1 and rat UGT1A7 are likely responsible for the glucuronidation of hesperetin.
Incubations with the human cytosolic fractions demonstrated a preferential sulfonation of position 3' of hesperetin (Table 6.4). Although SULT1A2, SULT1C4 and SULT1E1 demonstrate high catalytic efficiencies, based on expression levels[13,14] they are minor SULT isoforms in the intestine and liver. It is concluded that especially SULT1A1 is involved in the sulfonation of hesperetin in the human liver, while SULT1B1 and SULT1A3 will preferably contribute to the intestinal sulfonation of hesperetin. Our incubations with human cytosol demonstrating predominant formation of hesperetin 3'-*O*-sulfate, the major metabolite formed by SULT1A1 as

well as by SULT1B1 and SULT1A3, support such a notion. Hesperetin was not sulfonated by rat small intestinal cytosol, which corresponds with the negligible SULT expression in the small intestine of rats[26]. The hepatic expression of the rat ortholog of SULT1C4, a form not detected in human liver[37], probably explains the formation of hesperetin 7-*O*-sulfate by rat liver cytosol.

When both SULTs and UGTs play a role at the same time, such as in the *in vivo* situation, the existence of mixed conjugates has been reported as well. In a study in which human volunteers were given up to 1 liter of orange juice providing 444 mg/l hesperidin the circulating forms of hesperetin in the plasma consisted of glucuronides (87%) and sulfoglucuronides (13%) as determined after specific enzymatic hydrolysis[5]. In another study in which human volunteers were given 250 ml orange juice containing 410 mg/l hesperidin, only hesperetin glucuronides were detected in the plasma, however, substantial amounts of hesperetin sulfoglucuronides were detected in the urine as indicated by LC-MS/MS[8]. The authors argue that the kidney may be involved in post-absorption phase II metabolism, which could be explained by the expression of SULT1A1 in the kidneys[14,28], the enzyme for which we found a high affinity towards hesperetin resulting in sulfonation already at very low concentrations. In a third study in which human volunteers were given oranges or orange juice providing respectively 161 or 145 mg hesperidin, hesperetin 7-*O*-glucuronide and 3'-*O*-glucuronide were detected in blood and plasma, as well as hesperetin 3'-*O*-sulfate, as qualified by LC-MS/MS and metal complexation techniques[6]. The absence of hesperetin 7-*O*-sulfate in these human volunteers is supported by the sulfonation kinetics found in the present study.

Recently we analyzed the metabolism of hesperetin *in vitro* using Caco-2 cell monolayers as a model of the intestinal barrier. Interestingly, after incubations of hesperetin with Caco-2 cell monolayers formation of hesperetin 7-*O*-glucuronide and 7-*O*-sulfate was observed, while no metabolites of hesperetin conjugated at position 3' were detected. These observations could be explained by the relatively strong expression of SULT1C4[27,38] and UGT1A6[39], both enzymes specifically catalyzing the conjugation at position 7, compared to other SULT or UGT-forms in Caco-2 cells. Moreover, siRNA-mediated UGT1A6 silencing in this cell line heavily decreased the glucuronidation of the flavonoid apigenin demonstrating an important role for UGT1A6 in the glucuronidation by Caco-2 cells of a structurally related compound[40].

In conclusion, the results of the present study show that individual UGTs and SULTs demonstrate marked regioselective kinetics for conjugation of hesperetin. As a result variation in expression levels of these UGTs and SULTs give rise to different metabolite patterns in different biological systems. Since different flavonoid conjugates may have different physiological and/or biological properties, this

regioselective conjugation by different UGT and SULT enzymes should not be ignored in flavonoid research. Finally, given the high catalytic efficiency and expression levels of UGTs in intestinal tissue, it can be concluded that first pass metabolism within the intestinal cells contributes significantly to the formation of hesperetin 3'-*O*-glucuronide and 7-*O*-glucuronide, the major hesperetin metabolites found *in vivo*.

References

1 Tomás-Barberán FA, Clifford MN. Flavanones, chalcones and dihydrochalcones - nature, occurrence and dietary burden. *J Sci Food Agric* 80(7): 1073-1080, 2000.

2 Horcajada MN, Habauzit V, Trzeciakiewicz A, Morand C, Gil-Izquierdo A, Mardon J, Lebecque P, Davicco MJ, Chee WSS, Coxam V, Offord E. Hesperidin inhibits ovariectomized-induced osteopenia and shows differential effects on bone mass and strength in young and adult intact rats. *J Appl Physiol* 104(3): 648-654, 2008.

3 Németh K, Plumb GW, Berrin J-G, Juge N, Jacob R, Naim HY, Williamson G, Swallow DM, Kroon PA. Deglycosylation by small intestinal epithelial cell beta-glucosidases is a critical step in the absorption and metabolism of dietary flavonoid glycosides in humans. *Eur J Nutr* 42(1): 29-42, 2003.

4 Nielsen ILF, Chee WSS, Poulsen L, Offord-Cavin E, Rasmussen SE, Frederiksen H, Enslen M, Barron D, Horcajada M-N, Williamson G. Bioavailability is improved by enzymatic modification of the citrus flavonoid hesperidin in humans: a randomized, double-blind, crossover trial. *J Nutr* 136(2): 404-408, 2006.

5 Manach C, Morand C, Gil-Izquierdo A, Bouteloup-Demange C, Rémésy C. Bioavailability in humans of the flavanones hesperidin and narirutin after the ingestion of two doses of orange juice. *Eur J Clin Nutr* 57(2): 235-242, 2003.

6 Brett GM, Hollands W, Needs PW, Teucher B, Dainty JR, Davis BD, Brodbelt JS, Kroon PA. Absorption, metabolism and excretion of flavanones from single portions of orange fruit and juice and effects of anthropometric variables and contraceptive pill use on flavanone excretion. *Br J Nutr* 101(5): 664-675, 2009.

7 Matsumoto H, Ikoma Y, Sugiura M, Yano M, Hasegawa Y. Identification and quantification of the conjugated metabolites derived from orally administered hesperidin in rat plasma. *J Agric Food Chem* 52(21): 6653-6659, 2004.

8 Mullen W, Archeveque M-A, Edwards CA, Matsumoto H, Crozier A. Bioavailability and metabolism of orange juice flavanones in humans: impact of a full-fat yogurt. *J Agric Food Chem* 56(23): 11157-11164, 2008.

9 Silberberg M, Morand C, Mathevon T, Besson C, Manach C, Scalbert A, Remesy C. The bioavailability of polyphenols is highly governed by the capacity of the intestine and of the liver to secrete conjugated metabolites. *Eur J Nutr* 45(2): 88-96, 2006.

10 Liu Z, Hu M. Natural polyphenol disposition via coupled metabolic pathways. *Expert Opin Drug Metab Toxicol* 3(3): 389-406, 2007.

11 Brand W, Van der Wel PAI, Rein MJ, Barron D, Williamson G, Van Bladeren PJ, Rietjens IMCM. Metabolism and transport of the citrus flavonoid hesperetin in Caco-2 cell monolayers. *Drug Metab Dispos* 36(9): 1794-1802, 2008.

12 Mackenzie PI, Bock KW, Burchell B, Guillemette C, Ikushiro S, Iyanagi T, Miners JO, Owens IS, Nebert DW. Nomenclature update for the mammalian UDP glycosyltransferase (UGT) gene superfamily. *Pharmacogenet Genomics* 15(10): 677-685, 2005.

13 Teubner W, Meinl W, Florian S, Kretzschmar M, Glatt H. Identification and localization of soluble sulfotransferases in the human gastrointestinal tract. *Biochem J* 404(2): 207-215, 2007.

14 Riches Z, Stanley EL, Bloomer JC, Coughtrie MWH. Quantitative evaluation of the expression and activity of five major sulfotransferases (SULTs) in human tissues: the SULT "pie". *Drug Metab Dispos* 37(11): 2255-2261, 2009.

15 Meinl W, Donath C, Schneider H, Sommer Y, Glatt H. SULT1C3, an orphan sequence of the human genome, encodes an enzyme activating various promutagens. *Food Chem Toxicol* 46(4): 1249-1256, 2008.

16 Freimuth RR, Wiepert M, Chute CG, Wieben ED, Weinshilboum RM. Human cytosolic sulfotransferase database mining: identification of seven novel genes and pseudogenes. *Pharmacogenomics J* 4(1): 54-65, 2004.

17 Blanchard RL, Freimuth RR, Buck J, Weinshilboum RM, Coughtrie MWH. A proposed nomenclature system for the cytosolic sulfotransferase (SULT) superfamily. *Pharmacogenetics* 14(3): 199-211, 2004.

18 Boersma MG, Van der Woude H, Bogaards J, Boeren S, Vervoort J, Cnubben NHP, Van Iersel MLPS, Van Bladeren PJ, Rietjens IMCM. Regioselectivity of phase II metabolism of luteolin and quercetin by UDP-glucuronosyl transferases. *Chem Res Toxicol* 15(5): 662-670, 2002.

19 Otake Y, Hsieh F, Walle T. Glucuronidation versus oxidation of the flavonoid galangin by human liver microsomes and hepatocytes. *Drug Metab Dispos* 30(5): 576-581, 2002.

20 Zhang L, Lin G, Zuo Z. Involvement of UDP-glucuronosyltransferases in the extensive liver and intestinal first-pass metabolism of flavonoid baicalein. *Pharm Res* 24(1): 81-89, 2007.

21 Tang L, Singh R, Liu Z, Hu M. Structure and concentration changes affect characterization of UGT isoform-specific metabolism of isoflavones. *Mol Pharm* 6(5): 1466-1482, 2009.

22 Gregory PA, Lewinsky RH, Gardner-Stephen DA, Mackenzie PI. Regulation of UDP glucuronosyltransferases in the gastrointestinal tract. *Toxicol Appl Pharmacol* 199(3): 354-363, 2004.

23 Nakamura A, Nakajima M, Yamanaka H, Fujiwara R, Yokoi T. Expression of UGT1A and UGT2B mRNA in human normal tissues and various cell lines. *Drug Metab Dispos* 36(8): 1461-1464, 2008.

24 Ohno S, Nakajin S. Determination of mRNA expression of human UDP-glucuronosyltransferases and application for localization in various human tissues by real-time reverse transcriptase-polymerase chain reaction. *Drug Metab Dispos* 37(1): 32-40, 2009.

25 Izukawa T, Nakajima M, Fujiwara R, Yamanaka H, Fukami T, Takamiya M, Aoki Y, Ikushiro S, Sakaki T, Yokoi T. Quantitative analysis of UDP-glucuronosyltransferase (UGT) 1A and UGT2B expression levels in human livers. *Drug Metab Dispos* 37(8): 1759-1768, 2009.

26 Meinl W, Sczesny S, Brigelius-Flohé R, Blaut M, Glatt H. Impact of gut microbiota on intestinal and hepatic levels of phase 2 xenobiotic-metabolizing enzymes in the rat. *Drug Metab Dispos* 37(6): 1179-1186, 2009.

27 Meinl W, Ebert B, Glatt H, Lampen A. Sulfotransferase forms expressed in human intestinal Caco-2 and TC7 cells at varying stages of differentiation and role in benzo[a]pyrene metabolism. *Drug Metab Dispos* 36(2): 276-283, 2008.

28 Meinl W, Pabel U, Osterloh-Quiroz M, Hengstler JG, Glatt H. Human sulphotransferases are involved in the activation of aristolochic acids and are expressed in renal target tissue. *Int J Cancer* 118(5): 1090-1097, 2006.

29 Van der Woude H, Boersma MG, Vervoort J, Rietjens IMCM. Identification of 14 quercetin phase II mono- and mixed conjugates and their formation by rat and human phase II in vitro model systems. *Chem Res Toxicol* 17(11): 1520-1530, 2004.

30 Exarchou V, Nenadis N, Tsimidou M, Gerothanassis IP, Troganis A, Boskou D. Antioxidant activities and phenolic composition of extracts from Greek oregano, Greek sage, and summer savory. *J Agric Food Chem* 50(19): 5294-5299, 2002.

31 Zhang L, Zuo Z, Lin G. Intestinal and hepatic glucuronidation of flavonoids. *Mol Pharm* 4(6): 833-845, 2007.

32 Walle T, Otake Y, Galijatovic A, Ritter JK, Walle UK. Induction of UDP-glucuronosyltransferase UGT1A1 by the flavonoid chrysin in the human hepatoma cell line hep G2. *Drug Metab Dispos* 28(9): 1077-1082, 2000.

33 Nakano H, Ogura K, Takahashi E, Harada T, Nishiyama T, Muro K, Hiratsuka A, Kadota S, Watabe T. Regioselective monosulfation and disulfation of the phytoestrogens daidzein and genistein by human liver sulfotransferases. *Drug Metab Pharmacokinet* 19(3): 216-226, 2004.

34 Ung D, Nagar S. Variable sulfation of dietary polyphenols by recombinant human sulfotransferase (SULT) 1A1 genetic variants and SULT1E1. *Drug Metab Dispos* 35(5): 740-746, 2007.

35 Fujiwara R, Nakajima M, Yamanaka H, Katoh M, Yokoi T. Interactions between human UGT1A1, UGT1A4, and UGT1A6 affect their enzymatic activities. *Drug Metab Dispos* 35(10): 1781-1787, 2007.

36 Shelby MK, Cherrington NJ, Vansell NR, Klaassen CD. Tissue mRNA expression of the rat UDP-glucuronosyltransferase gene family. *Drug Metab Dispos* 31(3): 326-333, 2003.

37 Sakakibara Y, Yanagisawa K, Katafuchi J, Ringer DP, Takami Y, Nakayama T, Suiko M, Liu MC. Molecular cloning, expression, and characterization of novel human SULT1C sulfotransferases that catalyze the sulfonation of N-hydroxy-2-acetylamino- fluorene. *J Biol Chem* 273(51): 33929-33935, 1998.

38 Tamura H-O, Taniguchi K, Hayashi E, Hiyoshi Y, Nagai F. Expression profiling of sulfotransferases in human cell lines derived from extra-hepatic tissues. *Biol Pharm Bull* 24(11): 1258-1262, 2001.

39 Paine MF, Fisher MB. Immunochemical identification of UGT isoforms in human small bowel and in Caco-2 cell monolayers. *Biochem Biophys Res Commun* 273(3): 1053-1057, 2000.

40 Liu X, Tam VH, Hu M. Disposition of flavonoids via enteric recycling: determination of the

Chapter 7

Stereoselective conjugation, transport and bioactivity of *S*- and *R*-hesperetin enantiomers *in vitro*

Walter Brand, Jia Shao, Elisabeth F. Hoek-van den Hil, Kathelijn N. van Elk, Bert Spenkelink, Laura H.J. de Haan, Maarit J. Rein, Fabiola Dionisi, Gary Williamson, Peter J. van Bladeren, and Ivonne M.C.M. Rietjens

Journal of Agricultural and Food Chemistry, accepted for publication

Abstract

The flavanone hesperetin ((+/-)-4'-methoxy-3',5,7-trihydroxyflavanone) is the aglycone of the rutinoside hesperidin which is the major flavonoid present in sweet oranges. Like other flavanones, hesperetin contains a chiral C-atom and so can exist as an *S*- and *R*-enantiomer. In nature 2*S*-hesperidin and its *S*-hesperetin aglycone are the predominant chemical forms. In spite of this, many studies have been performed with the commercially available racemates of hesperidin and hesperetin. The present study reports a chiral HPLC method to separate *S*- and *R*-hesperetin on an analytical and semi-preparative scale. This allowed characterization of the stereoselective differences in metabolism and transport in the intestine and activity in a selected bioassay of the separated hesperetin enantiomers in *in vitro* model systems. To this end *S*- or *R*-hesperetin were treated in several assays: (1) with human small intestinal fractions containing UDP-glucuronosyl transferases (UGTs) or sulfotransferases (SULTs) and their cofactors; (2) with Caco-2 cell monolayers as a model for the intestinal transport barrier; (3) with mouse Hepa-1c1c7 cells transfected with human EpRE-controlled luciferase to test induction of EpRE-mediated gene expression. Although the results obtained indicate some significant differences in metabolism, the differences in the metabolism and transport characteristics of the two hesperetin enantiomers are relatively small, whereas at physiologically relevant concentrations the activation of EpRE mediated gene expression was similar. This indicates that for these endpoints, including intestinal metabolism and transport, experiments performed with racemic hesperetin may adequately reflect what can be expected for the naturally occurring *S*-enantiomer.

Introduction

The flavanone hesperetin ((+/-)-4'-methoxy-3',5,7-trihydroxyflavanone) (Figure 7.1 on page 125) is the aglycone of hesperidin (hesperetin 7-*O*-rutinoside), which is the major flavonoid present in sweet oranges (*Citrus sinensis*) and orange juice, but which can also be found in other citrus fruits including lemon, lime and mandarin and some herbs[1]. Hesperetin and hesperidin have been reported to provide health beneficial effects, including anticarcinogenic properties and a reduced risk of osteoporosis[2-4].

Upon ingestion, hesperidin has to be hydrolyzed into hesperetin aglycone by colonic microbiota prior to its absorption. Conversion of the disaccharide hesperidin into the monosaccharide hesperetin 7-*O*-glucoside prior to consumption has been demonstrated to lead to absorption already in the small intestine after deglucosilation by phloridzin hydrolase and/or by facilitated transport into the

intestinal cells by a sodium dependent glucose transporter (*e.g.* SGLT1) followed by intracellular deglucosylation[5]. In the intestinal cells, hesperetin aglycone can be conjugated by UDP-glucuronosyltransferases (UGTs) and sulfotransferases (SULTs) into glucuronidated and sulfonated metabolites respectively, which have been found *in vivo* in both rat and human plasma[6,7]. The intestinal barrier is believed to play a dominant role in the conjugation of hesperetin[8], and in its limited bioavailability because of efflux of the metabolites back to the intestinal lumen by ABC transport proteins[9,10].

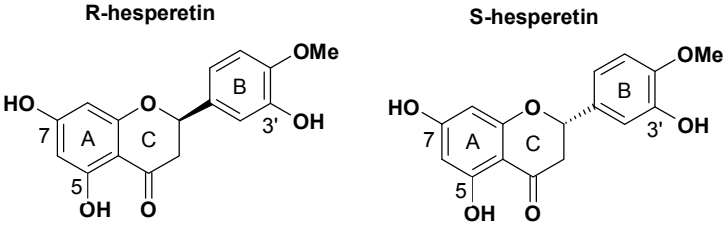

Figure 7.1 *Chemical structure of (-)-S- and (+)-R-hesperetin (4'-methoxy-3',5,7-trihydroxyflavanone).*

Unlike many other classes of flavonoids, flavanones, as well as flavanols, share a chiral carbon atom in position 2 and therefore exist in an *S*- and *R*-configuration (Figure 7.1). 2*S*-hesperidin is naturally predominant in citrus fruits[11-13], and hesperidin is present in fresh, sweet orange juice in an *S*:*R* ratio of at least 92:8 in favor of the 2*S*-epimer[14-16]. Although in nature the 2*S*-epimer of hesperidin, and subsequently the *S*-hesperetin enantiomer, is dominant, hesperetin and hesperidin are currently only commercially available as a mixture of both stereoisomers. As a result, studies on hesperetin and hesperidin generally do not take the chirality into account whereas in theory the two enantiomers may display distinct kinetic and dynamic properties[17]. For flavonoids, stereochemical properties have been reported to influence, for example, the bioavailability of the flavanol catechin[18], the estrogenic activity of the isoflavone metabolite equol[19,20] and the plasma and urinary kinetics of hesperetin[16,21], and may thus very well affect both the intestinal metabolism and transport of hesperetin, as well as its biological effects.

Although several studies reported analytical methods to analyze *S*- and *R*-enantiomers of hesperetin, as reviewed by Yáñez *et al.*[11], the kinetic differences of *S*- and *R*-hesperetin were only studied indirectly. After intravenous administration of racemic hesperetin to rats, *R*-hesperetin had a significant 3.3-fold higher area under the serum concentration-time curve (AUC) and a 1.9-fold longer half-life, compared to *S*-hesperetin (after enzymatic hydrolysis of the metabolites in plasma samples)[16].

The aim of the present study was to develop a method for separation of *S*- and *R*-hesperetin on an analytical and semi-preparative scale using chiral HPLC with α1-acid glycoprotein (AGP) as chiral selector, and to characterize differences in the intestinal conjugation and transport, and the activity in a selected bioassay, of the two hesperetin enantiomers in *in vitro* models. To that end we performed incubations with microsomal and cytosolic fractions of human small intestine with the separated enantiomers in order to determine the apparent kinetics for glucuronidation and sulfonation of *S*- and *R*-hesperetin. Furthermore, the stereoselective differences in intestinal metabolism and transport were assessed using Caco-2 cell monolayers in a two-compartment transwell system as a model for the intestinal barrier. In order to test differences in a selected bioassay *S*- and *R*-hesperetin were tested in a reporter gene based bioassay quantifying EpRE-(electrophile responsive element) mediated activation of gene expression. EpRE-mediated activation of gene expression is considered to contribute to the cancer preventive action of chemo-protective dietary compounds including flavonoids[22,23].

Materials and Methods

Materials

Alamethicin (from *Trichoderma viride*), ß-glucuronidase (from *Helix pomatia*) type HP-2, hesperetin (purity ≥95%, batch 015K1099), *L*-ascorbic acid and uridine 5'-diphosphoglucuronic acid (UDPGA) were obtained from Sigma (St. Louis, MO), 3'-phosphoadenosine 5'-phosphosulfate (PAPS) from Fluka (Buchs, Switzerland), dimethyl sulfoxide (DMSO), di-potassium hydrogen phosphate trihydrate, EDTA disodium salt dehydrate, glacial acetic acid, hydrochloric acid, potassium dihydrogen phosphate and sodium acetate trihydrate from Merck (Darmstadt, Germany), acetonitrile, isopropyl alcohol and methanol from Sigma-Aldrich (Steinheim, Germany), Tris from Invitrogen (Carlsbad, CA), and ammonium acetate and trifluoroacteic acid from J.T. Baker (Philipsburg, NJ). Authentic standards of hesperetin 7-*O*-glucuronide (purity >90%), hesperetin 3'-*O*-glucuronide (purity >90%) and hesperetin 7-*O*-sulfate (purity <50%) were provided by Nestlé Research Center (Lausanne, Switzerland). An orange (*Citrus sinensis*) from South-Africa was bought at a local store. All cell culture reagents were purchased from Invitrogen (Paisley, UK). Pooled human small intestinal microsomes (batch MIC318012) and pooled human small intestinal cytosol (batch CYT318004) were purchased from Biopredic (Rennes, France).

Cell lines

Caco-2 human colon carcinoma cells were obtained from the American Type Culture Collection (Manassas, VA), and were cultured as described earlier[9]. Passage number 39 to 47 were used for the experiments.

Hepa-1c1c7 mouse hepatoma cells stably transfected with the reporter vector pTI(hNQO1-EpRE)Luc+ from Promega (Leiden, The Netherlands) carrying the EpRE from the human NQO1 gene regulatory region between -470 to -448 (5'-AGT CAC AGT GAC TCA GCA GAA TC-3') coupled to a luciferase reporter gene, were obtained as described previously[24]. These transfected Hepa-1c1c7 cells will further be referred to as EpRE-LUX cells.

Identification of S-hesperetin

Hesperidin naturally occurs predominantly as the 2*S*-epimer[14-16]. To acquire *S*-hesperetin, 2*S*-hesperidin from an orange (*Citrus sinensis*) was deglycosylated. To this end, freshly prepared orange juice (0.5 ml) was added to 1 ml nanopure water, 110 µl 0.78 M sodium acetate (pH 4.8), 100 µl 0.1 M ascorbic acid and 200 µl crude preparation from *Helix pomatia* type HP-2 and incubated overnight at 37°C[16,25]. Then, 1 ml acetonitrile was added to precipitate the proteins, the mixture was vortexed for 1 min, and centrifuged at 16,000 *g* for 5 min. The supernatant was collected, the solvent evaporated under nitrogen gas and the residue was dissolved in the mobile phase for chiral HPLC analysis.

Chiral HPLC-DAD analysis

Chiral analyses of hesperetin were performed on an HPLC system consisting of a Waters (Milford, MA) Alliance 2695 separation module connected to a Waters 2996 photodiode array detector (DAD) equipped with a ChromTech (Cheshire, UK) analytical 150 × 4 mm Chiral-AGP column connected to a 10 × 4 mm guard column. Samples were centrifuged at 16,000 *g* for 4 min, and 20 µl was injected and isocratically eluted at a flow rate of 0.9 ml/min in 10 mM ammonium acetate (pH 5.0) containing 2% (v/v) isopropyl alcohol, filtered through a membrane filter with a pore size of 0.45 µm from Schleicher and Schuell (Dassel, Germany). The column was equilibrated for 10 min before injection, and washed with 15% (v/v) isopropyl alcohol in nanopure water. DAD-UV spectra were detected between 200 and 420 nm, and HPLC chromatograms acquired at 280 nm were used for quantification and presentation.

Semi-preparative separation of S- and R-hesperetin

Semi-preparative HPLC separation of the *S*- and *R*-enantiomers of hesperetin was performed on an HPLC system consisting of an Uniflows Degasys DG-2410 degasser (Tokyo, Japan), a Waters 600 fluid unit and controller connected to a Waters 996

DAD (Milford, MA), equipped with a ChromTech semi-preparative 100 × 10.0 mm Chiral-AGP column (Cheshire, UK). An injection volume of 100 µl of 500 µM of racemic hesperetin in 25% (v/v) isopropyl alcohol in nanopure water was injected and eluted at a flow rate of 5.6 ml/min in 10 mM ammonium acetate (pH 5.0) containing 2% (v/v) isopropyl alcohol, filtered through a membrane filter with a pore size of 0.45 µm from Schleicher and Schuell (Dassel, Germany). Elution of both hesperetin enantiomers was followed at 280 nm. Fractions containing the separate enantiomers were collected and divided into Eppendorf tubes, and freeze dried. The resulting products were dissolved in a small amount of methanol, pooled and dried under a flow of nitrogen and re-dissolved in a small amount of DMSO. In order to check the enantiomeric purity (>95%), a sample of each preparation, 100-fold diluted with 25% (v/v) isopropyl alcohol in nanopure water, was analyzed by chiral HPLC-DAD. To precisely determine the hesperetin concentration a 100- or 1000-fold diluted sample of each preparation in 20% acetonitrile (v/v) in 0.1% trifluoroacetic acid in nanopure water was analyzed by a-chiral HPLC-DAD based on detection at 280 nm using a 10-point linear (R^2>0.99) calibration line of relevant concentrations of racemic hesperetin. Based on the outcome of this quantification, the separated *S*- and *R*-hesperetin solutions in DMSO were further diluted with DMSO to create 10 mM stock solutions. A sample dissolved in cell culture medium did not demonstrate racemization after incubation at 37°C for 2 h (data not shown).

Microsomal and cytosolic incubations

To study intestinal glucuronidation of *S*- and *R*-hesperetin, incubations with human intestinal microsomes were performed as described before for racemic hesperetin[26]. The incubation mixtures (total volume 200 µl) contained 10 mM $MgCl_2$, 25 µg/ml alamethicin added from a 200 times concentrated stock solution in methanol (final concentration 0.5% methanol), 0.1 mg/ml microsomal protein and 1 mM uridine 5'-diphosphoglucuronic acid (UDPGA), in 50 mM Tris-HCl (pH 7.5). The reaction was started by addition of *S*- or *R*-hesperetin from a 200 times concentrated stock solution in DMSO (final concentration 0.5% DMSO) and incubated for 5 min at 37°C. The reaction was terminated by addition of 50 µl acetonitrile. Under these conditions formation of hesperetin glucuronides was linear in time and with the amount of protein (data not shown).

To study intestinal sulfonation of *S*- and *R*-hesperetin, incubations with human intestinal cytosol were performed as described before for racemic hesperetin[26]. The incubation mixtures (total volume 100 µl) contained 5 mM $MgCl_2$, 0.5 mg/ml cytosolic protein and 100 µM 3'-phosphoadenosine 5'-phosphosulfate (PAPS), in 50 mM potassium phosphate (pH 7.4). The reaction was started by addition of *S*- or *R*-hesperetin from a 100 times concentrated stock solution in DMSO (final concentration 1% DMSO) and incubated for 5 min at 37 °C. The reaction was

terminated by addition of 25 µl acetonitrile. Under these conditions formation of hesperetin sulfates was linear in time and with the amount of protein (data not shown).

Metabolism and transport by Caco-2 cell monolayers

Caco-2 cells were cultured in a humidified atmosphere of 5% CO_2 and 95% air at 37°C, and seeded at a density of 1×10^5 cells/cm^2 in Costar 12-well transwell plate inserts from Corning (Corning, NY) with an insert membrane pore size of 0.4 µm and growth area of 1.12 cm^2. The culture medium consisted of Dulbecco's modified Eagle's medium (DMEM) containing 25 mM HEPES buffer (pH 7.4), 4500 mg/ml glucose, *L*-glutamine, and phenol red, supplemented with 10% (v/v) heat inactivated (30 min at 56°C) fetal bovine serum, 1% (v/v) minimal essential medium nonessential amino acids (NEAA), and 0.1 mg/ml gentamicin. The medium was changed three times a week. Eighteen to 19 days post-seeding the transport experiment was performed for which the monolayers were washed and further incubated with DMEM without phenol red. The integrity of the monolayers was checked by measuring the trans-epithelial electrical resistance (TEER) values with a Millicell ERS volt/ohmmeter from Millipore (Bedford, MA). Only monolayers that demonstrated a TEER value between 500 and 1000 Ω·cm^2 were used. For the experiment, exposure medium was prepared consisting of DMEM (without phenol red) supplemented with 1% (v/v) NEAA and 1 mM *L*-ascorbic acid which was filtered through a sterile 0.2-µm filter unit from VWR (West Chester, PA). The monolayers were exposed at the apical side to exposure medium containing 10 µM *S*-hesperetin or *R*-hesperetin (final concentration 0.5% DMSO). Samples of 150 µl were taken from the apical and basolateral side 120 min upon addition, where after integrity of the monolayer was re-confirmed. All samples were stored at -80 °C until further HPLC-DAD analysis carried out as described earlier[9].

a-Chiral HPLC analysis

a-Chiral gradient HPLC on a C18 column was used to detect and quantify the amounts of hesperetin, hesperetin 7-*O*-glucuronide, hesperetin 3'-*O*-glucuronide, hesperetin 7-*O*-sulfate and hesperetin 3'-*O*-sulfate using methods previously described[9,26].

Enzyme kinetics

To determine the kinetics for glucuronidation and sulfonation, microsomal and cytosolic incubations were performed as described above varying the concentration of *S*- or *R*-hesperetin from 1 to 50 µM. Under the applied conditions the formation of hesperetin 7-*O*-glucuronide, hesperetin 3'-*O*-glucuronide, hesperetin 7-*O*-sulfate and hesperetin 3'-*O*-sulfate conjugates was linear in time and with the amount of

microsomal protein added (data not shown). The apparent maximum velocity ($V_{max(app)}$) and apparent Michaelis-Menten constant ($K_{m(app)}$) for the formation of the different phase II metabolites of *S*- and *R*-hesperetin were determined by fitting the data to the Michaelis-Menten steady-state model $v = V_{max} / (1 + (K_m / [S]))$, with [S] being the hesperetin concentration, using the LSW data analysis toolbox (version 1.1.1) from MDL Information Systems (San Ramon, CA).

EpRE-lux assay

EpRE-mediated induction of gene expression by *S*- and *R*-hesperetin was tested using the EpRE-LUX luciferase reporter gene assay as described earlier[24,27]. The EpRE-LUX cells were cultured in alpha modified Eagle's medium supplemented with 10% fetal bovine serum, 50 µg/ml gentamicin and 0.5 mg/ml G418 from Duchefa (Haarlem, The Netherlands), in a humidified atmosphere of 5% CO_2 and 95% air at 37°C. 100 µl Cell suspension with a density of 3×10^5 cells/ml was seeded per well in a 96 well view-plate (Corning, NY) and incubated for 24 h whereafter the cells had attached to the bottom and formed a confluent monolayer. The plates were exposed to different concentrations of *S*- or *R*-hesperetin. To this end the culture medium was removed and replaced by 100 µl of medium containing hesperetin at the required concentration (0.5% DMSO). The plates were incubated for another 24 h whereafter the cells were washed with 0.5 x PBS and lysed by addition of low salt buffer (10 mM Tris, 2 mM DTT and 2 mM *trans*-1,2-diaminocyclohexane-*N,N,N',N'*-tetra-acetic acid monohydrate, pH 7.8). After lysis, luciferase reagent (20 mM tricine, 1.07 mM $(MgCO_3)_4Mg(OH)_2$, 2.67 mM $MgSO_4$, 0.1 mM EDTA, 2 mM DTT, 0.47 mM D-luciferin, 5mM ATP; pH 7.8) was added and the luciferase activity was measured using a Luminoskan Ascent luminometer from Thermo electron corporation (Helsinki, Finland).

Results

Analytical and semi-preparative chiral HPLC-DAD analyses

Figure 7.2A depicts a chromatogram of the analytical chiral HPLC analysis of racemic hesperetin, demonstrating the two enantiomers at retention time (t_R) 25.5 min and 29.0 min in a 41:59 ratio. Both peaks demonstrated equivalent UV spectra with a UV_{max} at 285.9 nm. The limit of detection, defined as the lowest concentration which can be detected (signal-to-noise ratio 3) of this method was 0.6 µM, the limit of quantification, defined as the lowest concentration which can be quantitatively determined (signal-to-noise ratio 10) was 2 µM. To identify the *S*- and *R*-hesperetin enantiomers, hesperidin from fresh orange juice, mainly present as 2*S*-epimer, was deglycosylated to yield predominantly *S*-hesperetin and analyzed (Figure 7.2B). The

peak at t_R 29.0 min (UV_{max} 285.9 nm), was dominant in the hydrolyzed citrus sample identifying the corresponding metabolite as *S*-hesperetin. *S*- and *R*-hesperetin were successfully separated on a semi-preparative scale and concentrated, yielding sufficient amounts to perform small scale *in vitro* experiments. The racemic purity after vacuum concentration and pooling of the collected samples was >95% for both *S*- and *R*-hesperetin.

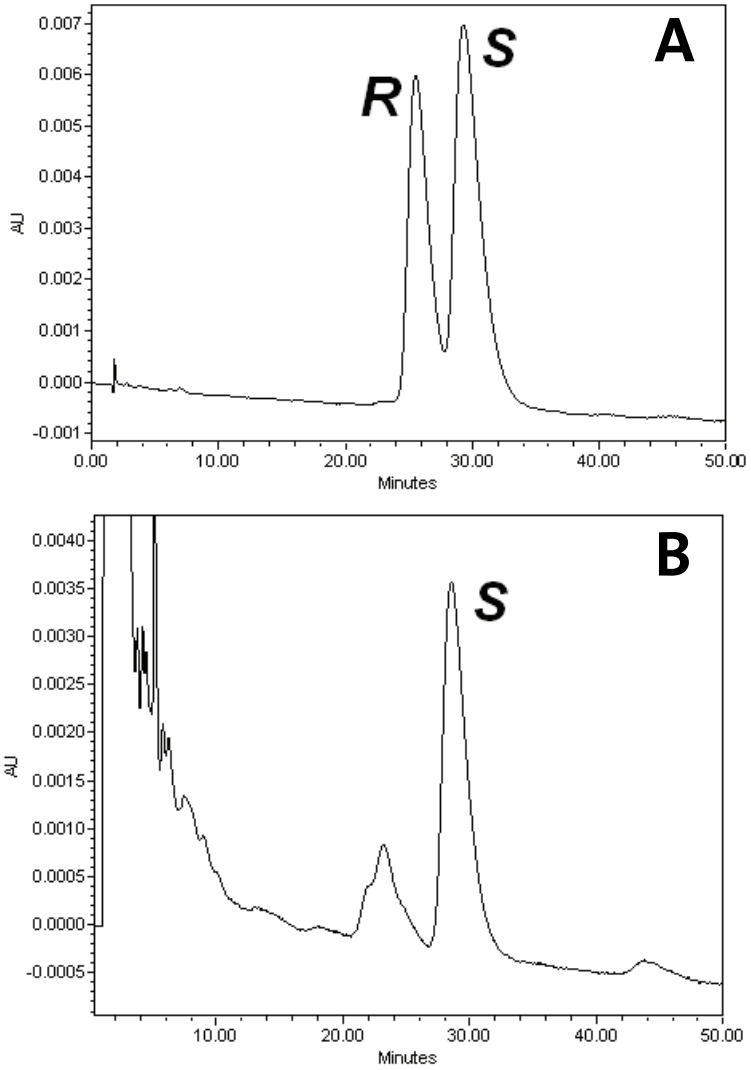

Figure 7.2 *Chiral HPLC chromatograms of A) racemic hesperetin, B) hesperetin resulting from deglycosylation of the 2S-hesperidin epimer from citrus.*

Microsomal glucuronidation

Hesperetin is glucuronidated by small intestinal microsomes into hesperetin 7-*O*-glucuronide and 3'-*O*-glucuronide metabolites[26]. The apparent V_{max} and K_m values derived from the concentration dependent formation of *S*-hesperetin 7-*O*-glucuronide and *S*-hesperetin 3-*O*-glucuronide (Figure 7.3A), and *R*-hesperetin 7-*O*-glucuronide and *R*-hesperetin 3'-*O*-glucuronide (Figure 7.3B) by human small intestinal microsomes are presented in table 1, as well as the apparent catalytic efficiencies (V_{max}/K_m). For comparison, Table 7.1 on page 133 also presents the kinetic data obtained previously for racemic hesperetin[26]. For the glucuronidation of both hesperetin enantiomers the relative contribution of the conjugation at position 7 and 3' is comparable. However, the affinity was higher (K_m lower) for the glucuronidation of *S*-hesperetin as compared to the glucuronidation of *R*-hesperetin. Together with a slightly higher capacity (V_{max}), this results in a 5.2-fold higher catalytic efficiency for the glucuronidation of *S*-hesperetin compared to *R*-hesperetin (Table 7.1). The catalytic efficiencies obtained for 7-*O*-glucuronide formation from *S*- and *R*-hesperetin were respectively 2.7-fold higher and 2.5-fold lower than the catalytic efficiencies observed with the racemic mixture, and the catalytic efficiencies obtained for 3'-*O*-glucuronide formation from *S*- and *R*-hesperetin were respectively 2.5-fold higher and 1.6-fold lower compared to the catalytic efficiencies observed with the racemic mixture.

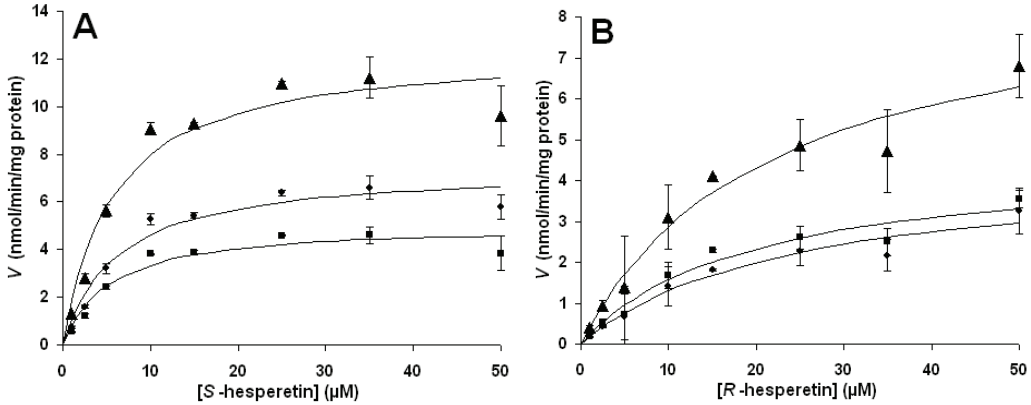

Figure 7.3 *Concentration dependent formation of hesperetin 7-O-glucuronide (●), hesperetin 3'-O-glucuronide (■) and total hesperetin glucuronides (▲) from S-hesperetin (A) and R-hesperetin (B) enantiomers by human small intestinal microsomes. Data points represent average activities of 2 measurements ± SD.*

Table 7.1 *Apparent V_{max}, K_m (±SEM) (n=2) and catalytic efficiency, calculated as $V_{max(app)}/K_{m(app)}$, for glucuronidation of S- and R-hesperetin by human small intestinal microsomes, as well as the kinetic data for racemic hesperetin, the latter taken from our previous work[26].*

	S-hesperetin			R-hesperetin			racemic hesperetin		
conjugation reaction	**K_m(app)** (µM)	**V_{max}(app)** (nmol min^{-1} mg $protein^{-1}$)	**Catalytic efficiency** (µl min^{-1} mg $protein^{-1}$)	**K_m(app)** (µM)	**V_{max}(app)** (nmol min^{-1} mg $protein^{-1}$)	**Catalytic efficiency** (µl min^{-1} mg $protein^{-1}$	**K_m(app)** (µM)	**V_{max}(app)** (nmol min^{-1} mg $protein^{-1}$)	**Catalytic efficiency** (µl min^{-1} mg $protein^{-1}$
Glucuronidation (total)	*5.7 ± 1.7*	*12.5 ± 0.99*	*2189*	*21.3 ± 6.5*	*8.95 ± 1.24*	*420*	*7.3 ± 1.4*	*6.26 ± 1.67*	*858*
7-O-glucuronidation	*6.1 ± 1.6*	*7.43 ± 0.56*	*1224*	*24.0 ± 8.0*	*4.40 ± 0.69*	*183*	*8.3 ± 1.9*	*3.80 ± 0.50*	*458*
3'-O-glucuronidation	*5.2 ± 1.7*	*5.08 ± 0.43*	*971*	*18.9 ± 6.1*	*4.55 ± 0.63*	*240*	*6.4 ± 1.2*	*2.49 ± 0.49*	*391*

Table 7.2 *Apparent V_{max}, K_m (±SEM) (n=2) and catalytic efficiency, calculated as V_{max}/K_m for sulfonation of S- and R-hesperetin by human small intestinal cytosol, as well as the kinetic data for racemic hesperetin, the latter taken from our previous work[26].*

	S-hesperetin			R-hesperetin			racemic hesperetin		
conjugation reaction	**K_m(app)** (µM)	**V_{max}(app)** (nmol min^{-1} mg $protein^{-1}$)	**Catalytic efficiency** (µl min^{-1} mg $protein^{-1}$)	**K_m(app)** (µM)	**V_{max}(app)** (nmol min^{-1} mg $protein^{-1}$)	**Catalytic efficiency** (µl min^{-1} mg $protein^{-1}$	**K_m(app)** (µM)	**V_{max}(app)** (nmol min^{-1} mg $protein^{-1}$)	**Catalytic efficiency** (µl min^{-1} mg $protein^{-1}$
Sulfonation (total)	*0.9 ± 0.2*	*0.96 ± 0.03*	*1067*	*1.6 ± 0.2*	*1.27 ± 0.04*	*803*	*0.8 ± 0.1*	*0.90 ± 0.29*	*1082*
7-O-sulfonation	*15.6 ± 2.5*	*0.25 ± 0.03*	*16*	*11.5 ± 2.1*	*0.51 ± 0.04*	*44*	*9.1 ± 1.5*	*0.14 ± 0.04*	*16*
3'-O-sulfonation	*0.6 ± 0.2*	*0.80 ± 0.03*	*1455*	*0.9 ± 0.3*	*0.89 ± 0.04*	*1000*	*0.6 ± 0.2*	*0.79 ± 0.14*	*1240*

Cytsosolic sulfonation

Hesperetin is sulfonated by human small intestinal cytosol into hesperetin 3'-*O*-sulfate and 7-*O*-sulfate metabolites[26]. The apparent V_{max} and K_m values derived from the concentration dependent formation of *S*-hesperetin 3'-*O*-sulfate and *S*-hesperetin 7-*O*-sulfate (Figure 7.4A), and *R*-hesperetin 3'-*O*-sulfate and *R*-hesperetin 7-*O*-sulfate (Figure 7.4B) by human small intestinal microsomes are shown in Table 7.2 on page 133, as well as the apparent catalytic efficiencies (V_{max}/K_m). For comparison, Table 7.2 also presents the kinetic data obtained previously for racemic hesperetin[26]. Both hesperetin enantiomers are predominantly sulfonated at position 3', although the capacity and the relative contribution of the formation of 7-*O*-sulfonation to the total sulfonation of *R*-hesperetin is higher as compared with the sulfonation of *S*-hesperetin (Table 7.2). The catalytic efficiency obtained for 3'-*O*-sulfate formation from *S*- and *R*-hesperetin were respectively 1.2-fold lower and 1.5-fold higher than the catalytic efficiencies observed with the racemic mixture, and the catalytic efficiency obtained for 7'-*O*-sulfate formation from *S*- and *R*-hesperetin were respectively equal and 2.8-fold higher compared to the catalytic efficiencies observed with the racemic mixture[26].

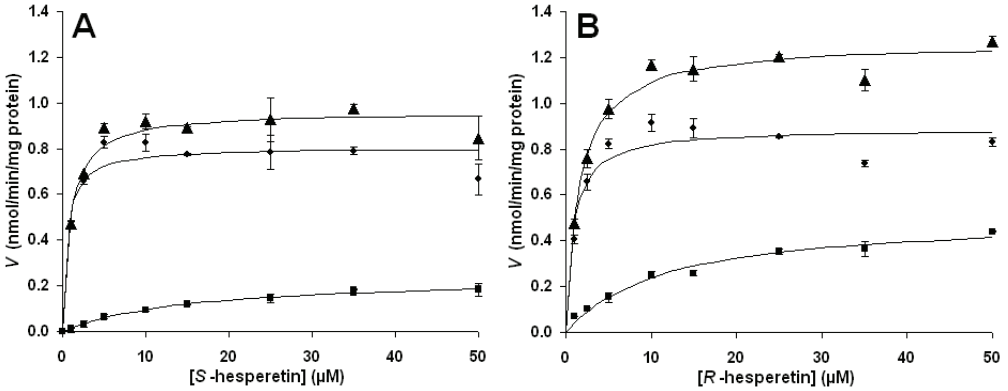

Figure 7.4 *Concentration dependent formation of hesperetin 7-O-sulfate (■), hesperetin 3'-O-sulfate (●) and total hesperetin sulfates (▲) from S-hesperetin (A) and R-hesperetin (B) enantiomers by human small intestinal cytosol. Data points represent average activities of 2 measurements ± SD.*

Metabolism and transport by Caco-2 cell monolayers

Caco-2 cell monolayers apically exposed to hesperetin metabolize it into hesperetin 7-*O*-glucuronide and hesperetin 7-*O*-sulfate, which are predominantly transported to the apical side of the monolayer[9]. Figure 7.5 shows the percentages of the applied amount of *S*-hesperetin or *R*-hesperetin that is metabolized into 7-*O*-glucuronide or 7-*O*-sulfate metabolites as well as the percentage which remained unmetabolized, and the disposition of the metabolites to the apical or basolateral side of the Caco-2 cell monolayer. Exposure to *R*-hesperetin resulted in a significantly ($p < 0.001$) higher amount of hesperetin 7-*O*-sulfate formed amounting to 129% (at the apical plus basolateral side) of the amount of hesperetin 7-*O*-sulfate formed upon exposure to *S*-hesperetin (Figure 7.5). The total amount of *R*-hesperetin 7-O-glucuronide formed was 8% lower compared to the amount of S-hesperetin 7-*O*-glucuronide formed, and this difference was not significant (Figure 7.5). The total amount of hesperetin metabolites and/or aglycone transported over the Caco-2 monolayer did not differ significantly for *S*- and *R*-hesperetin.

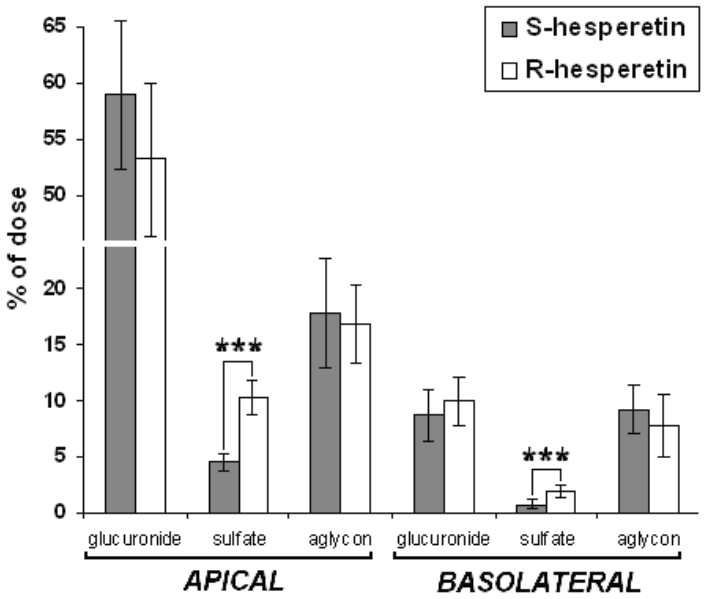

Figure 7.5 *Amount of hesperetin 7-O-glucuronide (glucuronide), hesperetin 7-O-sulfate (sulfate) and hesperetin aglycone detected at the apical and basolateral side of Caco-2 cell monolayers incubated for 120 min with 10 µM S-hesperetin or R-hesperetin added to the apical side. Mean ± SD values shown (n=8). ***, p<0.001 significantly different.*

Activation of EpRE-controlled gene expression by hesperetin

Figure 7.6 shows the concentration dependent induction of EpRE-mediated luciferase expression by *S*-hesperetin and *R*-hesperetin. Exposure to both hesperetin enantiomers resulted in a dose dependent induction of EpRE mediated gene expression: exposure to *S*-hesperetin led to an 8.2-fold (±0.6) induction at 50 µM, and exposure to *R*-hesperetin to a maximum induction of 6.0-fold (±0.2) at 25 µM and higher (Figure 7.6). Although at some of the concentrations significant differences are found between the induction factors by *S*- and *R*-hesperetin, the overall induction however, especially at lower, and thus physiologically relevant concentrations, does not demonstrate notable differences in activation of EpRE mediated gene expression between both hesperetin enantiomers.

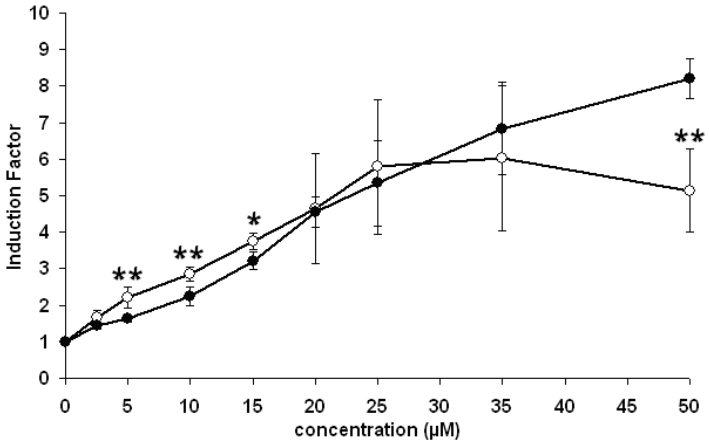

Figure 7.6 *Induction of EpRE-mediated gene transcription by R-hesperetin (O) and S-hesperetin (●). Data are presented as mean (±SD) (n=4). *, p <0.05; **, p <0.01 significantly different compared with the induction by the corresponding concentration of the other hesperetin enantiomer.*

Discussion

Although hesperidin naturally exists mainly as the 2*S*-epimer, which upon intake is subsequently transformed into *S*-hesperetin, practically all research on hesperidin and hesperetin using 'pure' compounds is actually on racemic mixtures, which are currently the only forms of hesperidin and hesperetin commercially available. Stereochemical differences have been proven to affect the bioavailability of flavonoids, as was shown for example for catechin. (+)-Catechin (2*R*,3*S*-catechin) has been demonstrated to be up to 2.1-fold more bioavailable compared to (-)-catechin (2*S*,3*R*-catechin), partly due to increased intestinal absorption[18].

In order to study the differences between the 'natural' *S*-hesperetin and *R*-hesperetin, the present paper reports a method to separate both enantiomers on

an analytical and semi-preparative scale, allowing small-scale *in vitro* experiments with the separated enantiomers. This allowed characterization of possible differences in intestinal metabolism and transport and the activity in a selected bioassay of *S*- and *R*-hesperetin, by incubating *S*- or *R*-hesperetin with human small intestinal microsomes and cytosol and cofactors for phase II conjugation, with Caco-2 cell monolayers in a transwell transport model, and with a transfected cell line to test induction of EpRE-mediated gene expression.

Although the results obtained indicate some significant differences in metabolism, the differences in the metabolism and transport of the two hesperetin enantiomers are relatively small. The higher affinity and capacity towards *S*-hesperetin resulted in an overall 5.2-fold higher catalytic efficiency for the formation of *S*-hesperetin glucuronides as compared to *R*-hesperetin glucuronides by human small intestinal microsomes (Table 7.1 on page 133). The differences between the sulfonation kinetics of *S*-hesperetin and *R*-hesperetin are marginal, although the capacity for the formation of 7-*O*-sulfate from *R*-hesperetin is 2.8-fold higher compared with the formation of 7-*O*-sulfate from *S*-hesperetin (Table 7.2 on page 133, Figure 7.4 on page 134). Although relatively small, together these kinetic differences might explain the increased formation of hesperetin 7-*O*-sulfate and reduced formation of hesperetin 7-*O*-glucuronide by Caco-2 cell monolayers exposed to *R*-hesperetin as compared to monolayers exposed to *S*-hesperetin (Figure 7.5 on page 135).

Differences in the kinetics between *S*-hesperetin and *R*-hesperetin have been observed indirectly *in vivo* after intravenous administration of racemic hesperetin (20 mg/kg bodyweight (bw)) to male Sprague-Dawley rats, demonstrating a significant ($p<0.05$) 3.2-fold higher area under the serum concentration-time curve (AUC) and 1.9-fold ($p<0.05$) longer serum half-life for *R*-hesperetin, compared to *S*-hesperetin which had a 3.3 fold ($p<0.05$) higher total clearance from serum[16]. The cumulative urinary excretion of *R*-hesperetin was 2.3-fold ($p<0.05$) higher compared to *S*-hesperetin[16]. In an earlier study, however, oral administration of racemic hesperidin (200 mg/kg bw) to a single rat revealed only slightly (~15%) increased cumulative 24 h urinary excretion of *R*-hesperetin compared to *S*-hesperetin, while the cumulative urinary excretion of *R*-hesperetin compared to *S*-hesperetin was only ~20% lower following the administration of orange juice (containing 7.3 mg/kg bw hesperidin in an *S*:*R* ratio of 6.8:1) to a healthy volunteer[21].

Although several of these effects appeared significant, they were moderate in size, showing, similar to the observations in the present study, differences between the kinetic parameters for the *S*- and *R*-enantiomer of less than 5-fold. In addition, the differences never resulted in the complete absence of a biochemical pathway or kinetic route for one of the hesperetin enantiomers. From this it is concluded that kinetic data obtained with the racemic mixture do give insight into what may happen to the naturally predominant *S*-enantiomer of hesperetin. It is of interest to

note that interindividual variation in kinetics may be in the same order of magnitude as or even larger than the differences now observed between *S*- and *R*-hesperetin.

In addition to possible differential kinetics for *S*- and *R*-hesperetin, it is of interest to study whether different hesperetin enantiomers would lead to different biological effects. It has been reported for instance that stereochemical differences greatly affect the estrogenic activity of the isoflavone metabolite equol: *S*(-)-equol demonstrated high affinity for estrogen receptor ERß (K_i = 0.73 nM), whereas *R*(+)-equol had a K_i of only 15.4 nM[19].

It has been reported that flavonols and catechins can activate EpRE mediated gene expression because of their pro-oxidant properties under certain conditions[27,28], by which these flavonoids could exert their chemopreventive action[23,27]. The present study revealed that, at physiologically relevant concentrations, *S*- and *R*-hesperetin were both able to induce EpRE mediated gene expression to a similar extent (Figure 7.6 on page 136). However, this assay represents only one of the possible mechanisms by which hesperetin could exert biological effects.

In conclusion, in the case of hesperetin, whenever differences were observed in the kinetics of *S*- and *R*-hesperetin they turned out to be moderate and generally within a 5-fold difference between the two enantiomers. The differences never resulted in the complete absence of a biochemical pathway or kinetic route for one of the hesperetin enantiomers. Also in a selected bioassay there the two enantiomers were equally active. Taken together, it is concluded that for the endpoints tested, including intestinal metabolism and transport, experiments performed with racemic hesperetin may adequately reflect what can be expected for the naturally occurring *S*-enantiomer.

References

[1] Tomás-Barberán FA, Clifford MN. Flavanones, chalcones and dihydrochalcones - nature, occurrence and dietary burden. *J Sci Food Agric* 80(7): 1073-1080, 2000.

[2] Chiba H, Uehara M, Wu J, Wang X, Masuyama R, Suzuki K, Kanazawa K, Ishimi Y. Hesperidin, a citrus flavonoid, inhibits bone loss and decreases serum and hepatic lipids in ovariectomized mice. *J Nutr* 133(6): 1892-1897, 2003.

[3] Garg A, Garg S, Zaneveld LJD, Singla AK. Chemistry and pharmacology of the citrus bioflavonoid hesperidin. *Phytother Res* 15(8): 655-669, 2001.

[4] Horcajada MN, Habauzit V, Trzeciakiewicz A, Morand C, Gil-Izquierdo A, Mardon J, Lebecque P, Davicco MJ, Chee WSS, Coxam V, Offord E. Hesperidin inhibits ovariectomized-induced osteopenia and shows differential effects on bone mass and strength in young and adult intact rats. *J Appl Physiol* 104(3): 648-654, 2008.

[5] Nielsen ILF, Chee WSS, Poulsen L, Offord-Cavin E, Rasmussen SE, Frederiksen H, Enslen M, Barron D, Horcajada M-N, Williamson G. Bioavailability is improved by enzymatic modification of the citrus flavonoid hesperidin in humans: a randomized, double-blind, crossover trial. *J Nutr* 136(2): 404-408, 2006.

[6] Matsumoto H, Ikoma Y, Sugiura M, Yano M, Hasegawa Y. Identification and quantification of the conjugated metabolites derived from orally administered hesperidin in rat plasma. *J Agric Food Chem* 52(21): 6653-6659, 2004.

[7] Mullen W, Archeveque M-A, Edwards CA, Matsumoto H, Crozier A. Bioavailability and metabolism of orange juice flavanones in humans: impact of a full-fat yogurt. *J Agric Food Chem* 56(23): 11157-11164, 2008.
[8] Silberberg M, Morand C, Mathevon T, Besson C, Manach C, Scalbert A, Remesy C. The bioavailability of polyphenols is highly governed by the capacity of the intestine and of the liver to secrete conjugated metabolites. *Eur J Nutr* 45(2): 88-96, 2006.
[9] Brand W, Van der Wel PAI, Rein MJ, Barron D, Williamson G, Van Bladeren PJ, Rietjens IMCM. Metabolism and transport of the citrus flavonoid hesperetin in Caco-2 cell monolayers. *Drug Metab Dispos* 36(9): 1794-1802, 2008.
[10] Liu Z, Hu M. Natural polyphenol disposition via coupled metabolic pathways. *Expert Opin Drug Metab Toxicol* 3(3): 389-406, 2007.
[11] Yáñez JA, Andrews PK, Davies NM. Methods of analysis and separation of chiral flavonoids. *J Chromatogr B Analyt Technol Biomed Life Sci* 848(2): 159-181, 2007.
[12] Arakawa H, Nakazaki M. Absolute configuration of (-)hesperetin and (-)liquiritigenin. *Chem Ind* 1960: 73, 1960.
[13] Arakawa H, Nakazaki M. Die absolute Konfigurationen der optisch aktiven Flavanone. *Liebigs Ann Chem* 636(1): 111-117, 1960.
[14] Aturki Z, Brandi V, Sinibaldi M. Separation of flavanone-7-O-glycoside diastereomers and analysis in citrus juices by multidimensional liquid chromatography coupled with mass spectrometry. *J Agric Food Chem* 52(17): 5303-5308, 2004.
[15] Gel-Moreto N, Streich R, Galensa R. Chiral separation of diastereomeric flavanone-7-O-glycosides in citrus by capillary electrophoresis. *Electrophoresis* 24(15): 2716-2722, 2003.
[16] Yáñez JA, Remsberg CM, Miranda ND, Vega-Villa KR, Andrews PK, Davies NM. Pharmacokinetics of selected chiral flavonoids: hesperetin, naringenin and eriodictyol in rats and their content in fruit juices. *Biopharm Drug Dispos* 29(2): 63-82, 2008.
[17] Ariëns EJ. Stereochemistry, a basis for sophisticated nonsense in pharmacokinetics and clinical pharmacology. *Eur J Clin Pharmacol* 26(6): 663-668, 1984.
[18] Donovan JL, Crespy V, Oliveira M, Cooper KA, Gibson BB, Williamson G. (+)-Catechin is more bioavailable than (-)-catechin: relevance to the bioavailability of catechin from cocoa. *Free Radic Res* 40(10): 1029-1034, 2006.
[19] Setchell KDR, Clerici C, Lephart ED, Cole SJ, Heenan C, Castellani D, Wolfe BE, Nechemias-Zimmer L, Brown NM, Lund TD, Handa RJ, Heubi JE. S-equol, a potent ligand for estrogen receptor beta, is the exclusive enantiomeric form of the soy isoflavone metabolite produced by human intestinal bacterial flora. *Am J Clin Nutr* 81(5): 1072-1079, 2005.
[20] Setchell KDR, Zhao X, Jha P, Heubi JE, Brown NM. The pharmacokinetic behavior of the soy isoflavone metabolite S-(-)equol and its diastereoisomer R-(+)equol in healthy adults determined by using stable-isotope-labeled tracers. *Am J Clin Nutr* 90(4): 1029-1037, 2009.
[21] Yáñez JA, Teng XW, Roupe KA, Davies NM. Stereospecific high-performance liquid chromatographic analysis of hesperetin in biological matrices. *J Pharm Biomed Anal* 37(3): 591-595, 2005.
[22] Chen C, Kong AN. Dietary chemopreventive compounds and ARE/EpRE signaling. *Free Radic Biol Med* 36(12): 1505-1516, 2004.
[23] Galati G, O'Brien PJ. Potential toxicity of flavonoids and other dietary phenolics: significance for their chemopreventive and anticancer properties. *Free Radic Biol Med* 37(3): 287-303, 2004.
[24] Boerboom AMJF, Vermeulen M, Van der Woude H, Bremer BI, Lee-Hilz YY, Kampman E, Van Bladeren PJ, Rietjens IMCM, Aarts JMMJG. Newly constructed stable reporter cell lines for mechanistic studies on electrophile-responsive element-mediated gene expression reveal a role for flavonoid planarity. *Biochem Pharmacol* 72(2): 217-226, 2006.
[25] Erlund I, Meririnne E, Alfthan G, Aro A. Plasma kinetics and urinary excretion of the flavanones naringenin and hesperetin in humans after ingestion of orange juice and grapefruit juice. *J Nutr* 131(2): 235-241, 2001.
[26] Brand W, Boersma MG, Bik H, Hoek-van den Hil EF, Vervoort J, Barron D, Meinl W, Glatt H, Williamson G, Van Bladeren PJ, Rietjens IMCM. Phase II metabolism of hesperetin by individual UDP-glucuronosyltransferases (UGTs) and sulfotransferases (SULTs) and rat and human tissue samples. *Drug Metab Dispos*, 38(4): 617-625, 2010.
[27] Lee-Hilz YY, Boerboom AMJF, Westphal AH, Berkel WJH, Aarts JMMJG, Rietjens IMCM. Pro-oxidant activity of flavonoids induces EpRE-mediated gene expression. *Chem Res Toxicol* 19(11): 1499-1505, 2006.
[28] Muzolf-Panek M, Gliszczyńska-Swigło A, de Haan L, Aarts JMMJG, Szymusiak H, Vervoort JM, Tyrakowska B, Rietjens IMCM. Role of catechin quinones in the induction of EpRE-mediated gene expression. *Chem Res Toxicol* 21(12), 2008.

Chapter 8

Summary and conclusions, concluding remarks and future perspectives

Summary and conclusions

Summary

The aim of the present thesis was to investigate whether the bioavailability of the selected model flavonoid hesperetin ((+/-)-4'-methoxy-3',5,7-trihydroxyflavanone) could be increased by modulation of its intestinal metabolism and transport by co-administering other flavonoids. Flavonoids form a large class of polyphenolic compounds omnipresent in plant derived products, often present in the form of ß-glycosides[1]. They have been frequently proposed to be associated with possible beneficial effects on health[2]. Hesperetin is the aglycone of the rutinoside hesperidin, which is present in large amounts in citrus fruits and orange juice (500 mg/L) and is deglycosylated upon oral uptake[3]. Hesperetin has been proposed to provide anti-carcinogenic effects[4], and also to reduce the risk of osteoporosis, which has been demonstrated in *in vivo* models[5-7]. Although the dietary intake can be considerable, the bioavailability of hesperetin is limited, a phenomenon observed for most subclasses of flavonoids[8]. An important mechanism behind this limited bioavailability is the metabolism and transport in intestinal cells: flavonoids are conjugated by phase II enzymes such as UDP-glucuronosyl transferases (UGTs), sulfotransferases (SULTs) or catechol-*O*-methyltransferases (COMT), and are subsequently transported from the intestinal cells back into the intestinal lumen by apically located ATP binding cassette (ABC) transporters[9]. Because specific flavonoids are known modulators of phase II metabolism and of ABC transporter activity, in this thesis it was hypothesized that simultaneous exposure to hesperetin and selected other flavonoids may increase hesperetin bioavailability by modulating its intestinal metabolism and transport.

To further support this hypothesis, **chapter 2** of the thesis presents a literature overview on the capacity of flavonoids to modulate the oral bioavailability of other compounds. This review reveals that the transport of compounds across the intestinal epithelial can be highly dependent on the activity of ABC transporters, especially those involved in the transport from the intestinal cells, either to the basolateral blood side, facilitating absorption, or back into the intestinal lumen, opposing bioavailability. The function of the ABC transporters in intestinal transcellular uptake also implies a role for inhibitors of these transporters in modulation of the bioavailability upon oral uptake. The role of flavonoids as important modulators or substrates of intestinal ABC transport proteins and their effect on the intestinal transport and bioavailability of other compounds is illustrated by several examples from *in vitro* and some *in vivo* studies. Chapter 2 concludes that future studies should focus on (1) *in vivo* validation of the flavonoid-mediated effects on bioavailability of drugs, toxins and beneficial bioactive food ingredients detected in *in vitro* models, and (2) on the role of the

phase II metabolism of flavonoids in modulating the activity of the flavonoids to act as ABC transporter inhibitors and/or substrates.

In the subsequent chapters of the thesis the concept of increasing the bioavailability of a compound by co-administration of inhibitors of phase II metabolism and/or ABC transporters, is tested for hesperetin using different *in vitro* and *in vivo* model systems. The *in vitro* models used to study intestinal metabolism and transport included a two-compartment transwell model with Caco-2 cell monolayers, simulating the intestinal transport barrier. After differentiation, Caco-2 cells are known to display morphological and biochemical characteristics of human enterocytes, including the expression of ABC transporters and phase II metabolizing enzymes, and to form a tight layer of polarized intestinal cells[10]. Grown on a membrane separating an apical compartment (simulating the intestinal lumen side) and a basolateral compartment (simulating the blood/plasma side) they form a well accepted *in vitro* model to study intestinal transport[11].

In **chapter 3**, this Caco-2 cell monolayer in a two-compartment transwell model system simulating the intestinal transport barrier was used to define the characteristics of the intestinal transport and metabolism of hesperetin *in vitro*. The metabolites of hesperetin formed by the Caco-2 cells were identified using HPLC-DAD and uPLC-DAD-MS-MS techniques and available reference compounds combined with specific enzymatic deconjugation reactions. The role of the apically located ABC transporters P-glycoprotein (Pgp), Multidrug Resistance Protein 2 (MRP2) and Breast Cancer Resistance Protein (BCRP) in the efflux of hesperetin and its metabolites was studied by co-administration of compounds known to inhibit several classes of ABC transporters. Furthermore, the cellular expression of these ABC transporters in Caco-2 cells was confirmed using reverse transcription quantitative polymerase chain reaction (RT-qPCR) analysis. It was shown that apically-applied hesperetin was metabolized into hesperetin 7-*O*-glucuronide and hesperetin 7-*O*-sulfate, which were transported predominantly to the apical side of the Caco-2 cell monolayer. Hesperetin aglycone permeated to the basolateral side, and this process was unaffected by the inhibitors used, possibly implying a passive diffusion process. The inhibition studies, however, showed that efflux of hesperetin conjugates to the apical side involved active transport, which from the pattern of inhibition, appeared to be mediated mainly by BCRP. Upon inhibition by the specific BCRP inhibitor Ko143[12], the apical efflux of hesperetin conjugates was significantly reduced by 1.9-fold and transport to the basolateral side was significantly increased by 3.1-fold. These findings elucidated a novel pathway of hesperetin metabolism and transport, and indicated that BCRP-mediated transport can be a limiting step for hesperetin bioavailability.

Because flavonoids can be expected to be converted by the same phase II enzymes and thus to interfere with hesperetin metabolism, and because, as reviewed in

chapter 2, specific flavonoids can also inhibit the apically located ABC transporter BCRP, it was studied in **chapter 4** to what extent flavonoids can modulate the metabolism and transport of hesperetin. To this end the effect of their co-administration with hesperetin on hesperetin metabolism and transport was studied using the Caco-2 cell monolayers two-compartment transwell model system. It was shown that co-administration of hesperetin with specific flavonoids reduced the ratio of apical to basolateral transport of hesperetin metabolites, and in some cases, also reduced the amount of hesperetin metabolites detected extracellularly. Flavonols and flavones were more potent inhibitors than isoflavones, with quercetin being the most potent compound, while co-administration of flavanols or glycosylated derivatives, reported not to inhibit BCRP, did not modulate the transport of hesperetin metabolites. Because intracellular accumulation of hesperetin metabolites did not account for the decrease in hesperetin metabolites detected extracellularly, inhibition of metabolism of hesperetin is likely the underlying mechanism for the reduced metabolite formation and excretion. In spite of the reduction in metabolism the amount of hesperetin metabolites transported to the basolateral side significantly increased upon co-exposure with specific flavonoids and therefore co-administration of specific flavonoids could be a strategy to improve the bioavailability of hesperetin.

In **chapter 5** it was investigated whether this *in vitro* observation, showing that co-administration of quercetin may increase the basolateral transport of hesperetin through Caco-2 cell monolayers at the cost of its apical transport, could be confirmed in an *in vivo* rat model. Therefore hesperetin 7-*O*-glucoside, a monosaccharide derivative of hesperidin, was administrated by oral gavage to Sprague-Dawley rats in the presence or absence of quercetin. In this *in vivo* study hesperetin 7-*O*-glucoside was used instead of hesperetin itself, because previous studies in rats revealed hesperetin to be already absorbed to a significant extent in the stomach excluding the possibility to study the effects of co-administering quercetin on intestinal uptake, while hesperetin 7-*O*-glucoside was found to be absorbed in the small intestine[13] and thus provided a better model compound to study the effect of quercetin on its intestinal uptake and subsequent bioavailability. Rats were orally administered hesperetin 7-*O*-glucoside (15 or 3 mg/kg bw), in the presence or absence of quercetin (15 mg/kg bw). Systemic blood was taken on 8 time points after dosing from 15 min up to 8 hr in order to determine the area under the concentration time curve (AUC) of plasma hesperetin and its demethylated and remethylated metabolites eriodictyol and homoeriodictyol after treatment of blood samples with ß-glucuronidase/sulfatase. Hesperetin, eriodictyol and homoeriodictyol were determined and quantified by uPLC-DAD. Co-administration of quercetin did especially increase hesperetin bioavailability in an early phase of the concentration

time curve (at 15 min) when elimination was not yet dominating over uptake, but did not significantly increase the AUC from time zero to 8 hr. It is concluded that the effect of co-administration of quercetin as an inhibitor of the intestinal BCRP mediated transport might result in increased bioavailability, especially during the early phase of exposure when absorption processes still dominate over elimination processes.

In **chapter 6** the phase II metabolism of hesperetin was further studied by determining the kinetics of hesperetin conversion by human or rat small intestinal, colonic and hepatic microsomal and cytosolic fractions. Furthermore, the kinetics for glucuronidation and sulfonation of hesperetin by, respectively, 12 individual UGT and 12 individual SULT enzymes were determined in order to identify the responsible UGT and SULT isoforms, of which the expression levels in different tissues are relatively well documented in literature[14-17]. Results obtained demonstrate that hesperetin is conjugated at positions 7 and 3', and that major enzyme-specific differences in kinetics and regioselectivity for the UGT and SULT catalyzed conjugations exist. UGT1A9, UGT1A1, UGT1A7, UGT1A8 and UGT1A3 are the major enzymes catalyzing hesperetin glucuronidation, the latter only producing 7-*O*-glucuronide, while UGT1A7 mainly produced 3'-*O*-glucuronide. Furthermore, UGT1A6 and UGT2B4 only produce hesperetin 7-*O*-glucuronide, while UGT1A1, UGT1A8, UGT1A9, UGT1A10, UGT2B7 and UGT2B15 conjugate both positions. SULT1A2 and SULT1A1 catalyze preferably and most efficiently the formation of hesperetin 3'-*O*-sulfate, and SULT1C4 preferably and most efficiently the formation of hesperetin 7-*O*-sulfate. Based on expression levels SULT1A3 and SULT1B1 will likely play a role in the sulfo-conjugation of hesperetin *in vivo*. The results help to explain discrepancies in metabolite patterns determined in tissues or systems with different expression levels of UGTs and SULTs, *e.g.* hepatic and intestinal fractions or Caco-2 cells. The incubations with rat and human tissue samples support an important role for the intestinal cells during first pass metabolism in the formation of hesperetin 3'-*O*-glucuronide and 7-*O*-glucuronide, which appear to be the major hesperetin metabolites found *in vivo*, as compared to metabolism by liver tissue.

Additionally, **chapter 7** pays attention to the stereochemistry of hesperetin which contains a chiral C-atom and therefore can exist as an *S*- and *R*-enantiomer. This is of importance because in nature 2*S*-hesperidin and its *S*-hesperetin aglycone are the predominant chemical forms. However, in spite of this, many studies have been performed with the commercially available racemates of hesperidin and hesperetin. In chapter 7 the transport and metabolism characteristics so far studied for the commercially available racemic mixture of hesperetin were investigated for the *S*- and *R*-hesperetin enantiomers. To this end a chiral separation method on an analytical and semi-preparative scale was developed allowing characterization of the stereoselective differences in metabolism and transport in the intestine and

activity in a selected bioassay of the separated hesperetin enantiomers in *in vitro* model systems. *S*- or *R*-hesperetin were compared in several assays: (1) in incubations with human small intestinal fractions containing UGTs or SULTs and their cofactors; (2) with Caco-2 cell monolayers as a model for the intestinal transport barrier; and (3) with mouse Hepa-1c1c7 cells transfected with human EpRE-controlled luciferase to test induction of EpRE-mediated gene expression. The results obtained indicate that although there are some significant differences in metabolism and transport characteristics between *S*- and *R*-hesperetin, these differences are relatively small. This indicates that for these endpoints, including intestinal metabolism and transport, experiments performed with racemic hesperetin may adequately reflect what can be expected for the naturally occurring *S*-enantiomer.

Conclusions

From the studies described in this thesis, the following can be concluded:

- Literature demonstrates that certain flavonoids are important modulators of intestinal ABC transporter proteins and therefore can modulate the bioavailability of other compounds upon oral uptake (**chapter 2**).
- The flavonoid hesperetin is metabolized into 7-*O*-glucuronide and 7-*O*-sulfate metabolites by Caco-2 cell monolayers, and these metabolites are predominantly transported to the apical side of the monolayer, representing the intestinal lumen side, by BCRP. Inhibition of this ABC transporter results in an up to 3.1-fold increased transport of hesperetin metabolites to the basolateral side of the monolayer, representing the blood side (**chapter 3**).
- Co-administration of specific flavonoids reported to inhibit BCRP, such as quercetin, results in an increased transport of hesperetin metabolites towards the basolateral side of Caco-2 cell monolayers, pointing at a possible way to increase *in vivo* bioavailability (**chapter 4**).
- The effect of co-administering quercetin *in vivo* in rat may result in an increased bioavailability of hesperetin, especially during the early phase of exposure when absorption dominates over elimination of hesperetin (**chapter 5**).
- Major differences in kinetics and regioselectivity of hesperetin by individual UGTs and SULTs exist, and incubations with rat and human tissue samples support an important role for the intestinal cells during first pass metabolism (**chapter 6**).
- Although there are some significant differences in metabolism and transport characteristics between *S*- and *R*-hesperetin, these differences are relatively small indicating that intestinal transport and metabolism performed with racemic hesperetin adequately reflects what can be expected from the naturally occurring *S*-enantiomer of hesperetin (**chapter 7**).

Concluding remarks and future perspectives

Flavonoid research dates back to the nineteen thirties, to the research of Dr. Albert Szent-Györgi and co-workers, who identified a compound in citrus peel that reduced capillary permeability and was effective in the treatment of purpura patients[18]. The compound was named vitamin P (P for 'Permeabilitätsfaktor')[18]. This compound was later reported to be a mixture of the flavonoids hesperidin and eriodictyol glucoside[19]. In the years onwards, the flavonoids hesperidin and hesperetin and its various derivatives were reported to possess a significant potential as therapeutic agents for a wide range of diseases and disorders, often explained by their anti-oxidant properties[4]. However, as for the biological effects of flavonoids in general, these biological activities are often assessed using *in vitro* test systems exposed to high concentrations of hesperetin aglycone. There are several flaws in this approach: the metabolism during first pass metabolism is ignored, and often non-physiologically relevant concentrations are being used. As a result, even up to date, research groups are ascribing health beneficial effects to the anti-oxidant properties of hesperetin or other flavonoids, based on data from *in vitro* assays in which biological systems are exposed to extremely high concentrations of flavonoids in a chemical form which cannot be detected in the blood. Given the actual physiological levels of flavonoids reached in plasma and most tissues *in vivo*, compared to the actual levels of other well known antioxidants like vitamin E, vitamin C and glutathione, it might be questioned whether flavonoids really exert their beneficial effects on health through their antioxidant activity. Recently, the biological effects of flavonoids are ascribed more and more to other mechanisms of action such as for example the modulation of factors within cell signaling pathways or the modulation of specific gene expression patterns, rather than to direct radical scavenging and antioxidant effects[20,21]. The induction of Electrophile Responsive Element (EpRE)-mediated gene expression by flavonoids, considered a beneficial response because its results in increased levels of phase II enzymes and other enzymes detoxifying electrophile compounds, has even been ascribed to their pro-oxidant chemistry[22].

During the first pass metabolism following intake, hesperetin is extensively metabolized and therefore only limited amounts, if any, of hesperetin aglycone are likely to be present in the systemic circulation. Since flavonoid conjugates and thus also the hesperetin conjugates are likely to possess different biological activities, as well as different distribution patterns than the parent aglycones, the results obtained in *in vitro* assays with the aglycones may not be extrapolated to the *in vivo* situation without taking the consequences of phase II metabolism into account. For hesperetin, apart from the aglycone, also its glucuronidated metabolites have been reported to provide some beneficial health effects such as the

protection against UV-A induced necrotic cell death in human skin fibroblasts[23], and recently, effects on several mechanisms or factors playing a role during osteoblast differentiation[24]. The latter may help to explain the role of hesperetin in the reduction of the risk on osteoporosis, which has been demonstrated in *in vivo* models with ovariectomized rats and mice[5-7]. Although the exact mechanism of action is still unknown, some research indicates that suppression of nuclear factor (NF)-κB activated mechanisms might play an important role[25].

Given this state-of-the-art it is concluded that future research on the biological activities of flavonoids should be directed at the phase II conjugates, which are the main circulating forms *in vivo,* and should define their mechanism and side of action as well as possibilities for their deconjugation upon or before cellular uptake. It can be envisaged that phase II metabolites of hesperetin may become deconjugated into the parent compound in order to exert their biological effects, as was demonstrated for the biological activity of quercetin glucuronides in the induction of EpRE-mediated gene expression [26]. Such a deconjugation may occur because cells can contain ß-glucuronidase able to deconjugate quercetin glucuronides[26,27].

In addition, further research should also take the physiologically relevant levels of hesperetin metabolites into account. Many of the effects reported in *in vitro* test systems result from exposure to concentrations up to thousand fold higher than the concentrations which can be detected in the blood after oral intake of hesperidin containing foods; *e.g.* consumption of 0.5 to 1 liter orange juice has been reported to result in maximum plasma concentrations (C_{max}) of only ~2 μM[28,29]. An important reason behind this low plasma concentration after consumption of orange juice is the fact that hesperidin is taken up only gradually after deglycosylation by microbiota in the colon. By enzymatic treatment hesperidin can be converted into hesperetin 7-*O*-glucoside, a form of hesperetin that is already taken up in the small intestine, at a faster rate, by which the C_{max} of hesperetin can be increased 4-fold[13]. However, even when co-administration with other flavonoids, as investigated in the present thesis, could potentially increase the C_{max} of hesperetin even further, the *in vivo* plasma levels of hesperetin metabolites would still be expected to amount to levels of at most 10 μM, consisting of mainly hesperetin phase II metabolites, and this should be taken into account when designing and interpreting *in vitro* studies.

A final issue which is generally overlooked in the research on hesperetin and some other flavonoids, and which should receive more attention in future research, is the fact that hesperetin has a chemical structure containing a chiral center, and therefore exists as *S*- and *R*-hesperetin enantiomers. While in nature *S*-hesperetin is predominant, most studies applying 'pure' compounds use a racemic mixture, containing two isomers with potentially distinct kinetic and dynamic behavior. This

not only applies to hesperetin but also to other flavanones such as naringenin, or other classes of flavonoids containing a chiral center in their structure, *e.g.* flavanols. In our studies on stereochemical differences in the metabolism and bioactive effects of the hesperetin enantiomers, using EpRE-mediated gene expression as a model assay, some significant differences were detected although they were generally small, leading to the conclusion that differences in metabolism and transport characteristics between *S*- and *R*-hesperetin are relatively small, indicating that intestinal transport and metabolism performed with racemic hesperetin adequately reflects what can be expected from the naturally occurring *S*-enantiomer of hesperetin. In the selected EpRE-reporter gene assay at physiologically relevant levels no major differences between the *S*- and *R*-enantiomer were detected. However, it should be recognized that bioassays that depend on selected receptor interactions may be more sensitive to stereochemical differences than the EpRE-reporter gene assay and the conversion of hesperetin by the phase II biotransformation enzymes or the ABC transporters with their wide substrate specificities. Thus, the possible impact of stereochemistry on the biological effects of flavonoids should be investigated to a further extent taking also other end-points into account.

Altogether, the studies described in this thesis belong to the only way forward in understanding and applying the physiological effects of flavonoids, and provide an insight in the mechanisms of bioavailability of hesperetin and the effect of co-administering other flavonoids hereon.

References

1 Scalbert A, Williamson G. Dietary intake and bioavailability of polyphenols. *J Nutr* 130(8S Suppl): 2073S-2085S, 2000.

2 Havsteen BH. The biochemistry and medical significance of the flavonoids. *Pharmacol Ther* 96(2-3): 67-202, 2002.

3 Tomás-Barberán FA, Clifford MN. Flavanones, chalcones and dihydrochalcones - nature, occurrence and dietary burden. *J Sci Food Agric* 80(7): 1073-1080, 2000.

4 Garg A, Garg S, Zaneveld LJD, Singla AK. Chemistry and pharmacology of the citrus bioflavonoid hesperidin. *Phytother Res* 15(8): 655-669, 2001.

5 Chiba H, Uehara M, Wu J, Wang X, Masuyama R, Suzuki K, Kanazawa K, Ishimi Y. Hesperidin, a citrus flavonoid, inhibits bone loss and decreases serum and hepatic lipids in ovariectomized mice. *J Nutr* 133(6): 1892-1897, 2003.

6 Habauzit V, Nielsen IL, Gil-Izquierdo A, Morand C, Chee W, Barron D, Davicco MJ, Coxam V, Williamson G, Offord E, Horcajada MN. Increased bioavailability of hesperetin-7-glucoside compared to hesperidin results in more efficient prevention of bone loss in adult ovariectomized rats. *Br J Nutr* 102(7): 976-984, 2009.

7 Horcajada MN, Habauzit V, Trzeciakiewicz A, Morand C, Gil-Izquierdo A, Mardon J, Lebecque P, Davicco MJ, Chee WSS, Coxam V, Offord E. Hesperidin inhibits ovariectomized-induced osteopenia and shows differential effects on bone mass and strength in young and adult intact rats. *J Appl Physiol* 104(3): 648-654, 2008.

8 Manach C, Williamson G, Morand C, Scalbert A, Remesy C. Bioavailability and bioefficacy of polyphenols in humans. I. Review of 97 bioavailability studies. *Am J Clin Nutr* 81(1 Suppl): 230S-242S, 2005.

9 Liu Z, Hu M. Natural polyphenol disposition via coupled metabolic pathways. *Expert Opin Drug Metab Toxicol* 3(3): 389-406, 2007.

10 Pinto M, Robine-Leon S, Appay M-D, Kedinger M, Triadou N, Dussaulx E, Lacroix B, Simon-Assmann P, Haffen K, Fogh J, Zweibaum A. Enterocyte-like differentiation and polarisation of the human colon carcinoma cell line Caco-2. *Biol Cell* 47: 323-330, 1983.

11 Karlsson J, Artursson P. A method for the determination of cellular permeability coefficients and aquous boundary layer thickness in monolayers of intestinal epithelial (Caco-2) cells grown in permeable filter chambers. *Int J Pharmaceutics* 71(1-2): 55-64, 1991.

12 Allen JD, Van Loevezijn A, Lakhai JM, Van der Valk M, Van Tellingen O, Reid G, Schellens JHM, Koomen G-J, Schinkel AH. Potent and specific inhibition of the breast cancer resistance protein multidrug transporter in vitro and in mouse intestine by a novel analogue of fumitremorgin C. *Mol Cancer Ther* 1(6): 417-425, 2002.

13 Nielsen ILF, Chee WSS, Poulsen L, Offord-Cavin E, Rasmussen SE, Frederiksen H, Enslen M, Barron D, Horcajada M-N, Williamson G. Bioavailability is improved by enzymatic modification of the citrus flavonoid hesperidin in humans: a randomized, double-blind, crossover trial. *J Nutr* 136(2): 404-408, 2006.

14 Nakamura A, Nakajima M, Yamanaka H, Fujiwara R, Yokoi T. Expression of UGT1A and UGT2B mRNA in human normal tissues and various cell lines. *Drug Metab Dispos* 36(8): 1461-1464, 2008.

15 Ohno S, Nakajin S. Determination of mRNA expression of human UDP-glucuronosyltransferases and application for localization in various human tissues by real-time reverse transcriptase-polymerase chain reaction. *Drug Metab Dispos* 37(1): 32-40, 2009.

16 Riches Z, Stanley EL, Bloomer JC, Coughtrie MWH. Quantitative evaluation of the expression and activity of five major sulfotransferases (SULTs) in human tissues: the SULT "pie". *Drug Metab Dispos* 37(11): 2255-2261, 2009.

17 Teubner W, Meinl W, Florian S, Kretzschmar M, Glatt H. Identification and localization of soluble sulfotransferases in the human gastrointestinal tract. *Biochem J* 404(2): 207-215, 2007.

18 Rusznyak S, Szent-Györgyi A. Vitamin P: flavonols as vitamins. *Nature* 138(3479): 27, 1936.

19 Bruckner V, Szent-Györgyi A. Chemical nature of citrin. *Nature* 138(3503): 1057, 1936.

20 Halliwell B, Rafter J, Jenner A. Health promotion by flavonoids, tocopherols, tocotrienols, and other phenols: direct or indirect effects? Antioxidant or not? *Am J Clin Nutr* 81(1 Suppl): 268S-276S, 2005.

21 Holst B, Williamson G. Nutrients and phytochemicals: from bioavailability to bioefficacy beyond antioxidants. *Curr Opin Biotechnol* 19(2): 73-82, 2008.

22 Lee-Hilz YY, Boerboom AMJF, Westphal AH, Berkel WJH, Aarts JMMJG, Rietjens IMCM. Pro-oxidant activity of flavonoids induces EpRE-mediated gene expression. *Chem Res Toxicol* 19(11): 1499-1505, 2006.

23 Proteggente AR, Basu-Modak S, Kuhnle G, Gordon MJ, Youdim K, Tyrrell R, Rice-Evans CA. Hesperetin glucuronide, a photoprotective agent arising from flavonoid metabolism in human skin fibroblasts. *Photochem Photobiol* 78(2): 256-261, 2003.

24 Trzeciakiewicz A, Habauzit V, Mercier S, Barron D, Urpi-Sarda M, Manach C, Offord E, Horcajada M-N. Molecular mechanism of hesperetin-7-O-glucuronide, the main circulating metabolite of hesperidin, involved in osteoblast differentiation. *J Agric Food Chem* 58(1): 668-675, 2010.

25 Kim JY, Jung KJ, Choi JS, Chung HY. Modulation of the age-related nuclear factor-kappaB (NF-kappaB) pathway by hesperetin. *Aging Cell* 5(5): 401-411, 2006.

26 Lee-Hilz YY, Stolaki M, Van Berkel WJH, Aarts JMMJG, Rietjens IMCM. Activation of EpRE-mediated gene transcription by quercetin glucuronides depends on their deconjugation. *Food Chem Toxicol* 46(6): 2128-2134, 2008.

27 O'Leary KA, Day AJ, Needs PW, Mellon FA, O'Brien NM, Williamson G. Metabolism of quercetin-7- and quercetin-3-glucuronides by an in vitro hepatic model: the role of human beta-glucuronidase, sulfotransferase, catechol-O-methyltransferase and multi-resistant protein 2 (MRP2) in flavonoid metabolism. *Biochem Pharmacol* 65(3): 479-491, 2003.

28 Erlund I, Meririnne E, Alfthan G, Aro A. Plasma kinetics and urinary excretion of the flavanones naringenin and hesperetin in humans after ingestion of orange juice and grapefruit juice. *J Nutr* 131(2): 235-241, 2001.

29 Manach C, Morand C, Gil-Izquierdo A, Bouteloup-Demange C, Rémésy C. Bioavailability in humans of the flavanones hesperidin and narirutin after the ingestion of two doses of orange juice. *Eur J Clin Nutr* 57(2): 235-242, 2003.

Samenvatting en conclusies

Samenvatting

Het doel van dit promotieonderzoek was te onderzoeken in welke mate de biobeschikbaarheid van de geselecteerde modelflavonoïde hesperetine ((+/-)-4'-methoxy-3',5,7-trihydroxyflavonone) zou kunnen worden verhoogd door het beïnvloeden van het metabolisme en het transport van hesperetine in de darmwand, door middel van gelijktijdige blootstelling aan andere flavonoïden. Flavonoïden vormen een grote groep polyfenolen en zijn aanwezig in veel voedingsmiddelen die afkomstig zijn van planten. Vaak zijn flavonoïden hierin aanwezig in de vorm van ß-glycosiden[1]. Flavonoïden zijn veelvuldig geassocieerd met allerhande, mogelijk gezondheidsbevorderende, effecten[2]. Hesperetine is het aglycon van de rutinoside hesperidine, dat in aanzienlijke hoeveelheden aanwezig kan zijn in citrusfruit en in sinaasappelsap[3]. Hesperidine wordt, na inname, in de darm gedeglycosyleerd tot hesperetine[3]. Hesperetine is in verband gebracht met anticarcinogene effecten[4], en ook met het verminderen van het risico op osteoporose, wat is aangetoond in *in vivo* modelsystemen[5-7]. Hoewel de inname via het dieet aanzienlijk kan zijn, is de biobeschikbaarheid van hesperetine beperkt; een fenomeen dat geldt voor de meeste subgroepen van flavonoïden[8]. Een belangrijk mechanisme dat hieraan ten grondslag ligt is het metabolisme en transport in de darmwand: flavonoïden worden geconjugeerd door zogenaamde fase-II-enzymen, zoals UDP-glucuronosyl tranferasen (UGT), sulfotransferasen (SULT) of catechol-*O*-methyltransferasen (COMT), in de cellen van de darmwand en worden vervolgens teruggetransporteerd naar het darmlumen door apicaal gelegen ABC-transporters[9]. Omdat specifieke flavonoïden bekendstaan als modulatoren van fase-II-enzymen en ABC-transporters, is in dit proefschrift de hypothese onderzocht of gelijktijdige blootstelling aan hesperetine en specifieke andere flavonoïden de biobeschikbaarheid van hesperetine zou kunnen verhogen door het moduleren van het metabolisme en het transport van hesperetine in de darmwand. Om deze hypothese te ondersteunen, geeft **hoofdstuk 2** van dit proefschrift een overzicht weer van literatuur over het vermogen van flavonoïden om de orale biobeschikbaarheid van bepaalde stoffen te moduleren. Het overzicht toont aan dat het transport van stoffen door de darmwand in grote mate afhankelijk kan zijn van de activiteit van ABC-transporters. Deze kunnen gelegen zijn aan de basolaterale zijde en absorptie faciliteren, of aan de apicale zijde en betrokken zijn bij het transport naar het darmlumen en daarmee de biobeschikbaarheid van bepaalde stoffen verminderen. Deze functie van de ABC- transporters houdt ook een rol in voor stoffen die deze transporters remmen (inhibitors) in het moduleren van orale biobeschikbaarheid. De rol van flavonoïden hierin kan worden geïllustreerd aan de hand van verschillende voorbeelden van *in vitro*- en *in vivo*-studies waarin

dergelijke effecten zijn waargenomen. Hoofdstuk 2 besluit met de conclusie dat toekomstige studies zich tevens zouden moeten richten op (1) *in vivo*-validatie van de effecten van flavonoïden op de biobeschikbaarheid van medicijnen, toxinen en bioactieve stoffen in het voedsel die zijn aangetoond in *in vitro*-modelsystemen, en (2) op de rol van het fase-II-metabolisme van flavonoïden op de functie van flavonoïden als ABC- transporter-inhibitor en/of -substraat.
In de daaropvolgende hoofdstukken van het proefschrift is het concept van het verhogen van de biobeschibaarheid van hesperetine door simultane blootstelling aan inhibitors van fase-II-metabolisme en/of ABC-transport onderzocht met behulp van verschillende *in vitro*- en *in vivo*-systemen. Als *in vitro*-modelsysteem is onder meer een tweecompartimenten transwellmodel met monolagen van Caco-2 cellen gebruikt om de darmwand te simuleren. Caco-2 cellen vertonen, na differentiatie, morfologische en biochemische karakteristieken van enterocyten, inclusief de expressie van ABC- transporters en fase II enzymen, en vormen een aaneengesloten laag van gepolariseerde cellen[10]. Gekweekt op een membraan dat een apicaal compartiment (dat het darmlumen vertegenwoordigt) scheidt van een basolateraal compartiment (dat de zijde van het bloed vertegenwoordigt), vormen monolagen van Caco-2 cellen een geaccepteerd *in vitro*-model om de opname door de darmwand te bestuderen[11].
In **hoofdstuk 3** zijn monolagen van Caco-2 cellen in het tweecompartimenten transwellmodel gebruikt om de eigenschappen van het metabolisme en het transport van hesperetine in de cellen van de darwmand *in vitro* te definiëren. De metabolieten van hesperetine, gevormd door de Caco-2 cellen zijn, daarbij geïdentificeerd door middel van HPLC-DAD en uPLC-DAD-MS-MS-technieken en beschikbare referentiestoffen in combinatie met specifieke deconjugatiereacties. De rol van de apicaal gelegen ABC-transporters P-glycoproteïne (Pgp), "Multidrug Resistance Protein 2" (MRP2) en "Breast Cancer Resistance Protein" (BCRP) in het transport van hesperetine en haar metabolieten is bestudeerd door gelijktijdige blootstelling aan remmers voor bepaalde klassen van ABC transporters. De cellulaire expressie van deze ABC-transporters in Caco-2 cellen is bevestigd door middel van RT-qPCR-analyse. De monolagen van Caco-2 cellen (apicaal blootgesteld) metaboliseerden hesperetine tot hesperetine 7-*O*-glucoronide en hesperetine 7-*O*-sulfaat, die voornamelijk naar de apicale zijde van de monolaag werden getransporteerd. Ongemetaboliseerd hesperetine drong door tot de basolaterale zijde en dit proces werd niet beïnvloed door de gebruikte remmers van ABC-transport, wat mogelijk op een passief diffusieproces duidt. Echter, de studies met de remmers toonden aan dat het transport van de metabolieten van hesperetine naar de apicale zijde een actief transport betrof, dat op basis van het patroon van remming hoofdzakelijk aan BCRP kon worden toegeschreven. Als gevolg van de specifieke BCRP-remmer K0143[12], werd het transport van de

hesperetine metabolieten naar de apicale zijde met een factor 1.9 verlaagd, en naar de basolaterale zijde met een factor 3.1 verhoogd. Deze resultaten werpen een nieuw licht op het metabolisme en transport van hesperetine, en tonen aan dat het transport door BCRP een beperkend mechanisme kan zijn in de biobeschikbaarheid van hesperetine.

Omdat verwacht kan worden dat andere flavonoïden worden omgezet door gelijke fase- II-enzymen als hesperetine en daarmee het metabolisme van hesperetine zouden kunnen beïnvloeden, en omdat bepaalde flavonoïden ook de apicaal gelegen ABC-transporter BCRP kunnen remmen, is in **hoofdstuk 4** het effect van verschillende flavonoïden op het metabolisme en het transport van hesperetine onderzocht. Dat is getest door monolagen van Caco-2 cellen in het tweecompartimenten transwellsysteem bloot te stellen aan combinaties van hesperetine met andere flavonoïden. Daarbij werd aangetoond dat blootstelling aan hesperetine in combinatie met specifieke flavonoïden de ratio van apicaal naar basolateraal transport verminderde, en in sommige gevallen ook de hoeveelheid gevormde, extracellulair gemeten hesperetine metabolieten verminderde. Flavonolen en flavonen hadden hierbij een groter effect dan isoflavonen, en de flavonol quercetine veroorzaakte het grootste effect, terwijl blootstelling aan flavanolen of geglycosyleerde derivaten, die volgens de literatuur BCRP niet remmen, geen effect hadden op het transport van de hesperetine metabolieten. Omdat intracellulaire ophoping van hesperetine metabolieten niet de verminderde hoeveelheid extracellulair gemeten hesperetine metabolieten kon verklaren, werd geconcludeerd dat remming van het metabolisme van hesperetine waarschijnlijk het mechanisme is voor de verminderde vorming en excretie van hesperetine metabolieten. Ondanks de reductie in metabolisme, was de hoeveelheid hesperetine metabolieten die naar de basolaterale zijde werden getransporteerd significant verhoogd door de gelijktijdige blootstelling aan specifieke flavonoïden en daarom zou gelijktijdige blootstelling aan bepaalde andere flavonoïden een strategie kunnen zijn waarmee de biobeschikbaarheid van hesperetine kan worden verhoogd.

In **hoofdstuk 5** is onderzocht of de *in vitro* bevindingen in het Caco-2 model, die aantoonden dat gelijktijdige blootstelling aan quercetine het basolaterale transport van hesperetine metabolieten vergrootte, zouden kunnen worden bevestigd in een *in vivo*-model. Daartoe werd hesperetine 7-*O*-glucoside, een monosaccharidederivaat van hesperetine, oraal toegediend aan Sprague-Dawley ratten in de aan- of afwezigheid van quercetine. In deze *in vivo*-studie werd hesperetine 7-*O*-glucoside gebruikt in plaats van hesperetine, omdat eerdere studies met ratten lieten zien dat hesperetine al voor een groot deel wordt opgenomen in de maag, wat de mogelijkheid uitsluit om het effect van quercetine op de opname in de darm te onderzoeken. Van hesperetine 7-*O*-glucoside is bekend dat het opgenomen

wordt in de dunne darm[13], en daarom is het een betere modelstof om het effect van quercetine op de opname en biobeschikbaarheid van hesperetine in de darm te onderzoeken. Ratten werd oraal hesperetine 7-*O*-glucoside (15 of 3 mg/kg lichaamsgewicht) toegediend, in de aan- of afwezigheid van quercetine (15 mg/kg lichaamsgewicht). Systemisch bloed werd afgenomen op 8 tijdspunten na toediening, tussen de 15 minuten en 8 uur, om de oppervlakte onder de concentratietijdcurve (AUC) van plasma-hesperetine en haar gedemethyleerde en geremethyleerde derivaten eriodictyol en homoeriodictyol te bepalen na behandeling van de bloedmonsters met ß-glucuronidase/sulfatase. De concentraties hesperetine, eriodictyol en homo-eriodictyol werden bepaald en gekwantificeerd middels uPLC-DAD. Gelijktijdige blootstelling aan hesperetine en quercetine verhoogde in het bijzonder de biobeschikbaarheid van hesperetine in de vroege fase van de concentratietijdcurve (bij 15 min) waar eliminatie nog niet domineert over opname, maar verhoogde niet de AUC van tijdstip nul tot 8 uur. Er kan worden geconcludeerd dat het effect van gelijktijdige blootstelling aan quercetine als een remmer van het transport van BCRP in de cellen van de darmwand, zou kunnen resulteren in een verhoogde biobeschikbaarheid van hesperetine, zeker tijdens de vroege fase van blootstelling waar absorptieprocessen nog domineren boven het proces van eliminatie.

In **hoofdstuk 6** werd het fase-II-metabolisme van hesperetine verder bestudeerd. In deze studie werd de kinetiek van de omzetting van hesperetine door microsomale en cytosolaire fracties van de dunne darm, dikke darm en lever van de mens en de rat bepaald. Ook werd de kinetiek onderzocht van de glucuronidering en sulfonering van hesperetine door respectievelijk 12 individuele UGT- en 12 individuele SULT-enzymen teneinde de verantwoordelijke UGTs en SULTs te bepalen. Van deze UGTs en SULTs zijn de expressieniveaus in verschillende weefsels betrekkelijk goed beschreven in de literatuur[14-17]. De verkregen resultaten toonden aan dat hesperetine wordt geconjugeerd op positie 7 en 3', en dat er belangrijke enzymspecifieke verschillen bestaan in de kinetiek en regioselectiviteit voor de door de UGTs en SULTs gekatalyseerde conjugatiereacties. UGT1A9, UGT1A1, UGT1A7, UGT1A8 en UGT1A3 zijn de belangrijkste UGTs die de glucuronidering van hesperetine katalyseren, waarvan de laatste alleen 7-*O*-glucuronide vormt, terwijl UGT1A7 hoofdzakelijk 3'-*O*-glucuronide produceert. UGT1A6 en UGT2B4 vormen enkel hesperetine 7-*O*-glucuronide, terwijl UGT1A1, UGT1A8, UGT1A9, UGT1A10 UGT2B7 en UGT2B15 beide posities conjugeren. SULT1A2 en SULT1A1 katalyseren het meest efficiënt de vorming van hesperetine 3'-*O*-sulfaat, en SULT1C4 vormt voornamelijk en het meest efficiënt de vorming van hesperetine 7-*O*-sulfaat. Gebaseerd op expressieniveaus ligt het ook voor de hand dat SULT1A3 en SULT1B1 een belangrijke rol spelen in de sulfonering in de darmcellen. Deze resultaten helpen verschillen in metabolietpatronen te verklaren die worden waargenomen in

weefsels of systemen met verschillende expressieniveaus van UGTs en SULTs, bijvoorbeeld lever- en darmfracties of Caco-2 cellen. Resultaten verkregen op basis van incubatie van hesperetine met de weefselfracties ondersteunden een belangrijke rol voor de darmcellen in het metabolisme van hesperetine tijdens de opname, resulterend in de vorming van hesperetine 3'-*O*-glucuronide en hesperetine 7-*O*-glucuronide, welke de belangrijkste metabolieten van hesperetine zijn die *in vivo* worden aangetroffen.

Hoofdstuk 7 belicht de stereochemie van hesperetine. Hesperetine bevat een chiraal C-atoom waardoor het kan voorkomen als *S*- en *R*-enantiomeer. Dit is van belang omdat in de natuur 2*S*-hesperidine en het afgeleide *S*-hesperetine verreweg de meest voorkomende chemische vormen zijn. Desondanks worden veel studies uitgevoerd met de commercieel verkrijgbare racemische mengsels van hesperidine en hesperetine. In hoofdstuk 7 zijn de eigenschappen van het transport en van het metabolisme die tot nu toe waren bestudeerd voor het commercieel beschikbare racemische mengsel van hesperetine, bestudeerd voor *S*- en *R*-hesperetine afzonderlijk. Hiertoe werd een chirale scheidingsmethode ontwikkeld die het mogelijk maakte op een analytische en semi-preperatieve schaal *S*- en *R*-hesperetine te isoleren. Vervolgens konden de stereoselectieve verschillen in metabolisme en transport tussen de twee hesperetine-enatiomeren in *in vitro*-modellen worden bestudeerd en tevens de activiteit van beide vormen in een geselecteerde *in vitro*-bioassay. *S*- en *R*-hesperetine zijn vergeleken in verschillende assays: (1) in incubatie met humane dunnedarmfracties die UGTs en SULTs bevatten, en de relevante co-facoren, (2) in het transwellsysteem met monolagen van Caco-2 cellen als model voor het metabolisme en het transport in de darmwand; en (3) in muizen Hepa-1c1c7-cellen getransfecteerd met humane EpRE-gereguleerde luciferase om de inductie van EpRE-gemedieerde genexpressie te onderzoeken. De resultaten lieten zien dat er enige significante verschillen bestaan tussen de kinetiek en de biologische activiteit van *S*- en *R*-hesperetine in deze assays, maar dat deze verschillen relatief klein zijn. Dit betekent dat voor de onderzochte eindpunten, namelijk darmmetabolisme en -transport, experimenten uitgevoerd met racemisch hesperetine, adequaat kunnen weergeven wat kan worden verwacht voor het natuurlijk voorkomende *S*-hesperetine.

Conclusies

Uit het onderzoek beschreven in dit proefschrift kan het volgende worden geconcludeerd:

- De literatuur toont aan dat bepaalde flavonoïden belangrijke modulatoren zijn van ABC-transporters in de darmwand en daarom de biobeschikbaarheid van andere stoffen na orale opname kunnen beïnvloeden (**hoofdstuk 2**).

- De flavonoïde hesperetine wordt door monolagen van Caco-2-cellen gemetaboliseerd in 7-*O*-glucuronide- en 7-*O*-sulfaat-metabolieten. Deze metabolieten worden hoofdzakelijk getransporteerd naar de apicale zijde van de monolaag, de zijde die het darmlumen simuleert, door de ABC-transporter BCRP. Remming van BCRP leidt in een tot 3.1-keer verhoogd transport van hesperetine metabolieten naar de basolaterale zijde van de monolaag, de zijde die het bloed vertegenwoordigt (**hoofdstuk 3**).
- Gelijktijdige blootstelling aan bepaalde flavonoïden die beschreven zijn als remmers van BCRP, waaronder quercetine, leidt tot een verhoogd transport van hesperetine metabolieten naar de basolaterale zijde van de monolagen van Caco-2 cellen, hetgeen wijst op een mogelijke manier om de biobeschikbaarheid *in vivo* te verhogen (**hoofdstuk 4**).
- Het effect van gelijktijdige blootstelling aan quercetine *in vivo* in ratten zou kunnen leiden tot een verhoogde biobeschikbaarheid van hesperetine, in het bijzonder gedurende de vroege fase van blootstelling wanneer de absorptie van hesperetine belangrijker is dan de uitscheiding (**hoofdstuk 5**).
- Er bestaan grote verschillen in kinetiek en regioselectiviteit van de omzetting van hesperetine door afzonderlijke UGTs en SULTs, en incubatie met weefselfracties van rat en mens ondersteunen een belangrijke rol voor de darmcellen tijdens het metabolisme van hesperetine gedurende de opname (**hoofdstuk 6**).
- Hoewel er enige significante verschillen bestaan in de karakteristieken van metabolisme en transport tussen *S*- en *R*-hesperetine, zijn deze relatief klein wat aantoont dat studies naar transport en metabolisme uitgevoerd met racemisch hesperetine adequaat weerspiegelen wat kan worden verwacht voor de natuurlijk voorkomende *S*-enanatiomeer van hesperetine (**hoofdstuk 7**).

Referenties

1 Scalbert A, Williamson G. Dietary intake and bioavailability of polyphenols. *J Nutr* 130(8S Suppl): 2073S-2085S, 2000.

2 Havsteen BH. The biochemistry and medical significance of the flavonoids. *Pharmacol Ther* 96(2-3): 67-202, 2002.

3 Tomás-Barberán FA, Clifford MN. Flavanones, chalcones and dihydrochalcones - nature, occurrence and dietary burden. *J Sci Food Agric* 80(7): 1073-1080, 2000.

4 Garg A, Garg S, Zaneveld LJD, Singla AK. Chemistry and pharmacology of the citrus bioflavonoid hesperidin. *Phytother Res* 15(8): 655-669, 2001.

5 Chiba H, Uehara M, Wu J, Wang X, Masuyama R, Suzuki K, Kanazawa K, Ishimi Y. Hesperidin, a citrus flavonoid, inhibits bone loss and decreases serum and hepatic lipids in ovariectomized mice. *J Nutr* 133(6): 1892-1897, 2003.

6 Habauzit V, Nielsen IL, Gil-Izquierdo A, Morand C, Chee W, Barron D, Davicco MJ, Coxam V, Williamson G, Offord E, Horcajada MN. Increased bioavailability of hesperetin-7-glucoside compared to hesperidin results in more efficient prevention of bone loss in adult ovariectomized rats. *Br J Nutr* 102(7): 976-984, 2009.

7 Horcajada MN, Habauzit V, Trzeciakiewicz A, Morand C, Gil-Izquierdo A, Mardon J, Lebecque P, Davicco MJ, Chee WSS, Coxam V, Offord E. Hesperidin inhibits ovariectomized-induced osteopenia and shows differential effects on bone mass and strength in young

and adult intact rats. *J Appl Physiol* 104(3): 648-654, 2008.
8 Manach C, Williamson G, Morand C, Scalbert A, Remesy C. Bioavailability and bioefficacy of polyphenols in humans. I. Review of 97 bioavailability studies. *Am J Clin Nutr* 81(1 Suppl): 230S-242S, 2005.
9 Liu Z, Hu M. Natural polyphenol disposition via coupled metabolic pathways. *Expert Opin Drug Metab Toxicol* 3(3): 389-406, 2007.
10 Pinto M, Robine-Leon S, Appay M-D, Kedinger M, Triadou N, Dussaulx E, Lacroix B, Simon-Assmann P, Haffen K, Fogh J, Zweibaum A. Enterocyte-like differentiation and polarisation of the human colon carcinoma cell line Caco-2. *Biol Cell* 47: 323-330, 1983.
11 Karlsson J, Artursson P. A method for the determination of cellular permeability coefficients and aquous boundary layer thickness in monolayers of intestinal epithelial (Caco-2) cells grown in permeable filter chambers. *Int J Pharmaceutics* 71(1-2): 55-64, 1991.
12 Allen JD, Van Loevezijn A, Lakhai JM, Van der Valk M, Van Tellingen O, Reid G, Schellens JHM, Koomen G-J, Schinkel AH. Potent and specific inhibition of the breast cancer resistance protein multidrug transporter in vitro and in mouse intestine by a novel analogue of fumitremorgin C. *Mol Cancer Ther* 1(6): 417-425, 2002.
13 Nielsen ILF, Chee WSS, Poulsen L, Offord-Cavin E, Rasmussen SE, Frederiksen H, Enslen M, Barron D, Horcajada M-N, Williamson G. Bioavailability is improved by enzymatic modification of the citrus flavonoid hesperidin in humans: a randomized, double-blind, crossover trial. *J Nutr* 136(2): 404-408, 2006.
14 Nakamura A, Nakajima M, Yamanaka H, Fujiwara R, Yokoi T. Expression of UGT1A and UGT2B mRNA in human normal tissues and various cell lines. *Drug Metab Dispos* 36(8): 1461-1464, 2008.
15 Ohno S, Nakajin S. Determination of mRNA expression of human UDP-glucuronosyltransferases and application for localization in various human tissues by real-time reverse transcriptase-polymerase chain reaction. *Drug Metab Dispos* 37(1): 32-40, 2009.
16 Riches Z, Stanley EL, Bloomer JC, Coughtrie MWH. Quantitative evaluation of the expression and activity of five major sulfotransferases (SULTs) in human tissues: the SULT "pie". *Drug Metab Dispos* 37(11): 2255-2261, 2009.
17 Teubner W, Meinl W, Florian S, Kretzschmar M, Glatt H. Identification and localization of soluble sulfotransferases in the human gastrointestinal tract. *Biochem J* 404(2): 207-215, 2007.

Dankwoord

Promoveren doe je niet alleen en ik heb het genoegen gehad met veel mensen te hebben mogen samenwerken. Graag wil ik hier iedereen bedanken die, op welke wijze dan ook, heeft geholpen bij het totstandkomen van dit proefschrift. In het bijzonder, allereerst mijn prima promotoren en begeleiders: Beste Ivonne, ontzettend bedankt voor de efficiënte wijze waarin je me de afgelopen jaren hebt begeleid! Dank ook voor het altijd supersonisch snel nakijken van mijn schrijfsels en je scherpe commentaar, maar ook voor de vrijheid die je me hebt gelaten om zelf dingen te ontdekken (en daarbij ook de nodige fouten te maken). Ik heb ontzettend veel van je geleerd! Beste Peter, dank voor het mogelijk maken van de samenwerking met Nestlé. Ik heb onze gesprekken altijd enorm gewaardeerd en bedankt voor de vele goede raad! Onze lunches zal ik nooit vergeten, zowel die in Lausanne (a la carte in het Nestlé restaurant) als in de universiteitskantine (kroketten, witte bolletjes). Dear Gary, it was an honor to have you as a supervisor on our project. Thank you very much for all your comments and help. The time spent at 'your' ICPH in Harrogate in December 2009 was the best part of my whole PhD, and I truly regret I've not been to Leeds more often.

Als deel van het onderzoek was het voor mij een groot genoegen om zeven master studenten ('mijn hesperiden') tijdens hun afstudeervak te mogen begeleiden: Inge, Karin, Bea, Jia, Kathelijn, Hanneke en Elise - thank you very much for your help unravelling the secrets of the most interesting flavonoid in the world! Also you will never be able to drink a glass of orange juice without thinking about ABC transporters, bioavailability, UGTs, etcetera... I do hope you learned as much from me as I did from you. The fact that three of you are now PhD-candidates yourself (even one at toxicology), fulfills me with proudness! I wish you all the best!

Alle technische en administratieve staf van de leerstoelgroep verdient ook veel dank. In het bijzonder: Marelle (dankjewel voor alle hulp bij de incubaties en de HPLC- en uPLC-analyses), Bert (dankjewel voor het onophoudelijke preparatief HPLC-en en het opwerken van de plasmamonsters, je onvermoeibare interesse in mijn onderzoek - en dat ene artikel), Laura (dankjewel voor je hulp bij de cellen en moleculaire biologie, en dat je altijd voor me klaar stond) en Irene (dankjewel voor alle bestellingen en hulp met administratie, formulieren en alle bureaucratie waar je tegenwoordig zelfs als promovendus mee te maken hebt! -en voor het nakijken van de Nederlandse samenvatting bovendien). Ook alle andere stafleden: bedankt voor jullie tips en interesse, en bovenal voor de huiselijke sfeer op de leerstoelgroep. Een bijzonder wens voor alle AiO's, waarvan ik er eerst veel zag gaan en later veel zag komen: veel succes met jullie carriere en/of onderzoek! En dank voor alle gezelligheid! Special thanks to my roommates, first: Ans (fijn dat ik al even bij jou op het podium mocht oefenen!) and Elton, then: Linda and Erry; thanks for the nice

atmosphere at room 1.021!
Part of this research was performed at Nestlé, and I would like to express my appreciation to all the people who have helped me in Laussanne. Special thanks to Denis, Fabiola, Inge-lise, Maarit and Sylvie, and of course all (other) people from the bioavailability group for their presence and feedback during presentations!
Jacques en Sjef, dank jullie wel voor jullie hulp met de LC-MS en NMR bij biochemie en Biqualys. Alle mensen van het CKP: bedankt voor jullie tijd en uitstekende assistentie bij de dierproeven en de goede sfeer! Bert, dankjewel voor alle hulp hierbij! Sehr geehrte professor Glatt und Walter (eins): herzlichen Dank für eure Beiträge an Kapitel sechs! Sjoerd Knibbeler, bedankt voor het opmaken en beschikbaar stellen van die mooie foto op de cover.
Al mijn nieuwe (inmiddels ex-)collega's bij MSD, dank voor de fijne sfeer in Schaijk en voor jullie begrip en interesse in de tijd dat ik twee banen met elkaar wist te combineren. Marlou, dankjewel voor het creëren van deze kans, en de enorm leerzame tijdbij MSD. Jammer dat de overname roet in het eten gooide. Ook Arne, bedankt voor de fijne sfeer op ons kantoor en alles wat ik van je heb geleerd. Veel succes allemaal!
Mijn paranimfen Jochem en Joost, fijn dat jullie me op de dag van de verdediging terzijde willen staan! Jochem, je bent een uitstekende collega en wetenschapper en ik weet zeker dat je een mooie carrière tegemoet gaat! Joost, beste vriend, het is heel fijn dat je wederom aan mijn zijde staat!
Lieve vrienden en familie, ontzettend bedankt voor al jullie interesse. Het laatste halve jaar was niet altijd even gemakkelijk -dank voor jullie begrip en jullie steun. Mathieu, broertjuh, hartstikke bedankt voor het layout-en van het boekje! Het is erg mooi geworden!
Lieve Janneke, naast de vele gezichten die ons werk liet zien hebben we de afgelopen jaren (ook) daarbuiten heel veel mooie en bijzondere momenten meegemaakt. En er ligt nog veel op de plank. Dankjewel voor alle liefde, steun en vertrouwen. Je hebt me er de laatste maanden vaak aan moeten herinneren hoe leuk ik het vond om AiO te zijn. Ik beloof dat jij te zijner tijd ook op dat begrip mag rekenen. We leven het leven wel!

-Walter

Curriculum Vitae

Walter Brand werd geboren op 29 juli 1979 te Nijmegen, groeide op in Nijmegen, Aalst-Waalre, en wederom in Nijmegen waar hij in 1998 zijn VWO diploma aan het R.K. lyceum Dominicus college behaalde. Datzelfde jaar begon hij de studie Bioprocestechnologie aan de toenmalige Landbouwuniversiteit Wageningen, maar verruilde deze studie na een jaar voor de studie Voeding & gezondheid en volgde de afstudeerrichting toxicologie. Hij verrichte een afstudeervak biochemie onder begeleiding van Hanem Awad, dr. Jacques Vervoort en professor dr. ir. Ivonne Rietjens, getiteld 'Biochemical and toxicological studies on the allylbenzene safrole', en een afstudeervak toxicologie bij de afdeling Ernährungstoxikologie van het Deutsches Institut für Ernährungswissenschaft (DIfE) te Potsdam-Rehbrücke onder begeleiding van dr. Walter Meinl, dr. Heiko Schneider en professor dr. Hansruedi Glatt, getiteld 'Genotype-phenotype correlations for human SULT1A1', waarvoor hij een beurs ontving van de KWF kankerbestrijding. Tijdens zijn studie behaalde hij zijn certificaat proefdierkunde (art. 9) en in het laatste jaar van zijn studie volgde hij met een Radboudbeurs verschillende vakken filosofie en ethiek aan de Radbouduniversiteit Nijmegen. In september 2005 behaalde hij zijn ingenieursdiploma Voeding & gezondheid en twee maanden later werd hij aangesteld als onderwijsassistent bij de sectie toxicologie van Wageningen University. In januari 2006 begon hij er zijn promotieonderzoek in een project in samenwerking met Nestlé Research Center, Lausanne, Zwitserland, waarvan de resultaten beschreven zijn in dit proefschrift. Tijdens zijn promotie werden alle certificaten van de postdoctorale opleiding toxicologie benodigd voor de registratie als erkend toxicoloog behaald. Van november 2009 tot mei 2010 was Walter werkzaam als trainee study director en scientist metabolite identification bij MSD (voormalig Schering-Plough), toxicology and drug disposition, te Schaijk.

List of publications

Scientific articles

Walter Brand, Jia Shao, Elisabeth F. Hoek-van den Hil, Kathelijn N. van Elk, Bert Spenkelink, Laura H.J. de Haan, Maarit J. Rein, Fabiola Dionisi, Gary Williamson, Peter J. van Bladeren, and Ivonne M.C.M. Rietjens. Stereoselective conjugation, transport and bioactivity of *S*- and *R*-hesperetin enantiomers *in vitro*. *Journal of Agricultural & Food Chemistry, accepted for publication.*

Walter Brand, Beatriz Padilla, Peter J. van Bladeren, Gary Williamson, and Ivonne M.C.M. Rietjens. Effect of co-administered flavonoids on the metabolism of hesperetin and the disposition of its metabolites in Caco-2 cell monolayers. *Molecular Nutrition & Food Research*, *in press*.

Walter Brand, Marelle G. Boersma, Hanneke Bik, Elise F. Hoek-van den Hil, Jacques Vervoort, Denis Barron, Walter Meinl, Hansruedi Glatt, Gary Williamson, Peter J. van Bladeren, and Ivonne M.C.M. Rietjens. Phase II metabolism of hesperetin by individual UDP-glucuronosyltransferases and sulfotransferases and rat and human tissue samples. *Drug Metabolism and Disposition,* 38(4): 617-625, 2010.

Walter Brand, Petronella A.I. van der Wel, Maarit J. Rein, Denis Barron, Gary Williamson, Peter J. van Bladeren, and Ivonne M.C.M. Rietjens. Metabolism and transport of the citrus flavonoid hesperetin in Caco-2 cell monolayers. *Drug Metabolism and Disposition* 36(9): 1794-1802, 2008.

Walter Brand, Maaike E. Schutte, Gary Williamson, Jelmer J. van Zanden, Nicole H.P. Cnubben, John P. Groten, Peter J. van Bladeren, and Ivonne M.C.M. Rietjens. Flavonoid-mediated inhibition of intestinal ABC transporters may affect the oral bioavailability of drugs, food-borne toxic compounds and bioactive ingredients. *Biomedicine & Pharmacotherapy* 60(9): 508-519, 2006.

Suzanne M.F. Jeurissen, Jan J.P. Bogaards, Hanem M. Awad, Marelle G. Boersma, **Walter Brand**, Yiannis C. Fiamegos, Teris A. van Beek, Gerrit M. Alink, Ernst J.R. Südholter, Nicole H.P. Cnubben, and Ivonne M.C.M. Rietjens. Human cytochrome P450 enzyme specificity for bioactivation of safrole to the proximate carcinogen 1'-hydroxy-safrole. *Chemical Research in Toxicology* 17(9): 1245-1250, 2004.

Ana M. Sotoca, Toine F.H. Bovee, **Walter Brand**, Nadya Velikova, Sjef Boeren, Albertinka J. Murk, Jacques Vervoort, and Ivonne M.C.M. Rietjens. On the mechanism of superinduction of estrogen receptor mediated gene expression in luciferase based reporter gene assays. *Submitted.*

Patents

Brand W, Williamson G, Van Bladeren PJ, Rietjens IMCM. Increasing the bioavailability of hesperetin. European patent application 09156910.3-2123 (filed 31.03.09)

Abstracts

Brand W, Rietjens IMCM, Van Bladeren PJ, Williamson G. Modulating of flavonoid bioavailability at the level of the intestinal metabolism and transport. In: *Current research 2010, graduate school VLAG, in press.*

Brand W, Padilla B, Van Bladeren PJ, Williamson G, Rietjens IMCM. Increasing the bioavailability of the flavanone hesperetin by co-administration of other flavonoids. In: *4th International Conference on Polyphenols and Health (ICPH2009)*: 229, 2009.

Brand W, Van Bladeren PJ, Williamson G, Rietjens IMCM. Modulating intestinal metabolism and transport of the citrus flavonoid hesperetin. In: *30th anniversary meeting of the Netherlands Society of Toxicology*: 43-44, 2009.

Brand W, Bik H, Van den Hil EF, Meinl W, Glatt H, Van Bladeren PJ, Williamson G, Rietjens IMCM. Conjugation of hesperetin by individual isoforms of UDP-glucuronosyl transferase (UGT) and sulfotransferase (SULT). In: *30th anniversary meeting of the Netherlands Society of Toxicology*: 81, 2009.

Brand W, Shao J, Rein MJ, Barron D, Williamson G, Van Bladeren PJ, Rietjens IMCM. Stereoselective kinetics of *R*- and *S*-enantiomers of the citrus flavonoid hesperetin *in vitro*. In: Abstracts from the 11th European regional ISSX meeting, May 17-20, Portugal, Lisbon. *Drug Metabolism Reviews* 41(Suppl 1): 83, 2009.

Brand W, Van der Wel PAI, Williamson G, Van Bladeren PJ, Rietjens IMCM. Modulating hesperetin bioavailability at the level of its intestinal metabolism and ABC transporter mediated efflux studied in Caco-2 monolayers. In: *Abstracts of the 44th congress of the European societies of toxicology, EUROTOX 2007. Toxicology Letters* 172S: S101, 2007. And in: *Abstracts of the Dutch toxicology days, 12th-13th June 2007. Chemico-Biological Interactions* 169(2): 132-133, 2007.

Brand W, Van Bladeren PJ, Rietjens IMCM, Williamson G. Modulating and modeling of flavonoid bioavailability at the level of the intestinal metabolism and transport. In: *Current research 2007, graduate school VLAG*: 132, 2007.

Brand W, Williamson G, Van Bladeren PJ, Rietjens IMCM. Modulation and modelling of flavonoid bioavailability at the level of its intestinal metabolism and transport. In: *Abstracts of the Dutch toxicology days, 13th-14th June 2006. Chemico-Biological Interactions* 161(2): 165, 2006.

Overview of completed training activities

Courses
Risk Assessment, PET, Wageningen, 2006
Ecotoxicology, PET, Wageningen/Utrecht, 2007
Medical, Forensic and Regulatory Toxicology, PET, Utrecht, 2007
Reproductive Toxicology, PET, Utrecht, 2008
Immunotoxicology, PET, Utrecht, 2008
Organtoxicology, PET, Utrecht, 2008
Physiologically Based Pharmacokinetic (PBBK) Modeling, Wageningen, 2009

Meetings
Biomedical Symposium, WUR, Wageningen, 2006
PhD Student Meeting, NVT, Wageningen, 2006
PhD Student Meeting, NVT, Wageningen, 2007
44th Congress of the European Society of Toxicology, Amsterdam, 2007
NMR and MRI applications in food systems, VLAG, Wageningen, 2008
30th Anniversary Meeting of the NVT, Veldhoven, 2009
11th European Meeting of the ISSX, Lisbon, 2009
4th International Conference on Polyphenols and Health, Harrogate, 2009

General courses
Organising and supervising MSc thesis work, OWU, Wageningen, 2006
VLAG PhD course, Ermelo, 2006
Techniques for writing and presenting a scientific paper, WGS, Wageningen, 2007
Effective behaviour in your professional surroundings, WGS, Wageningen, 2008

Optionals
Preparation PhD research proposal
Literature discussions, Division of Toxicology, Wageningen, 2006-2010
Theses and research in progress presentations, Division of Toxicology, Wageningen, 2006-2010

Approved by the graduate school VLAG.

Abbreviations

ABC	ATP binding cassette
ADP	adenine diphosphate
AGP	α_1-acid glycoprotein
AP	apical
ATP	adenine triphosphate
AUC_{o-xh}	area under the concentration time curve from time zero to x hours
BCRP	breast cancer resistance protein
BL	basolateral
bw	body weight
CsA	Cyclosporin A
CYP	cytochrome P450
DAD	diode-array detector
DEC	Dier Expereimenten Commissie
DMEM	Dulbecco's modified eagle medium
DMSO	dimethyl sulfoxide
EDTA	ethylene dinitrilotetraacetic acid
EGCG	(-)-epigallocatechin gallate
EpRE	electrophile-responsive element
FTC	Fumitremorgin C
GF120918	*N*-(4-[2-(1,2,3,4-tetrahydro-6,7-dimethoxy-2-isoquinolinyl)ethyl]-phenyl)-9,10-dihydro-5-methoxy-9-oxo-4- acridine carboxamide
GSH	Glutathione
GSSG	oxidized gluthatione
GV196771	*E*-4,6-dichloro-3-(2-oxo-1-phenyl-pyrrolidin-3-glydenemethyl)-1*H*-indole-2 carboxylic acid
HEPES,	4-(2-hydroxyethyl)-1-piperazineethanesulphonic acid
HIV	human immunodeficiency virus
HPLC,	high performance liquid chromatography
IS	internal standard
Ki	inhibitor constant
K_m	Michaelis-Menten constant
Ko143	3-(6-isobutyl-9-methoxy-1,4-dioxo-1,2,3,4,6,7,12,12*a*-octahydropyrazino-[1',2':1,6]pyrido[3,4-*b*]indol-3-yl)-propionic acid *tert*-butyl ester
LTC_4	Leukotriene C_4
LPH	lactase phloridzin hydrolase
MCF	Michigan Cancer Foundation
MDCK	Madin-Darby canine kidney
MDR	multidrug resistance
MDR1	multidrug resistance protein (=Pgp)
MEM,	minimal essential medium
MK571	3-[[3-[2-(7-chloroquinolin-2-yl)vinyl]-phenyl]-(2-dimethylcarbamoylethyl-sulfanyl)methylsulfanyl] propionic acid
MRP	multidrug resistance protein
MS-MS	tandem mass spectrometry
NEAA	nonessential amino acids
NMDA	*N*-methyl-*D*-aspartate
NMR	nuclear magnetic resonance
NRC	Nestlé Research Center
NVT	Netherlands Society of Toxicology
OWU	Onderwijsondersteuning Wageningen University
PAH	polycyclic aromatic hydrocarbon
PAPS	3'-phosphoadenosine 5'-phosphosulfate
PET	Postgraduate Education in Toxicology
PBS	phosphate buffered saline
PCR	polymerase chain reaction
PhIP	2-amino-1-methyl-6-phenylimidazo-[4,5-*b*]pyridine
Pgp	P-glycoprotein
PSC-833	Valspodar
RT-qPCR	reverse transcription quantitative PCR
SD-rat	Sprague-Dawley rat
SD	standard deviation
SEM	standard error of mean
SGLT1	sodium-dependent glucose transporter 1
SIR	selective ion recording
SULT	sulfotransferase
TEER	trans-epithelial electrical resistance
t_R	retention time
UDPGA	UDP-glucuronic acid
UGT	UDP-glucuronosyltransferase
uPLC	ultra performance liquid chromatography
WGS	Wageningen Graduate Schools
Vmax	maximum velocity
WGS	Wageningen Graduate Schools

The studies in this thesis were financially supported by Nestlé Research Center, Nestec Ltd., Lausanne, Swizterland. The publication of this thesis was financially supported by Wageningen University.

The cover photo was originally published in the book
'Ertussenuit' ('Going out') by Sjoerd Knibbeler.
It shows 'service to the intestinal tract', and was made
in Corpus, Oestgeest, The Netherlands.

The thesis was printed by
GVO drukkers & vormgevers B.V. / Ponsen & Looijen,
Ede, The Netherlands, on FSC and PEFC certified paper.

Lay-out thesis: Mathieu Brand
Foto cover and cover design: Sjoerd Knibbeler